INVESTIGATION OF THE MOLECULAR ROLE(S) OF YOP1 AND RTN1 SHAPING THE PERIPHERAL ER

A Dissertation

Presented to the Faculty of the Graduate School

of Cornell University

In Partial Fulfillment of the Requirements for the Degree of

Doctor of Philosophy

by

David Jeffrey Cragun

January 2011

INVESTIGATION OF THE MOLECULAR ROLE(S) OF YOP1 AND RTN1 SHAPING THE PERIPHERAL ER

David Jeffrey Cragun, Ph. D.

Cornell University 2011

A defining feature of eukaryotic life is the presence of membrane-bound organelles. While the energetically most stable shape for a membrane is likely a sphere, many organelles possess much more complex shapes within cells which contributes to their proper function. There has been an explosion in the field of membrane bending proteins in recent years giving new insights into how a cell forms and maintains organelle structures. Two ER resident proteins have recently been implicated in the formation of the tubular network of the ER in both higher and lower eukaryotes. Both Rtn1p and Yop1p contain two long hydrophobic domains, ~40 amino acids in length, which are thought to act as wedges within the outer leaflet of the ER membrane and drive membrane deformation.

Using a mutagenic approach I have determined that both of the hydrophobic domains of Yop1p are critical for its ability to generate the tubules of the peripheral ER. The overexpression of Yop1p produces long, unbranched tubules in cells. I have developed an initial strategy for the enrichment of these Yop1p formed tubules for further study outside the context of the cell. Biochemical analysis of these tubular structures has revealed they are composed of protein and lipid components. Electron microscopy of enriched tubules indicates they have a small diameter, ~15 nm, and are

often bundled together into rope-like structures. This work underscores the importance of Yop1p in the generation of the tubular network of the peripheral ER and provides evidence deepening our understanding of the molecular mechanism of Yop1p action on membranes that generates membrane tubules.

BIOGRAPHICAL SKETCH

The author of this thesis was born in Los Angeles, California but spent his formative years in Davis, California. He graduated from Granite Bay High School in 1999 and went on to complete a BA in Cell and Molecular Biology and a BS in Microbiology from the University of Montana, Missoula in 2005 where he graduated with high honors. During his studies at U of M he was awarded two consecutive years of NSF EPSCoR fellowships for research conducted with Dr. Scott Samuels on the transmission of *Borrelia burgdorferi*. He subsequently was accepted into the graduate program at Cornell University in the field of Biochemistry, Molecular and Cell Biology.

Dedicated to my wife and son, where would I be without you?

ACKNOWLEDGMENTS

First I would like to thank my mentor, Dr. Ruth Collins. Her passion for science and the pursuit of knowledge has been truly inspirational and is something I will take with me as I pursue my own career. She has pushed me to become a better scientist and person. Her support, not only of my scientific endeavors but also of my personal ambitions, has been key in helping me to become the person that I am today. She provided me with a scientifically stimulating work place that acted as a platform to further develop my critical thinking skills and pushed me to seek the knowledge I would need to experimentally answer difficult scientific questions. For her mentorship and guidance, I am truly thankful and will never forget her contribution to the person I have become.

I was also very fortunate to have an extremely supportive and helpful committee. Dr. William Brown, Dr. Thomas Fox and Dr. Gary Whittaker have all provided me with constructive criticism with regards to my thesis project that has been instrumental in guiding me to necessary experiments. They have all been present at every committee meeting and actively engaged in the progress of my project, for which I am greatly indebted to all of them. Dr. Nick Davis (Wayne State University) and Dr. Stanley Perlman (University of Iowa) also deserve special thanks for collaborations on the reticulon palmitoylation and SARS-CoV ORF6 projects, respectively. I am grateful that they both were willing to share information and constructs that provided the basis for these two side-projects.

There have been many past and present Collins lab members who have made my time in Ithaca so much more enjoyable. Thanks to Dr. Pete Rahl who taught me all the technical aspects of microscopy, which became a staple in my day-to-day lab bench-work. Also, thanks to Dr. Chris Heger who showed me the ropes in the Collins

lab and taught me much of the technical aspects of working with yeast. Other members, Dr. Ian Berke, Dr. Catherine Chen, Dr. Carrie DeRegis, Dr. Duane Hoch, Mengqiao Wang and Dr. Fabio Renaldi have all provided me with invaluable conversations and input on my work and all have become great friends. I would like to thank all of them for their support and friendship and know we will remain in touch as we all move forward in our careers.

There have been incredible staff members at Cornell that have been instrumental in my success here. First, I would like to give Dr. Volker Vogt special thanks for offering me so many supportive conversations. He selflessly devoted many hours to ensure my success here at Cornell. He also offered immense guidance on the content of my thesis for which I cannot express my gratitude enough. I would also like to thank Diane Colf who has helped me navigate the behind-the-scenes paperwork and scheduling that is required to complete the graduate program at Cornell. I would also like to thank Vicki Shaff, Debbie Crane, Valerie Moore, Cindy Westmiller, Casey Isham, Janna Lamey, Greg Mitchell and Blake Werner for ensuring the day-to-day operations ran smoothly.

I would also like to thank my wife, Jenni, for all of the support she has offered me over the last 13 years. Without her dedication and love I would not have made it through high school, let alone college or graduate school. She, and my son Elliott, have been a guiding light through these long hours and difficult times, and I am fortunate to have them both in my life. In addition I would like to thank my parents, Jeff and Lisa, for all the support they have given me throughout my life. They both are truly inspirational and have instilled in me a strong work ethic and dedication to the task at hand. Also, Jenni's parents, Steve and Pam, deserve a special thanks as well for their support of all my endeavors, as well as everything they have done for me and my family over the years.

TABLE OF CONTENTS

LIST OF FIGURES

LIST OF TABLES

CHAPTER 1

INTRODUCTION

Eukaryotic membrane trafficking

One of the defining characteristics of eukaryotic cells is the presence of membrane bound organelles. The lipid bilayers of these structures serve as barriers between the cytoplasm and the contents of the organelle. Transfer of cellular material between organelles occurs through a complex process of budding vesicles/tubules from one organelle, transport through the cell and ultimately fusion with an acceptor membrane. During this process luminal and membrane components are transferred from one organelle to another. The transfer of organellular components is a highly regulated process where specific loading of cargo within the membrane bound vesicles/tubule aids in maintaining organelle identity and delivering specific cargo to designated locations [1]. Factors present on the budded membrane direct the cargo to designated acceptor membranes containing the necessary components for fusion [2-4].

A number of factors have been identified that direct the formation of membrane buds and select the cargo components for transfer to an accepter organelle (Figure 1.1). Clathrin forms coated pits on the cytoplasmic face of the plasma membrane during endocytosis, as well as from the trans Golgi network and endosomes [2, 3, 5]. Clathrin monomers aggregate at the bud site to begin bud formation. The adaptor proteins (AP1, AP2, AP3 and AP4) interact with clathrin and the selected cargo and effectively hold the cargo in place to be loaded into the forming vesicle [6-10]. COPI coated vesicles traffic materials retrograde from the Golgi to the ER, as well as between the cisternae of the Golgi complex [11]. COPI is thought to function in formation of the membrane bud as well as in cargo selection during this process [12-14]. COPII coated vesicles traffic material from the ER to the Golgi [15, 16].

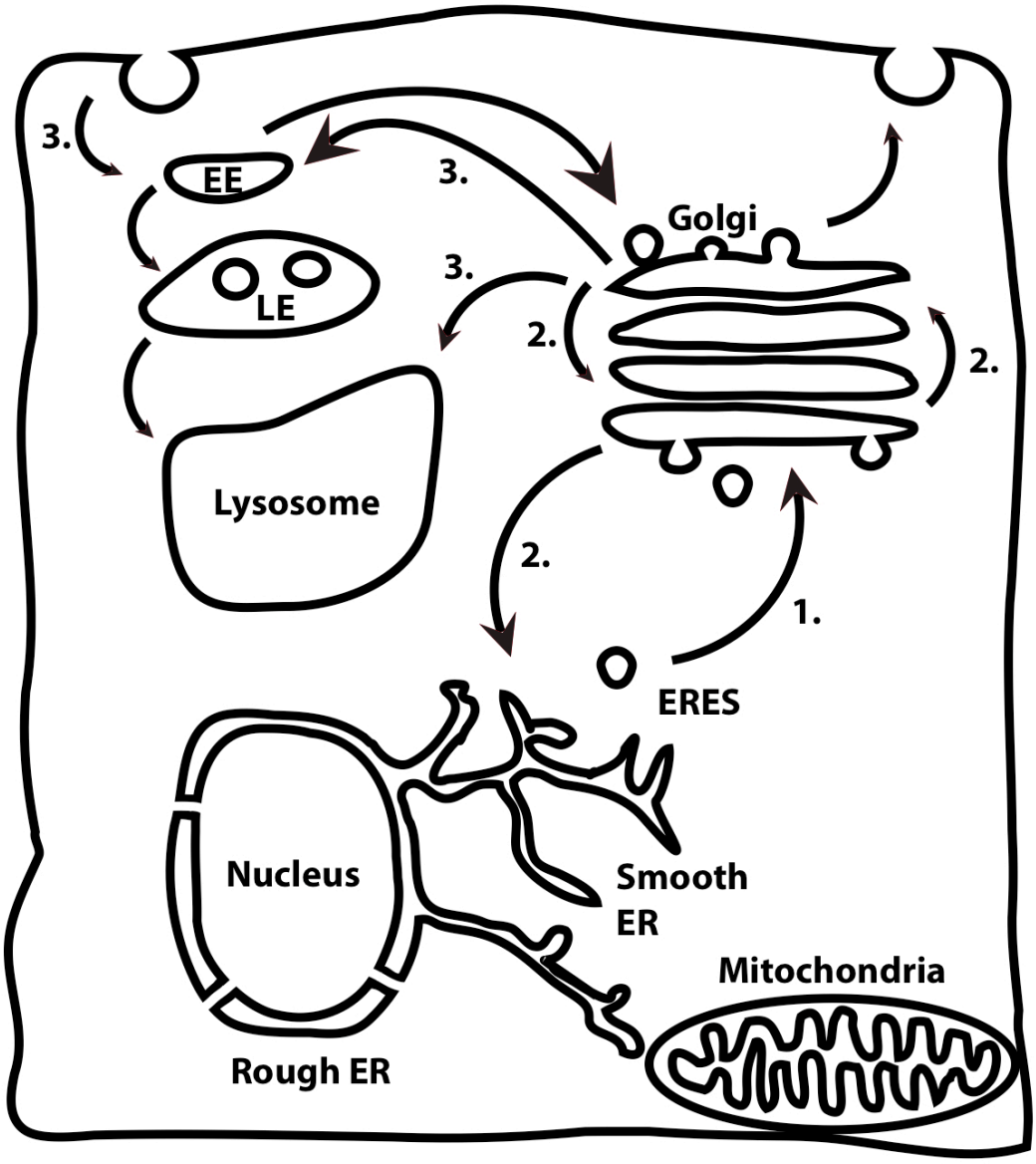

Figure 1.1 Schematic representation of eukaryotic membrane trafficking. Also included are some of the major proteins responsible for steps in membrane trafficking. 1. COPII, 2. COPI, 3. Clathrin. Abbreviations: ERES ER exit sites, EE early endosome, LE late endosome.

Activation of Sar1p by exchange of GDP with GTP exposes an NH_2 terminal amphipathic helix, which is inserted into the membrane, recruiting the two protein complexes, Sec13p-Sec31p and Sec23p-Sec24p and together drives membrane deformation [17-32]. This complex interacts with the adaptor protein, p24, which binds to cargo and Sec24p, loading the appropriate cargo into the forming vesicle known as an ER exit site (ERES) [31, 33-43].

Tethering proteins and SNAREs (soluble N-ethylmaleimide sensitive factor attachment receptors) present on the surface of the vesicles and acceptor membranes serve to facilitate binding of the vesicle to the correct acceptor membrane and are also thought to drive fusion of the two membranes [44]. Tethering complex on the acceptor membrane, along with its cognate Rab protein serves to identify the correct destination for the vesicle and acts to bring the vesicle physically close to the acceptor membrane [45-48]. A number of potential tethering complexes have been identified on various acceptor membranes, for example the exocyst complex on the plasma membrane [49], TRAPP and COG complexes on the Golgi [50-56], and the HOPS complex on the vacuole [57, 58]. Target SNAREs (t-SNAREs) and vesicle SNAREs (v-SNAREs) are present on the acceptor and vesicle membranes, respectively, and function in fusing the two membranes. SNARES are long coiled-coil proteins that interact specifically with another SNARE when two membranes are brought into close proximity to one another. It is thought that the SNAREs serve as a bridge between the two membranes and together with SM/Sec1p, function in fusing the two membranes through a yet undetermined mechanism [44, 59-63].

Complex morphology of organelles

The morphology of each organelle manifests as distinct membrane shapes that are evolutionarily conserved (Figure 1.1). For example, mitochondria contain two

distinct membranes, the inner and outer membranes. The outer membrane is relatively flat and serves as a barrier between the mitochondrial matrix and the cytoplasmic space. On the other hand, the inner membrane is highly convoluted into structures called cristae [64-66]. These membrane invaginations serve to increase the surface area of the inner membrane to increase the energy production of the mitochondria [67, 68]. The membrane cristae have a very narrow diameter, ~10-15 nm, thought to slow the diffusion of proteins from the mitochondrial interior and regulate the energy state of the mitochondria [69]. Formation of the proton gradient that drives ATP production occurs across the inner membrane and it is thought that slowing the diffusion of factors to the peripheral ends of the cristae regulates the rate of energy production. When a cell needs a higher energy level the diameter of the mitochondrial cristae can widen to increase the diffusion rate and thus increase energy output [70, 71]. The morphology of these membrane invaginations has a direct effect on the function of the mitochondria.

The nuclear envelope provides another example of how the morphology of a membrane can aid in the proper function of the organelle. The nuclear envelope is composed of two relatively flat, large membrane sheets attached together through nuclear pores that connect the aqueous environments of the nucleus and the cytoplasm [72]. Between the two membranes is the lumen of the ER. The presence of nuclear pores is required for the exchange of macromolecules between the nucleus and the cytoplasm and is also essential for cell division and differentiation [73-75]. Nuclear pores are large complex structures that have defined morphologies with a diameter of 40-90 nm connecting the two membranes approximately 50-100 nm apart [76-78]. The specific structure of these pores controls the diffusion of macromolecules through them, providing another example of how the morphology of the nuclear envelope can dictate its proper function [79-83]. Nuclear pores consist of more than 30 individual

proteins bound very specifically between the membranes and is ~40 Mda in the budding yeast, *S. cerevisiae* [84]. In higher eukaryotes, the nuclear envelope is broken down during mitosis and must be reformed after [85]. This process also necessitates that nuclear pores must be broken down and reformed as well [86, 87]. In order for the inner and outer nuclear membranes to be connected through the formation of a pore the two membranes must be brought close together and a localized area of extremely high curvature must be generated between the two membranes where the pore is to form. Two ER resident proteins, Rtn1p and Yop1p, were recently identified as factors required for the formation of nuclear pores [88]. Although, Rtn1p and Yop1p localize mainly to peripheral ER structures where they are thought to function in generating membrane tubules, a small amount can be found on the nuclear envelope as well [89-91]. It has been proposed that this small pool of Rtn1p and Yop1p are critical factors in generating the high level of curvature required for proper nuclear pore formation [88, 92].

The Golgi complex is another organelle that is composed of a specific morphology that is critical for proper function. In mammalian cells the Golgi is composed of a series of cisternae, each a flat disc-like structure sandwiched together and connected by small membrane tubules [93-95]. Each of the cisternea of the Golgi contains distinct components that function in a different step during the post-translational modification of proteins [96-99]. Protein glycosylation is a modification that can regulate the turnover of a protein, proper protein folding, the localization of a protein, or be necessary for the function of a protein [100-104]. Glycosylation occurs through a distinct series of enzymatic reactions that must occur in the correct order to result in the proper glycosylation pattern. Cells divide the machinery for glycosylation between the Golgi cisternae so that early acting processing enzymes are found in the *cis*-Golgi and later acting enzymes are found in the *trans*-Golgi. Thus as proteins

progress through each cisternae they receive the correct glycosylation in the correct order [105-107]. It is the structure of the Golgi complex that allows the separation of these reactions to achieve the proper modification of proteins, thus providing another example of how the morphology of an organelle can be critical for its function.

The endoplasmic reticulum

The endoplasmic reticulum (ER) is ubiquitously found in all eukaryotic organisms and provides the cell with many essential functions. The ER is the major site of lipid synthesis which serves as the source of lipids for the biogenesis of many organelles [111, 112]. ER membranes, in close apposition to other organelles, are believed to transfer lipids and/or proteins to the mitochondria, peroxisomes, endosomes and the plasma membrane directly as well [112]. The ER also acts as the entry portal into the secretory system. The ribosomes of the rough ER produce integral membrane proteins and luminal proteins that are distributed throughout the cell. The lumen of the ER contains many enzymes essential for protein glycosylation, detoxification of harmful compounds and quality control of proteins through the unfolded protein response [113, 114]. Additionally, the lumen of the ER acts as a Ca+2 storage and signaling repository for the cell, regulating many Ca+2 dependant processes [115]. Thus, the ER functions as a master organelle in the biosynthesis of other organelles, synthesis of macromolecules, storage of signaling molecules and protein quality control providing the cell with many other functions essential for eukaryotic life.

Morphology of the Endoplasmic Reticulum

In mammalian cells, the ER is a membrane-enclosed organelle composed of at least three morphologically distinct regions that contain a continuous luminal space

[116]. The rough ER is found close to the nucleus and is composed of relatively flat membrane sheets studded with ribosomes while the smooth ER consists of a polygonal array of highly curved tubules which extend throughout the entire cytoplasm [116-119]. ER exit sites (ERES) are specialized regions of the ER where COPII coated vesicles form and bud during membrane trafficking [120, 121]. These sites are spread throughout the ER and are composed of protein complexes that aid in the formation of COPII coated vesicles and the packaging of material destined to enter the secretory system [36]. Little is known about how all of these subdomains of the ER are formed and maintained as morphologically distinct structures, however conservation of this ER morphology is observed in other eukaryotes demonstrating the significance of these distinct ER subdomains.

Budding yeast contains a similarly structured ER, which enables examination of the conserved mechanisms cells use to generate these subdomains in a genetically amenable system. In yeast, the flat sheet-like ER surrounds the nucleus (the nuclear ER) and is connected to the peripheral ER by a few cytoplasmic tubules, making a continuous luminal space between these two ER subdomains (Figure 1.2 A). The peripheral ER is found at the extreme periphery of the cell in a network of tubules connected by junction points just beneath the plasma membrane [119, 122, 123] (Figure 1.2 B). In yeast, ERES are found mainly in the tubules of the peripheral ER, possibly suggesting the high curvature present in these tubules may aid in vesicle formation [119]. The conserved morphology of ER membranes in eukaryotic cells implies the existence of conserved mechanisms for generating and maintaining the membrane curvature of these differently structured domains.

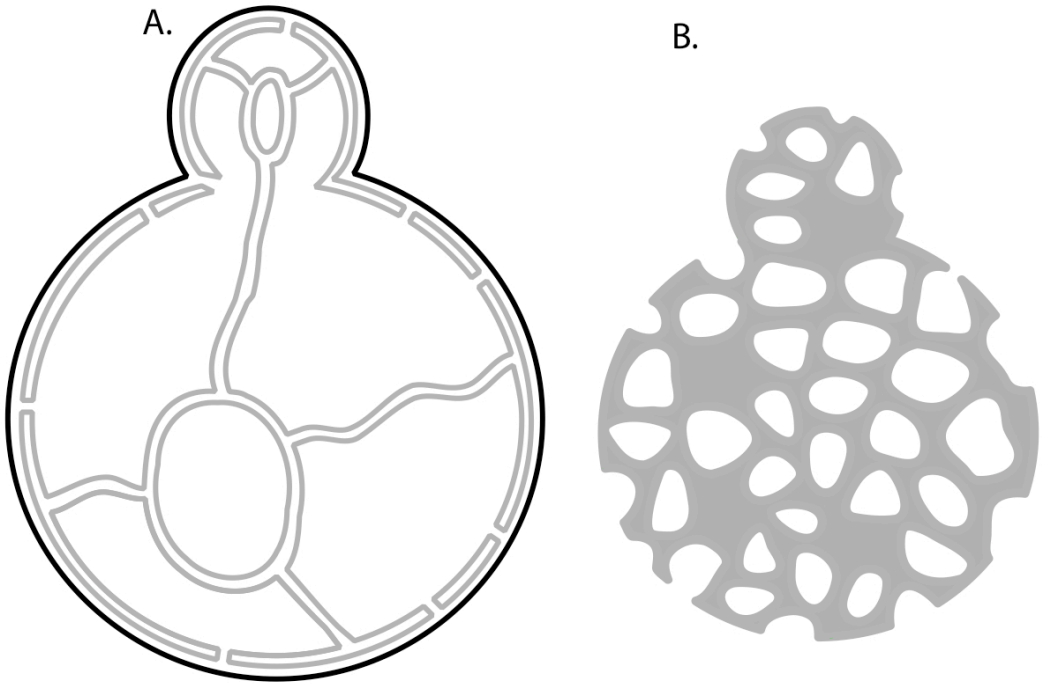

Figure 1.2 Structure of the ER in *S. cerevisiae*. A. Cross sectional view through the center of a cell depicting ER membranes, colored grey. B. Cross sectional view of the periphery of a cell depicting the tubular network of the peripheral ER found just beneath the plasma membrane.

The ER is a dynamic structure

During mammalian mitosis the nuclear envelope is disassembled, and with it the ER is also broken into vesicular structures distributed throughout the cell [122, 124]. This large-scale alteration of ER membranes, and the subsequent reformation of the ER after mitosis, suggests that the mechanism driving the formation of these structures must be reversible. In yeast however, the nuclear ER is not broken down during mitosis, but instead remains intact. A tubule of the peripheral ER is inherited by the daughter cell early in bud formation. Actin cables direct the movement of a peripheral ER tubule into the newly forming daughter cell where it is anchored to the plasma membrane [125, 126]. Rtn1p has been shown to bind directly to Sec6p, a subunit of the exocyst complex [89]. The exocyst complex is an octameric complex that localizes to sites of secretion, such as the bud tip and septum, and functions to tether secretory vesicles to the plasma membrane [49, 127]. The delivery of a peripheral ER tubule to the bud tip of a growing daughter cell involves this tubule moving along an actin filament and attaching at the bud tip. The tubule is then anchored at the bud tip and subsequently spreads throughout the inner plasma membrane of the bud through an unknown mechanism. The initial movement of the peripheral ER tubule requires the action of Myo4p and She3p, however, no mechanism is known for attachment of the tubule to the daughter cell plasma membrane [125, 128]. It has been suggested that the binding of Rtn1p to the exocyst complex aids in the attachment of the peripheral ER tubule to the daughter cell plasma membrane, perhaps directly anchoring the peripheral ER at the bud tip where it can subsequently spread along the plasma membrane of the daughter cell [89]. However, considering *rtn1Δ* cells do not have defects in ER inheritance there must be some other redundant mechanism of tubule attachment [89].

Additionally, the tubular ER is a highly dynamic structure constantly undergoing rearrangements [124]. New tubules can branch from existing ones, grow, and then fuse with other tubules. Tubules can also slide along one another, changing the arrangement of the tubular network. In addition, tubules can be removed when a sliding tubule fuses with an adjacent one, a process called ring closure [122, 124, 129]. How this dynamic behavior is regulated is unclear, but actin filaments play a critical role in the dynamics of the ER in yeast, while microtubules appear to serve this function in the smooth ER of higher eukaryotes [122, 130, 131]. Actin depolymerization reduces the peripheral ER movements dramatically in yeast, though appears to have little effect on the structure of tubules, suggesting actin may regulate these tubule movements but is not responsible for forming the tubular structure [123].

Mechanisms of Membrane Bending

While the most energetically stable form for a membrane bound compartment is likely to be roughly a sphere consisting of a single, relatively flat membrane sheet, many eukaryotic organelles maintain a distinct and highly specialized membrane morphology critical for their function. This conservation suggests the presence of evolutionarily conserved means to form/maintain the specific morphology of each organelle. Several conserved mechanisms for generating membrane curvature have been discovered (Figure 1.3) [132, 133]. For example, varying the lipid composition between leaflets of a lipid bilayer can induce spontaneous membrane curvature. The varied polar tail regions and charged head groups of lipids can alter their packing within the membrane, ultimately changing the membrane curvature (Figure 1.3 A). Alternatively, soluble protein coats can oligomerize on a membrane surface, imposing their intrinsic curvature on a localized region of the membrane (Figure 1.3 B). Furthermore, the insertion of a proteins hydrophobic domain part of the way through

the lipid bilayer can increase the surface area of one leaflet, forcing deformation of the membrane through a wedging mechanism (Figure 1.3 C). These mechanisms are not exclusive to one another and may act in concert to generate the curved membranes of many organelle structures within the cell.

Lipid composition and membrane curvature

A common mechanism of generating morphological alterations of membranes is through changes in lipid composition between the two leaflets of a bilayer [108, 134, 135]. Lipids are composed of polar head groups and hydrophobic tails. The size and charge of the polar head group influences the amount of space occupied by the lipid on the membrane surface while the length of the hydrophobic tail and the number of double bonds present have effects on the packaging of the lipids within the interior of the membrane. These two factors govern the ability of the lipid composition to drive membrane deformation through the shape of the lipids that make up the membrane. In order for the lipid composition to drive membrane curvature the different lipid species must be asymmetrically distributed between the two leaflets of the bilayer, and this asymmetry must be maintained in order for the curvature generated to be maintained for long periods of time. There is an intrinsic low level of lipid flipping that occurs between the two leaflets of a membrane that would eventually redistribute the lipids between the two leaflets [136-142]. Perhaps once a small, localized area of curvature has been generated, the lipids with large head groups prefer to be on the leaflet with a larger surface area, with more space between the large, charged head groups. Flippases have the ability to flip lipids from one leaflet to another and may act to generate and/or maintain the lipid asymmetry that results in membrane deformation as well [143-145].

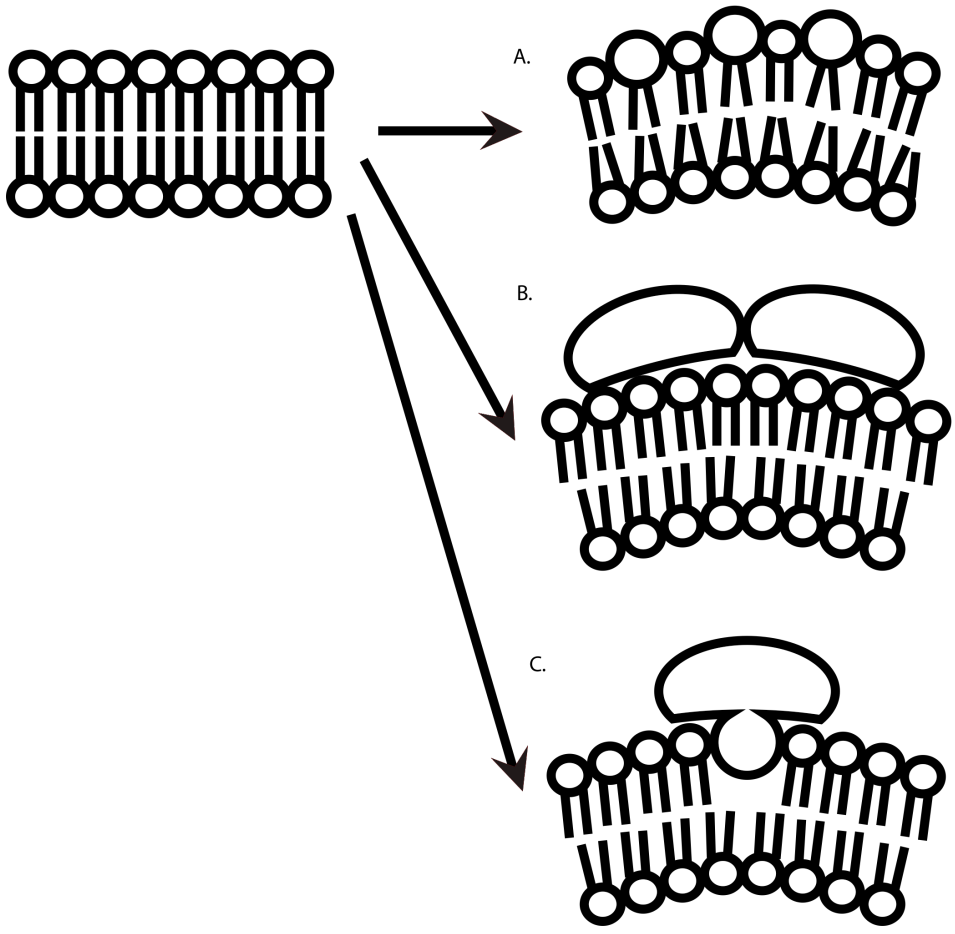

Figure 1.3 Three ways to generate membrane curvature. A. Altering the lipid composition of a normally flat membrane can curve the membrane. B. Coat proteins can bind to the surface of a flat membrane and impose their intrinsic curvature on the membrane. C. Hydrophobic "wedging" can increase the surface area of one leaflet, generating membrane curvature.

Furthermore, the enzymes that generate the different lipid species may form the asymmetric lipid distribution that results in generating membrane curvature. These enzymes chemically convert one lipid species into another, altering the lipid composition of the membrane and potentially the shape of that membrane. Trafficking in the Golgi occurs, in part, through the action of phospholipase A2, which increases the concentration of inverted, cone-shaped lysophospholipids in the membrane of the Golgi, TGN, and endosomes and results in the formation of tubular structures [109, 146-148]. The increase in inverted cone shaped lipid species specifically localized within the cytoplasmic leaflet of these organelles results in the formation of 60-80 nm tubular structures and promotes trafficking between membranes [149-151]. This is one example of how altering the enzymatic action of a protein can alter the lipid composition of a membrane and thus change the morphology of an organelle.

Coat proteins and membrane curvature

Coat proteins are soluble proteins that have the capacity to bind to membrane surfaces, sensing and/or forming curved membranes. These proteins often contain intrinsic curvature on their positively charged membrane-binding surface and can force this intrinsic curvature on the membrane [32, 152]. BAR domain proteins function as banana shaped homodimers that bind membranes on their concave surfaces. The interaction between two or more of these complexes can induce large areas of curvature over great distances resulting in the formation of membrane tubules [153, 154]. Coat proteins often also contain amphipathic helices that are inserted into the surface of the membrane to stabilize the interaction between the coat protein and the membrane. These helices are also thought to act in generating membrane curvature through a wedging effect, expanding the outer leaflet of the bilayer and driving membrane curving [155, 156].

Clathrin is another coat protein that functions in generating membrane curvature. Clathrin drives the formation of clathrin-coated pits through its interaction with the plasma membrane and other accessory proteins. Clathrin polymerization at the surface of the membrane with epsin and AP-2 is thought to begin bud formation from the relatively flat plasma membrane [156]. Cargo selection is mediated through interactions between AP-2 and specifically selected cargo and it is believed that the accumulation of cargo may further drive bud formation. Epsin and other F-BAR proteins continue to accumulate at the bud site and function in forming the vesicle, as clathrin is not believed to be capable of polymerizing into a symmetrical vesicular structure [157, 158]. Scission of the clathrin-coated vesicle is thought to occur through the combined action of dynamin, amphiphysin, endophilin and SNX9 binding to the very narrow neck of the vesicle and pinching it off [159-162]. The combined action of all these factors results in the endocytosis of specific cargo from the extracellular environment into the cytoplasm through the regulated formation of a localized area of membrane curvature.

Hydrophobic domains and membrane curvature

The insertion of the hydrophobic regions of a protein part of the way into a membrane can result in the expansion of the surface area of one leaflet of the bilayer, driving membrane deformation. The amphipathic helices of many BAR domain proteins provide an example of how hydrophobic insertion can alter membrane structure through a wedging mechanism [155, 156].

Another protein, caveolin, contains a single COOH terminal hydrophobic domain of ~40 amino acids believed to form a hydrophobic hairpin within one leaflet of the membrane [163]. Aggregation of caveolin within the membrane drives the formation of caveolae during endocytosis [164-169]. Caveolin is specifically attracted

to plasma membrane subdomains enriched in cholesterol and sphingolipids and the presence of these molecules with the hydrophobic domain of caveolin are believed to increase the fluidity of this localized region of the membrane, aiding in membrane deformation [170-175]. It is thought that the hydrophobic domain provides the driving force in generating membrane curvature while the NH_2 and COOH terminal hydrophilic domains aid in oligomerization of caveolin monomers. Modeling of the hydrophilic regions of caveolin suggests they may have the ability to form amphipathic helices and may further drive membrane deformation similar to the BAR domain protein's helices [176]. An additional class of proteins, cavin proteins, also localize to caveolae and appear to aid in forming the typical morphology of these budding vesicular structures, though their contribution to this process is poorly understood [177-180].

Two ER resident proteins, Rtn1p and Yop1p, also each contain these long hydrophobic domains thought to drive membrane deformation. Although Rtn1p and Yop1p do not share sequence homology, they both have two long hydrophobic domains (~40 amino acids in length) predicted to be membrane embedded. Together they have been proposed play redundant roles in the formation and/or maintenance of the highly curved membranes of the ER [90, 181-183].

Rtn1p and Yop1p Family Proteins

Rtn1p belongs to the eukaryotic reticulon family of integral membrane proteins, characterized by a reticulon homology domain (RHD). This domain contains two long hydrophobic stretches (~40 amino acids) separated by a hydrophilic loop (~60 amino acids) (Figure 1.4 A) [89, 90]. Additionally, reticulons contain a variable NH_2 terminal hydrophilic segment, suggesting divergent functions may exist for different family members. Although reticulon homologs exist in all sequenced

eukaryotic genomes, none are found in prokaryotic ones [184], implying an evolutionarily conserved function that arose after the development of membrane-bound organelles.

Mammalian cells contain 4 reticulon genes with many isoforms differentially expressed in different cell types [184]. Reticulon proteins studied to date localize primarily ER membranes, with enrichment on tubular ER structures [91, 181, 185-188]. Mammalian reticulons are highly expressed in neuronal cells and have been implicated in a variety of diseases including Alzheimer's and autism [189-193], indicating a role for these proteins in proper nerve cell function, although no mechanism has been identified [191, 194]. Furthermore, reticulons have predicted functions as neurite outgrowth inhibitors, regulators of apoptosis through interactions with Bcl-2, and as regulators of amyloid precursor protein processing which may represent some of the divergent functions of this protein family [195-200]. In addition, reticulons have been recently implicated in the formation and/or maintenance of the peripheral ER tubules in both lower and higher eukaryotes [90, 181].

Yop1p/DP1 family proteins represent a distinct family from reticulons, but interestingly also contain two long hydrophobic segments separated by a hydrophilic loop (Figure 1.4 B) [90]. Yop1p/DP1 family proteins have homologs in eukaryotic organisms but not in prokaryotic ones [195, 196]. The mammalian homolog of *YOP1*, the deleted in polyposis gene 1 (DP1), localizes to tubular ER membranes [90]. A recent study identified another mammalian *YOP1* homolog called REEP3. Truncation in the promoter region of this gene abolishes its expression, which correlates with development of autism, indicating a potential role for this protein in proper nerve cell function [190]. Yop1p has also recently been implicated in the formation and/or maintenance of peripheral ER tubules in both higher and lower eukaryotes, perhaps even sharing redundant functions with Rtn1p [90, 181].

Figure 1.4 Sequence alignment of Reticulon and Yop1p/DP1 family homologs. A. Sequence aligment of the reticulon homology domain of selected reticulon family members, bars indicate the predicted hydrophobic domains. B. Sequence alignment of Yop1p/DP1 family homologs, bars indicate predicted hydrophobic domains. *S. cerevisiae* (yeast), *H. sapiens* (human), *M. musculus* (mouse), *S. pombe* (pombe), *D. melanogaster* (fly), *C. elegans* (worm), *A. thaliana* (plant).

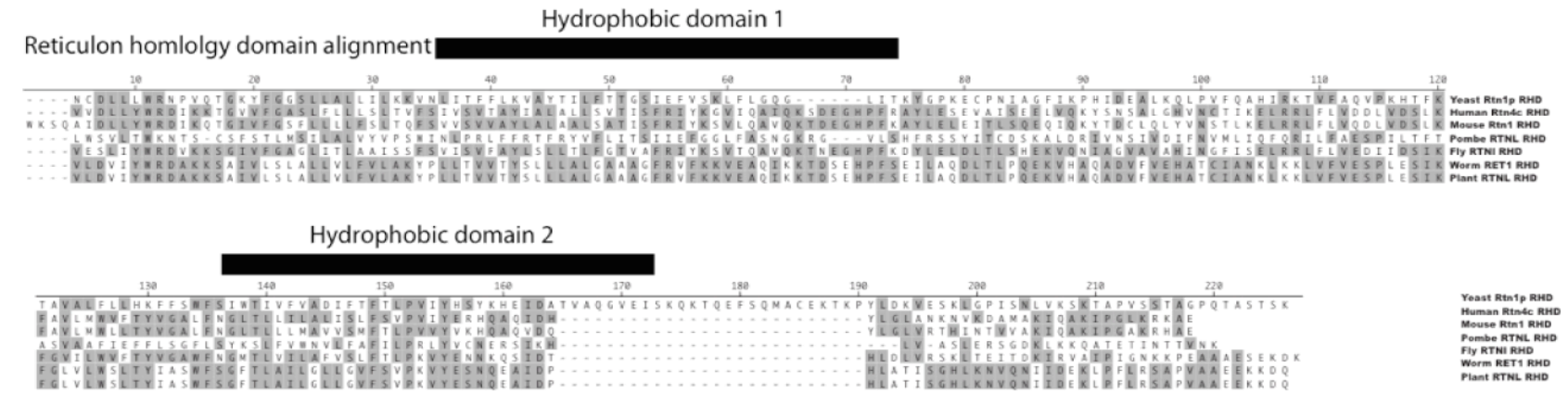
Hydrophobic domain 1
Reticulon homlolgy domain alignment
Yeast Rtn1p RHD
Human Rtn4c RHD
Mouse Rtn1 RHD
Pombe RTNL RHD
Fly RTNI RHD
Worm RET1 RHD
Plant RTNL RHD
Hydrophobic domain 2
Yeast Rtn1p RHD
Human Rtn4c RHD
Mouse Rtn1 RHD
Pombe RTNL RHD
Fly RTNI RHD
Worm RET1 RHD
Plant RTNL RHD

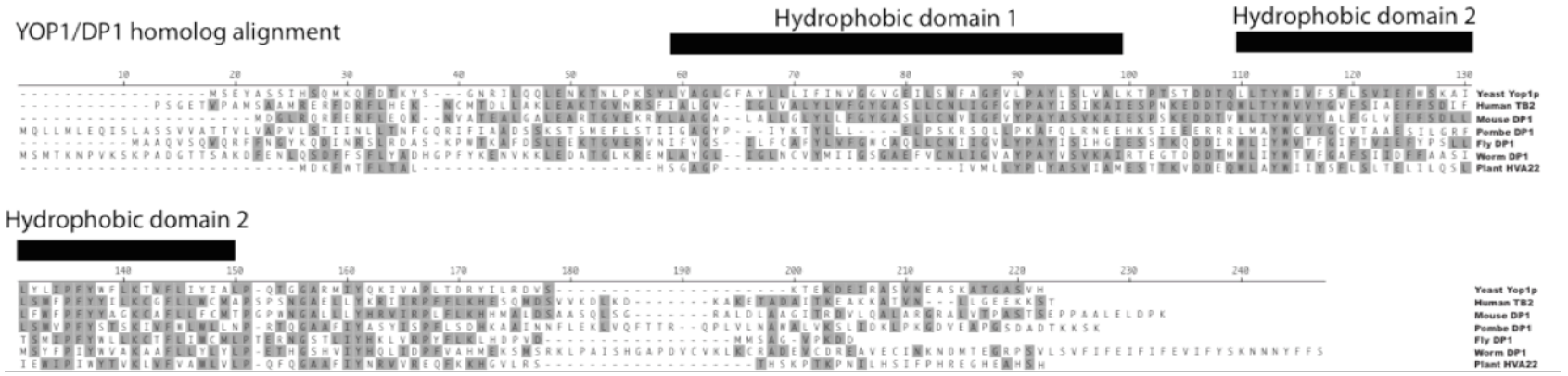
YOP1/DP1 homolog alignment
Hydrophobic domain 1
Hydrophobic domain 2
Yeast Yop1p
Human TB2
Mouse DP1
Pombe DP1
Fly DP1
Worm DP1
Plant HVA22
Hydrophobic domain 2
Yeast Yop1p
Human TB2
Mouse DP1
Pombe DP1
Fly DP1
Worm DP1
Plant HVA22

Rtn1p and Yop1p form oligomeric complexes with each other and Yip family proteins

Tubules are specifically organized structures, characterized by highly curved membranes in cross section, but low curvature along the length of the tubule. This organization implies that the proteins responsible for generating this curvature may be assembled into highly ordered complexes [181].

Rtn1p interacts with a number of proteins all implicated in the formation of peripheral ER tubules. The binding of Rtn1p to itself and Yop1p are required for the generation of peripheral ER tubules in vivo. Indeed, mutations of *RTN1* have been identified that abolish its ability to function in tubule formation as well as its ability to oligomerize [181]. Rtn1p also binds to Yip3p, a protein related to the YIP family proteins which are believed to be involved in membrane trafficking [197]. Yop1p was originally identified as a Yip1p interacting protein (Yip One Partner) in a two-hybrid screen [198]. YIP family proteins are a class of proteins that bind Rabs in a prenylation-dependent manner [199-201], however the exact function of YIP family proteins is not understood. Recent work has linked YIP family proteins to the regulation COPII coated vesicle biogenesis [202]. Mutants of *YIP1* result in both an inability for COPII vesicle biogenesis to occur (a severe secretion defect) and an accumulation of sheet-like ER membranes in place of the tubular peripheral ER [198, 200, 201, 203]. Perhaps Yop1p, Rtn1p and YIP family proteins act in concert to regulate the formation and maintenance of ER tubules. The formation of oligomeric complexes between these proteins may be critical for their proper organization within the membrane, ultimately being responsible for generating the highly organized structure of a tubule.

Rtn1p and Yop1p Share a Unique Topology within the Membrane

Both Rtn1p and Yop1p are predicted to contain two long hydrophobic segments, each ~40 amino acids in length, separated by a hydrophilic loop (Figure 1.4 A, B). These two hydrophobic segments are considerably longer than a normal transmembrane domain which typically consists of 18-20 amino acids [204] . Examination of the topology of mammalian Rtn4a and DP1 suggests that the NH_2 and COOH termini reside on the cytoplasmic face of the ER membrane. In addition, the hydrophilic internal loop region resides on the cytoplasmic face of the ER which might cause the long hydrophobic domains to fold into two hairpins, each dipping into the membrane without passing through the other side (Figure 1.4 C) [90]. The additional space taken up by each of the hydrophobic segments may result in expansion of the outer leaflet, forcing localized deformation of the membrane.

Figure 1.5 Model of the mechanism of Yop1p/Rtn1p in generating membrane curvature. A. MpeX hydrophobicity plot of the primary amino acid sequence of Rtn1p. Positive values represent hydrophobic residues, negative values represent hydrophilic residues. B. MpeX hydrophobicity plot of the primary amino acid sequence of Yop1p. Positive values represent hydrophobic residues, negative values represent hydrophilic residues. C. Model of the mechanism of hydrophobic "wedging" used by Rtn1p/Yop1p in the generation of membrane curvature.

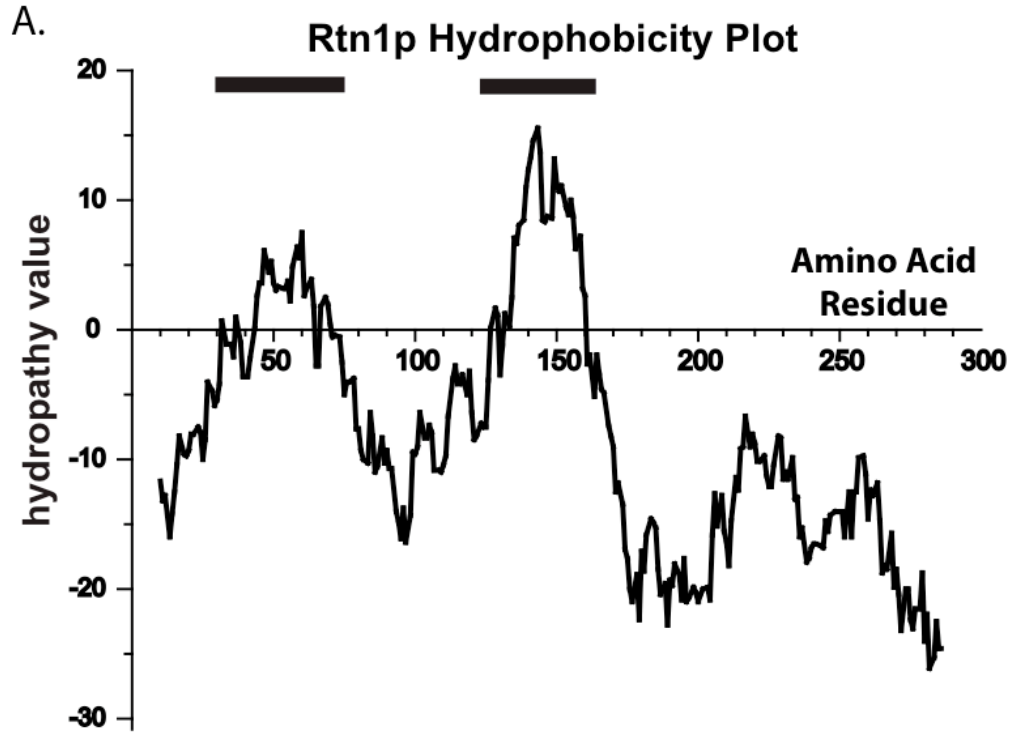
A.
Rtn1p Hydrophobicity Plot
hydropathy value
Amino Acid Residue
20
10
0
-10
-20
-30
50
100
150
200
250
300

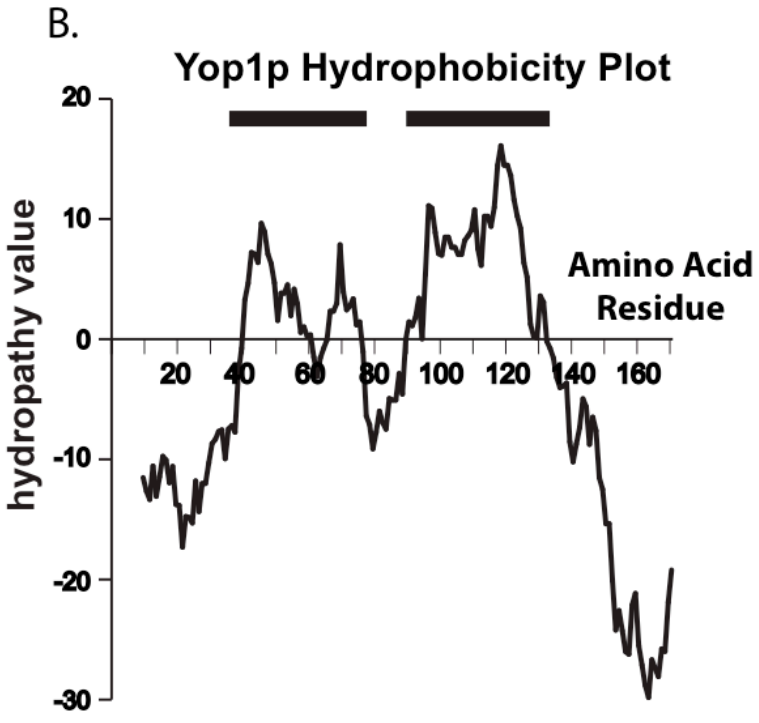
B.
Yop1p Hydrophobicity Plot
hydropathy value
Amino Acid Residue
20
10
0
-10
-20
-30
20
40
60
80
100
120
140
160

Figure 1.5 Continued

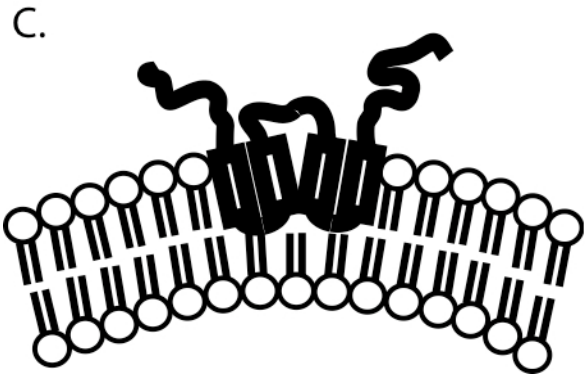

OVERVIEW

The purpose of this thesis is to investigate the mechanism of action of Yop1p and Rtn1p in their function in generating the highly curved tubules of the peripheral ER.

In chapter 2, I investigate the mechanism of Yop1p action on membranes to generate the tubules of the peripheral ER. To accomplish this goal I utilized a mutational approach to dissect the domains of Yop1p that are critical for its ability to generate peripheral ER tubules. I have identified the two long hydrophobic domains of Yop1p to be necessary and sufficient to function in membrane tubule formation. Furthermore, my work suggests a minimal linker length requirement between the two hydrophobic domains of Yop1p for the generation of membrane tubules as well as a role for the length of the individual hydrophobic domains for this process. Additionally, I have identified two putative membrane-embedded residues, both highly charged, that appear to be critical for Yop1p function. The studies in chapter 2 deepen our understanding of the model for Yop1p action on membranes.

In chapter 3, I investigate the morphology of tubular structures formed by the overexpression of Yop1p. I determined that Rtn1p is not necessary for the formation of Yop1p tubules. Furthermore, I developed an enrichment process to isolate the tubules formed by Yop1p overexpression and analyzed the morphology of these tubular structures by electron microscopy. The tubular structures were found to have a very narrow diameter when compared to the diameter of the peripheral ER tubules. Analysis of the tubular structures formed by Yop1p overexpression deepens our understanding of the types of membrane alterations Yop1p is capable of forming in vivo and suggests a mechanism may exist to modulate the membrane-bending activity of Yop1p for the formation of the larger diameter tubules of the peripheral ER.

I investigate the ability of Rtn1p to function in the generation of peripheral ER tubules in chapter 4. Rtn1p is palmitoylated at 4 cysteine residues, all located in close proximity to the two hydrophobic domains of Rtn1p. I found that the palmitoylation of Rtn1p is not necessary for Rtn1p to form a tubular peripheral ER or for the formation of the junction points between these tubules. Furthermore, I have found that the palmitoylation of Rtn1p may play a role in the normal localization of this protein. Chapter 4 identifies a potential role for the palmitoylation of Rtn1p and provides evidence that this modification is not strictly required for the generation of membrane tubules by Rtn1p.

Additionally, in the appendix chapter I investigate the function of a SARS-CoV protein, ORF6, using yeast as a model. I found that ORF6 localizes to ER membranes and upon overexpression induces the formation of vesicular structures from the membranes of the ER. Through mutational analysis, I identified the single long hydrophobic domain of ORF6 to be sufficient for ER localization as well as for the formation of the vesicular structures. This chapter elucidates a potential role for ORF6 in the formation of viral replication sites, either directly or through recruitment of host factors, and provides a platform for further studies aimed at investigating the mechanism of ORF6 action on membranes to form the viral replication sites.

REFERENCES

1. Bonifacino, J.S. and B.S. Glick, *The mechanisms of vesicle budding and fusion*. Cell, 2004. **116**(2): p. 153-66.
2. McMahon, H.T. and I.G. Mills, *COP and clathrin-coated vesicle budding: different pathways, common approaches*. Curr Opin Cell Biol, 2004. **16**(4): p. 379-91.
3. Tang, B.L., et al., *COPII and exit from the endoplasmic reticulum*. Biochim Biophys Acta, 2005. **1744**(3): p. 293-303.
4. Rothman, J.E., *The protein machinery of vesicle budding and fusion*. Protein Sci, 1996. **5**(2): p. 185-94.
5. Edeling, M.A., C. Smith, and D. Owen, *Life of a clathrin coat: insights from clathrin and AP structures*. Nat Rev Mol Cell Biol, 2006. **7**(1): p. 32-44.
6. Dell'Angelica, E.C., et al., *AP-3: an adaptor-like protein complex with ubiquitous expression*. EMBO J, 1997. **16**(5): p. 917-28.
7. Dell'Angelica, E.C., C. Mullins, and J.S. Bonifacino, *AP-4, a novel protein complex related to clathrin adaptors*. J Biol Chem, 1999. **274**(11): p. 7278-85.
8. Dell'Angelica, E.C., et al., *Association of the AP-3 adaptor complex with clathrin*. Science, 1998. **280**(5362): p. 431-4.
9. Pearse, B.M. and M.S. Robinson, *Clathrin, adaptors, and sorting*. Annu Rev Cell Biol, 1990. **6**: p. 151-71.
10. Pearse, B.M. and M.S. Robinson, *Purification and properties of 100-kd proteins from coated vesicles and their reconstitution with clathrin*. EMBO J, 1984. **3**(9): p. 1951-7.

11. Reilly, B.A., et al., *Golgi-to-endoplasmic reticulum (ER) retrograde traffic in yeast requires Dsl1p, a component of the ER target site that interacts with a COPI coat subunit*. Mol Biol Cell, 2001. **12**(12): p. 3783-96.
12. DeRegis, C.J., et al., *Mutational analysis of betaCOP (Sec26p) identifies an appendage domain critical for function*. BMC Cell Biol, 2008. **9**: p. 3.
13. Hoffman, G.R., et al., *Conserved structural motifs in intracellular trafficking pathways: structure of the gammaCOP appendage domain*. Mol Cell, 2003. **12**(3): p. 615-25.
14. Waters, M.G., T. Serafini, and J.E. Rothman, *'Coatomer': a cytosolic protein complex containing subunits of non-clathrin-coated Golgi transport vesicles*. Nature, 1991. **349**(6306): p. 248-51.
15. Sato, K. and A. Nakano, *[COPII-dependent vesicle formation and protein sorting from endoplasmic reticulum]*. Tanpakushitsu Kakusan Koso, 2004. **49**(7 Suppl): p. 910-3.
16. Palmer, K.J. and D.J. Stephens, *Biogenesis of ER-to-Golgi transport carriers: complex roles of COPII in ER export*. Trends Cell Biol, 2004. **14**(2): p. 57-61.
17. Stagg, S.M., et al., *Structure of the Sec13/31 COPII coat cage*. Nature, 2006. **439**(7073): p. 234-8.
18. Barlowe, C. and R. Schekman, *SEC12 encodes a guanine-nucleotide-exchange factor essential for transport vesicle budding from the ER*. Nature, 1993. **365**(6444): p. 347-9.
19. Salama, N.R., J.S. Chuang, and R.W. Schekman, *Sec31 encodes an essential component of the COPII coat required for transport vesicle budding from the endoplasmic reticulum*. Mol Biol Cell, 1997. **8**(2): p. 205-17.

20. Barlowe, C., C. d'Enfert, and R. Schekman, *Purification and characterization of SAR1p, a small GTP-binding protein required for transport vesicle formation from the endoplasmic reticulum*. J Biol Chem, 1993. **268**(2): p. 873-9.

21. Barlowe, C., et al., *COPII: a membrane coat formed by Sec proteins that drive vesicle budding from the endoplasmic reticulum*. Cell, 1994. **77**(6): p. 895-907.

22. Salama, N.R., T. Yeung, and R.W. Schekman, *The Sec13p complex and reconstitution of vesicle budding from the ER with purified cytosolic proteins*. EMBO J, 1993. **12**(11): p. 4073-82.

23. Pryer, N.K., et al., *Cytosolic Sec13p complex is required for vesicle formation from the endoplasmic reticulum in vitro*. J Cell Biol, 1993. **120**(4): p. 865-75.

24. Antonny, B., et al., *Self-assembly of minimal COPII cages*. EMBO Rep, 2003. **4**(4): p. 419-24.

25. Futai, E., et al., *GTP/GDP exchange by Sec12p enables COPII vesicle bud formation on synthetic liposomes*. EMBO J, 2004. **23**(21): p. 4146-55.

26. Huang, M., et al., *Crystal structure of Sar1-GDP at 1.7 A resolution and the role of the NH2 terminus in ER export*. J Cell Biol, 2001. **155**(6): p. 937-48.

27. Lee, M.C., et al., *Sar1p N-terminal helix initiates membrane curvature and completes the fission of a COPII vesicle*. Cell, 2005. **122**(4): p. 605-17.

28. Matsuoka, K., et al., *Surface structure of the COPII-coated vesicle*. Proc Natl Acad Sci U S A, 2001. **98**(24): p. 13705-9.

29. Matsuoka, K., et al., *COPII-coated vesicle formation reconstituted with purified coat proteins and chemically defined liposomes*. Cell, 1998. **93**(2): p. 263-75.

30. Bi, X., J.D. Mancias, and J. Goldberg, *Insights into COPII coat nucleation from the structure of Sec23.Sar1 complexed with the active fragment of Sec31*. Dev Cell, 2007. **13**(5): p. 635-45.

31. Fath, S., et al., *Structure and organization of coat proteins in the COPII cage*. Cell, 2007. **129**(7): p. 1325-36.

32. Bi, X., R.A. Corpina, and J. Goldberg, *Structure of the Sec23/24-Sar1 pre-budding complex of the COPII vesicle coat*. Nature, 2002. **419**(6904): p. 271-7.

33. Mancias, J.D. and J. Goldberg, *The transport signal on Sec22 for packaging into COPII-coated vesicles is a conformational epitope*. Mol Cell, 2007. **26**(3): p. 403-14.

34. Belden, W.J. and C. Barlowe, *Role of Erv29p in collecting soluble secretory proteins into ER-derived transport vesicles*. Science, 2001. **294**(5546): p. 1528-31.

35. Aridor, M., et al., *Cargo can modulate COPII vesicle formation from the endoplasmic reticulum*. J Biol Chem, 1999. **274**(7): p. 4389-99.

36. Budnik, A. and D.J. Stephens, *ER exit sites--localization and control of COPII vesicle formation*. FEBS Lett, 2009. **583**(23): p. 3796-803.

37. Muniz, M., et al., *The Emp24 complex recruits a specific cargo molecule into endoplasmic reticulum-derived vesicles*. J Cell Biol, 2000. **148**(5): p. 925-30.

38. Belden, W.J. and C. Barlowe, *Distinct roles for the cytoplasmic tail sequences of Emp24p and Erv25p in transport between the endoplasmic reticulum and Golgi complex*. J Biol Chem, 2001. **276**(46): p. 43040-8.

39. Belden, W.J. and C. Barlowe, *Erv25p, a component of COPII-coated vesicles, forms a complex with Emp24p that is required for efficient endoplasmic reticulum to Golgi transport*. J Biol Chem, 1996. **271**(43): p. 26939-46.

40. Appenzeller, C., et al., *The lectin ERGIC-53 is a cargo transport receptor for glycoproteins*. Nat Cell Biol, 1999. **1**(6): p. 330-4.

41. Miller, E.A., et al., *Multiple cargo binding sites on the COPII subunit Sec24p ensure capture of diverse membrane proteins into transport vesicles*. Cell, 2003. **114**(4): p. 497-509.

42. Miller, E., et al., *Cargo selection into COPII vesicles is driven by the Sec24p subunit*. EMBO J, 2002. **21**(22): p. 6105-13.

43. Dominguez, M., et al., *gp25L/emp24/p24 protein family members of the cis-Golgi network bind both COP I and II coatomer*. J Cell Biol, 1998. **140**(4): p. 751-65.

44. Jahn, R. and R.H. Scheller, *SNAREs--engines for membrane fusion*. Nat Rev Mol Cell Biol, 2006. **7**(9): p. 631-43.

45. Sztul, E. and V. Lupashin, *Role of vesicle tethering factors in the ER-Golgi membrane traffic*. FEBS Lett, 2009. **583**(23): p. 3770-83.

46. Sztul, E. and V. Lupashin, *Role of tethering factors in secretory membrane traffic*. Am J Physiol Cell Physiol, 2006. **290**(1): p. C11-26.

47. Cai, H., K. Reinisch, and S. Ferro-Novick, *Coats, tethers, Rabs, and SNAREs work together to mediate the intracellular destination of a transport vesicle*. Dev Cell, 2007. **12**(5): p. 671-82.

48. Collins, R.N., *Rab and ARF GTPase regulation of exocytosis*. Mol Membr Biol, 2003. **20**(2): p. 105-15.

49. Guo, W., et al., *The exocyst is an effector for Sec4p, targeting secretory vesicles to sites of exocytosis*. EMBO J, 1999. **18**(4): p. 1071-80.

50. Morozova, N., et al., *TRAPPII subunits are required for the specificity switch of a Ypt-Rab GEF*. Nat Cell Biol, 2006. **8**(11): p. 1263-9.

51. Wang, W., M. Sacher, and S. Ferro-Novick, *TRAPP stimulates guanine nucleotide exchange on Ypt1p*. J Cell Biol, 2000. **151**(2): p. 289-96.

52. Smith, R.D., et al., *The COG complex, Rab6 and COPI define a novel Golgi retrograde trafficking pathway that is exploited by SubAB toxin*. Traffic, 2009. **10**(10): p. 1502-17.

53. Smith, R.D. and V.V. Lupashin, *Role of the conserved oligomeric Golgi (COG) complex in protein glycosylation*. Carbohydr Res, 2008. **343**(12): p. 2024-31.

54. Sohda, M., et al., *The interaction of two tethering factors, p115 and COG complex, is required for Golgi integrity*. Traffic, 2007. **8**(3): p. 270-84.

55. Vasile, E., et al., *IntraGolgi distribution of the Conserved Oligomeric Golgi (COG) complex*. Exp Cell Res, 2006. **312**(16): p. 3132-41.

56. Ungar, D., et al., *Characterization of a mammalian Golgi-localized protein complex, COG, that is required for normal Golgi morphology and function*. J Cell Biol, 2002. **157**(3): p. 405-15.

57. Hickey, C.M. and W. Wickner, *HOPS initiates vacuole docking by tethering membranes before trans-SNARE complex assembly*. Mol Biol Cell, 2010. **21**(13): p. 2297-305.

58. Starai, V.J., C.M. Hickey, and W. Wickner, *HOPS proofreads the trans-SNARE complex for yeast vacuole fusion*. Mol Biol Cell, 2008. **19**(6): p. 2500-8.

59. Jena, B.P., *Assembly and disassembly of SNAREs in membrane fusion*. Methods Cell Biol, 2008. **90**: p. 157-82.

60. Scales, S.J., et al., *SNAREs contribute to the specificity of membrane fusion*. Neuron, 2000. **26**(2): p. 457-64.

61. Gerst, J.E., *SNAREs and SNARE regulators in membrane fusion and exocytosis*. Cell Mol Life Sci, 1999. **55**(5): p. 707-34.

62. Fasshauer, D., et al., *Conserved structural features of the synaptic fusion complex: SNARE proteins reclassified as Q- and R-SNAREs*. Proc Natl Acad Sci U S A, 1998. **95**(26): p. 15781-6.

63. Nichols, B.J., et al., *Homotypic vacuolar fusion mediated by t- and v-SNAREs*. Nature, 1997. **387**(6629): p. 199-202.

64. Palade, G.E., *The fine structure of mitochondria*. Anat Rec, 1952. **114**(3): p. 427-51.

65. Frey, T.G. and C.A. Mannella, *The internal structure of mitochondria*. Trends Biochem Sci, 2000. **25**(7): p. 319-24.

66. Mannella, C.A., et al., *The internal compartmentation of rat-liver mitochondria: tomographic study using the high-voltage transmission electron microscope*. Microsc Res Tech, 1994. **27**(4): p. 278-83.

67. Parsons, D.F., *Recent advances correlating structure and function in mitochondria*. Int Rev Exp Pathol, 1965. **4**: p. 1-54.

68. Mannella, C.A., *The relevance of mitochondrial membrane topology to mitochondrial function*. Biochim Biophys Acta, 2006. **1762**(2): p. 140-7.

69. Mannella, C.A., et al., *Topology of the mitochondrial inner membrane: dynamics and bioenergetic implications*. IUBMB Life, 2001. **52**(3-5): p. 93-100.

70. Hackenbrock, C.R., *Ultrastructural bases for metabolically linked mechanical activity in mitochondria. II. Electron transport-linked ultrastructural transformations in mitochondria*. J Cell Biol, 1968. **37**(2): p. 345-69.

71. Hackenbrock, C.R., *Ultrastructural bases for metabolically linked mechanical activity in mitochondria. I. Reversible ultrastructural changes with change in*

metabolic steady state in isolated liver mitochondria. J Cell Biol, 1966. **30**(2): p. 269-97.

72. Kirschner, R.H., M. Rusli, and T.E. Martin, *Characterization of the nuclear envelope, pore complexes, and dense lamina of mouse liver nuclei by high resolution scanning electron microscopy*. J Cell Biol, 1977. **72**(1): p. 118-32.
73. Terry, L.J. and S.R. Wente, *Nuclear mRNA export requires specific FG nucleoporins for translocation through the nuclear pore complex*. J Cell Biol, 2007. **178**(7): p. 1121-32.
74. Lang, I. and R. Peters, *Nuclear envelope permeability: a sensitive indicator of pore complex integrity*. Prog Clin Biol Res, 1984. **164**: p. 377-86.
75. Terry, L.J., E.B. Shows, and S.R. Wente, *Crossing the nuclear envelope: hierarchical regulation of nucleocytoplasmic transport*. Science, 2007. **318**(5855): p. 1412-6.
76. Fahrenkrog, B., J. Koser, and U. Aebi, *The nuclear pore complex: a jack of all trades?* Trends Biochem Sci, 2004. **29**(4): p. 175-82.
77. Schwartz, T.U., *Modularity within the architecture of the nuclear pore complex*. Curr Opin Struct Biol, 2005. **15**(2): p. 221-6.
78. Lim, R.Y. and B. Fahrenkrog, *The nuclear pore complex up close*. Curr Opin Cell Biol, 2006. **18**(3): p. 342-7.
79. Maco, B., et al., *Nuclear pore complex structure and plasticity revealed by electron and atomic force microscopy*. Methods Mol Biol, 2006. **322**: p. 273-88.
80. Fahrenkrog, B. and U. Aebi, *The vertebrate nuclear pore complex: from structure to function*. Results Probl Cell Differ, 2002. **35**: p. 25-48.
81. Miller, M., M.K. Park, and J.A. Hanover, *Nuclear pore complex: structure, function, and regulation*. Physiol Rev, 1991. **71**(3): p. 909-49.

82. Akey, C.W., *Probing the structure and function of the nuclear pore complex*. Semin Cell Biol, 1991. **2**(3): p. 167-77.

83. Starr, C.M. and J.A. Hanover, *Structure and function of the nuclear pore complex: new perspectives*. Bioessays, 1990. **12**(7): p. 323-30.

84. Alber, F., et al., *The molecular architecture of the nuclear pore complex*. Nature, 2007. **450**(7170): p. 695-701.

85. Webster, M., K.L. Witkin, and O. Cohen-Fix, *Sizing up the nucleus: nuclear shape, size and nuclear-envelope assembly*. J Cell Sci, 2009. **122**(Pt 10): p. 1477-86.

86. Antonin, W., J. Ellenberg, and E. Dultz, *Nuclear pore complex assembly through the cell cycle: regulation and membrane organization*. FEBS Lett, 2008. **582**(14): p. 2004-16.

87. Maul, G.G., J.W. Price, and M.W. Lieberman, *Formation and distribution of nuclear pore complexes in interphase*. J Cell Biol, 1971. **51**(21): p. 405-18.

88. Dawson, T.R., et al., *ER membrane-bending proteins are necessary for de novo nuclear pore formation*. J Cell Biol, 2009. **184**(5): p. 659-75.

89. De Craene, J.O., et al., *Rtn1p is involved in structuring the cortical endoplasmic reticulum*. Mol Biol Cell, 2006. **17**(7): p. 3009-20.

90. Voeltz, G.K., et al., *A class of membrane proteins shaping the tubular endoplasmic reticulum*. Cell, 2006. **124**(3): p. 573-86.

91. Kiseleva, E., et al., *Reticulon 4a/NogoA locates to regions of high membrane curvature and may have a role in nuclear envelope growth*. J Struct Biol, 2007. **160**(2): p. 224-35.

92. Antonin, W., *Nuclear envelope: membrane bending for pore formation?* Curr Biol, 2009. **19**(10): p. R410-2.

93. Mogelsvang, S., et al., *Predicting function from structure: 3D structure studies of the mammalian Golgi complex*. Traffic, 2004. **5**(5): p. 338-45.

94. James Morre, D. and H.H. Mollenhauer, *Microscopic morphology and the origins of the membrane maturation model of Golgi apparatus function*. Int Rev Cytol, 2007. **262**: p. 191-218.

95. Rambourg, A. and Y. Clermont, *Three-dimensional electron microscopy: structure of the Golgi apparatus*. Eur J Cell Biol, 1990. **51**(2): p. 189-200.

96. Dean, N., *Asparagine-linked glycosylation in the yeast Golgi*. Biochim Biophys Acta, 1999. **1426**(2): p. 309-22.

97. Helenius, A. and M. Aebi, *Intracellular functions of N-linked glycans*. Science, 2001. **291**(5512): p. 2364-9.

98. Lowe, J.B. and J.D. Marth, *A genetic approach to Mammalian glycan function*. Annu Rev Biochem, 2003. **72**: p. 643-91.

99. Opat, A.S., C. van Vliet, and P.A. Gleeson, *Trafficking and localisation of resident Golgi glycosylation enzymes*. Biochimie, 2001. **83**(8): p. 763-73.

100. Matsuda, K., et al., *N-linked glycosylation sites of the motor protein prestin: effects on membrane targeting and electrophysiological function*. J Neurochem, 2004. **89**(4): p. 928-38.

101. O'Connor, S.E. and B. Imperiali, *Modulation of protein structure and function by asparagine-linked glycosylation*. Chem Biol, 1996. **3**(10): p. 803-12.

102. Hounsell, E.F., M.J. Davies, and D.V. Renouf, *O-linked protein glycosylation structure and function*. Glycoconj J, 1996. **13**(1): p. 19-26.

103. Gentzsch, M., T. Immervoll, and W. Tanner, *Protein O-glycosylation in Saccharomyces cerevisiae: the protein O-mannosyltransferases Pmt1p and Pmt2p function as heterodimer*. FEBS Lett, 1995. **377**(2): p. 128-30.

104. Welply, J.K., *Protein glycosylation: function and factors that regulate oligosaccharide structure*. Biotechnology, 1991. **17**: p. 59-72.

105. Farquhar, M.G. and G.E. Palade, *The Golgi apparatus (complex)-(1954-1981)-from artifact to center stage*. J Cell Biol, 1981. **91**(3 Pt 2): p. 77s-103s.

106. Kweon, H.S., et al., *Golgi enzymes are enriched in perforated zones of golgi cisternae but are depleted in COPI vesicles*. Mol Biol Cell, 2004. **15**(10): p. 4710-24.

107. Martinez-Menarguez, J.A., et al., *Peri-Golgi vesicles contain retrograde but not anterograde proteins consistent with the cisternal progression model of intra-Golgi transport*. J Cell Biol, 2001. **155**(7): p. 1213-24.

108. Brown, W.J., K. Chambers, and A. Doody, *Phospholipase A2 (PLA2) enzymes in membrane trafficking: mediators of membrane shape and function*. Traffic, 2003. **4**(4): p. 214-21.

109. Polizotto, R.S., P. de Figueiredo, and W.J. Brown, *Stimulation of Golgi membrane tubulation and retrograde trafficking to the ER by phospholipase A(2) activating protein (PLAP) peptide*. J Cell Biochem, 1999. **74**(4): p. 670-83.

110. Chan, D., et al., *Inhibition of membrane tubule formation and trafficking by isotetrandrine, an antagonist of G-protein-regulated phospholipase A2 enzymes*. Mol Biol Cell, 2004. **15**(4): p. 1871-80.

111. Vidugiriene, J. and A.K. Menon, *Early lipid intermediates in glycosyl-phosphatidylinositol anchor assembly are synthesized in the ER and located in the cytoplasmic leaflet of the ER membrane bilayer*. J Cell Biol, 1993. **121**(5): p. 987-96.

112. Dennis, E.A. and E.P. Kennedy, *Intracellular sites of lipid synthesis and the biogenesis of mitochondria*. J Lipid Res, 1972. **13**(2): p. 263-7.

113. Kleizen, B. and I. Braakman, *Protein folding and quality control in the endoplasmic reticulum*. Curr Opin Cell Biol, 2004. **16**(4): p. 343-9.

114. Ellgaard, L. and A. Helenius, *Quality control in the endoplasmic reticulum*. Nat Rev Mol Cell Biol, 2003. **4**(3): p. 181-91.

115. Verkhratsky, A., *The endoplasmic reticulum and neuronal calcium signalling*. Cell Calcium, 2002. **32**(5-6): p. 393-404.

116. Estrada de Martin, P., P. Novick, and S. Ferro-Novick, *The organization, structure, and inheritance of the ER in higher and lower eukaryotes*. Biochem Cell Biol, 2005. **83**(6): p. 752-61.

117. Vedrenne, C. and H.P. Hauri, *Morphogenesis of the endoplasmic reticulum: beyond active membrane expansion*. Traffic, 2006. **7**(6): p. 639-46.

118. Palade, G.E., *The endoplasmic reticulum*. J Biophys Biochem Cytol, 1956. **2**(4 Suppl): p. 85-98.

119. Voeltz, G.K., M.M. Rolls, and T.A. Rapoport, *Structural organization of the endoplasmic reticulum*. EMBO Rep, 2002. **3**(10): p. 944-50.

120. Bevis, B.J., et al., *De novo formation of transitional ER sites and Golgi structures in Pichia pastoris*. Nat Cell Biol, 2002. **4**(10): p. 750-6.

121. Hammond, A.T. and B.S. Glick, *Dynamics of transitional endoplasmic reticulum sites in vertebrate cells*. Mol Biol Cell, 2000. **11**(9): p. 3013-30.

122. Terasaki, M., *Recent progress on structural interactions of the endoplasmic reticulum*. Cell Motil Cytoskeleton, 1990. **15**(2): p. 71-5.

123. Prinz, W.A., et al., *Mutants affecting the structure of the cortical endoplasmic reticulum in Saccharomyces cerevisiae*. J Cell Biol, 2000. **150**(3): p. 461-74.

124. Lee, C. and L.B. Chen, *Dynamic behavior of endoplasmic reticulum in living cells*. Cell, 1988. **54**(1): p. 37-46.

125. Estrada, P., et al., *Myo4p and She3p are required for cortical ER inheritance in Saccharomyces cerevisiae*. J Cell Biol, 2003. **163**(6): p. 1255-66.

126. Fehrenbacher, K.L., et al., *Endoplasmic reticulum dynamics, inheritance, and cytoskeletal interactions in budding yeast*. Mol Biol Cell, 2002. **13**(3): p. 854-65.

127. TerBush, D.R., et al., *The Exocyst is a multiprotein complex required for exocytosis in Saccharomyces cerevisiae*. EMBO J, 1996. **15**(23): p. 6483-94.

128. Du, Y., et al., *Aux1p/Swa2p is required for cortical endoplasmic reticulum inheritance in Saccharomyces cerevisiae*. Mol Biol Cell, 2001. **12**(9): p. 2614-28.

129. Waterman-Storer, C.M. and E.D. Salmon, *Endoplasmic reticulum membrane tubules are distributed by microtubules in living cells using three distinct mechanisms*. Curr Biol, 1998. **8**(14): p. 798-806.

130. Terasaki, M., L.B. Chen, and K. Fujiwara, *Microtubules and the endoplasmic reticulum are highly interdependent structures*. J Cell Biol, 1986. **103**(4): p. 1557-68.

131. Liebe, S. and D. Menzel, *Actomyosin-based motility of endoplasmic reticulum and chloroplasts in Vallisneria mesophyll cells*. Biol Cell, 1995. **85**(2-3): p. 207-22.

132. McMahon, H.T. and J.L. Gallop, *Membrane curvature and mechanisms of dynamic cell membrane remodelling*. Nature, 2005. **438**(7068): p. 590-6.

133. Farsad, K. and P. De Camilli, *Mechanisms of membrane deformation*. Curr Opin Cell Biol, 2003. **15**(4): p. 372-81.

134. Kooijman, E.E., et al., *Spontaneous curvature of phosphatidic acid and lysophosphatidic acid*. Biochemistry, 2005. **44**(6): p. 2097-102.

135. Farge, E. and P.F. Devaux, *Shape changes of giant liposomes induced by an*

asymmetric transmembrane distribution of phospholipids. Biophys J, 1992. **61**(2): p. 347-57.

136. Smith, R.J. and C. Green, *The rate of cholesterol 'flip-flop' in lipid bilayers and its relation to membrane sterol pools*. FEBS Lett, 1974. **42**(1): p. 108-11.

137. Anglin, T.C., et al., *Free energy and entropy of activation for phospholipid flip-flop in planar supported lipid bilayers*. J Phys Chem B, 2010. **114**(5): p. 1903-14.

138. Contreras, F.X., et al., *Transbilayer (flip-flop) lipid motion and lipid scrambling in membranes*. FEBS Lett, 2010. **584**(9): p. 1779-86.

139. Ramachandran, S., P.B. Kumar, and M. Laradji, *Lipid flip-flop driven mechanical and morphological changes in model membranes*. J Chem Phys, 2008. **129**(12): p. 125104.

140. Gurtovenko, A.A. and I. Vattulainen, *Molecular mechanism for lipid flip-flops*. J Phys Chem B, 2007. **111**(48): p. 13554-9.

141. Winschel, C.A., et al., *New noninvasive methodology for real-time monitoring of lipid flip*. Bioconjug Chem, 2007. **18**(5): p. 1507-15.

142. Anzai, K., *[Sidedness of biomembrane: asymmetrical distribution and flip-flop of phospholipids across lipid bilayer]*. Tanpakushitsu Kakusan Koso, 1995. **40**(16): p. 2418-26.

143. Graham, T.R., *Flippases and vesicle-mediated protein transport*. Trends Cell Biol, 2004. **14**(12): p. 670-7.

144. Farge, E., et al., *Enhancement of endocytosis due to aminophospholipid transport across the plasma membrane of living cells*. Am J Physiol, 1999. **276**(3 Pt 1): p. C725-33.

145. Hua, Z. and T.R. Graham, *Requirement for neo1p in retrograde transport from the Golgi complex to the endoplasmic reticulum*. Mol Biol Cell, 2003. **14**(12): p. 4971-83.

146. de Figueiredo, P., et al., *Inhibition of transferrin recycling and endosome tubulation by phospholipase A2 antagonists*. J Biol Chem, 2001. **276**(50): p. 47361-70.

147. de Figueiredo, P., et al., *Evidence that phospholipase A2 activity is required for Golgi complex and trans Golgi network membrane tubulation*. Proc Natl Acad Sci U S A, 1998. **95**(15): p. 8642-7.

148. de Figueiredo, P., et al., *Membrane tubule-mediated reassembly and maintenance of the Golgi complex is disrupted by phospholipase A2 antagonists*. Mol Biol Cell, 1999. **10**(6): p. 1763-82.

149. Burger, K.N., *Greasing membrane fusion and fission machineries*. Traffic, 2000. **1**(8): p. 605-13.

150. Huijbregts, R.P., L. Topalof, and V.A. Bankaitis, *Lipid metabolism and regulation of membrane trafficking*. Traffic, 2000. **1**(3): p. 195-202.

151. Huttner, W.B. and A.A. Schmidt, *Membrane curvature: a case of endofeelin'*. Trends Cell Biol, 2002. **12**(4): p. 155-8.

152. Musacchio, A., et al., *Functional organization of clathrin in coats: combining electron cryomicroscopy and X-ray crystallography*. Mol Cell, 1999. **3**(6): p. 761-70.

153. Peter, B.J., et al., *BAR domains as sensors of membrane curvature: the amphiphysin BAR structure*. Science, 2004. **303**(5657): p. 495-9.

154. Zimmerberg, J. and S. McLaughlin, *Membrane curvature: how BAR domains bend bilayers*. Curr Biol, 2004. **14**(6): p. R250-2.

155. Farsad, K., et al., *Generation of high curvature membranes mediated by direct endophilin bilayer interactions*. J Cell Biol, 2001. **155**(2): p. 193-200.

156. Ford, M.G., et al., *Curvature of clathrin-coated pits driven by epsin*. Nature, 2002. **419**(6905): p. 361-6.

157. Schmid, E.M. and H.T. McMahon, *Integrating molecular and network biology to decode endocytosis*. Nature, 2007. **448**(7156): p. 883-8.

158. Traub, L.M., *Tickets to ride: selecting cargo for clathrin-regulated internalization*. Nat Rev Mol Cell Biol, 2009. **10**(9): p. 583-96.

159. Takei, K., et al., *Functional partnership between amphiphysin and dynamin in clathrin-mediated endocytosis*. Nat Cell Biol, 1999. **1**(1): p. 33-9.

160. Gallop, J.L., et al., *Mechanism of endophilin N-BAR domain-mediated membrane curvature*. EMBO J, 2006. **25**(12): p. 2898-910.

161. Masuda, M., et al., *Endophilin BAR domain drives membrane curvature by two newly identified structure-based mechanisms*. EMBO J, 2006. **25**(12): p. 2889-97.

162. Pylypenko, O., et al., *The PX-BAR membrane-remodeling unit of sorting nexin 9*. EMBO J, 2007. **26**(22): p. 4788-800.

163. Glenney, J.R., Jr. and D. Soppet, *Sequence and expression of caveolin, a protein component of caveolae plasma membrane domains phosphorylated on tyrosine in Rous sarcoma virus-transformed fibroblasts*. Proc Natl Acad Sci U S A, 1992. **89**(21): p. 10517-21.

164. Schlegel, A. and M.P. Lisanti, *A molecular dissection of caveolin-1 membrane attachment and oligomerization. Two separate regions of the caveolin-1 C-terminal domain mediate membrane binding and oligomer/oligomer interactions in vivo*. J Biol Chem, 2000. **275**(28): p. 21605-17.

165. Schlegel, A., et al., *A role for the caveolin scaffolding domain in mediating the*

membrane attachment of caveolin-1. The caveolin scaffolding domain is both necessary and sufficient for membrane binding in vitro. J Biol Chem, 1999. **274**(32): p. 22660-7.

166. Das, K., et al., *The membrane-spanning domains of caveolins-1 and -2 mediate the formation of caveolin hetero-oligomers. Implications for the assembly of caveolae membranes in vivo*. J Biol Chem, 1999. **274**(26): p. 18721-8.

167. Westermann, M., H. Leutbecher, and H.W. Meyer, *Membrane structure of caveolae and isolated caveolin-rich vesicles*. Histochem Cell Biol, 1999. **111**(1): p. 71-81.

168. Sargiacomo, M., et al., *Oligomeric structure of caveolin: implications for caveolae membrane organization*. Proc Natl Acad Sci U S A, 1995. **92**(20): p. 9407-11.

169. Monier, S., et al., *VIP21-caveolin, a membrane protein constituent of the caveolar coat, oligomerizes in vivo and in vitro*. Mol Biol Cell, 1995. **6**(7): p. 911-27.

170. Sonnino, S. and A. Prinetti, *Sphingolipids and membrane environments for caveolin*. FEBS Lett, 2009. **583**(4): p. 597-606.

171. Le Lan, C., J.M. Neumann, and N. Jamin, *Role of the membrane interface on the conformation of the caveolin scaffolding domain: a CD and NMR study*. FEBS Lett, 2006. **580**(22): p. 5301-5.

172. Graziani, A., et al., *Cholesterol- and caveolin-rich membrane domains are essential for phospholipase A2-dependent EDHF formation*. Cardiovasc Res, 2004. **64**(2): p. 234-42.

173. Daniel, E.E., et al., *Changes in membrane cholesterol affect caveolin-1 localization and ICC-pacing in mouse jejunum*. Am J Physiol Gastrointest Liver Physiol, 2004. **287**(1): p. G202-10.

174. Evans, W.E.t., et al., *Characterization of membrane rafts isolated from rat sertoli cell cultures: caveolin and flotillin-1 content*. J Androl, 2003. **24**(6): p. 812-21.

175. Travis, A.J., et al., *Expression and localization of caveolin-1, and the presence of membrane rafts, in mouse and Guinea pig spermatozoa*. Dev Biol, 2001. **240**(2): p. 599-610.

176. Parton, R.G., M. Hanzal-Bayer, and J.F. Hancock, *Biogenesis of caveolae: a structural model for caveolin-induced domain formation*. J Cell Sci, 2006. **119**(Pt 5): p. 787-96.

177. Bastiani, M., et al., *MURC/Cavin-4 and cavin family members form tissue-specific caveolar complexes*. J Cell Biol, 2009. **185**(7): p. 1259-73.

178. Hill, M.M., et al., *PTRF-Cavin, a conserved cytoplasmic protein required for caveola formation and function*. Cell, 2008. **132**(1): p. 113-24.

179. Hansen, C.G., et al., *SDPR induces membrane curvature and functions in the formation of caveolae*. Nat Cell Biol, 2009. **11**(7): p. 807-14.

180. McMahon, K.A., et al., *SRBC/cavin-3 is a caveolin adapter protein that regulates caveolae function*. EMBO J, 2009. **28**(8): p. 1001-15.

181. Shibata, Y., et al., *The reticulon and DP1/Yop1p proteins form immobile oligomers in the tubular endoplasmic reticulum*. J Biol Chem, 2008. **283**(27): p. 18892-904.

182. Hu, J., et al., *A class of dynamin-like GTPases involved in the generation of the tubular ER network*. Cell, 2009. **138**(3): p. 549-61.

183. Hu, J., et al., *Membrane proteins of the endoplasmic reticulum induce high-curvature tubules*. Science, 2008. **319**(5867): p. 1247-50.

184. Oertle, T., et al., *A reticular rhapsody: phylogenic evolution and nomenclature of the RTN/Nogo gene family*. FASEB J, 2003. **17**(10): p. 1238-47.

185. Wakefield, S. and G. Tear, *The Drosophila reticulon, Rtnl-1, has multiple differentially expressed isoforms that are associated with a sub-compartment of the endoplasmic reticulum*. Cell Mol Life Sci, 2006. **63**(17): p. 2027-38.

186. Nziengui, H., et al., *Reticulon-like proteins in Arabidopsis thaliana: structural organization and ER localization*. FEBS Lett, 2007. **581**(18): p. 3356-62.

187. Sparkes, I., et al., *Five Arabidopsis reticulon isoforms share endoplasmic reticulum location, topology, and membrane-shaping properties*. Plant Cell, 2010. **22**(4): p. 1333-43.

188. Tolley, N., et al., *Overexpression of a plant reticulon remodels the lumen of the cortical endoplasmic reticulum but does not perturb protein transport*. Traffic, 2008. **9**(1): p. 94-102.

189. He, W., et al., *Reticulon family members modulate BACE1 activity and amyloid-beta peptide generation*. Nat Med, 2004. **10**(9): p. 959-65.

190. Castermans, D., et al., *Identification and characterization of the TRIP8 and REEP3 genes on chromosome 10q21.3 as novel candidate genes for autism*. Eur J Hum Genet, 2007. **15**(4): p. 422-31.

191. Hu, X., et al., *Transgenic mice overexpressing reticulon 3 develop neuritic abnormalities*. EMBO J, 2007. **26**(11): p. 2755-67.

192. Wildasin, K., *Role of reticulon proteins in Alzheimer's disease*. Lancet Neurol, 2004. **3**(10): p. 576.

193. Buss, A., et al., *Expression pattern of NOGO-A protein in the human nervous system*. Acta Neuropathol, 2005. **110**(2): p. 113-9.

194. Yan, R., et al., *Reticulon proteins: emerging players in neurodegenerative diseases*. Cell Mol Life Sci, 2006. **63**(7-8): p. 877-89.

195. Shen, Q., et al., *The stress- and abscisic acid-induced barley gene HVA22: developmental regulation and homologues in diverse organisms*. Plant Mol Biol, 2001. **45**(3): p. 327-40.

196. Chen, C.N., et al., *AtHVA22 gene family in Arabidopsis: phylogenetic relationship, ABA and stress regulation, and tissue-specific expression*. Plant Mol Biol, 2002. **49**(6): p. 633-44.

197. Geng, J., et al., *Saccharomyces cerevisiae Rab-GDI displacement factor ortholog Yip3p forms distinct complexes with the Ypt1 Rab GTPase and the reticulon Rtn1p*. Eukaryot Cell, 2005. **4**(7): p. 1166-74.

198. Calero, M., G.R. Whittaker, and R.N. Collins, *Yop1p, the yeast homolog of the polyposis locus protein 1, interacts with Yip1p and negatively regulates cell growth*. J Biol Chem, 2001. **276**(15): p. 12100-12.

199. Chen, C.Z. and R.N. Collins, *Insights into biological functions across species: examining the role of Rab proteins in YIP1 family function*. Biochem Soc Trans, 2005. **33**(Pt 4): p. 614-8.

200. Chen, C.Z., et al., *Genetic analysis of yeast Yip1p function reveals a requirement for Golgi-localized rab proteins and rab-Guanine nucleotide dissociation inhibitor*. Genetics, 2004. **168**(4): p. 1827-41.

201. Calero, M. and R.N. Collins, *Saccharomyces cerevisiae Pra1p/Yip3p interacts with Yip1p and Rab proteins*. Biochem Biophys Res Commun, 2002. **290**(2): p. 676-81.

202. Heidtman, M., et al., *A role for Yip1p in COPII vesicle biogenesis*. J Cell Biol, 2003. **163**(1): p. 57-69.

203. Heidtman, M., et al., *Yos1p is a novel subunit of the Yip1p-Yif1p complex and is required for transport between the endoplasmic reticulum and the Golgi complex*. Mol Biol Cell, 2005. **16**(4): p. 1673-83.

204. Fariselli, P., et al., *MaxSubSeq: an algorithm for segment-length optimization. The case study of the transmembrane spanning segments*. Bioinformatics, 2003. **19**(4): p. 500-5.

CHAPTER 2

Mutational analysis of Yop1p reveals a minimal linker requirement for the generation of a tubular ER morphology

ABSTRACT

A role for Yop1p in the generation of the tubules of the peripheral ER has recently been proposed, though Yop1p likely functions redundantly with Rtn1p in this role. Deletion of Yop1p alone has no apparent phenotype, but *rtn1Δyop1Δ* cells contain sheet-like peripheral ER structures in place of the normally tubular network. A model has emerged for the action of Yop1p on membranes based on the presence of the two long hydrophobic regions of Yop1p, both predicted to be membrane embedded. It is thought that these hydrophobic domains are inserted into the membrane but do not penetrate the opposite face, giving Yop1p a "wedge-like" shape within the membrane that drives membrane deformation. Here I provide experimental evidence that Yop1p generates membrane curvature through a wedging mechanism and begin to elucidate the details that govern its ability to form the tubules of the peripheral ER.

INTRODUCTION

A role for Yop1p in generating the tubules of the peripheral ER has been suggested by previous studies, in combination with a related protein, Rtn1p [1-4]. Rtn1p adopts a similar topology within the membrane, contains a similar domain organization and is thought to provide a redundant function in tubule formation through a similar mechanism of action as Yop1p [1]. Deletion of either *YOP1* or *RTN1* alone in cells is known to have no effect on the morphology of the peripheral ER, however deletion of both results in a dramatic conversion of much of the normal tubular peripheral ER into largely sheet-like structures. Although the *rtn1Δyop1Δ* cells have large areas of membrane sheets in their peripheral ER, some area of membrane tubules can still be seen, suggesting there may be other factors that contribute to the formation of peripheral ER tubules besides Rtn1p and Yop1p. Yeast contain two reticulon homologs, Rtn1p and Rtn2p. Rtn1p is the predominantly expressed form, but Rtn2p expression can be induced under stressed conditions [5]. *Rtn1Δrtn2Δyop1Δ* cells contain a similar ER morphology defect as the *rtn1Δyop1Δ* cells with large peripheral ER sheets, but also some areas of tubules still present. The altered ER morphology in the *rtn1Δrtn2Δyop1Δ* cells can be reversed by the expression of genomic *YOP1* as well as COOH terminally tagged *YOP1-GFP* [1, 2]. The mechanism used by Yop1p in generating the tubules of the peripheral ER has been suggested based on the presence of two unique hydrophobic domains, each ~40 amino acids in length [1]. The length of these hydrophobic domains is considerably longer than a typical transmembrane spanning domain [6, 7], suggesting perhaps a more complex structuring of these regions of Yop1p within the membrane.

Further evidence that Yop1p is a player in the formation of the tubules of the peripheral ER comes from the fact that overexpression of Yop1p results in the formation of long, unbranched tubular structures within the cell (investigated further

in Chapter 3) [1, 4]. These tubules form from ER membranes and most likely contain a contiguous lumen, although luminal proteins appear to be excluded from the tubules due to their extremely small diameter [4, 8]. Additionally, studies have shown that purified Yop1p has the ability to generate small membrane tubules from lipids in vitro [4].

Yop1p forms oligomeric complexes with many other proteins, for example Rtn1p, Yip1p, Sey1p and itself [1-3, 9]. Previous studies have implicated Yop1p homo-oligomerization to be critical for its ability to function in generating membrane tubules. Relatively immobile oligomeric complexes of 6-7 Yop1p monomers were identified through crosslinking experiments and the authors suggested that these small "arcs" of oligomerized Yop1p, distributed randomly along the tubule length, could maintain the tubule structure without further organization [2].

Yop1p was identified as a Yip1p interacting partner (Yip One Partner) [9]. Yip1p is an integral membrane protein thought to function in COPII vesicle biogenesis [10-12]. It is possible that interactions between Yop1p and Yip1p are necessary for ER tubule formation. YIP family proteins also bind to Rab proteins [10, 12-15], perhaps providing a level of regulation for YIP family proteins and Yop1p in generating curved ER membranes. YIP family proteins contain extensive, conserved COOH terminal hydrophobic regions, and work in our lab has demonstrated that interactions between Rabs and YIP1 family members are critical for their ability to function [10, 12, 14, 15]. Perhaps the binding of a Rab to a YIP1 protein transmits a signal to Yop1p, regulating the formation of tubular ER structures.

Yop1p contains two long hydrophobic regions ~40 amino acids in length, separated by a 9 amino acid hydrophilic linker region (see Figure 1.4). Hydrophobicity prediction software identifies these two long regions as extremely hydrophobic and likely membrane embedded (MpeX Hydrophobicity Predictor, see Figure 1.5).

Previous results have determined that the NH_2 and COOH termini of Yop1p are located on the cytoplasmic face of the ER membrane, as well as the linker region between the two hydrophobic domains [1]. These results suggest that the hydrophobic domains are inserted into the membrane part way and adopt a hairpin structure within the bilayer. The insertion of these hairpins only part way through the membrane is thought to result in an expansion of the outer leaflet of the bilayer, creating a localized area of membrane curvature. The aggregation of many Yop1p proteins together could drive the deformation of the membrane into membrane tubules [1, 2].

This study aims to investigate the molecular mechanism Yop1p utilizes to form the tubules of the peripheral ER. I employ a mutational analysis of the different domains of *YOP1* to dissect the contribution each part of Yop1p provides to the formation of membrane tubules and to identify the function of each domain. I identify the minimal functional domains of Yop1p to be its two hydrophobic domains, while the hydrophilic regions of the protein appear to be dispensable. I also show the two hydrophobic domains must be at least 5-6 amino acids apart for proper function, deepening our understanding of the mechanism of Yop1p that generates the tubules of the peripheral ER.

MATERIALS AND METHODS

Yeast strains and plasmids used in this study

S. cerevisiae strains used in this study are listed in table 2.1. All manipulations of these yeast strains were conducted using standard biological methods. Cell density was determined using a Thermo Spectronic Genesys 10UV spectrophotometer (Rochester, NY) at 600 nm.

Table 2.1 *S. cerevisiae* strains used in this study

RCY Strain	Genotype	Source
RCY239	*MAT***a** *ura3-52 leu2-3,112*	This lab
RCY4164	*MAT***a**, *yop1ΔHIS5*, *ura3*Δ0, *leu2*Δ0, *his3*Δ0	This study
RCY4169	*MAT***a**, *yop1ΔHIS5*, *ura3*Δ0, *leu2*Δ0, *his3*Δ0	This study
RCY4168	*MAT*α, *rtn1ΔKAN*^{R} *yop1ΔHIS5 ura3Δ0 leu2Δ0 his3Δ0 lys2Δ0*	This study
RCY4323	*MAT***a** *rtn1*ΔKAN^{R} *rtn2*ΔKAN^{R} *yop1ΔHIS5*, *ura3Δ0*, *leu2Δ0*, *his3*Δ0, *lys2Δ0*, *met15*Δ0	This lab

Plasmids used in this study were created by standard biological methods and are listed in table 2.2. All mutant *YOP1* constructs were created by overlap PCR recombination using overlap sites within the ORF as needed for each *yop1* mutant.

Table 2.2 Plasmids used in this study

Plasmid number	Construct	Description	Source	Sequencing Number
pRC504	pRS316 *GFP-YOP1*		This lab	N/A, previously made
pRC2239	pRS316 *SEC13-RFP*		This lab	N/A
pRC3484	pRS316 *SEC63-GFP*		This lab	N/A
pRC3588	pRS315 *RFP-KDEL*		This lab	N/A
pRC3589	pRS316 *RFP-KDEL*		This lab	N/A
pRC3822	pRS315 *RFP-RTN1*		This lab	N/A
pRC3825	pRS426 *GFP-YOP1*		This study	10113880
pRC4436	pRS426 *YOP1-GFP*		This study	10156999
pRC4444	pRS316 *YOP1-GFP*		This study	10158255
pRC4523	pRS315 *GFP-YOP1ΔH1*	Δ39-79	This study	10174565

Table 2.2 Continued

pRC4524	pRS315 *GFP-YOP1ΔH2*	Δ90-130	This study	10174565
pRC4525	pRS315 *GFP-H1*	Amino acids 39-79	This study	10174565
pRC4526	pRS315 *GFP-H2*	Amino acids 90-130	This study	10174565
pRC4559	pRS315 *GFP-H1-H2*	Linker KTASAGSSA	This study	10178698
pRC4560	pRS316 *GFP-H1*	Amino acids 39-79	This study	10178698
pRC4562	pRS316 *YOP1*	Genomic *YOP1*	This study	10178698
pRC4573	pRS316 *GFP-YOP1ΔH1*	Δ39-79	This study	10183352
pRC4674	pRS315 *GFP-H2-H1*	Linker KTASAGSSA	This study	10201684
pRC4705	pRS315 *GFP-H1-H1*	Linker KTASAGSSA	This study	10204713
pRC4706	pRS315 *GFP-H2-H2*	Linker KTASAGSSA	This study	10204713
pRC4709	pRS315 *H1-H2-GFP*	Linker KTASAGSSA	This study	10205453
pRC4710	pRS315 *H2-H1-GFP*	Linker KTASAGSSA	This study	10205453
pRC4711	pRS315 *GFP-H1-7a-H2*	Linker KTSKTDE	This study	10205453
pRC4712	pRS315 *GFP-H1-16-H2*	Linker KTASASSKTDEKTSSGSSA	This study	10205453
pRC4713	pRS315 *GFP-H1-9-H2*	Linker KTSSKTDEK	This study	10205453
pRC4714	pRS315 *GFP-H1-2-H2*	Linker KT	This study	10205453
pRC4715	pRS315 *GFP-H1-KTG-H2*	Linker KTG	This study	10205453
pRC4716	pRS315 *GFP-H1-KTD-H2*	Linker KTD	This study	10205453
pRC4717	pRS315 *GFP-H1-8a-H2*	Linker KTSSKTDE	This study	10205453
pRC4777	pRS315 *YOP1-Hs1-GFP*	Shortened H1 (Δ55-67)	This study	10211866

Table 2.2 Continued

pRC4778	pRS315 *GFP-Hs1-H2*	Amino acids 39-54, 68-79-(linker KTASAGSSA) 90-130	This study	10211866
pRC4779	pRS315 *YOP1-Hs2-GFP*	Shortened H2 (Δ99-111)	This study	10213773
pRC4780	pRS315 *GFP-H1-Hs2*	Amino acids 39-79-(linker KTASAGSSA)-90-98, 112-130	This study	10213773
pRC4783	pRS315 *GFP-H1-6a-H2*	Linker KTASAG	This study	10211866
pRC4784	pRS315 *GFP-H1-6b-H2*	Linker KTGSSA	This study	10211866
pRC4786	pRS315 *GFP-H1-7b-H2*	Linker ASAGSSA	This study	10211866
pRC4787	pRS315 *GFP-H1-H2*[30]	Amino acids 39-79-(linker KTASAGSSA)-101-130	This study	10211866
pRC4788	pRS315 *H1-GFP-H2*	Linker GFP	This study	10211866
pRC4789	pRS315 *GFP-H1-8b-H2*	Linker KTASAGSS	This study	10211866
pRC4790	pRS315 *GFP-H1-7c-H2*	Linker KTASAGS	This study	10211866
pRC4791	pRS315 *GFP-YOP1 K121E*		This study	10211866
pRC4792	pRS315 *GFP-YOP1 K108E*		This study	10211866
pRC4793	pRS315 *GFP-YOP1 E104K*		This study	10211866
pRC4794	pRS315 *GFP-YOP1 E61K*		This study	10211866
pRC4795	pRS315 *GFP-YOP1 E61K K121E*		This study	10211866
pRC4796	pRS315 *GFP-YOP1 E61K K108E*		This study	10211866
pRC4797	pRS315 *GFP-H1*[37]*-H2*	Linker KTASAGSSA	This study	10211866
pRC4798	pRS315 *GFP-H1-H2*[34]	Linker KTASAGSSA	This study	10211866
pRC4799	pRS315 *GFP-H1*[37]*- H2*[34]	Linker KTASAGSSA	This study	10211866

Table 2.2 Continued

pRC4816a	pRS315 *GFP-H1-S7-H2*	Linker KTSSSSSSS	This study	10213773
pRC4823	pRS315 *GFP-H1-S6-H2*	Linker KTSSSSSS	This study	10225045
pRC4824	pRS315 *GFP-H1-S5-H2*	Linker KTSSSSS	This study	10225045
pRC4825	pRS315 *GFP-H1-S4-H2*	Linker KTSSSS	This study	10225045
pRC4826	pRS315 *GFP-H1-S3-H2*	Linker KTSSS	This study	10225045
pRC4827	pRS315 *GFP-H1-S2-H2*	Linker KTSS	This study	10225045
pRC4828	pRS315 *GFP-H1-S-H2*	Linker KTS	This study	10225045
pRC4829	pRS315 *GFP-YOP1 E104K K108E*		This study	10225045
pRC4816b	pRS315 *GFP-H1-KTS11-H2*	Linker KTSSSSSSSSSSS	This study	10213773

Fluorescence Microscopy

GFP fusions of each protein were created by fusing 238 amino acids of yeast enhanced green fluorescence protein (yEGFP) to either the NH_2 or COOH terminus and separated by a unique linker sequence (GGPGG). Expression of each GFP fusion construct is driven by the endogenous promotor of that gene. NH_2 terminal GFP fusions contain the endogenous terminator sequences from each ORF, ~500 bp downstream from the stop codon of that gene. For COOH terminal GFP fusions, termination is controlled by 573 bp of DNA downstream of the *ADH1* ORF. All fusion constructs were created using overlap PCR recombination with ~20 bp overlapping sequences for all PCR fragments and recombined into the specified CEN plasmid at the multiple cloning site.

RFP-tagged proteins were constructed as described above, using *Discosoma* red fluorescent protein (DsRed) T4 as a template [16]. RFP-KDEL was constructed

with DsRed fused to the NH_2 terminus of the yeast ER retrieval signal HDEL separated by the linker ASAGGSAGGGSASAGGPGG. RFP fusion constructs are NH_2 terminal fusions separated by a GGPGG linker sequence (RFP-RTN1).

Cells were grown overnight in minimal media to mid-log phase. Fluorescence images were taken using a Nikon Eclipse E600 equipped with a 100X (1.4NA) objective and 1x optivar (typically RFP constructs were exposed for 150-300 msec, while GFP constructs were exposed for 350-450 msec). DIC images were collected from a single plane while fluorescence images were gathered as a series of 20-30 z steps of 0.2 μm. A CCD camera (Sensicam EM High Performance, The Cook Corporation) was used to collect images (software IP Lab version 3.6.5, Scanalytics). Blind deconvolution of each z-series was done using AutoQuant X2 program (Media Cybernetics) for 30 iterations. Single planes were identified from either the center or periphery of the cell. Typically between 3 and 20 images were collected for each.

Analysis of peripheral ER morphology

To perform the quantification of cells containing a normal tubular peripheral ER, either *rtn1Δyop1Δ* or *rtn1Δrtn2Δyop1Δ* cells were transformed with one of the GFP-tagged constructs and RFP-KDEL and analyzed by fluorescence microscopy. Using the TxRED filter and focusing on peripheral ER structures, cells were visually categorized as having either an all-tubular peripheral ER (normal phenotype) or having some areas of peripheral ER sheet-like structures (mutant phenotype). Only cells expressing the GFP construct were included in this analysis. From a single microscope slide 100 cells were analyzed and this procedure was always performed in triplicate from a single liquid culture. Quantification numbers are all reported as average +/- standard deviation of cells with a normal peripheral ER morphology (level of rescue).

RESULTS

Yop1p is involved in the formation of peripheral ER tubules

Previous studies have shown that both *rtn1Δyop1Δ* and *rtn1Δrtn2Δyop1Δ* cells contain sheet-like peripheral ER membranes in place of the normal peripheral ER tubular membranes, suggesting that both Yop1p and Rtn1p are involved in the formation of the tubules of the peripheral ER. Furthermore, the sheet-like peripheral ER morphology can be restored to a wild-type tubular morphology by the expression of genomic *YOP1* [1]. These mutant cells can be used to analyze mutant *YOP1* constructs for their ability to restore a tubular morphology in the peripheral ER of these cells to elucidate the molecular mechanism utilized by Yop1p to generate these membrane tubules. To demonstrate that, in my hands, the *rtn1Δrtn2Δyop1Δ* cell's mutant sheet-like phenotype can be restored to a tubular morphology, these cell lines were analyzed by fluorescence microscopy (using RFP-KDEL expression to visualize ER structures, see materials and methods section) and categorized as having either a sheet-like peripheral ER (mutant phenotype) or a tubular peripheral ER (normal phenotype). From a single, overnight liquid culture 100 cells were analyzed in this manner (performed in triplicate) and reported as an average +/- standard deviation. Vector control wild-type cells almost all contain a tubular peripheral ER (99 +/- 1% cells with normal ER, Table 2.3, Figure 2.1), as do vector control *rtn1Δ* cells (93.6 +/- 1.5% cells with normal ER, Table 2.3) and vector control *yop1Δ* cells (96 +/- 4% cells with normal ER, table 2.3). Almost all of the *rtn1Δyop1Δ* cells and *rtn1Δrtn2Δyop1Δ* cells contained sheet-like peripheral ER (9.3+/- 2.6% and 5 +/- 3.6 cells with normal ER, respectively). Expression of genomic *YOP1* from a single copy plasmid was found to restore a tubular morphology to the peripheral ER in many *rtn1Δrtn2Δyop1Δ* cells (77.3 +/- 4.1% cells with normal ER, Table 2.3), demonstrating that I can use this mutant cell line to analyze the functionality of mutant *YOP1* constructs.

Figure 2.1. Yop1p is involved in forming peripheral ER tubules. A. Wild-type (RCY239), *yop1Δ* (CY4169), *rtn1Δ* (RCY4164), *rtn1Δyop1Δ* (RCY4168) and *rtn1Δrtn2Δyop1Δ* (RCY4323) cells expressing RFP-KDEL to visualize ER structures. B. Quantification of number of each cell type containing a normal, tubular peripheral ER. Numbers are presented as average +/- standard deviation.

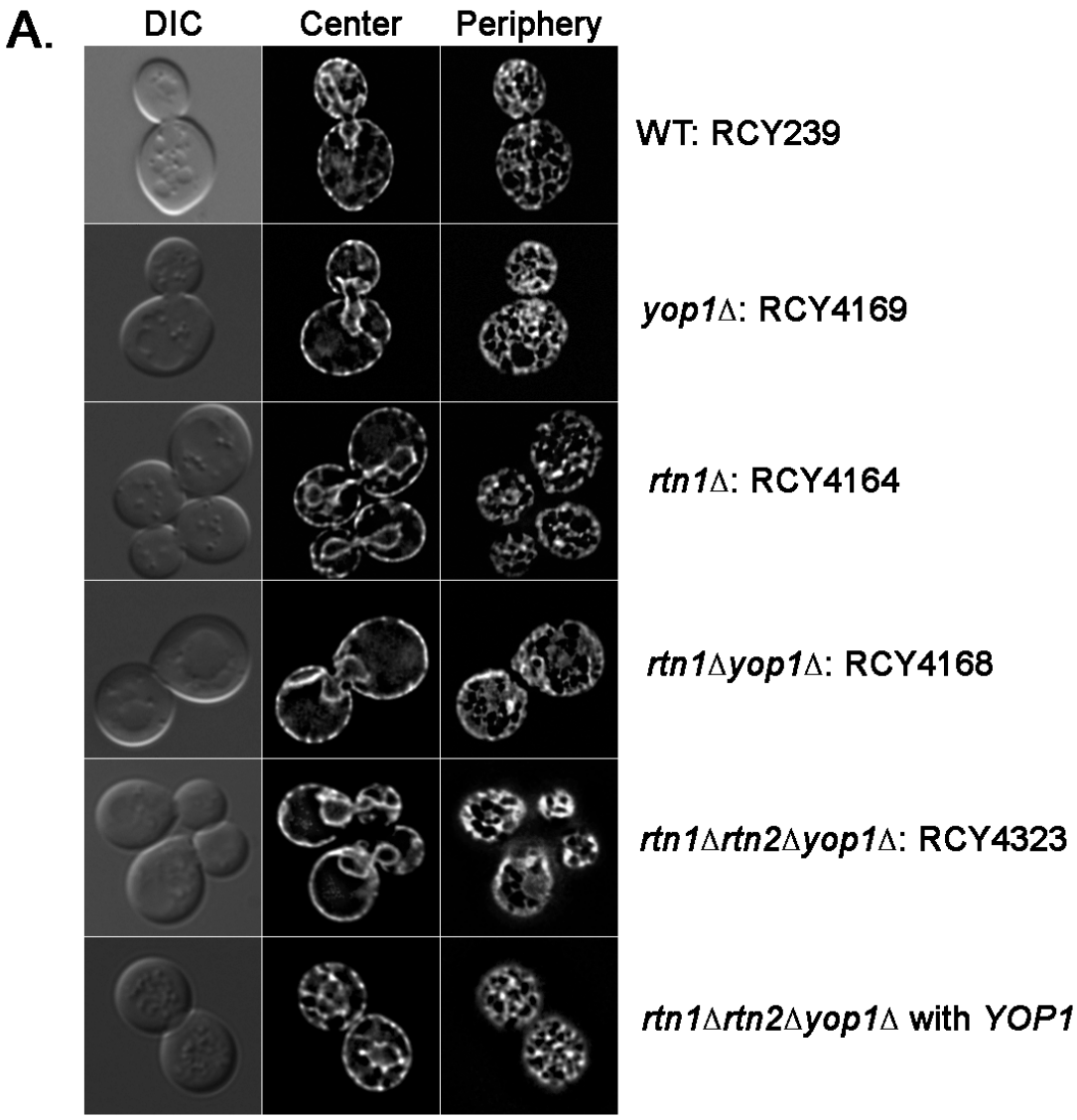
A.
DIC
Center
Periphery
WT: RCY239
yop1Δ: RCY4169
rtn1Δ: RCY4164
rtn1Δyop1Δ: RCY4168
rtn1Δrtn2Δyop1Δ: RCY4323
rtn1Δrtn2Δyop1Δ with YOP1

Figure 2.1 continued

B.

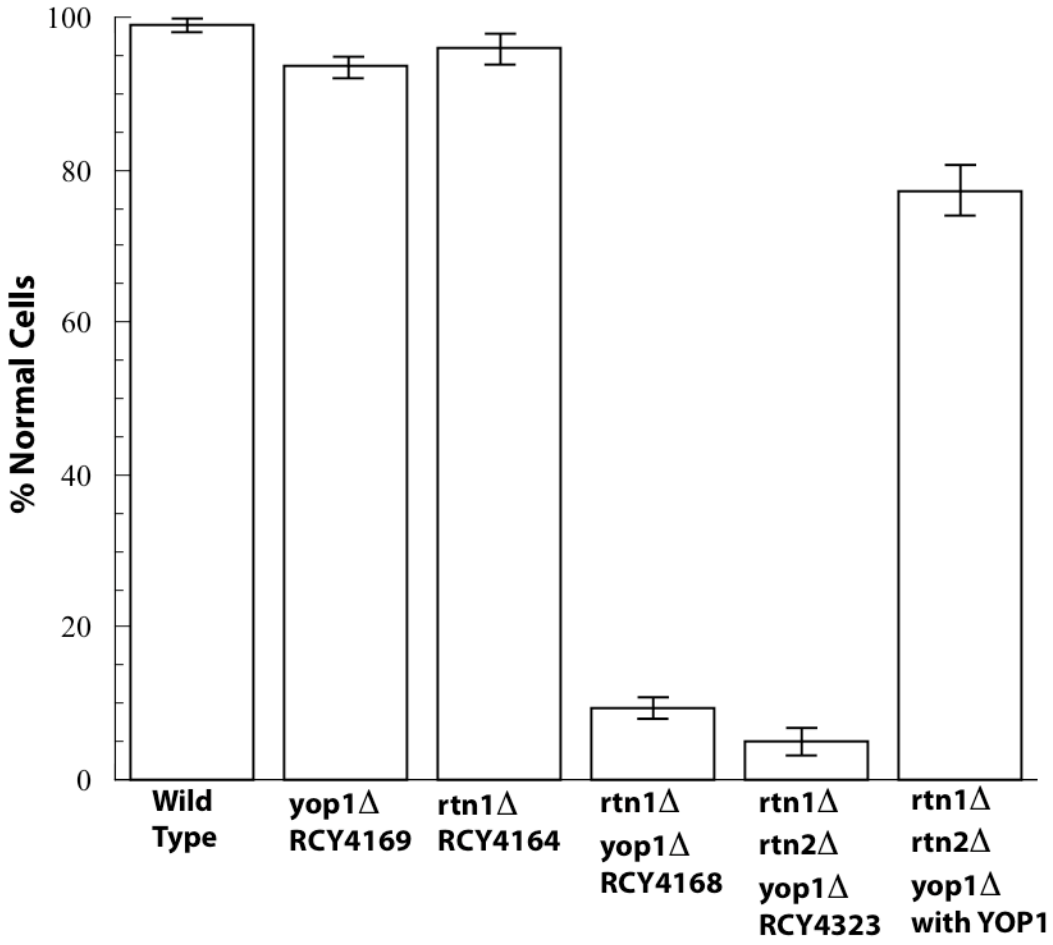

Table 2.3 Quantification of cells with normal ER morphology, Yop1p generates the tubules of the peripheral ER

RCY strain	Plasmid(s)	Slide 1 100 cells counted	Slide 2 100 cells counted	Slide 3 100 cells counted	Average	Standard Deviation	Date analysis performed
239	pRC3588	100	98	99	99	1	7/29/08
4169	pRC3588	94	92	95	93.6	1.5	9/16/08
4164	pRC3588	94	96	97	96	4	8/26/08
4168	pRC3588	6	10	11	9.3	2.6	7/29/08
4323	pRC3588	6	8	1	5	3.6	7/31/08
4323	pRC3588, pRC4562	82	76	74	77.3	4.1	1/27/09

GFP-Yop1p is functional in restoring a tubular peripheral ER morphology

Previous studies have demonstrated that a COOH terminal GFP tag does not interfere with Yop1p function [1]. However, the same studies suggest that tagging Yop1p on the NH_2 terminus resulted in disruption of the ability for Yop1p to function in tubule formation. I created NH_2 terminally tagged *GFP-YOP1* with a linker separating GFP from Yop1p (GGPGG) and analyzed for function as previously described. My findings indicate that NH_2 terminally tagged GFP-Yop1p is just as functional as Yop1p or Yop1p-GFP in restoring tubules in *rtn1Δrtn2Δyop1Δ* cells (68.3 +/- 14.1%, 77.3 +/- 4.1, and 57.6 +/- 3.5% cells with normal ER, respectively, Table 2.4, Figure 2.2), while expression of a vector control or a control protein (GFP-Sec63p) were both unable to restore a tubular peripheral ER (8.0 +/- 3.6% and 0.6 +/- 0.5% cells with normal ER, respectively) (Figure 2.2, Table 2.4). It is possible that the separation of GFP from Yop1p by the GGPGG linker may provide enough flexibility for the NH_2 terminal GFP tag to not interfere with Yop1p function. Alternatively, differences in the genetic background of strains used in the Voeltz et al study [1] and our studies may account for the differences in the ability of GFP-Yop1p to function.

Figure 2.2. GFP-Yop1p expression restores tubules in *rtn1Δrtn2Δyop1Δ* cells. A. Fluorescence images of *rtn1Δrtn2Δyop1Δ* (RCY4323) expressing genomic *YOP1, SEC63-GFP, YOP1-GFP,* and *GFP-YOP1*. RFP-KDEL allows visualization of ER structures. B. Quantification of number of each cell type with a tubular peripheral ER. Numbers presented are average+/- standard deviation.

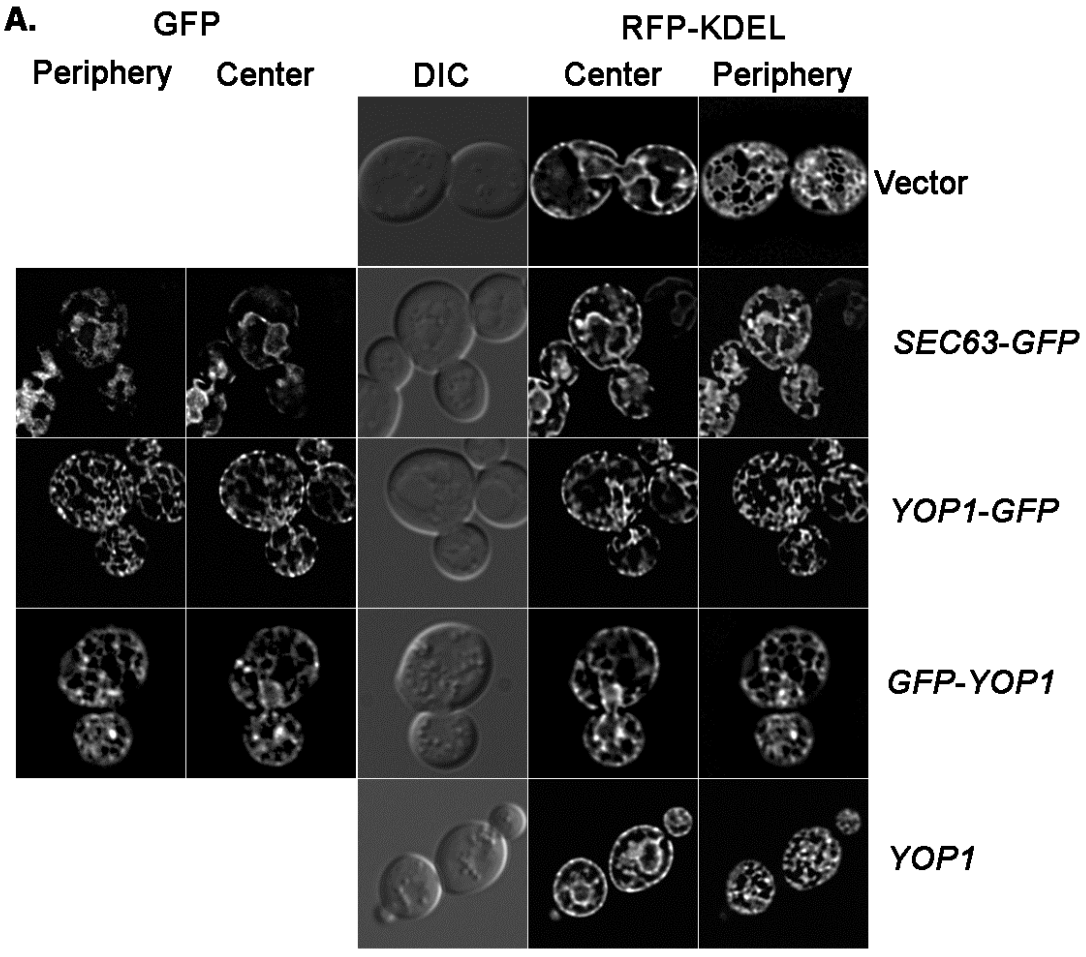
A.
GFP
RFP-KDEL
Periphery
Center
DIC
Center
Periphery
Vector
SEC63-GFP
YOP1-GFP
GFP-YOP1
YOP1

Figure 2.2 continued

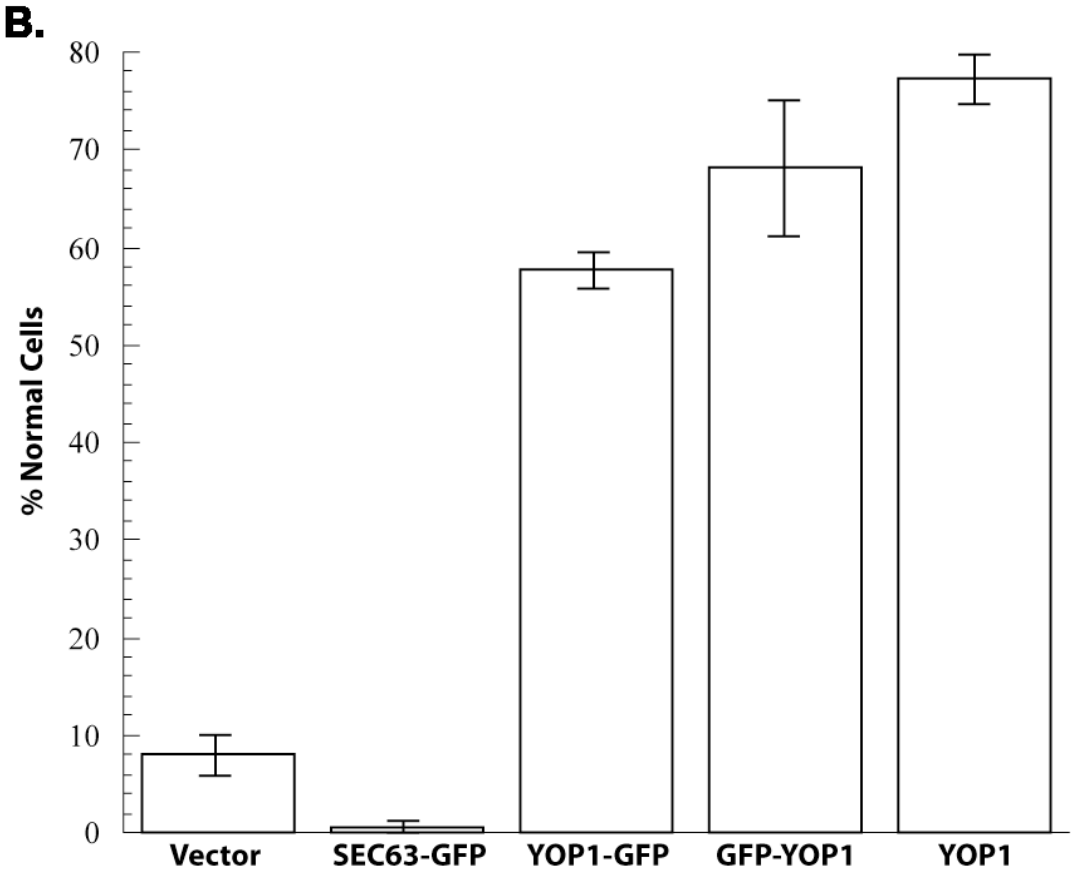

Table 2.4 Quantification of cells with normal ER morphology, GFP-Yop1p is functional

RCY strain	Plasmid(s)	Slide 1 100 cells counted	Slide 2 100 cells counted	Slide 3 100 cells counted	Average	St. Dev.	Date Analysis Performed
4323	pRS315	12	5	7	8	3.6	1/27/09
4323	pRC3484	1	0	1	0.6	0.5	1/27/09
4323	pRC4444	61	58	54	57.6	3.5	1/27/09
4323	pRC504	52	76	77	68.3	14.1	1/27/09
4323	pRS4562	82	76	74	77.3	4.1	1/27/09

Yip1/Yif1p expression does not functionally complement *rtn1Δyop1Δ* cells

Another family of proteins, the YIP1/YIF1 family, are known to bind to Yop1p and may aid in the formation of the peripheral ER tubules. In order to assess the ability of these proteins to restore a normal peripheral ER morphology in *rtn1Δrtn2Δyop1Δ* cells, multi-copy plasmids overexpressing genomic copies of the YIP1 family members Yip1p, Yif1p, or both were introduced into these cells and peripheral ER morphology was analyzed by fluorescence microscopy. This analysis (performed as previously described) revealed that neither Yip1p nor Yif1p overexpression was capable of restoring peripheral ER tubules more than vector alone (5.1 +/- 2.5%, 9.6 +/- 1.5% and 5 +/- 2.3% cells with normal ER, respectively, Table 2.5, Figure 2.3). Additionally, expression of both Yip1p and Yif1p together was unable to restore a normal peripheral ER morphology in the *rtn1Δrtn2Δyop1Δ* cells (5.3 +/- 3.2% cells with normal ER, Figure 2.3, Table 2.5). These results suggest that the ability of Yip1p/Yif1p to generate curvature of ER membranes requires the presence of Yop1p and/or Rtn1p.

To further analyze the interaction between Yip1p and Yop1p, as well as investigate whether Yop1p requires Yip1p for its function, *yip1-40* cells expressing endogenous levels of Yop1p were analyzed for peripheral ER morphology. *Yip1-40*

cells contain normal peripheral ER tubules at the permissive temperature (30°C), but upon a shift to 37°C these tubules are rapidly converted to peripheral ER sheets [10]. Interestingly, *yip1-40* cells at the restrictive temperature do not appear to contain any areas of peripheral ER tubules, a more severe mutant phenotype than the *rtn1Δrtn2Δyop1Δ* cells have, highlighting the importance of Yip1p in the formation of these structures. As expected, at the permissive temperature these cells have mainly a tubular peripheral ER (Figure 2.3 C) while upon shift to the restrictive temperature these tubules are converted into sheet-like structures, despite the expression of Yop1p (Figure 2.3 D). This result further suggests that Yop1p may act in concert with Yip1p to form and maintain the tubules of the peripheral ER in yeast, and that Yop1p requires Yip1p to accomplish this task.

Table 2.5 Quantification of indicated cell type with normal ER morphology, *YIP1/YIF1* expression cannot function without Rtn1p/Yop1p

RCY strain	Plasmid(s)	Slide 1 100 cells counted	Slide 2 100 cells counted	Slide 3 100 cells counted	Average	St. Dev.	Date Analysis Performed
4323	pRS315	4	1	8	5	2.3	3/8/09
4323	pRC1037	4	5	6	5.1	2.5	3/8/09
4323	pRC3146	8	10	11	9.6	1.5	3/8/09
4323	pRC1037 pRC3146	4	8	4	5.3	3.2	3/8/09
4323	pRC504	62	59	49	58	17.7	3/8/09

Figure 2.3. YIP1 family proteins and Yop1p act together to form peripheral ER tubules. A. Fluorescence images of *rtn1Δrtn2Δyop1Δ*cells overexpressing genomic *YIP1*, *YIF1* or both. RFP-KDEL was also expressed to visualize peripheral ER structures. B. Quantification of number of each cell type containing a tubular peripheral ER. Numbers presented are average+/- standard deviation. C, D. *yip1-40* cells expressing GFP-Yop1p at permissive (C, 30°C) and restrictive (D, 37°C) temperatures. RFP-KDEL expression allows visualization of ER structures.

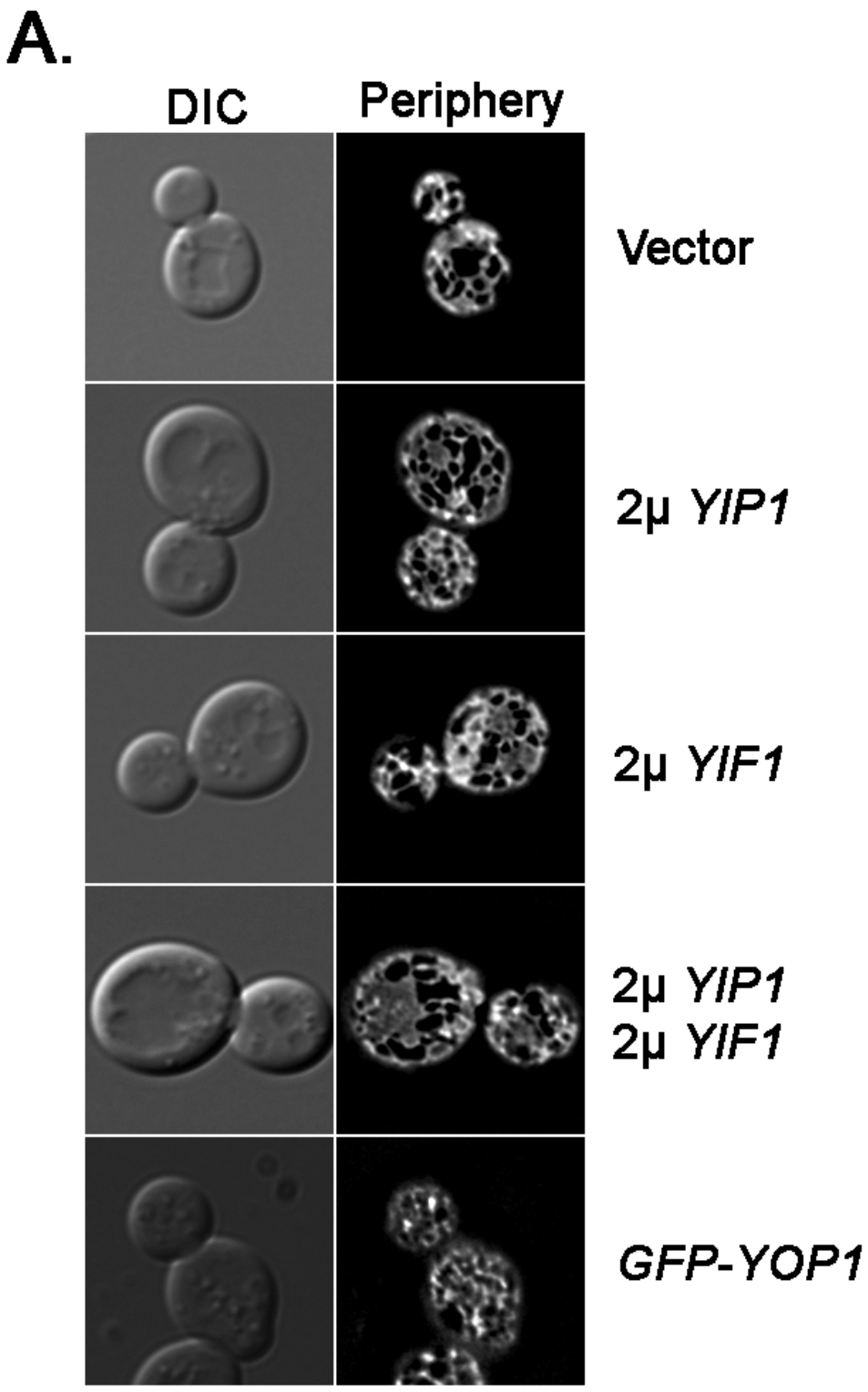
A.
DIC
Periphery
Vector
2μ YIP1
2μ YIF1
2μ YIP1
2μ YIF1
GFP-YOP1

Figure 2.3 continued

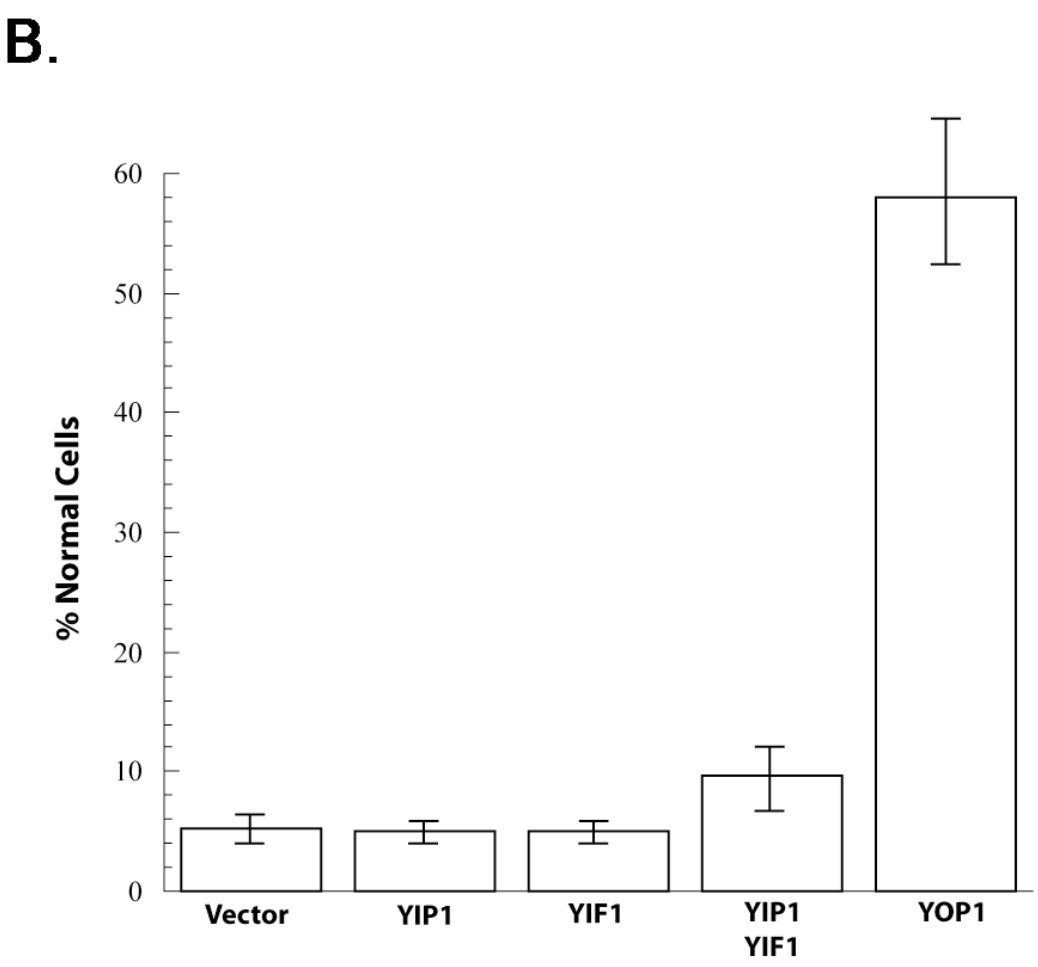

Figure 2.3 continued

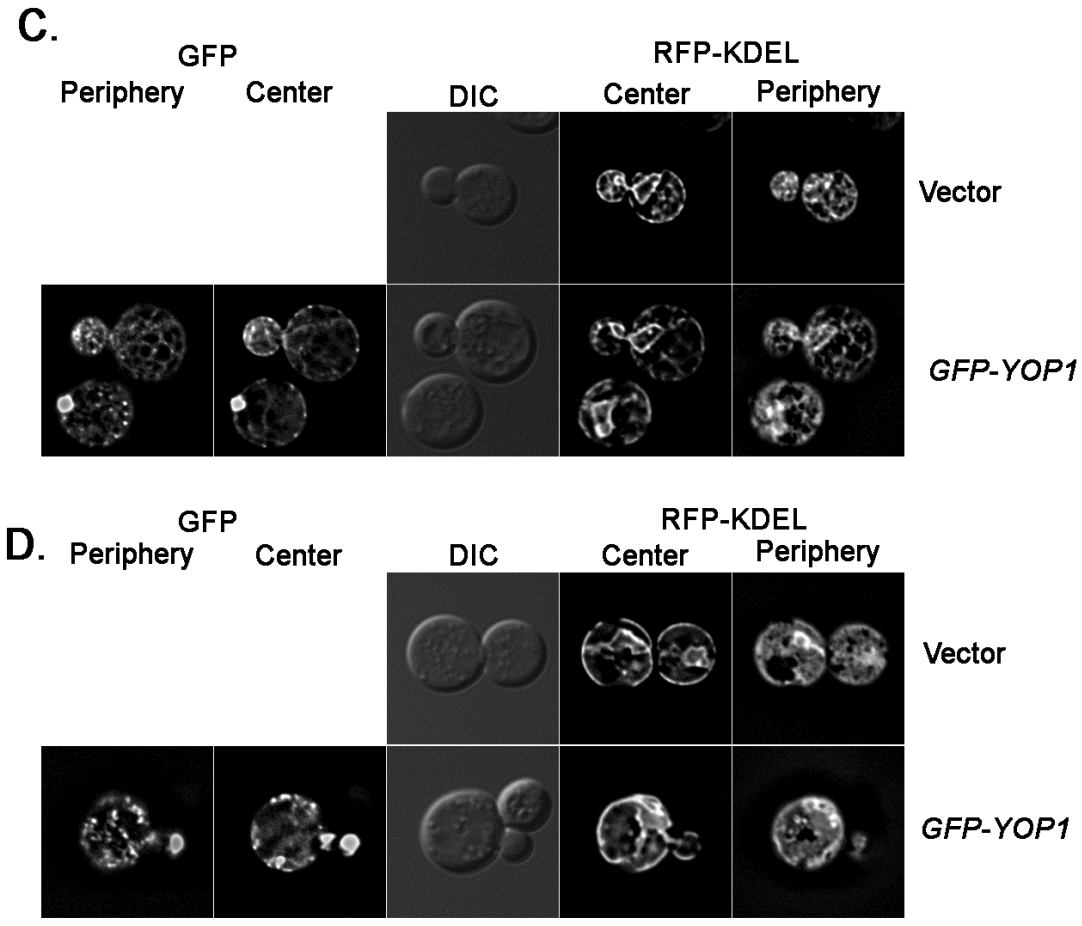

Membrane trafficking appears unaffected in *rtn1Δrtn2Δyop1Δ* cells

There is evidence that a block in membrane trafficking from the ER to the Golgi can results in an accumulation of cisternal ER membranes and an expansion of the surface area of the ER [17]. In order to test the possibility that the presence of peripheral ER sheets in the *rtn1Δrtn2Δyop1Δ* cells is a consequence of a membrane trafficking block and an accumulation of ER membranes, the number of ER exit sites (ERES) in wild-type and *rtn1Δrtn2Δyop1Δ* cells was analyzed. A halt in ER to Golgi trafficking would lead to an accumulation of ERES present in the peripheral ER. To accomplish this analysis, *SEC13-RFP* was expressed to visualize ERES, which appear as puncta on the peripheral ER. Sec13p is a component of COPII vesicles and aggregates at ERES [18, 19]. GFP-KDEL expression allowed visualization of the ER structures and the number of ERES was quantified within each cell (6 cells analyzed). This analysis revealed there was no difference in the number of ERES between the wild-type (23.1 +/- 7.4 ERES/cell) and *rtn1Δrtn2Δyop1Δ* cells (22.3 +/- 8.4 ERES/cell) (Figure 2.4, Table 2.6). The apparently normal number of ERES in the *rtn1Δrtn2Δyop1Δ* cells suggests that trafficking between the ER and Golgi is functioning despite the lack of Yop1p and Rtn1p in these cells. This result also suggests that the presence of membrane sheets in the peripheral ER of the *rtn1Δrtn2Δyop1Δ* cells is likely not due to an accumulation of ER membranes but is rather a specific morphological change due to the lack of Rtn1p and Yop1p.

Table 2.6 Analysis of number of ERES in the indicated cell type

RCY strain	Cell 1	Cell 2	Cell 3	Cell 4	Cell 5	Cell 6	Average	St. Dev.
239	18	24	29	11	31	26	23.1	7.4
4168	28	10	34	19	18	25	22.3	8.4

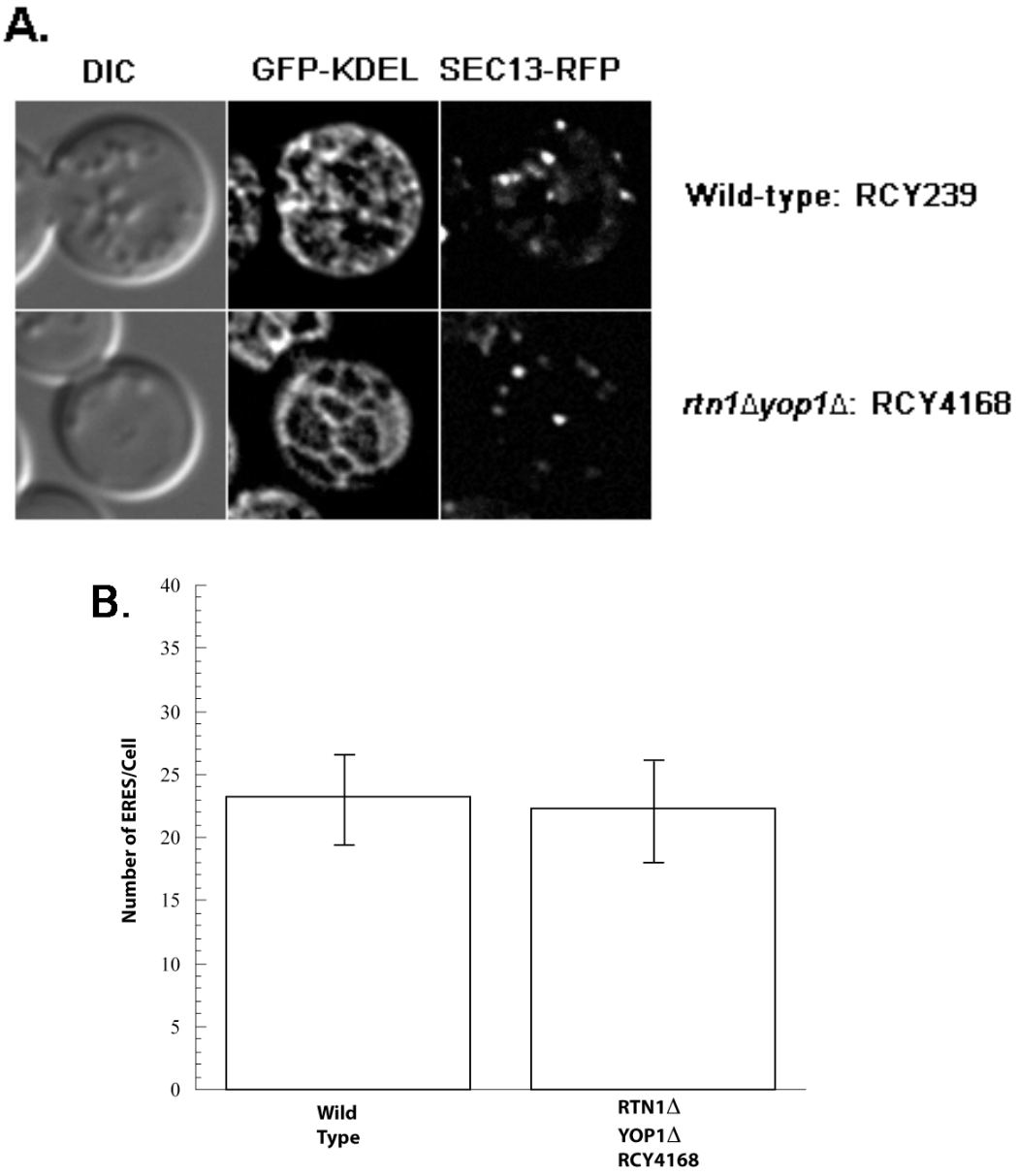

Figure 2.4. ERES appear unaffected in *rtn1Δyop1Δ* cells. A. Fluorescence images of wild-type (RCY239) and *rtn1Δyop1Δ* (RCY4168) cells expressing *SEC13-RFP* to visualize ERES and GFP-KDEL to visualize ER structures. Peripheral view of ER is shown. B. Quantification of number of ERES from both cells types, six individual cells were analyzed from each type. Numbers presented are average+/- standard deviation.

Both hydrophobic domains of Yop1p are required for function

The current model for the mechanism of Yop1p in generating membrane curvature suggests that the presence of the two hydrophobic hairpins within the lipid bilayer expands the surface area of one leaflet, forming a localized area of curvature [1]. To test the accuracy of this model the role of each hydrophobic hairpin was analyzed individually for its contribution to tubule formation. Mutant *YOP1* constructs were generated lacking either the first or second hydrophobic domain (*yop1ΔH1* and *yop1ΔH2*, respectively). These mutants were tagged with GFP on their NH_2 terminus, expressed in *rtn1Δrtn2Δyop1Δ* cells and peripheral ER morphology was analyzed by fluorescence microscopy as previously described. Each of these mutants allowed me to test the individual contribution of the hydrophobic domains to the ability of Yop1p to function in tubule formation. This analysis revealed that neither GFP-Yop1ΔH1 or GFP-Yop1ΔH2 were able to function in peripheral ER tubule formation (17.5 +/- 8.5% and 18.5 +/- 11.1% cells with normal ER, respectively, Table 2.7, Figure 2.5), indicating a critical role for each of these hydrophobic domains for Yop1p function. Furthermore, these studies indicate an absolute requirement for both hydrophobic domains for Yop1p to function normally, providing further evidence that Yop1p functions in tubule formation through the presence both hydrophobic domains. Interestingly, both GFP-Yop1ΔH1 and GFP-Yop1ΔH2 localized not only to the peripheral ER tubules, but to the nuclear ER as well (Figure 2.5). This is an unexpected localization, considering Yop1p is enriched on the peripheral ER structures with very little found on the nuclear ER [1]. It is possible that the ability of Yop1p to function in tubule formation is connected to its proper localization exclusively to the peripheral ER and when that localization is disrupted Yop1p loses its ability to function.

Figure 2.5. The two hydrophobic domains of Yop1p are necessary to form peripheral ER tubules. A. ER structure was monitored in *rtn1Δrtn2Δyop1Δ* cells expressing *GFP-YOP1, GFP-yop1ΔH1, GFP-yop1ΔH2*, and both *GFP-yop1ΔH1* and *GFP-yop1ΔH2* by fluorescence microscopy. B. Quantification of number of each cell type with a tubular peripheral ER. Numbers presented are average+/- standard deviation. C. Sequence alignment of above constructs.

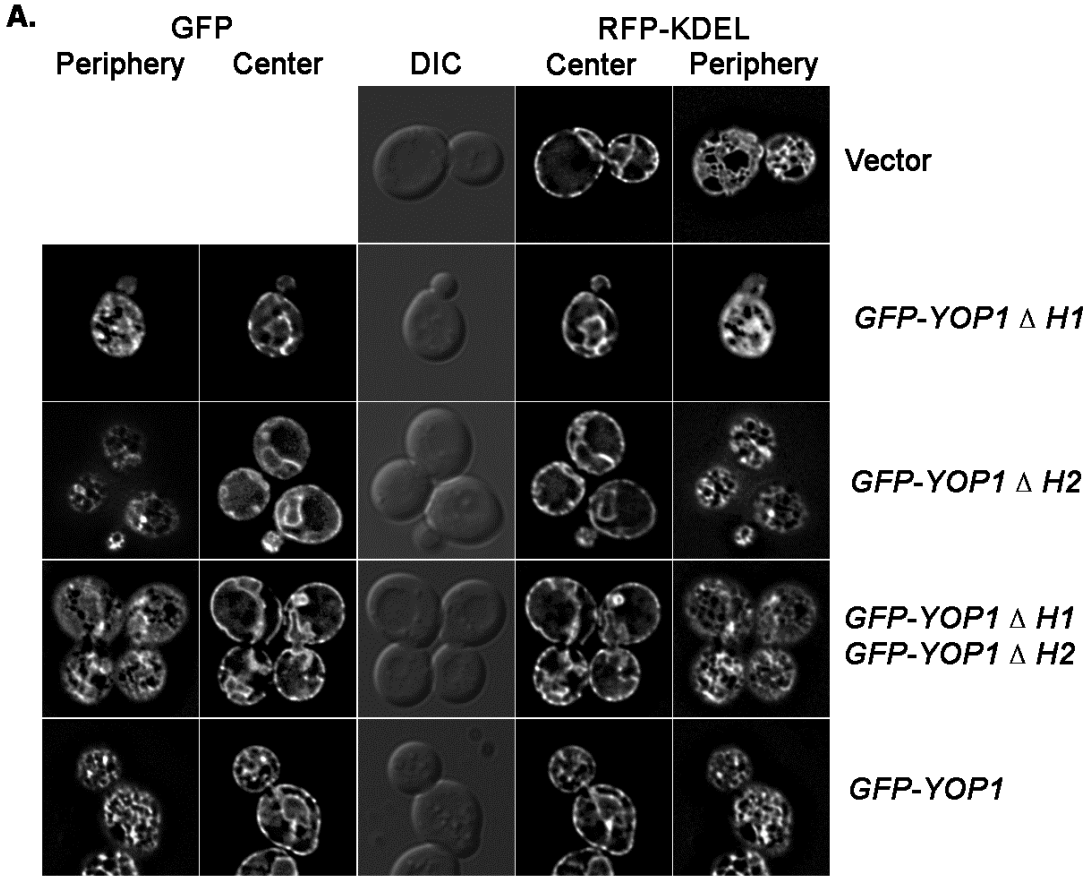
A.
GFP
Periphery
Center
DIC
RFP-KDEL
Center
Periphery
Vector
GFP-YOP1 Δ H1
GFP-YOP1 Δ H2
GFP-YOP1 Δ H1
GFP-YOP1 Δ H2
GFP-YOP1

Figure 2.5 continued

B.

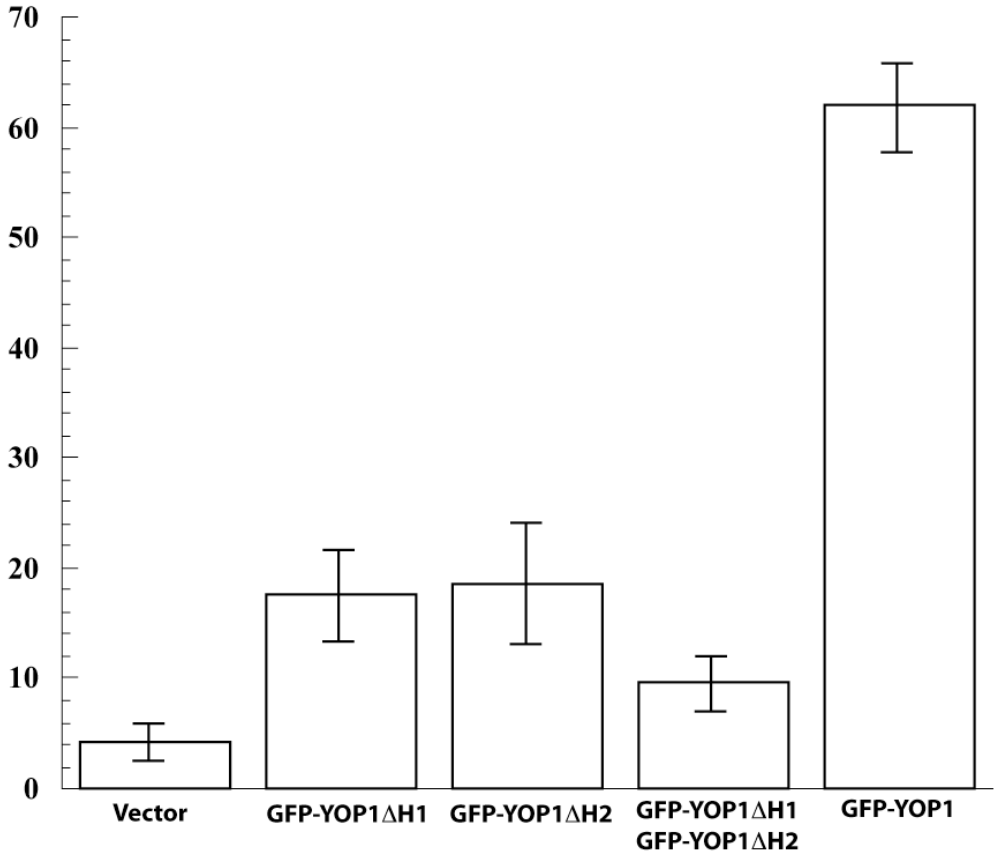

C.

```
MSEYASSIHS QMKQFDTKYS GNRILQQLEN KTNLPKSYLV AGLGFAYLLL IFINVGGVGE ILSNFAGFVL PAYLSLVALK TPTSTDDTQL      YOP1
MSEYASSIHS QMKQFDTKYS GNRILQQLEN KTNLPKSY---------- ---------- ---------- ----------TPTSTDDTQL      YOP1ΔH1
MSEYASSIHS QMKQFDTKYS GNRILQQLEN KTNLPKSYLV AGLGFAYLLL IFINVGGVGE ILSNFAGFVL PAYLSLVALK TPTSTDDTQ-      YOP1ΔH2

LTYWIVFSFL SVIEFWSKAI LYLIPFYWFL KTVFLIYIAL PQTGGARMIY QKIVAPLTDR YILRDVSKTE KDEIRASVNE ASKATGASVH    YOP1
LTYWIVFSFL SVIEFWSKAI LYLIPFYWFL KTVFLIYIAL PQTGGARMIY QKIVAPLTDR YILRDVSKTE KDEIRASVNE ASKATGASVH    YOP1ΔH1
---------- ---------- ---------- ---------- ----------RMIY QKIVAPLTDR YILRDVSKTE KDEIRASVNE ASKATGASVH    YOP1ΔH2
```

Table 2.7 Quantification of indicated cell type with normal ER morphology, both hydrophobic domains of Yop1p are required for peripheral ER tubule formation

RCY strain	Plasmid(s)	Slide 1 100 cells counted	Slide 2 100 cells counted	Slide 3 100 cells counted	Average	St. Dev.	Date Analysis Performed
4323	pRS315	4	6	12	7.3	4.1	4/7/09
4323	pRC4523	25	14	9	17.5	8.7	4/7/09
4323	pRC4524	28	19	14	18.5	11.1	4/7/09
4323	pRC4523 pRS4524	16	6	7	9.6	5.5	4/7/09
4323	pRC504	60	56	70	62	7.2	4/7/09

Removal of either hydrophobic domain results in non-functional Yop1p, however it is possible that by expressing both GFP-Yop1ΔH1 and GFP-Yop1ΔH2 together in *rtn1Δrtn2Δyop1Δ* cells may provide the cell with both hydrophobic domains on separate polypeptides, perhaps complementing the cell with all of the functional domains of Yop1p that are needed to form membrane tubules. I assessed this possibility by expressing both GFP-Yop1ΔH1 and GFP-Yop1ΔH2 together in *rtn1Δrtn2Δyop1Δ* cells and analyzing peripheral ER morphology by fluorescence microscopy as previously described. I found that expression of both of these constructs within the *rtn1Δrtn2Δyop1Δ* cells did not functionally complement the lack of reticulons/Yop1p, with most cells still containing peripheral ER sheets (9.6 +/- 5.5% cells with normal ER, Table 2.7, Figure 2.5). This result further confirms that each hydrophobic hairpin is critical for Yop1p function and suggests that both hydrophobic hairpins must be physically linked on the same polypeptide to generate membrane tubules (as in Yop1p). Despite the fact that Yop1p forms homo-oligomeric complexes [2, 4], expression of both of the hydrophobic deletion mutants together was unable to restore peripheral ER tubules. This result could be due to an inability of the two mutant proteins to interact inter-molecularly and form the oligomeric complexes,

suggesting that higher order complex formation may be mediated through interactions of the hydrophobic domains. Alternatively, this result may suggest some specific intra-molecular interaction between the hydrophobic domains of Yop1p occurs. The interaction between these domains may give Yop1p a conformation/shape within the membrane that is necessary for the generation of membrane tubules (ie. "wedge").

A previous study found that the factors that generate ER tubules in vitro (later identified as Rtn1p and Yop1p) have the ability to maintain the tubular structures after random proteolysis of the hydrophilic regions of the proteins, suggesting that tubule structure may be maintained by the hydrophobic regions of Rtn1p/Yop1p alone [1, 4, 20]. To further investigate the role that the hydrophobic domains of Yop1p play in generating membrane tubules, GFP fusions to each of the individual hydrophobic domains were created which lack all of the surrounding hydrophilic regions (*GFP-H1* and *GFP-H2*). When these constructs were expressed in cells they localized to ER membranes (Figure 2.6), indicating that the ER localization of Yop1p is directed by information present in either of the hydrophobic domains. Interestingly, I found these mutants were no longer restricted to the peripheral ER tubules, perhaps suggesting that the restriction of Yop1p to the tubular peripheral ER is controlled by information in the hydrophilic domains. It is possible that the hydrophilic regions of Yop1p mediate interactions with other proteins that direct its localization to the peripheral ER.

Each individual mutant was then tested for its ability to restore peripheral ER tubules in the *rtn1Δrtn2Δyop1Δ* cells as previously described. Neither GFP-H1 nor GFP-H2 was found to function in restoring a tubular ER morphology in these cells (12 +/- 4.9% and 12 +/- 3.2% cells with normal ER, respectively, Table 2.8) (Figure 2.6). Even when expressed at the same time in *rtn1Δrtn2Δyop1Δ* cells the peripheral ER was composed mainly of membrane sheets (7.3 +/- 4.6% cells with normal ER, Table 2.8) (Figure 2.6). These results further confirm that both of the hydrophobic domains

are necessary for Yop1p function and that these domains together, on two separate polypeptides, are not sufficient to restore normal Yop1p function.

To test the hypothesis that the hydrophobic domains of Yop1p must interact specifically to give Yop1p the proper shape within the membrane necessary for function a minimal *YOP1* hydrophobic domain mutant was created containing both hydrophobic domains separated by a unique linker (KTASAGSSA, mimicking the length of this region in wild-type Yop1p) and fused NH_2 terminally to GFP (*GFP-H1-H2*). This construct localized to ER membranes, including the nuclear ER (Figure 2.6). Upon testing for function in restoring peripheral ER tubules in the *rtn1Δrtn2Δyop1Δ* cells as previously described I discovered that this protein functioned to a similar level as GFP-Yop1p in restoring a tubular peripheral ER (57.6 +/- 7.7% and 59.3 +/- 3.5% cells with normal ER, respectively, Table 2.8) (Figure 2.6). This result confirms that both of the hydrophobic domains of Yop1p are necessary for generating membrane tubules and sufficient to function in this task in place of Yop1p, as long as they are present on a single protein. Furthermore, all of the hydrophilic domains of Yop1p appear to be dispensable for normal function suggesting their contribution to the generation of membrane tubules by Yop1p is minimal. Interestingly, the GFP-H1-H2 construct localized to the entire ER membrane, including the relatively flat nuclear ER, but was still able to function in tubule formation (Figure 2.6). This fact indicates that the ability of Yop1p to function in tubule formation is distinct from its exclusive localization to the peripheral ER tubules, suggesting a more complex mechanism of regulating the activity of Yop1p than its localization alone. These results further strengthen our understanding of the mechanism of Yop1p action, suggesting specific interaction between the two hydrophobic domains is necessary to give Yop1p a conformation required to function in forming the tubules of the peripheral ER. Considering the model that Yop1p is shaped like a wedge within the membrane, the

spacing between these domains may also be an important feature of Yop1p in maintaining a functional conformation by holding the two domains apart at the membrane surface (investigated later in this chapter).

Table 2.8 Quantification of indicated cell type with normal ER morphology, the two hydrophobic domains of Yop1p are sufficient to form peripheral ER tubules

RCY strain	Plasmid(s)	Slide 1 100 cells counted	Slide 2 100 cells counted	Slide 3 100 cells counted	Average	St. Dev.	Date Analysis Performed
4323	pRS315	6	4	12	7.3	4.1	4/7/09
4323	pRC4525	21	13	8	12	4.9	4/7/09
4323	pRC4526	13	9	10	12	3.2	4/7/09
4323	pRC4525 pRC4526	13	9	2	7.3	4.6	4/7/09
4323	pRC504	56	63	59	59.3	3.5	4/7/09
4323	pRC4559	70	63	44	57.6	7.7	4/7/09

Figure 2.6. The two hydrophobic domains of Yop1p are sufficient to form peripheral ER tubules. A. *rtn1Δrtn2Δyop1Δ* cells expressing *GFP-H1*, *GFP-H2*, both *GFP-H1* and *GFP-H2*, *GFP-YOP1,* and *GFP-H1-H2* were monitored for ER structure using RFP-KDEL expression. B. Quantification of number of each cell type with a tubular peripheral ER. Numbers presented are average+/- standard deviation. C. Sequence alignment of the above constructs.

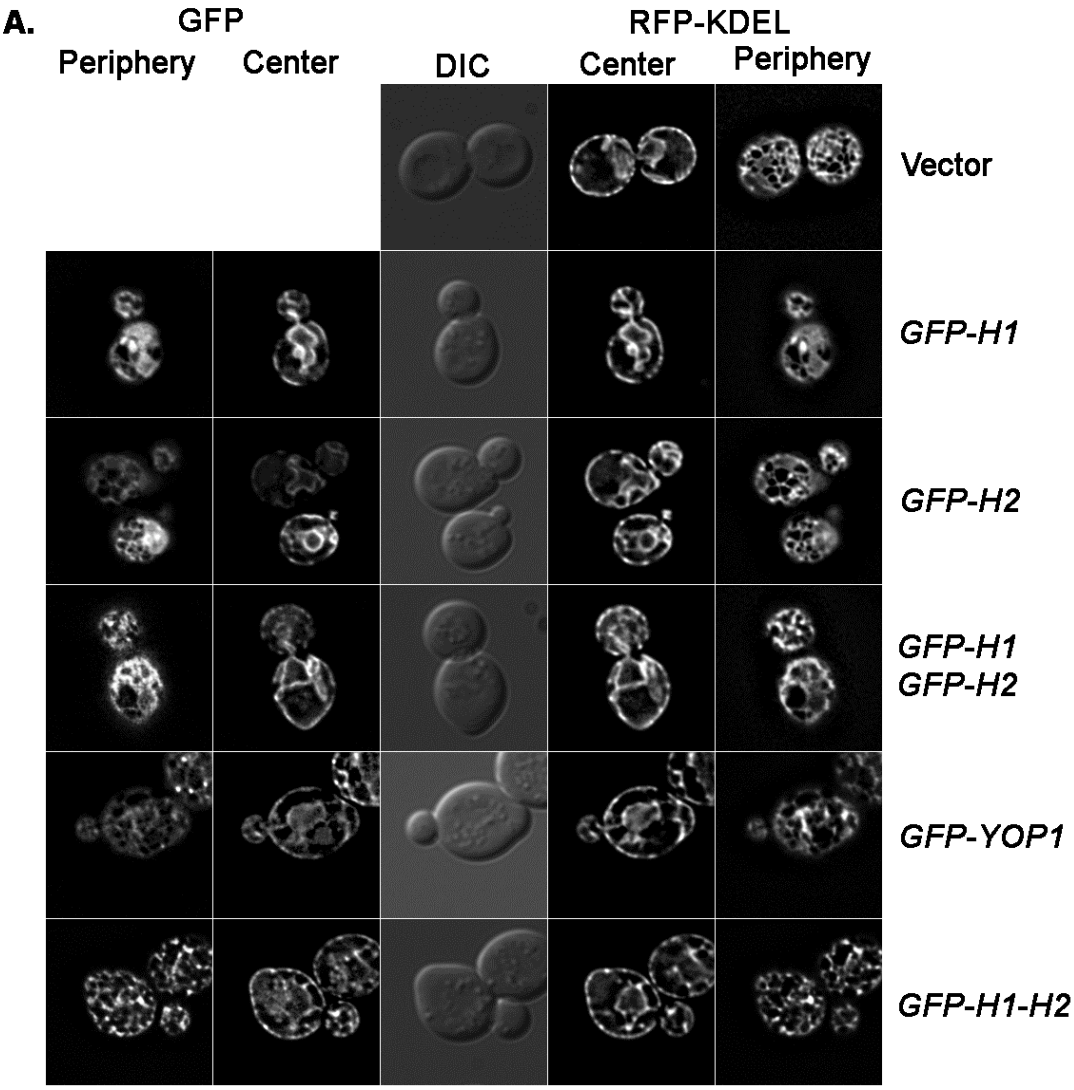
A.
GFP
Periphery
Center
DIC
RFP-KDEL
Center
Periphery
Vector
GFP-H1
GFP-H2
GFP-H1
GFP-H2
GFP-YOP1
GFP-H1-H2

Figure 2.6 Continued

B.

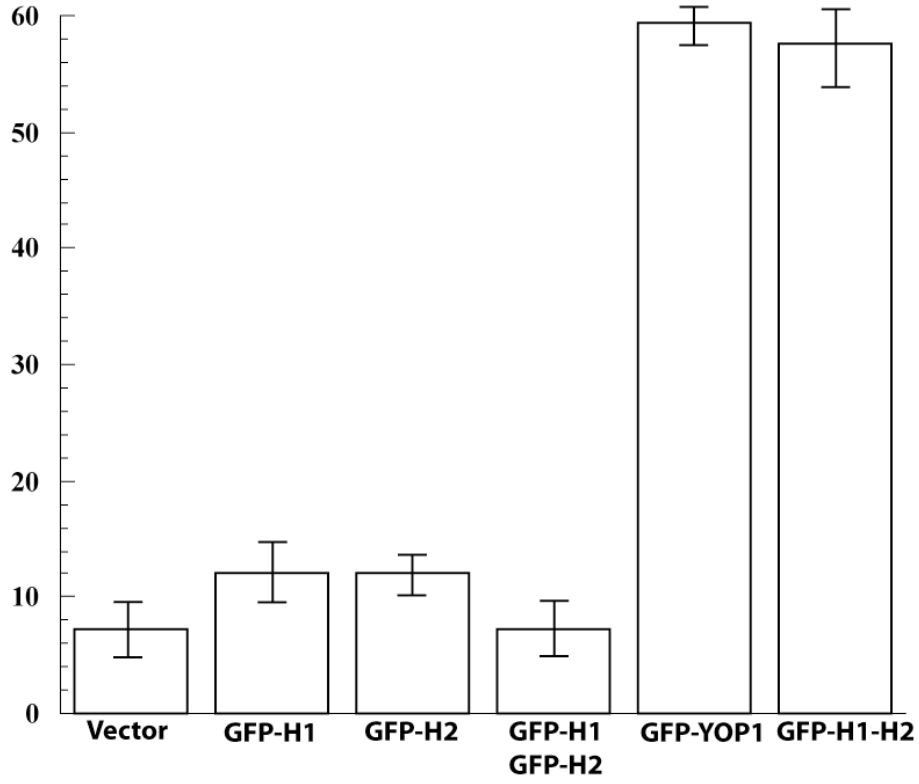

C.

```
MSEYASSIHS QMKQFDTKYS GNRILQQLEN KTNLPKSYLV AGLGFAYLLL IFINVGGVGE  ILSNFAGFVL PAYLSLVALK TPTSTDDTQL        YOP1
---------- ---------- ---------- KTNLPKSYLV AGLGFAYLLL IFINVGGVGE  ILSNFAGFVL PAYLSLVAL- ----------        H1
---------- ---------- ---------- ---------- ---------- ---------- ---------- ---------- ----------L       H2
---------- ---------- ---------- KTNLPKSYLV AGLGFAYLLL IFINVGGVGE  ILSNFAGFVL PAYLSLVALK TASAGSSA--L       H1-H2


LTYWIVFSFL SVIEFWSKAI LYLIPFYWFL  KTVFLIYIAL PQTGGARMIY QKIVAPLTDR YILRDVSKTE KDEIRASVNE ASKATGASVH        YOP1
---------- ---------- ---------- ---------- ---------- ---------- ---------- ---------- ----------        H1
LTYWIVFSFL SVIEFWSKAI LYLIPFYWFL  KTVFLIYI AL ---------- ---------- ---------- ---------- ----------        H2
LTYWIVFSFL SVIEFWSKAI LYLIPFYWFL  KTVFLIYI AL PQTGGA----- ---------- ---------- ---------- ----------        H1-H2
```

Interaction between H1 and H2 is specific

There is evidence that some integral membrane proteins may interact through specific attractions of their hydrophobic domains embedded within the membrane [21]. To further test the specificity of the interaction between the hydrophobic domains of Yop1p and whether this interaction is a specific one rather than a general property of long hydrophobic domains, a series of *yop1* constructs were generated using different combinations of the hydrophobic domains (separated by an KTASAGSSA linker). GFP was fused to the NH_2 terminus of *H1-H1*, *H2-H2*, and *H2-H1*. Altering the identity and location of the hydrophobic domains allowed me to analyze the specificity of the interaction between H1 and H2. Each of these constructs was analyzed for its ability to restore a tubular peripheral ER in the *rtn1Δrtn2Δyop1Δ* cells as previously described. In all three cases expression of the *yop1* mutant resulted in cells with peripheral ER sheets, indicating that the interaction between H1 and H2 is specific and likely not a result of non-specific hydrophobic attractions (H1-H1 7.3 +/- 4.5%, H2-H2 5.3 +/- 2%, H2-H1 3.6 +/- 2% cells with normal ER, respectively, Table 2.9) (Figure 2.7). Interestingly, I found the *GFP-H2-H1* construct to be non-functional despite the fact that both H1 and H2 are present on the same polypeptide. This is an unexpected result because both hydrophobic domains are present, however the orientation of these domains is reversed when compared to GFP-H1-H2. To further analyze this result, H2-H1-GFP was constructed to mimic the GFP-H1-H2 with an opposite orientation by moving the GFP tag to the COOH terminus. When tested for functionality in the *rtn1Δrtn2Δyop1Δ* cells I found that this construct was also unable to restore a tubular peripheral ER (21 +/- 6.5% cells with normal ER, Table 2.9) (Figure 2.7). This unexpected result may indicate that the conformation of Yop1p is asymmetrical and that the interaction between the two hydrophobic domains can only occur if H1 is upstream of H2. It is also possible that reversing the orientation of the

hydrophobic domains decreases the stability of Yop1p or alters the folding and/or membrane insertion, thus decreasing the ability of these mutants (GFP-H2-H1 and H2-H1-GFP) to function in forming the tubules of the peripheral ER.

Table 2.9 Quantification of indicated cell type with normal ER morphology, the interaction between H1 and H2 is specific

RCY strain	Plasmid(s)	Slide 1 100 cells counted	Slide 2 100 cells counted	Slide 3 100 cells counted	Average	St. Dev.	Date analysis performed
4323	pRS315	6	3	9	5.3	2	10/28/09
4323	pRC4559	70	59	52	63.6	5.6	9/4/09
4323	pRC4674	6	3	2	3.6	2	9/4/09
4323	pRC4710	27	14	22	21	6.5	10/28/09
4323	pRC4705	3	12	7	7.3	4.5	10/28/09
4323	pRC4706	9	12	8	5.3	2	10/28/09

Figure 2.7. Peripheral ER tubule formation requires a specific interaction between H1 and H2. A. Fluorescence microscopy was used to monitor peripheral ER morphology in *rtn1Δrtn2Δyop1Δ* cells using RFP-KDEL expression. Cells expressing *GFP-H1-H2, GFP-H2-H1, H2-H1-GFP, GFP-H1-H1* and *GFP-H2-H2* are shown. B. Quantification of number of each cell type with a tubular peripheral ER. Numbers presented are average+/- standard deviation.

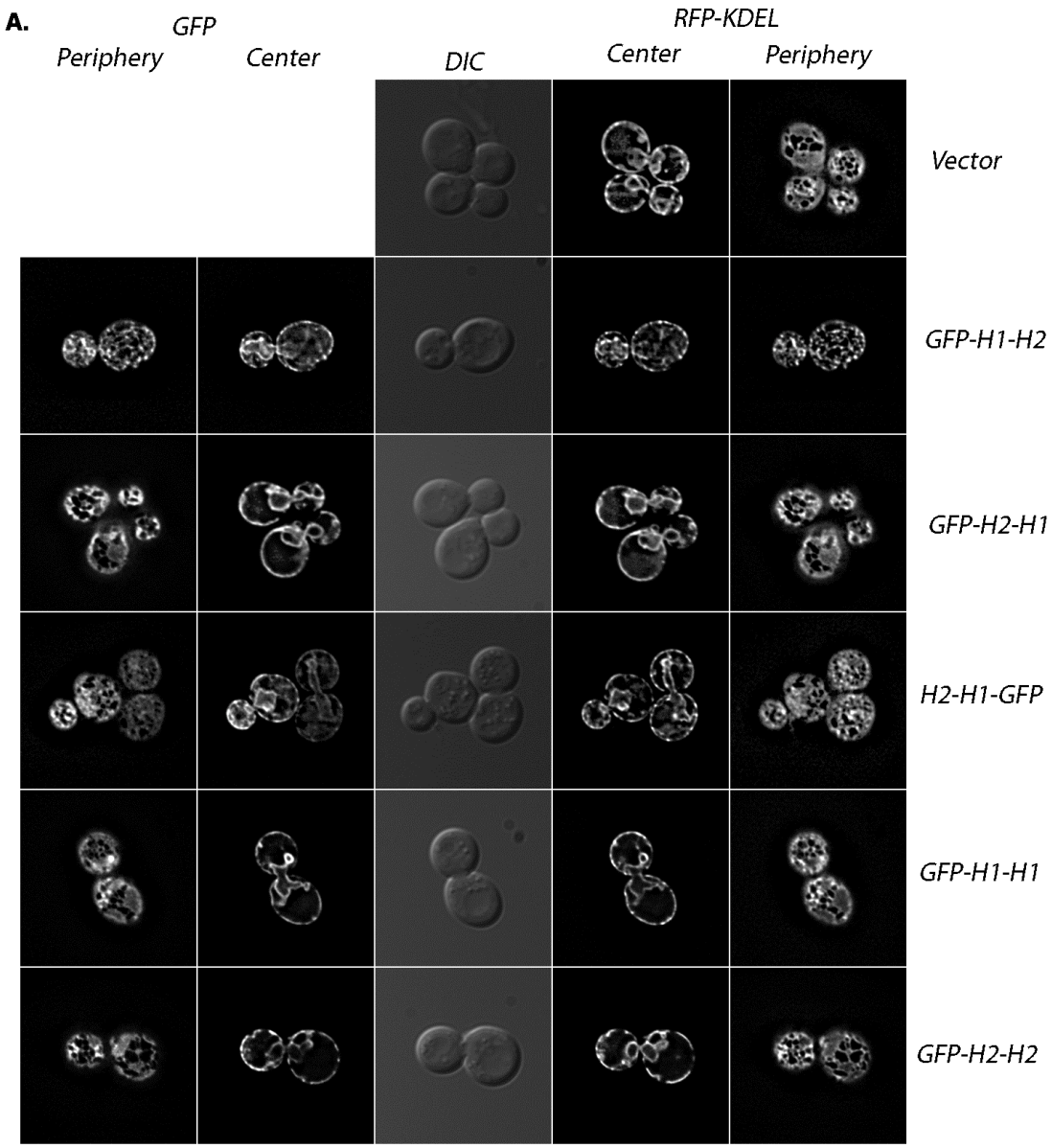
A.
GFP
Periphery
Center
DIC
RFP-KDEL
Center
Periphery
Vector
GFP-H1-H2
GFP-H2-H1
H2-H1-GFP
GFP-H1-H1
GFP-H2-H2

Figure 2.7 continued

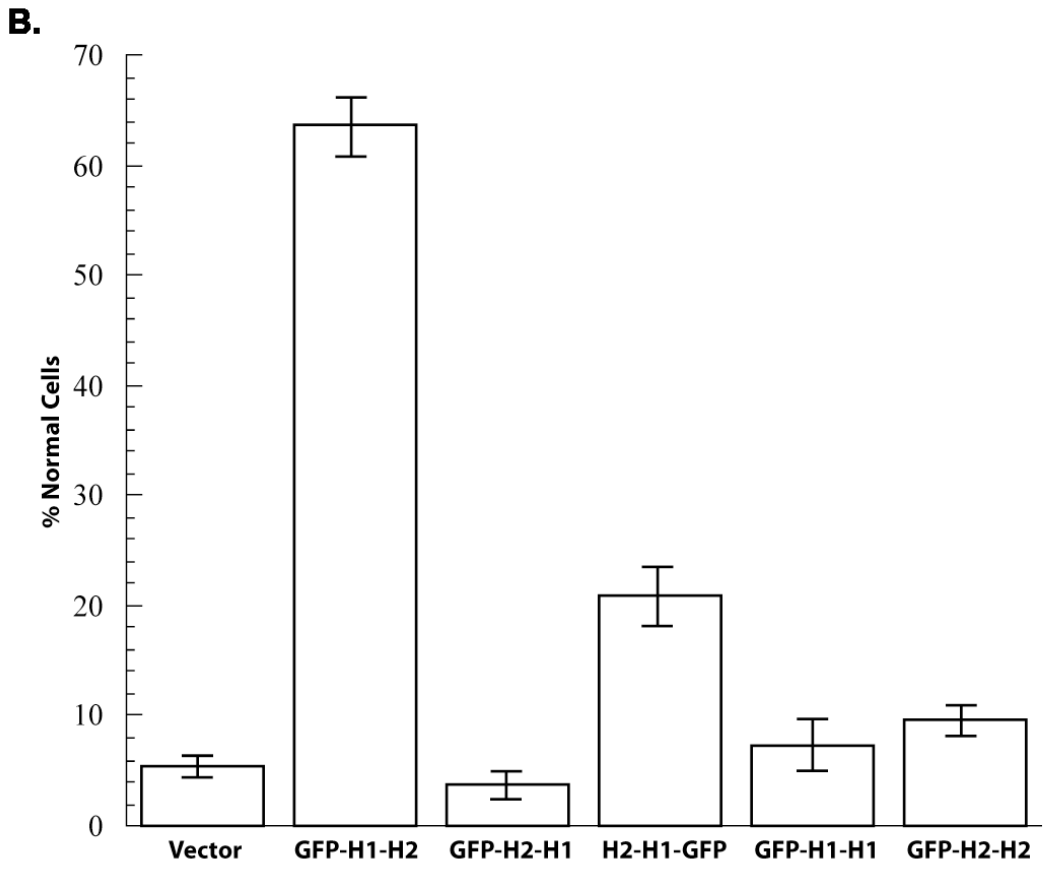

The length of the linker region between H1 and H2 is critical for Yop1p function

Having determined that the interaction between the two hydrophobic domains is likely necessary for Yop1p to adopt a conformation that generates the tubules of the peripheral ER, I sought to investigate if the spacing between these two domains also contributes to the ability of Yop1p to alter membrane architecture. I reasoned that in order for the hydrophobic domains of Yop1p to adopt a wedge-like shape within the membrane the cytosol-exposed ends would need to be held apart, while the membrane embedded ends would need to be held together (see Figure 1.5). Both Yop1p and GFP-H1-H2 contain hydrophilic linker regions between H1 and H2 that are ~9 amino acids in length. To determine if the linker region between the hydrophobic domains functions in spacing these domains and if this spacing is critical for Yop1p function, a series of *YOP1* mutants were made with successively longer or shorter linker regions.

First, mutants were constructed where the linker region was lengthened to 13 (GFP-H1-KTS11-H2) or 19 (GFP-H1-19-H2) amino acids and tested for their ability to restore a tubular peripheral ER in the *rtn1Δrtn2Δyop1Δ* cells as described previously. Both of these long linker mutants were found to function as well as GFP-H1-H2 in restoring the peripheral ER tubules in the *rtn1Δrtn2Δyop1Δ* cells. However, when the linker was lengthened using GFP (238 amino acids with a GGPGG linker NH_2 terminally and ASAGSSA linker COOH terminally for flexibility, H1-GFP-H2) the protein lost its ability to function normally, suggesting that the hydrophobic domains have a requirement to be in relatively close proximity to each other, but this spacing can be lengthened up to 19 amino acids and still function. These results suggest the spacing between the hydrophobic domains may play a role in giving Yop1p a conformation conducive to deforming membranes. Alternatively, the presence of GFP between the two hydrophobic domains may interfere with the orientation of these domains or their ability to be inserted into the membrane properly.

Although my results suggest that the linker region of Yop1p can be lengthened to 19 amino acids and still function normally, I next wanted to investigate if the spacing could be shortened, restricting the distance between the two hydrophobic domains. Considering the model for Yop1p function, where the protein adopts a wedge-like shape within the membrane, by shortening the linker region between the two hydrophobic domains I may alter the shape of this "wedge" and affect the ability of Yop1p to alter membrane curvature. To test this possibility GFP-H1-H2 constructs were made where the linker region was shortened successively (from 9 amino acids down to 2 amino acids) and tested for their ability to restore a tubular morphology in the peripheral ER in the *rtn1Δrtn2Δyop1Δ* cells. I found that when the linker region was 9 (GFP-H1-H2 61.6 +/- 3.2%, GFP-H1-9-H2 62 +/- 7% cells with normal ER), 8 (GFP-H1-8a-H2 69.3 +/- 8.7%, GFP-H1-8b-H2 68 +/- 6.5% cells with normal ER) or 7 (GFP-H1-7a-H2 59.6 +/- 7.5%, GFP-H1-7b-H2 82 +/- 8.2%, GFP-H1-7c-H2 68.3 +/- 10.1% cells with normal ER) amino acids in length the GFP-H1-H2 construct was functional in restoring a tubular peripheral ER in the *rtn1Δrtn2Δyop1Δ* cells (Figure 2.8, Table 2.10). Shortening the linker region to 6 (GFP-H1-6a-H2 32.3 +/- 3.5%, GFP-H1-6b-H2 34.6 +/- 4.9% cells with normal ER) amino acids resulted in a significantly decreased ability of the GFP-H1-H2 construct to function in tubule formation, though these constructs appeared to function better than the vector control (4.3 +/- 3.2% cells with normal ER, Figure 2.8, Table 2.10). Shortening the linker to 3 (GFP-H1-KTD-H2 14.6 +/- 7.6%, GFP-H1-KTG-H2 16.3 +/- 5.5% cells with normal ER) or 2 (GFP-H1-2-H2 17.6 +/- 4.0% cells with normal ER) amino acids abolished the ability of the GFP-H1-H2 construct to function in the generation of a tubular peripheral ER in the *rtn1Δrtn2Δyop1Δ* cells (Figure 2.8, Table 2.10). In summary, I found that the linker could be shortened down to 7 amino acids and still maintain function and that a 6 amino acid linker resulted in a partially functional protein.

Figure 2.8. Mutational analysis of the length of the linker between H1 and H2. A. Fluorescence microscopy was used to monitor peripheral ER morphology in *rtn1Δrtn2Δyop1Δ* cells using RFP-KDEL expression. Cells expressing *H1-GFP-H2, GFP-H1-19-H2, GFP-H1-KTS11-H2, GFP-H1-H2, GFP-H1-9-H2, GFP-H1-8a-H2, GFP-H1-8b-H2, GFP-H1-7a-H2, GFP-H1-7b-H2, GFP-H1-7c-H2, GFP-H1-6a-H2, GFP-H1-6b-H2, GFP-H1-KTG-H2, GFP-H1-KTD-H2, GFP-H1-KT-H2, GFP-H1-KTS7-H2, GFP-H1-KTS6-H2, GFP-H1-KTS5-H2, GFP-H1-KTS4-H2, GFP-H1-KTS3-H2, GFP-H1-KTS2-H2* and *GFP-H1-KTS-H2* are shown. B. Quantification of number of each cell type from A with a tubular peripheral ER. Numbers presented are presented as average+/- standard deviation. C. Sequence alignment of the above constructs.

A.

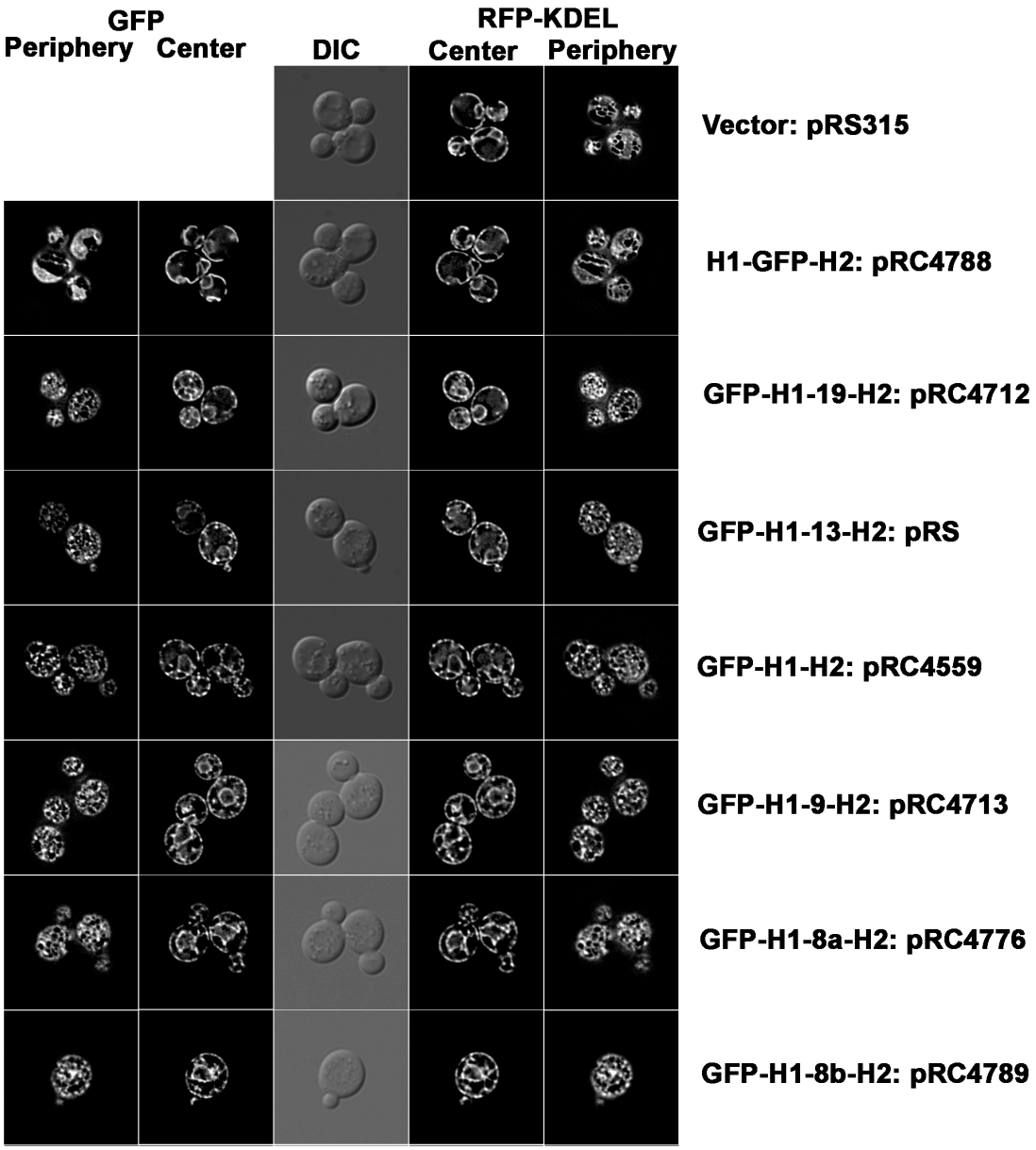
GFP
Periphery
Center
DIC
RFP-KDEL
Center
Periphery
Vector: pRS315
H1-GFP-H2: pRC4788
GFP-H1-19-H2: pRC4712
GFP-H1-13-H2: pRS
GFP-H1-H2: pRC4559
GFP-H1-9-H2: pRC4713
GFP-H1-8a-H2: pRC4776
GFP-H1-8b-H2: pRC4789

Figure 2.8 A continued

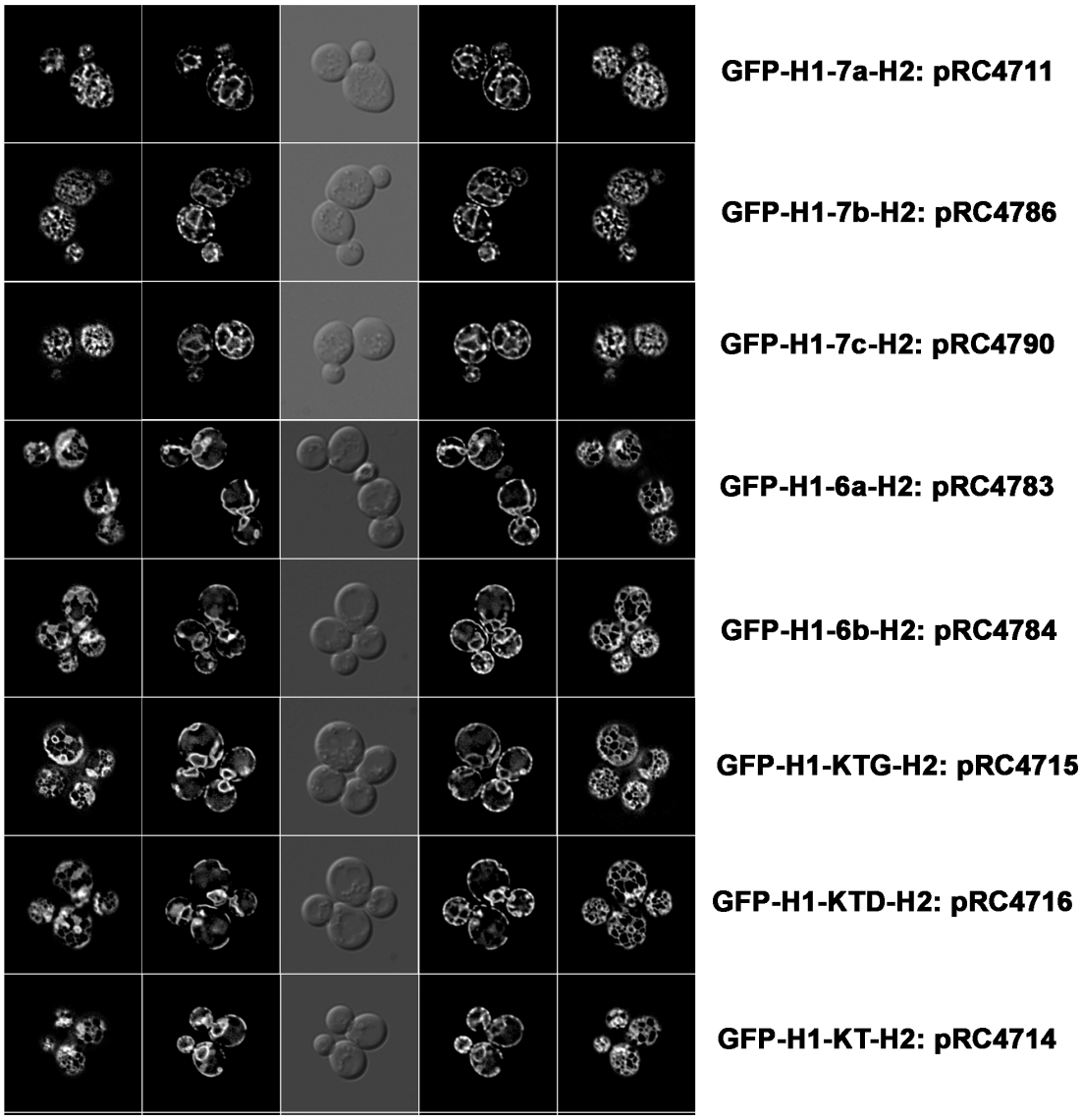

Figure 2.8 A continued

Figure 2.8 continued

B.

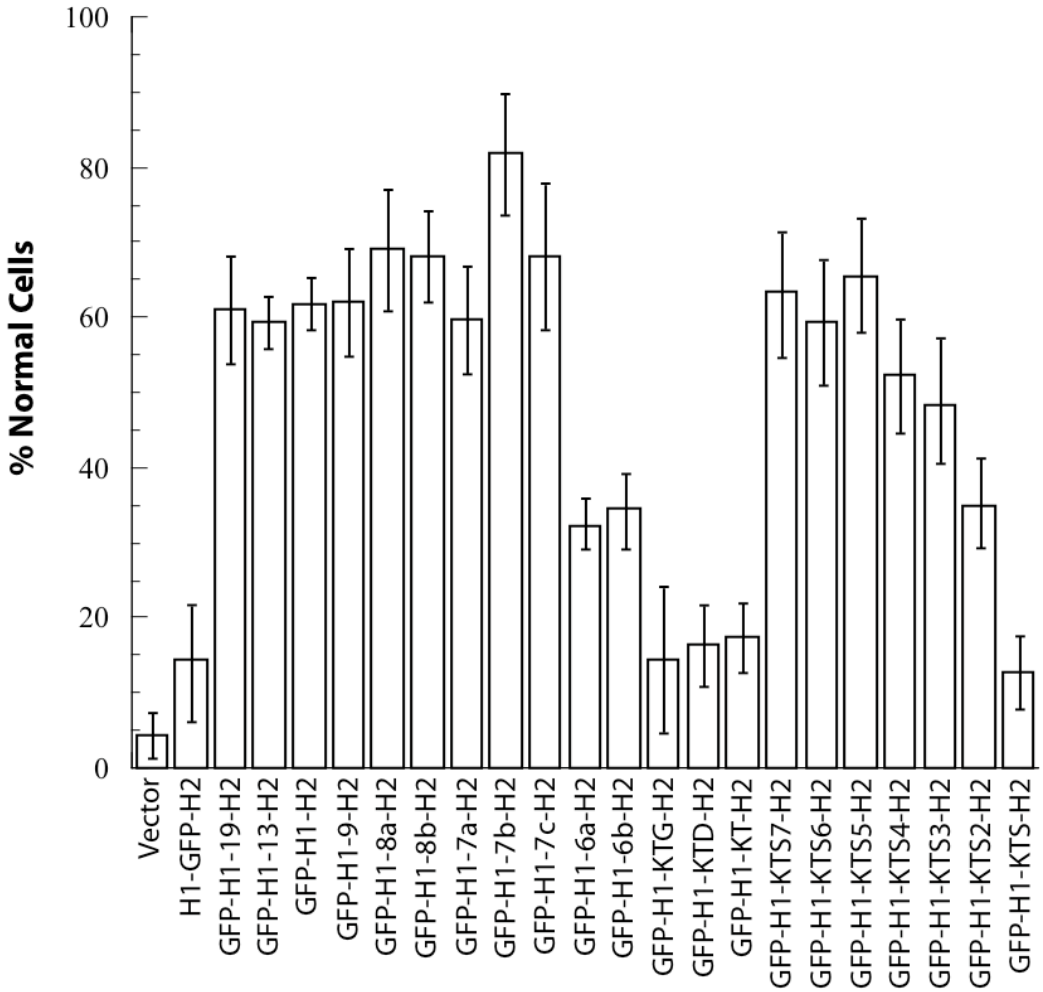

Figure 2.8 Continued

C.

```
KTNLPKSYLV AGLGFAYLLL IFINVGGVGE ILSNFAGFVL PAYLSLVALK TASASSKTDE KTSSGSSALL TYWIVFSFLS VIEFWSKAIL YLIPFYWFLK TVFLIYIAL   H1-19-H2
KTNLPKSYLV AGLGFAYLLL IFINVGGVGE ILSNFAGFVL PAYLSLVALK TSSSSSSSSS S----------LL TYWIVFSFLS VIEFWSKAIL YLIPFYWFLK TVFLIYIAL   H1-13-H2
KTNLPKSYLV AGLGFAYLLL IFINVGGVGE ILSNFAGFVL PAYLSLVALK TASAGSSA  --  ----------LL TYWIVFSFLS VIEFWSKAIL YLIPFYWFLK TVFLIYIAL   H1-H2
KTNLPKSYLV AGLGFAYLLL IFINVGGVGE ILSNFAGFVL PAYLSLVALK TSSKTDEK ---  ----------LL TYWIVFSFLS VIEFWSKAIL YLIPFYWFLK TVFLIYIAL   H1-9-H2
KTNLPKSYLV AGLGFAYLLL IFINVGGVGE ILSNFAGFVL PAYLSLVALK TSSKTDE -----  ----------LL TYWIVFSFLS VIEFWSKAIL YLIPFYWFLK TVFLIYIAL   H1-8a-H2
KTNLPKSYLV AGLGFAYLLL IFINVGGVGE ILSNFAGFVL PAYLSLVALK TASAGSS -----  ----------LL TYWIVFSFLS VIEFWSKAIL YLIPFYWFLK TVFLIYIAL   H1-8b-H2
KTNLPKSYLV AGLGFAYLLL IFINVGGVGE ILSNFAGFVL PAYLSLVALK TSKTDE -------  ----------LL TYWIVFSFLS VIEFWSKAIL YLIPFYWFLK TVFLIYIAL   H1-7a-H2
KTNLPKSYLV AGLGFAYLLL IFINVGGVGE ILSNFAGFVL PAYLSLVAL-  -ASAGSSA ---  ----------LL TYWIVFSFLS VIEFWSKAIL YLIPFYWFLK TVFLIYIAL   H1-7b-H2
KTNLPKSYLV AGLGFAYLLL IFINVGGVGE ILSNFAGFVL PAYLSLVALK TASAGS ------  ----------LL TYWIVFSFLS VIEFWSKAIL YLIPFYWFLK TVFLIYIAL   H1-7c-H2
KTNLPKSYLV AGLGFAYLLL IFINVGGVGE ILSNFAGFVL PAYLSLVALK TASAG  -------  ----------LL TYWIVFSFLS VIEFWSKAIL YLIPFYWFLK TVFLIYIAL   H1-6a-H2
KTNLPKSYLV AGLGFAYLLL IFINVGGVGE ILSNFAGFVL PAYLSLVALK TGSSA --------  ----------LL TYWIVFSFLS VIEFWSKAIL YLIPFYWFLK TVFLIYIAL   H1-6b-H2
KTNLPKSYLV AGLGFAYLLL IFINVGGVGE ILSNFAGFVL PAYLSLVALK TG ------------  ----------LL TYWIVFSFLS VIEFWSKAIL YLIPFYWFLK TVFLIYIAL   H1-KTG-H2
KTNLPKSYLV AGLGFAYLLL IFINVGGVGE ILSNFAGFVL PAYLSLVALK TD ------------  ----------LL TYWIVFSFLS VIEFWSKAIL YLIPFYWFLK TVFLIYIAL   H1-KTD-H2
KTNLPKSYLV AGLGFAYLLL IFINVGGVGE ILSNFAGFVL PAYLSLVALK T---------------  ----------LL TYWIVFSFLS VIEFWSKAIL YLIPFYWFLK TVFLIYIAL   H1-KT-H2
KTNLPKSYLV AGLGFAYLLL IFINVGGVGE ILSNFAGFVL PAYLSLVALK TSSSSSSS ----  ----------LL TYWIVFSFLS VIEFWSKAIL YLIPFYWFLK TVFLIYIAL   H1-S7-H2
KTNLPKSYLV AGLGFAYLLL IFINVGGVGE ILSNFAGFVL PAYLSLVALK TSSSSSS ------  ----------LL TYWIVFSFLS VIEFWSKAIL YLIPFYWFLK TVFLIYIAL   H1-S6-H2
KTNLPKSYLV AGLGFAYLLL IFINVGGVGE ILSNFAGFVL PAYLSLVALK TSSSSS -------  ----------LL TYWIVFSFLS VIEFWSKAIL YLIPFYWFLK TVFLIYIAL   H1-S5-H2
KTNLPKSYLV AGLGFAYLLL IFINVGGVGE ILSNFAGFVL PAYLSLVALK TSSSS ---------  ----------LL TYWIVFSFLS VIEFWSKAIL YLIPFYWFLK TVFLIYIAL   H1-S4-H2
KTNLPKSYLV AGLGFAYLLL IFINVGGVGE ILSNFAGFVL PAYLSLVALK TSSS ----------  ----------LL TYWIVFSFLS VIEFWSKAIL YLIPFYWFLK TVFLIYIAL   H1-S3-H2
KTNLPKSYLV AGLGFAYLLL IFINVGGVGE ILSNFAGFVL PAYLSLVALK TSS ------------  ----------LL TYWIVFSFLS VIEFWSKAIL YLIPFYWFLK TVFLIYIAL   H1-S2-H2
KTNLPKSYLV AGLGFAYLLL IFINVGGVGE ILSNFAGFVL PAYLSLVALK TS -------------  ----------LL TYWIVFSFLS VIEFWSKAIL YLIPFYWFLK TVFLIYIAL   H1-S-H2
```

Table 2.10 Quantification of the indicated cell type with a normal peripheral ER morphology, linker manipulated Yop1p mutants

RCY strain	Plasmid(s)	Slide 1 100 cells counted	Slide 2 100 cells counted	Slide 3 100 cells counted	Average	St. Dev.	Date analysis performed
4323	pRS315	3	2	8	4.3	3.2	12/21/09
4323	pRC4788	14	23	6	14.3	8.5	12/21/09
4323	pRC4712	59	55	69	61	7.2	10/29/09
4323	pRC4816b	67	62	60	59.3	3.1	2/12/10
4323	pRC4559	63	64	58	61.6	3.2	12/21/09
4323	pRC4713	57	59	70	62	7	10/29/09
4323	pRC4776	67	79	62	69.3	8.7	12/21/09
4323	pRC4789	74	69	61	68	6.5	12/21/09
4323	pRC4711	51	65	63	59.6	7.5	10/29/09
4323	pRC4786	89	73	84	82	8.1	12/21/09
4323	pRC4790	69	78	58	68.3	10	12/21/09
4323	pRC4783	36	32	29	32.3	3.5	12/21/09
4323	pRC4784	37	29	38	34.6	4.9	12/21/09
4323	pRC4715	8	13	23	14.6	7.6	10/29/09
4323	pRC4716	16	13	20	16.3	5.5	10/29/09
4323	pRC4714	17	22	14	17.6	4	10/29/09
4323	pRC4816	67	70	54	63.6	8.5	2/12/10
4323	pRC4823	69	55	54	59.3	8.4	7/20/10
4323	pRC4824	61	74	62	65.6	7.2	7/20/10
4323	pRC4825	51	60	46	52.3	7.1	7/20/10
4323	pRC4826	58	46	41	48.3	8.7	7/20/10
4323	pRC4827	40	28	37	35	6.2	7/20/10
4323	pRC4828	18	9	11	12.7	4.7	7/20/10

Table 2.11 Quantification of the indicated cell type with a normal peripheral ER morphology, linker manipulated Yop1p A7/K7 mutants

RCY strain	Plasmid(s)	Slide 1 100 cells counted	Slide 2 100 cells counted	Slide 3 100 cells counted	Average	St. Dev.	Date analysis performed
4323	4785	1	0	0	0.3	0.6	12/21/09
4323	4817	63	59	61	59	8.9	2/12/10

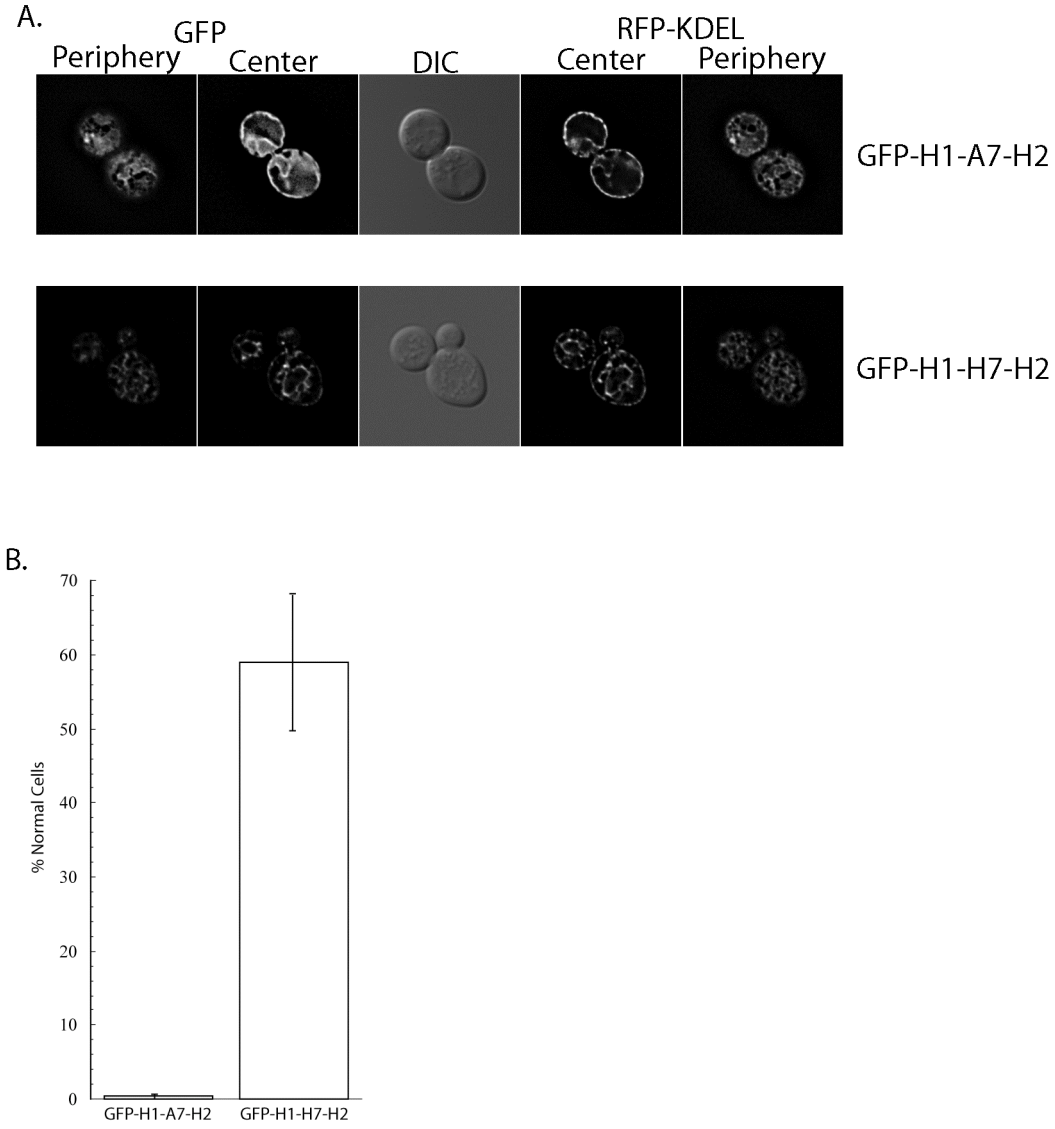

Figure 2.9 Mutational analysis of all alanine (A7) and all histidine (H7) linkers. A. Fluorescence microscopy was used to monitor peripheral ER morphology in *rtn1Δrtn2Δyop1Δ* cells using RFP-KDEL expression. Images of GFP-H1-A7-H2 and GFP-H1-H7-H2 are shown. B. Quantification of number of each cell type from A with a tubular peripheral ER. Numbers presented are presented as average+/- standard deviation.

Shortening the linker to 3 amino acids or shorter resulted in non-functional proteins suggesting the linker region acts as a spacer holding the two hydrophobic domains apart at the surface of the membrane and this spacing is critical for Yop1p to function in tubule formation. There appears to be some allowance for a slightly longer and a slightly shorter linker region between the two hydrophobic domains for Yop1p to function normally, but shortening this linker to less than 6 amino acids decreases function. Taken with the fact that the interaction between H1 and H2 may be holding the membrane embedded domains together, these results support the model that Yop1p adopts a wedge-like conformation within the membrane and that this shape is critical for Yop1p to function in generating the tubules of the peripheral ER.

The above studies were done using a unique linker with the sequence KTASAGSSA or other variations of this sequence. It is possible that the GFP-H1-H2 construct was functional due to the particular linker sequence chosen for these studies. To confirm the accuracy of the previous results I created a series of GFP-H1-H2 constructs, each with serine-only linkers, from KTS7 (9 amino acids) to KTS (3 amino acids), and tested these mutants for their ability to restore tubules in the *rtn1Δrtn2Δyop1Δ* cells as previously described. I found that the H1-H2 construct was able to function only when the serine linker was longer than 5 amino acids, but shorter linker regions resulted in decreased function (GFP-H1-KTS7-H2 63.6 +/- 8.5%, GFP-H1-KTS6-H2 59.3 +/- 8.4%, GFP-H1-KTS5-H2 65.6 +/- 7.2%, GFP-H1-KTS4-H2 52.3 +/- 7.1%, GFP-H1-KTS3-H2 48.3 +/- 8.7%, GFP-H1-KTS2-H2 35 +/- 6.2%, GFP-H1-KTS-H2 12.7 +/- 4.7% cells with normal ER, Table 2.10, Figure 2.8). These results are similar to my previous findings that indicate the linker likely needs to be about 6 amino acids in length for function. I found that shorter linkers (KTS4 to KTS)

were found to not restore peripheral ER tubules in these cells, similar to the results I obtained previously. The fact that these serine linker mutants support our previous results shows that the function seen with GFP-H1-H2 previously was not due to the sequence of the linker tested, but is in fact likely a result of the spacing of the hydrophobic domains.

Deletion of hydrophobic residues impairs Yop1p function

The current model of the mechanism of Yop1p acting on membranes suggests that each of the two hydrophobic domains spans the lipid bilayer only part of the way, without penetrating the opposite face of the membrane. This model also suggests that the hydrophobic domains are the driving force in generating membrane curvature [1]. I decided to investigate what role the length of each hydrophobic domain, and therefore how far they extend through the lipid bilayer, plays in the ability of Yop1p to generate membrane tubules. Both hydrophobic domains of wild-type Yop1p are ~40 amino acids in length, thus, mutants were constructed where each hydrophobic domain was shortened in length. These shortened hydrophobic domain mutants were constructed in both the full length GFP-Yop1p (GFP-YOP1-Hs1^{28}, GFP-YOP1-Hs2^{29}) and in the functional GFP-H1-H2 construct (GFP-Hs1^{28}-H2, GFP-H1-Hs2^{29}, GFP-H1-H2^{30}, GFP-H1^{37}-H2, GFP-H1-H2^{34}, GFP-H1^{37}-H2^{34}). All of these shortened hydrophobic domain mutants were found to localize to ER membranes (Figure 2.10) and were tested for their ability to restore a tubular peripheral ER in the *rtn1Δrtn2Δyop1Δ* cells. Shortening the first hydrophobic domain to 28 or 30 amino acids resulted in non-functional proteins, with a majority of these cells containing peripheral ER sheets (4 +/- 4.3%, 22 +/- 6% cells with normal ER, respectively, Table 2.12) (Figure 2.10). However, shortening the first hydrophobic domain to 37 amino acids did not abolish the function of this protein, restoring a tubular morphology to the peripheral ER of the

rtn1Δrtn2Δyop1Δ cells (60 +/- 6.5% cells with normal ER, Table 2.12) (Figure 2.10). The inability of the 28 or 30 amino acid H1 mutants to restore peripheral ER tubules in the *rtn1Δrtn2Δyop1Δ* cells shows a strict requirement that the length of the first hydrophobic domain of Yop1p be greater than 30 amino acids, suggesting that this domain is, in part, the driving force in generating membrane curvature.

Shortening the second hydrophobic domain to 29 or 30 amino acids abolished the ability of these constructs to form a tubular peripheral ER in the *rtn1Δrtn2Δyop1Δ* cells (20.3 +/- 6.5%, 12.6 +/- 4.0% cells with normal ER, respectively, Table 2.12) (Figure 2.10), while shortening this domain to 34 amino acids did not affect its function (59.3 +/- 8.7% cells with normal ER, Table 2.12) (Figure 2.10). This result confirms that the second hydrophobic domain also contributes to the function of Yop1p and must be greater than 34 amino acids in length. Taken with the shortened H1 results, these results indicate that Yop1p deforms membranes through the presence of its long hydrophobic domains, and these domains must be at least 37 and 34 amino acids in length, for H1 and H2 respectively, in order to generate membrane tubules.

Table 2.12 Quantification of the indicated cell type with a normal peripheral ER, the length of the hydrophobic domain is critical for Yop1p function

RCY strain	Plasmid(s)	Slide 1 100 cells counted	Slide 2 100 cells counted	Slide 3 100 cells counted	Average	St. Dev.	Date analysis performed
4323	pRS315	6	3	7	5.33	2.08	1/12/10
4323	pRC4559	70	69	62	63.67	5.68	1/12/10
4323	pRC4797	61	66	53	60	6.55	1/12/10
4323	pRC4798	57	69	52	59.33	8.73	1/12/10
4323	pRC4799	48	67	59	58	9.53	1/12/10
4323	pRC4778	2	1	9	4	4.35	12/21/09
4323	pRC4780	17	9	12	12.67	4.04	2/12/10
4323	pRC4787	24	8	11	14.33	8.50	12/21/09
4323	pRC4777	16	22	28	22	6	12/21/09
4323	pRC4779	14	27	20	20.33	6.50	2/12/10

Figure 2.10. The length of the hydrophobic domain of Yop1p is critical for function. A. Fluorescence microscopy was used to monitor peripheral ER morphology in *rtn1Δrtn2Δyop1Δ* cells using RFP-KDEL expression. Cells expressing *GFP-H1-H2*, *GFP-Hs1*^{28}*-H2*, *GFP-H1-Hs2*^{29}, *GFP-H1-H2*^{30}, *GFP-H1*^{37}*-H2*, *GFP-H1-H2*^{34}, *GFP-H1*^{37}*-H2*^{34}, *GFP-YOP1-Hs1*^{28} and *GFP-YOP1-Hs2*^{29} are shown. B. Quantification of number of each cell type from A with a tubular peripheral ER. Numbers presented are presented as average+/- standard deviation. C. Sequence alignment of above constructs.

A.

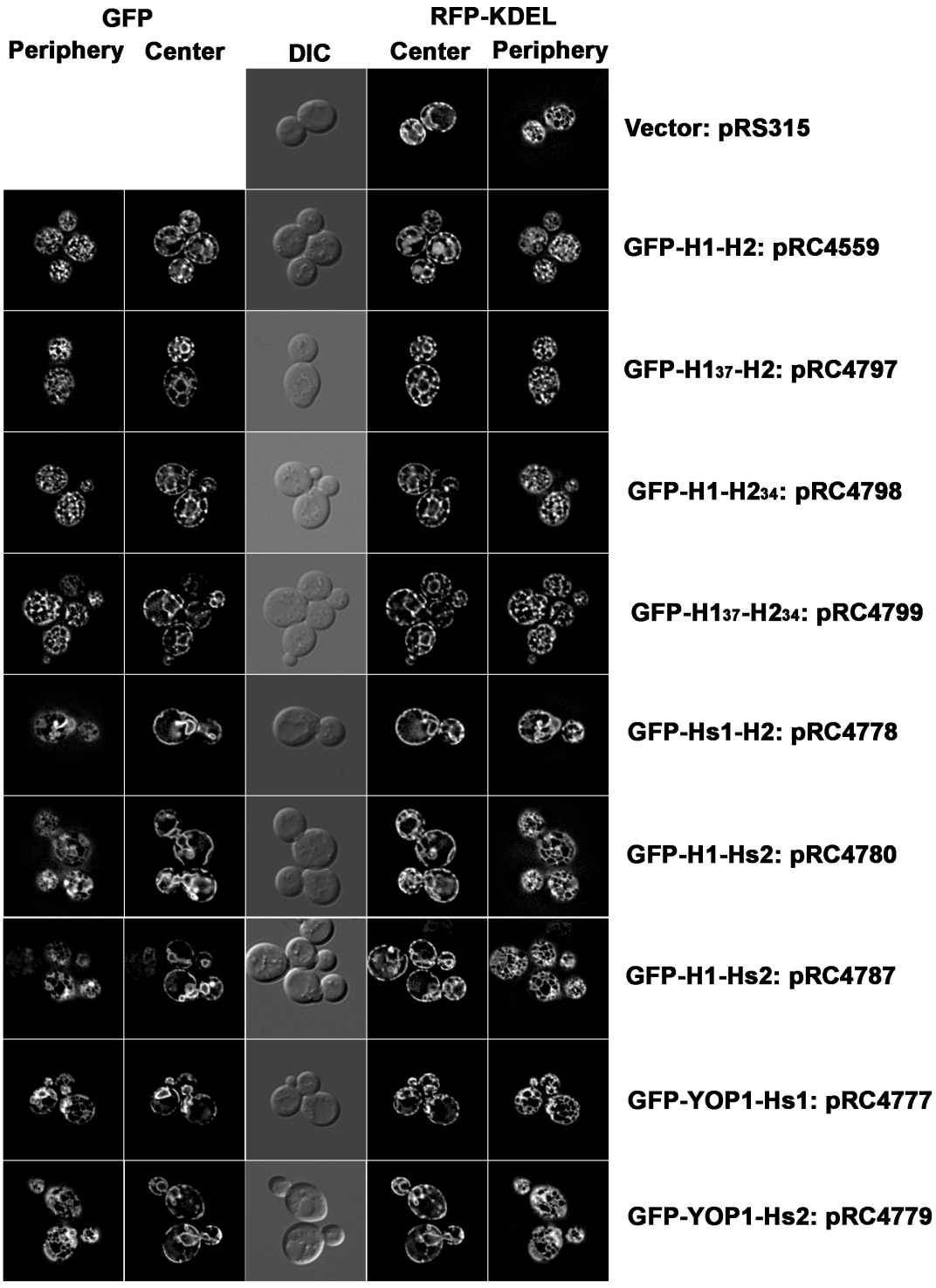
GFP
Periphery
Center
DIC
RFP-KDEL
Center
Periphery
Vector: pRS315
GFP-H1-H2: pRC4559
GFP-H1$_{37}$-H2: pRC4797
GFP-H1-H2$_{34}$: pRC4798
GFP-H1$_{37}$-H2$_{34}$: pRC4799
GFP-Hs1-H2: pRC4778
GFP-H1-Hs2: pRC4780
GFP-H1-Hs2: pRC4787
GFP-YOP1-Hs1: pRC4777
GFP-YOP1-Hs2: pRC4779

Figure 2.10 Continued

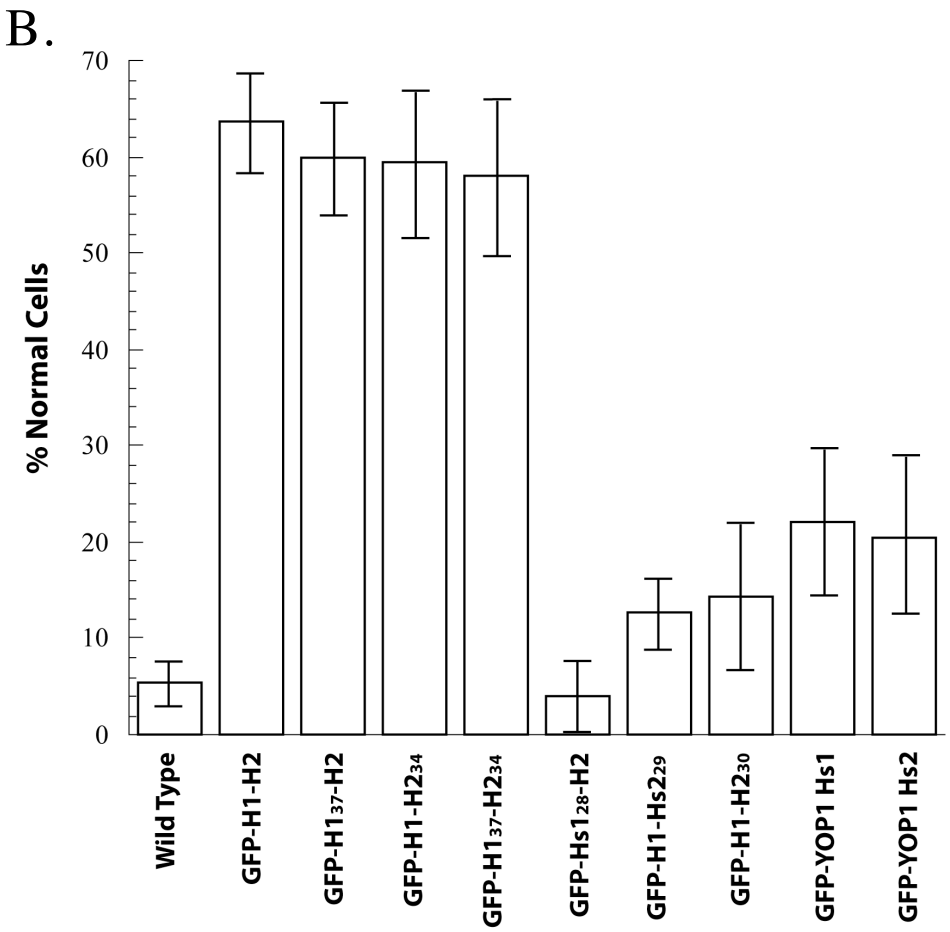

Figure 2.10 continued

C.

```
MSEYASSIHS QMKQFDTKYS GNRILQQLEN KTNLPKSYLV AGLGFAYLLL IFINVGGVGE ILSNFAGFVL PAYLSLVALK TPTSTDDTQL  YOP1
---------- ---------- ---------- KTNLPKSYLV AGLGFAYLLL IFINVGGVGE ILSNFAGFVL PAYLSLVALK TASAGSSA--L  H1-H2
---------- ---------- ---------- KTNLPKSYLV AGLGFAYLLL IFINVGGVGE ILSNFAG ---- ----------K TASAGSSA--L  H1[37]-H2
---------- ---------- ---------- KTNLPKSYLV AGLGFAYLLL IFINVGGVGE ILSNFAGFVL PAYLSLVALK TASAGSSA--L  H1-H2[34]
---------- ---------- ---------- KTNLPKSYLV AGLGFAYLLL IFINVGGVGE ILSNFAG ---- ----------K TASAGSSA--L  H1[37]-H2[34]
---------- ---------- ---------- KTNLPKSYLV ---------- ----------GE ILSNFAGFVL PAYLSLVALK TASAGSSA--L  Hs1[28]-H2
---------- ---------- ---------- KTNLPKSYLV AGLGFAYLLL IFINVGGVGE ILSNFAGFVL PAYLSLVALK TASAGSSA--L  H1-Hs2[29]
---------- ---------- ---------- KTNLPKSYLV AGLGFAYLLL IFINVGGVGE ILSNFAGFVL PAYLSLVALK TASAGSSA----  H1-H2[30]
MSEYASSIHS QMKQFDTKYS GNRILQQLEN KTNLPKSYLV AGLGFAYLLL ---------- ----------FVL PAYLSLVALK TPTSTDDTQL  YOP1-Hs1
MSEYASSIHS QMKQFDTKYS GNRILQQLEN KTNLPKSYLV AGLGFAYLLL IFINVGGVGE ILSNFAGFVL PAYLSLVALK TPTSTDDTQL  YOP1-Hs2

 LTYWIVFSFL SVIEFWSKAI LYLIPFYWFL KTVFLIYIAL PQTGGARMIY QKIVAPLTDR YILRDVSKTE KDEIRASVNE ASKATGASVH  YOP1
 LTYWIVFSFL SVIEFWSKAI LYLIPFYWFL KTVFLIYIAL PQTGGA------ ---------- ---------- ---------- ----------  H1-H2
 LTYWIVFSFL SVIEFWSKAI LYLIPFYWFL KTVFLIYIAL PQTGGA------ ---------- ---------- ---------- ----------  H1[37]-H2
 LTYWIVFSFL SVIEFWSKAI LYLIPFYWFL KTVF ------- ---------- ---------- ---------- ---------- ----------  H1-H2[34]
 LTYWIVFSFL SVIEFWSKAI LYLIPFYWFL KTVF-------- ---------- ---------- ---------- ---------- ----------  H1[37]-H2[34]
 LTYWIVFSFL SVIEFWSKAI LYLIPFYWFL KTVFLIYIAL ---------- ---------- ---------- ---------- ----------  Hs1[28]-H2
 LTYWIVFS--- ---------- LYLIPFYWFL KTVFLIYIAL ---------- ---------- ---------- ---------- ----------  H1-Hs2[29]
 ----------L SVIEFWSKAI LYLIPFYWFL KTVFLIYIAL ---------- ---------- ---------- ---------- ----------  H1-H2[30]
 LTYWIVFSFL SVIEFWSKAI LYLIPFYWFL KTVFLIYIAL PQTGGARMIY QKIVAPLTDR YILRDVSKTE KDEIRASVNE ASKATGASVH  YOP1-Hs1
 ----------  ---------- LYLIPFYWFL KTVFLIYIAL PQTGGARMIY QKIVAPLTDR YILRDVSKTE KDEIRASVNE ASKATGASVH  YOP1-Hs2
```

Putative membrane-embedded charged residues are critical for Yop1p function

Upon closer inspection of the primary amino acid sequence of the hydrophobic domains of *YOP1*, I noticed a few interesting, conserved residues, all highly charged and predicted to be buried within the membrane. These highly charged residues (E61, E104, K108 and K121) are all found within the putative hydrophobic domains and it is unlikely that these amino acids would be membrane embedded without their charge being neutralized (Figure 2.11). E and K are often found in salt bridges that neutralize their charges [22]. Considering the specificity of the interaction between H1 and H2 it is possible these residues interact to hold the two hydrophobic domains together within the membrane, giving Yop1p a wedge shape within the membrane or some other more complex structure. I constructed GFP-*yop1* point mutants where each E was replaced with a K, and visa versa (GFP-*yop1* E61K, GFP-*yop1* E104K, GFP-*yop1* K108E, GFP-*yop1* K121E). If any of these residues are critical for Yop1p function and are involved in salt bridge formation I would expect the single mutant to be non-functional. Creating the complementary double mutant (E to K and K to E) should restore the ability to form the salt bridge and thus restore Yop1p function. GFP-*yop1* E61K and GFP-*yop1* K108E were both found to function in restoring a tubular peripheral ER in the *rtn1Δrtn2Δyop1Δ* cells (60.3 +/- 8.5%, 58.7 +/- 6.1% cells with normal ER, respectively, Table 2.13) (Figure 2.12), suggesting these two residues are not critical for Yop1p function, or that the substitutions do not disrupt the structure of Yop1p enough to abolish activity. GFP-*yop1* E104K and GFP-*yop1* K121E were both found to be unable to restore a tubular morphology to the peripheral ER of the *rtn1Δrtn2Δyop1Δ* cells (28.3 +/- 3.2%, 28.6 +/- 6.6% cells with normal ER, respectively, Table 2.13) (Figure 2.12). These results confirm that the identities of these residues are critical for Yop1p to restore tubules in the peripheral ER, suggesting that both of these residues (E104 and K121) play a role in Yop1p function. However, I

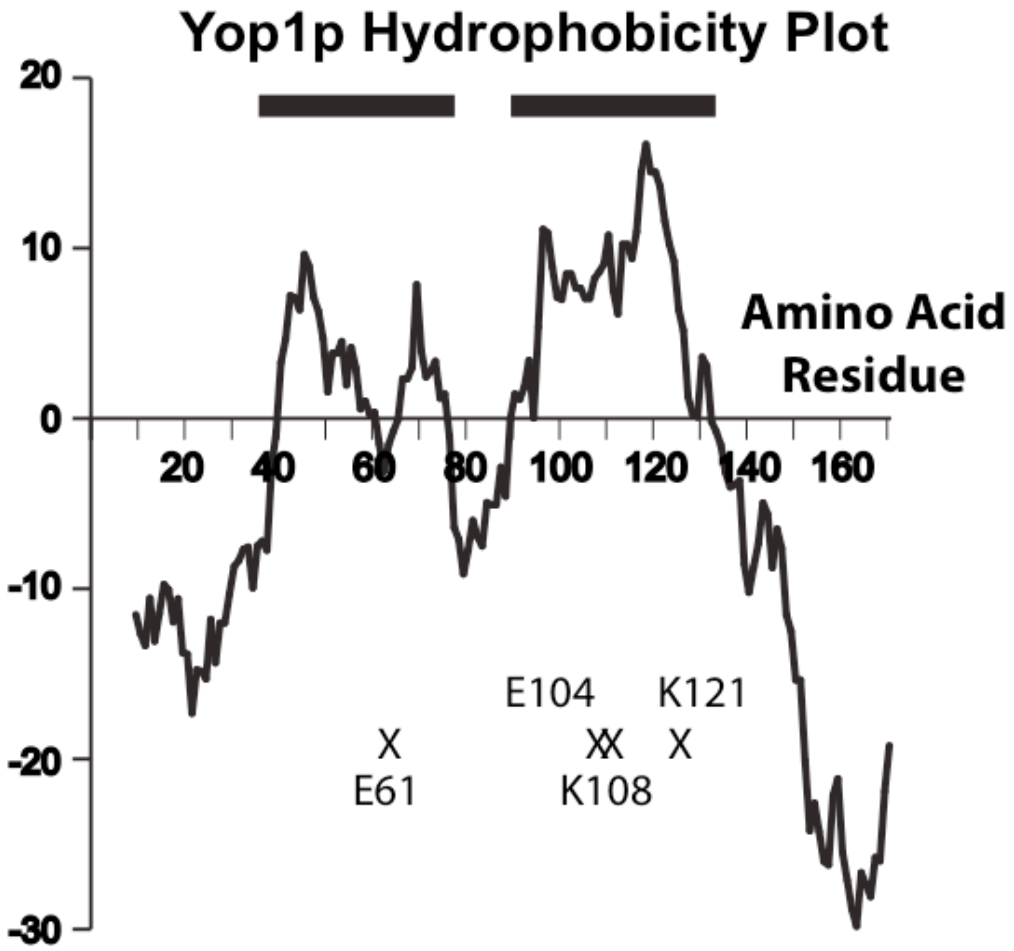

Figure 2.11. Yop1p hydrophobicity plot indicating the positions of the four putative membrane-embedded charged residues. Note their locations within the long hydrophobic domains of Yop1p.

cannot rule out the possibility that these mutations may decrease the stability of Yop1p, thereby affecting the ability to function in membrane tubulation. It is also possible that these residues contribute to the formation of membrane curvature through their charged state, which would repel the hydrophobic tails of lipids within the membrane. By replacing these residues with hydrophobic amino acids I could test this possibility more directly.

Table 2.13 Quantification of cells with a normal peripheral ER morphology, putative charge embedded residues critical for Yop1p function

RCY strain	Plasmid(s)	Slide 1 100 cells counted	Slide 2 100 cells counted	Slide 3 100 cells counted	Average	St. Dev.	Date Analysis Performed
4323	pRS315	3	2	8	4.3	3.2	1/12/10
4323	pRC504	54	62	68	63.6	8.3	1/12/10
4323	pRC4794	70	54	57	60.3	8.5	1/12/10
4323	pRC4793	32	26	27	28.3	3.2	1/12/10
4323	pRC4792	52	64	60	58.6	6.1	1/12/10
4323	pRC4791	23	36	27	28.6	6.5	1/12/10
4323	pRC4795	29	18	26	24.3	5.6	1/12/10
4323	pRC4796	66	51	62	60	6.5	1/12/10
4323	pRC4819	28	34	17	26.3	8.2	1/12/10
4323	pRC4829	6	11	6	7.7	2.9	7/20/10

Figure 2.12 Membrane embedded residues critical for Yop1p function. A. Fluorescence microscopy was used to monitor peripheral ER morphology in *rtn1Δrtn2Δyop1Δ* cells using RFP-KDEL expression. Cells expressing *GFP-yop1 E61K, GFP-yop1 E104K, GFP-yop1 K108E, GFP-yop1 K121E, GFP-yop1 E61K K108E, GFP-yop1 E104K K108E, GFP-yop1 E61K K121E* and *GFP-yop1 E104K K121E* are shown. B. Quantification of number of each cell type from A with a tubular peripheral ER. Numbers presented are presented as average+/- standard deviation.

A.

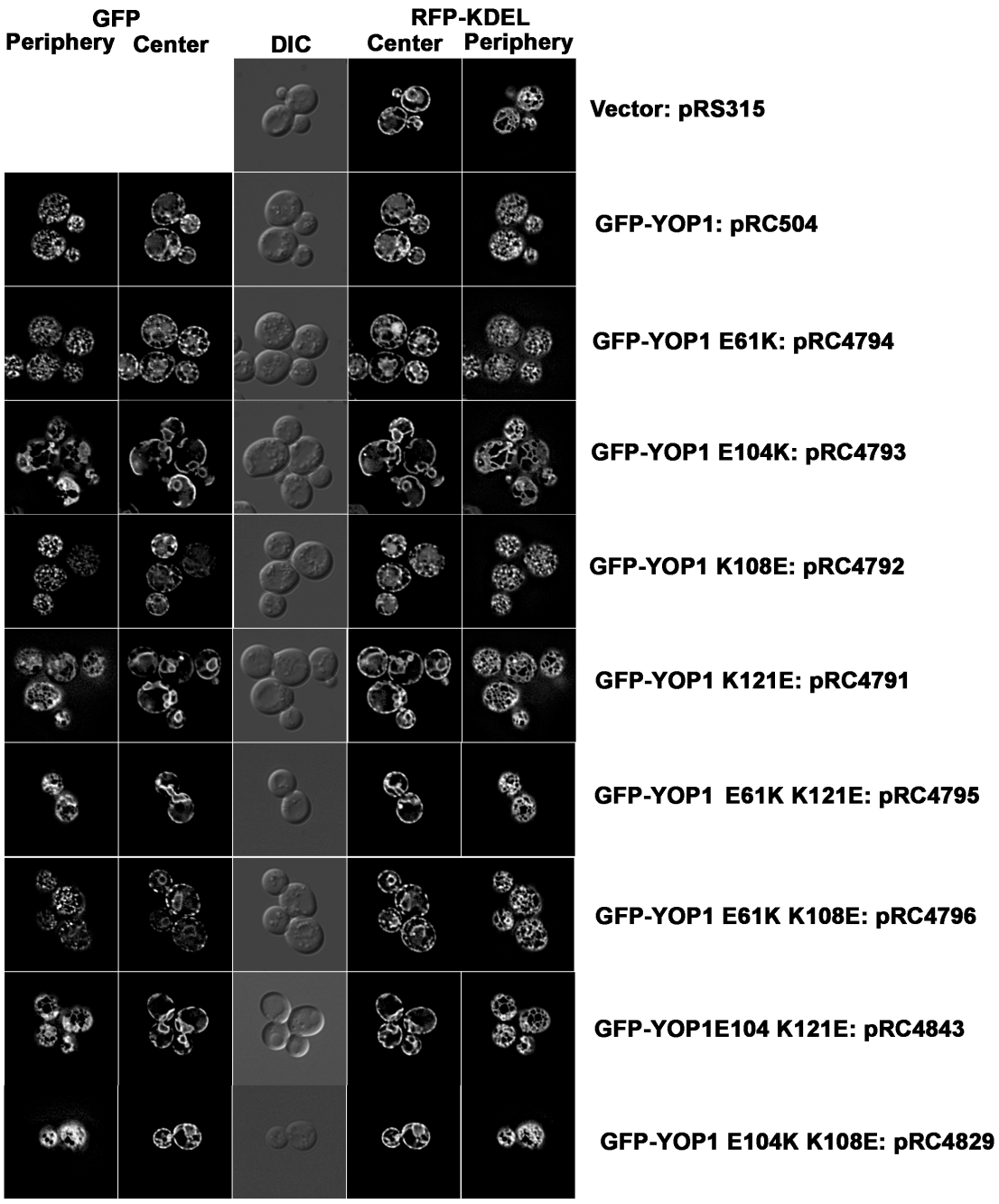
GFP
Periphery
Center
DIC
RFP-KDEL
Center
Periphery
Vector: pRS315
GFP-YOP1: pRC504
GFP-YOP1 E61K: pRC4794
GFP-YOP1 E104K: pRC4793
GFP-YOP1 K108E: pRC4792
GFP-YOP1 K121E: pRC4791
GFP-YOP1 E61K K121E: pRC4795
GFP-YOP1 E61K K108E: pRC4796
GFP-YOP1E104 K121E: pRC4843
GFP-YOP1 E104K K108E: pRC4829

Figure 2.12 continued

B.

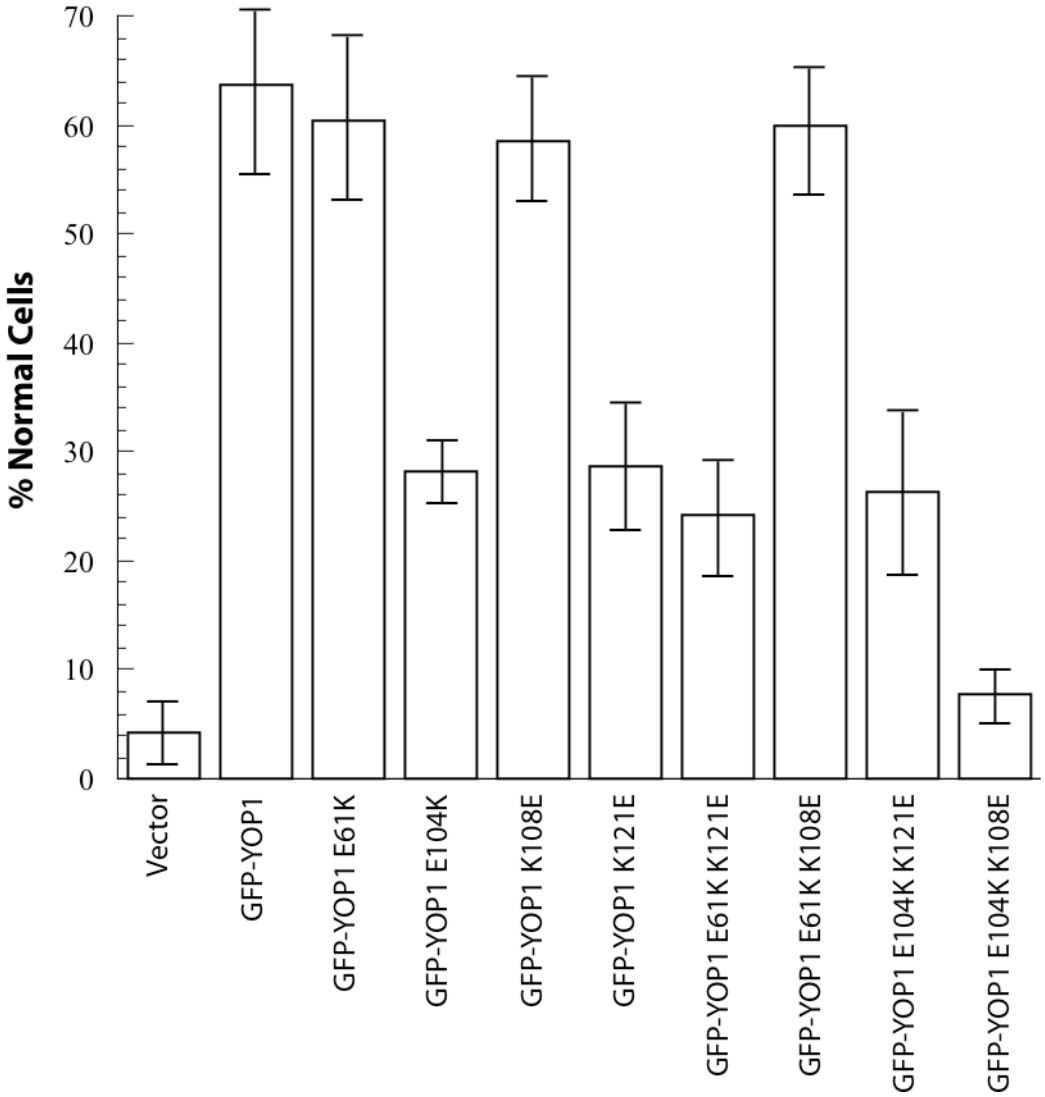

I then created each combination of double mutant (GFP-*yop1* E61K K108E, GFP-*yop1* E104K K108E, GFP-*yop1* E61K K121E and GFP-*yop1* E104K K121E) to account for the possibility that E61 or E104 could be bridging with K108 or K121 to give the hydrophobic domains of Yop1p the necessary conformation to function in tubule formation. I found that only the GFP-*yop1* E61K K108E mutant was functional in restoring a tubular peripheral ER in the *rtn1Δrtn2Δyop1Δ* cells (60 +/- 6.5% cells with normal ER, Table 2.12) (Figure 2.11). All the other double mutants were found to be non-functional (GFP-*yop1* E104K K108E 7.7 +/- 2.9%, GFP-*yop1* E61K K121E 24.3 +/- 5.7%, GFP-*yop1* E104K K121E 26.3 +/- 8.3% cells with normal ER, Table 2.12) (Figure 2.11). It is likely that the E61K K108E mutant was functional because neither of these residues were found to be critical for Yop1p function in the single point mutants. Also, all of the other double mutants contain either the E104K mutation or the K121E mutation and are likely non-functional due to the presence of one of these point mutations (found to be non-functional in the single point mutants) and not because of the secondary mutation (either E61K or K108E). Considering the single mutants E104K and K121E were both non-functional, it was possible that these two residues may be involved in the formation of a salt-bridge. However, I found that the double mutant (E104K K121E) was unable to restore a tubular peripheral ER, thus it is unlikely that these residues are neutralized through a salt bridge. This result suggests that these residues (E104 and K121) are important for Yop1p to function but assert their affect through some as yet undetermined means. How these residues contribute to the function of Yop1p is unclear but considering the length of the hydrophobic domains, ~40 amino acids, each hydrophobic domain could theoretically span the lipid bilayer and penetrate the opposite leaflet or have some more complex and less defined structure within the membrane. Perhaps these charged residues are exposed to the

aqueous environment of either the ER lumen (if they span the bilayer) or the cytosol (if they form some other more complex structure) to aid in Yop1p adopting a functional conformation. Further studies are needed to determine the structure of the hydrophobic domains of Yop1p.

DISCUSSION

Previous studies have provided evidence supporting a role for Yop1p in the formation of the tubules of the peripheral ER [1-4]. Voeltz et al [1] have proposed a model for the mechanism of Yop1p action on membranes that results in membrane deformation. These studies suggest that the two hydrophobic domains of Yop1p drive membrane deformation through their presence within the membrane, though the molecular details that govern Yop1p function are poorly understood. A previous study has suggested that the ability of Yop1p to form homo-oligomeric complexes is critical for tubule formation and the formation of these complexes may be mediated through interactions of the hydrophobic regions of Yop1p [2]. To dissect the individual role each hydrophobic domain of Yop1p plays in its ability to function in tubule formation I generated mutants lacking H1 or H2 and tested them for their ability to restore a tubular peripheral ER in *rtn1Δrtn2Δyop1Δ* cells. Deletion of either hydrophobic domain from Yop1p resulted in a loss of function (Figure 2.5), indicating that these regions contribute to the ability of Yop1p to form tubular membranes. Expression of GFP-Yop1ΔH1 and GFP-Yop1ΔH2 together were also unable to function (Figure 2.5), indicating that both hydrophobic domains need to be physically linked together to function (as in Yop1p). It is possible that these two mutants are unable to bind to one another, which would suggest that oligomer formation is mediated through interactions of the hydrophobic domains and that the hydrophilic regions of Yop1p are not required to generate higher order complex formation. It is also possible that, if H1

and H2 cannot interact intramolecularly in these mutants (because one is missing), the shape of Yop1p is altered and thus its ability to generate membrane curvature is decreased. Further studies aimed at the ability of these proteins to oligomerize would distinguish between these possibilities. Analysis of the level of expression of these constructs is also needed to ensure that the lack of function noted in my results is due to the missing hydrophobic domain and not because the mutant protein is expressed at a lower level than GFP-Yop1p.

The model proposed by Voeltz et al [1] suggests that the insertion of the hydrophobic domains into the membrane is the driving force in tubule formation. To understand more clearly the role of each hydrophobic domain in this process, as well as to investigate if the hydrophilic regions of Yop1p are dispensable for function, I tested just the hydrophobic domains of Yop1p, fused to GFP, for their ability to function in peripheral ER tubule formation in the *rtn1Δrtn2Δyop1Δ* cells. Expression of the individual hydrophobic domains, GFP-H1 or GFP-H2, were both unable to restore a tubular peripheral ER in the *rtn1Δrtn2Δyop1Δ* cells (Figure 2.6). Even when expressed together these proteins could not function. These results may indicate that these two domains must be held in close proximity to one another to interact properly for function. It is also possible that the hydrophilic regions of Yop1p are in fact critical for membrane tubulation and being absent from these mutants is the reason they cannot function. Western blot analysis investigating the level of expression of these mutant constructs would rule out the possibility that the lack of function is due to a decreased expression level/stability.

To determine if the hydrophilic regions of Yop1p are necessary for function and if the two hydrophobic domains need to be held close together to form the tubules of the peripheral ER, I generated a construct with both H1 and H2 separated by an artificial linker (KTASAGSSA), GFP-H1-H2. *rtn1Δrtn2Δyop1Δ* cells expressing this

construct were found to have a normal tubular peripheral ER, similar to GFP-Yop1p expressing cells (Figure 2.6). This result shows that the information necessary for tubule formation is contained within the hydrophobic domains of Yop1p, both of which are critical for function. Furthermore, the hydrophilic regions of Yop1p appear to be dispensable for normal function. This result suggests the physical presence of the hydrophobic domains within the membrane drives membrane tubulation and that the hydrophobic domains need to be physically close to one another to form membrane tubules. Further studies are needed to determine exactly how the hydrophobic domains interact within the membrane.

To determine if H1 and H2 interact specifically or if this interaction is simply due to hydrophobic attractions, I designed constructs in which the identity and organization of the hydrophobic domains of Yop1p were reorganized. GFP-H1-H2 is able to function like wild-type Yop1p; however, any alteration of the organization of the hydrophobic domains (GFP-H1-H1, GFP-H2-H2) abolishes their ability to restore a tubular peripheral ER in the *rtn1Δrtn2Δyop1Δ* cells (Figure 2.7). This fact suggests that H1 interacts in a specific manner with H2 within the membrane and that both H1 and H2 are absolutely required for function. Also, these results suggest it is unlikely that the interaction between H1 and H2 is due to non-specific hydrophobic clustering of these domains. The proposed model suggests that Yop1p adopts a wedge-like conformation within the membrane, a shape that drives disruption of the outer leaflet of the membrane generating membrane curvature [1]. My results confirm there is likely a specific interaction between H1 and H2 and that this interaction may aid in Yop1p forming this wedge-like structure. Interestingly, a reversal of the functional, GFP-H1-H2 construct, namely H2-H1-GFP, was unable to restore a tubular peripheral ER in the *rtn1Δrtn2Δyop1Δ* cells (Figure 2.7). This fact suggests that the interaction between H1 and H2 has an asymmetry that cannot be mimicked in the reversed H2-

H1-GFP. The H2-H1-GFP construct may not fold into the proper shape during synthesis due to the reversed order of the hydrophobic domains, which could have drastic effects on its ability to function. Alternatively, it is possible that this protein is expressed at a lower level or has a decreased stability and is rapidly degraded. Further studies are needed to distinguish these possibilities.

The interaction between H1 and H2 appears to be a critical factor in Yop1p function, likely contributing to formation of a conformation that drives membrane deformation. In order for Yop1p to adopt the proposed wedge-like shape within the membrane, the two hydrophobic domains must be physically linked. The linker region between H1 and H2 is approximately 9 amino acids long in wild-type Yop1p as well as in the GFP-H1-H2 construct. Considering the requirement for H1 and H2 to be physically linked for function, I sought to understand if this linker region plays a role in the ability of Yop1p to function, and thus to investigate its role in generating a functional conformation. To accomplish this analysis the linker region between H1 and H2 was lengthened to 13 and 19 amino acids and tested for function in the *rtn1Δrtn2Δyop1Δ* cells. Both of these constructs were found to be functional (Figure 2.8), suggesting that the hydrophobic domains are in close enough proximity to interact in these mutants to give Yop1p a functional conformation. However, when GFP was inserted between H1 and H2, H1-GFP-H2, this protein lost the ability to restore tubules in the peripheral ER (Figure 2.8). These results show that slightly longer linker regions do not disrupt the ability of H1 and H2 to interact, but too much distance between the two hydrophobic domains does not allow this interaction to occur.

To further investigate the possibility that this linker region acts as a spacer, holding the surface exposed ends of the hydrophobic domains apart, I created a series of H1-H2 constructs where the linker region was shortened successively. I tested these

mutants for function in the *rtn1Δrtn2Δyop1Δ* cells to determine if there is a minimum spacing required for Yop1p to function normally. The results of these experiments suggest that the linker region between H1 and H2 must be at least 5-6 amino acids to maintain normal function. Shorter linker regions result in non-functional proteins (Figure 2.8) indicating that the linker region likely acts as a spacer, holding the cytosol-exposed ends of the hydrophobic domains apart. This result, taken with the model that the hydrophobic domains interact within the membrane, suggests that Yop1p adopts a wedge-like conformation with the linker region acting to hold the ends of H1 and H2 apart, while interactions between H1 and H2 within the membrane maintain the wedge-like shape. Analysis of the expression level of these constructs is still needed to confirm that their ability to function (or lack thereof) can be attributed to their specific mutation rather than to a lower expression level or decreased stability. Additionally, the analysis of the functionality of each of the constructs in this chapter were conducted on a single YOP1 mutant. In order to confirm these results independently created constructs will need to be tested.

The hydrophobic domains of Yop1p both contain a number of conserved charged residues, predicted to be membrane embedded (E61, E104, K108 and K121, Figure 2.11). It is unlikely that these charged amino acids would be present in a charged state within the hydrophobic environment of the membrane. My results suggesting an interaction between H1 and H2 that is necessary for Yop1p function led me to consider the possibility that these charged residues are involved in this interaction. E is capable of forming a salt bridge with K, neutralizing both charges in the process [22]. To test the possibility that the charged residues in the hydrophobic domains of Yop1p are involved in the interaction between H1 and H2, single point mutants were first created that would disrupt any salt bridge formation (E61K, E104K, K108E and K121E respectively). I tested these single point mutants for function in

restoring peripheral ER tubules in the *rtn1Δrtn2Δyop1Δ* cells. Both mutations E61K and K108E did not disrupt Yop1p function, but mutations in E104K and K121E both abolished the ability of Yop1p to form peripheral ER tubules (Figure 2.11). These results identified two residues, E104 and K121 (both in H2), that are required for Yop1p to form the tubules of the peripheral ER and suggest these amino acids may be involved in maintaining a functional conformation. While these residues may be neutralized in a salt bridge, this would not contribute to the interaction between H1 and H2, as both E104 and K121 are located within H2. Perhaps these residues contribute to the structuring of the second hydrophobic domain within the membrane.

Double point mutants were next constructed to determine if any combination of these 4 residues are involved in the formation of a salt bridge. By replacing E with K, and K with E, any possible salt bridge formation (that was lost in the single mutant) would be restored in the double mutant. E61K K121E, E104K K121E, and E104K K108E all tested for function in the *rtn1Δrtn2Δyop1Δ* cells were found to be non-functional. E61K K108E was however found to retain the ability to restore a tubular peripheral ER (Figure 2.11). These results do not confirm the presence of salt bridge neutralization between any of the amino acids tested, as none of the double mutants regained function. These results did however identify two charged amino acids located within H2 that are important for Yop1p function, E104 and K121, which is likely the reason any double mutant containing these individual mutations were found to be non-functional. Perhaps these charged residues contribute to the conformation of the second hydrophobic domain, thus affecting the shape of Yop1p within the membrane. These residues may be exposed to the cells aqueous environment, altering the proposed hairpin structure of this domain (H2) into something more complex than an alpha helix. Further studies investigating the topology of Yop1p within the membrane more closely would elucidate whether these residues are indeed cytosol exposed or if

they assert their effect on Yop1p function through other means. Analysis of the level of expression of each of these constructs is needed to validate the above results and rule out the possibility that decreased expression/stability is not the reason for their lack of function.

REFERENCES

1. Voeltz, G.K., et al., *A class of membrane proteins shaping the tubular endoplasmic reticulum*. Cell, 2006. **124**(3): p. 573-86.
2. Shibata, Y., et al., *The reticulon and DP1/Yop1p proteins form immobile oligomers in the tubular endoplasmic reticulum*. J Biol Chem, 2008. **283**(27): p. 18892-904.
3. Hu, J., et al., *A class of dynamin-like GTPases involved in the generation of the tubular ER network*. Cell, 2009. **138**(3): p. 549-61.
4. Hu, J., et al., *Membrane proteins of the endoplasmic reticulum induce high-curvature tubules*. Science, 2008. **319**(5867): p. 1247-50.
5. Oertle, T., et al., *A reticular rhapsody: phylogenic evolution and nomenclature of the RTN/Nogo gene family*. FASEB J, 2003. **17**(10): p. 1238-47.
6. Papaloukas, C., et al., *Estimating the length of transmembrane helices using Z-coordinate predictions*. Protein Sci, 2008. **17**(2): p. 271-8.
7. Krishnakumar, S.S. and E. London, *Effect of sequence hydrophobicity and bilayer width upon the minimum length required for the formation of transmembrane helices in membranes*. J Mol Biol, 2007. **374**(3): p. 671-87.
8. Tolley, N., et al., *Overexpression of a plant reticulon remodels the lumen of the cortical endoplasmic reticulum but does not perturb protein transport*. Traffic, 2008. **9**(1): p. 94-102.
9. Calero, M., G.R. Whittaker, and R.N. Collins, *Yop1p, the yeast homolog of the polyposis locus protein 1, interacts with Yip1p and negatively regulates cell growth*. J Biol Chem, 2001. **276**(15): p. 12100-12.

10. Chen, C.Z., et al., *Genetic analysis of yeast Yip1p function reveals a requirement for Golgi-localized rab proteins and rab-Guanine nucleotide dissociation inhibitor*. Genetics, 2004. **168**(4): p. 1827-41.
11. Heidtman, M., et al., *A role for Yip1p in COPII vesicle biogenesis*. J Cell Biol, 2003. **163**(1): p. 57-69.
12. Calero, M. and R.N. Collins, *Saccharomyces cerevisiae Pra1p/Yip3p interacts with Yip1p and Rab proteins*. Biochem Biophys Res Commun, 2002. **290**(2): p. 676-81.
13. Chen, C.Z. and R.N. Collins, *Insights into biological functions across species: examining the role of Rab proteins in YIP1 family function*. Biochem Soc Trans, 2005. **33**(Pt 4): p. 614-8.
14. Calero, M., et al., *Dual prenylation is required for Rab protein localization and function*. Mol Biol Cell, 2003. **14**(5): p. 1852-67.
15. Calero, M., N.J. Winand, and R.N. Collins, *Identification of the novel proteins Yip4p and Yip5p as Rab GTPase interacting factors*. FEBS Lett, 2002. **515**(1-3): p. 89-98.
16. Bevis, B.J. and B.S. Glick, *Rapidly maturing variants of the Discosoma red fluorescent protein (DsRed)*. Nat Biotechnol, 2002. **20**(1): p. 83-7.
17. Prinz, W.A., et al., *Mutants affecting the structure of the cortical endoplasmic reticulum in Saccharomyces cerevisiae*. J Cell Biol, 2000. **150**(3): p. 461-74.
18. Bevis, B.J., et al., *De novo formation of transitional ER sites and Golgi structures in Pichia pastoris*. Nat Cell Biol, 2002. **4**(10): p. 750-6.
19. Hammond, A.T. and B.S. Glick, *Dynamics of transitional endoplasmic reticulum sites in vertebrate cells*. Mol Biol Cell, 2000. **11**(9): p. 3013-30.

20. Dreier, L. and T.A. Rapoport, *In vitro formation of the endoplasmic reticulum occurs independently of microtubules by a controlled fusion reaction*. J Cell Biol, 2000. **148**(5): p. 883-98.

21. Feng, D., et al., *The transmembrane domain is sufficient for Sbh1p function, its association with the Sec61 complex, and interaction with Rtn1p*. J Biol Chem, 2007. **282**(42): p. 30618-28.

22. Marqusee, S. and R.L. Baldwin, *Helix stabilization by Glu-...Lys+ salt bridges in short peptides of de novo design*. Proc Natl Acad Sci U S A, 1987. **84**(24): p. 8898-902.

CHAPTER 3

MORPHOLOGICAL AND BIOCHEMICAL ANALYSIS OF YOP1-INDUCED MEMBRANE TUBULES

ABSTRACT

There is recent evidence that Yop1p functions in the formation of the tubules of the peripheral ER through a membrane wedging mechanism, likely a redundant function shared with Rtn1p. Furthermore, purified Yop1p has been shown to form membrane tubules in vitro, though these tubules have a narrow diameter compared to the peripheral ER tubules. Here I show that Yop1p overexpression results in an accumulation of tubular structures and these tubules form from ER membranes. Furthermore, I show that the formation of Yop1p tubular structures does not require Rtn1p. I also developed a means to enrich for these tubular structures and show they contain a very narrow diameter, similar to the in vitro formed Yop1p tubules. These results strengthen our understanding of how Yop1p is acting on membranes in vivo and the types of membrane alterations Yop1p is capable of accomplishing.

INTRODUCTION

Previous studies have provided evidence that Yop1p is involved in the process of tubule formation in the peripheral ER [1-4]. Furthermore, purified Yop1p is capable of forming tubules from lipids in vitro. Interestingly, the tubules formed by purified Yop1p in vitro have a very small diameter [4], ~10-15 nm, compared to the diameter of the tubules in the peripheral ER (50-100 nm) [5]. Hu et al [4] have suggested that the diameter of the in vitro formed tubules is considerably smaller than those of the ER due to the high concentration of Yop1p in this artificial setting [2, 6, 7]. It is also possible that Yop1p acts in concert with other ER resident proteins and that these other proteins modulate Yop1p function and thereby contribute to the formation of the larger tubules of the peripheral ER.

Yop1p is known to interact with many ER resident proteins, which may also aid in the formation of the peripheral ER tubules. For example, Rtn1p is also thought to redundantly function in the formation and/or maintenance of the peripheral ER tubules and is known to form oligomeric complexes with Yop1p [1]. Additionally, YIP1/YIF1 family proteins physically interact with Yop1p and Rtn1p [8, 9]. It is possible that the tubules of the peripheral ER are formed through the combined action of all of these proteins together.

YIP1/YIF1 family proteins bind to Rab proteins in a prenylation-dependant manner [10, 11]. The binding of Rab proteins to YIP1/YIF1 family proteins may act as a signal, controlling the activity of YIP1/YIF1 family members as they interact with Yop1p. The Rab signal may alter the activity of Yop1p, Rtn1p, and other YIP1/YIF1 family proteins to regulate the generation of the tubules of the peripheral ER.

Sey1p is a dynamin-like GTPase that resides on the membranes of the ER, mainly on the tubules of the peripheral ER. Sey1p binds to Yop1p and is thought to aid in the formation of the junction points that connect the peripheral ER tubules [12,

13]. Considering the fact that Yop1p acts to form membrane tubules it is possible that Sey1p may function to form junction points by altering the ability of Yop1p to act on membranes, thereby facilitating the negative curvature required for a junction point to form when two tubules fuse. Furthermore, overexpression of Yop1p results in the formation of long, unbranched tubular structures perhaps due to an inability of these small diameter tubules to be acted upon by Sey1p [4].

This study aims to investigate the morphology of tubular structures formed by overexpression of Yop1p in vivo. I show that overexpression of Yop1p forms long, unbranched tubular structures from ER membranes, and the formation of these tubular structures does not require Rtn1p. I have developed an enrichment protocol to partially purify these tubular structures for further analysis. Furthermore, I show that the tubules formed by Yop1p overexpression have a morphology that is similar to the tubules generated by purified Yop1p from lipids in vitro strengthening our understanding of the function of Yop1p in vivo.

MATERIALS AND METHODS

Yeast strains and Plasmids

All *S. cerevisiae* strains used in this study are listed in table 3.1. Manipulations of these strains were using standard biological techniques. Cell density was determined using a Thermo Spectronic Genesys 10UV spectrophotometer (Rochester, NY) at 600nm. Overexpression studies were performed in *reg1Δ* cells. Overexpression of constructs under *GAL1/10* promotor control was performed by growing cells overnight in SD media to a density of 0.4-0.8. Cells were pelleted, washed once in ddH20, and resuspended in 1mL ddH20. Washed cells were inoculated into minimal media containing 2% galactose to an initial density of 0.05-0.2, depending on the length of induction.

Table 3.1 *S. cerevisiae* strains used in this study

RCY Strain	Genotype	Source
RCY239	*MAT***a** *ura3-52 leu2-3,112*	This lab
RCY4274	*MAT***a/α** *reg1*ΔKAN^R/ *reg1*ΔKAN^R *ura3Δ0/ ura3Δ0*, *leu2Δ0/ leu2Δ0*, *his3*Δ0/ *his3*Δ0, *lys2Δ0/ lys2Δ0*, *met15*Δ0/*MET15*	This lab
RCY4164	*MAT***a**, *yop1ΔHIS5*, *ura3*Δ0, *leu2*Δ0, *his3*Δ0	This lab
RCY4169	*MAT***a**, *yop1ΔHIS5*, *ura3*Δ0, *leu2*Δ0, *his3*Δ0	This lab
RCY4168	*MATα*, *rtn1ΔKAN^R yop1ΔHIS5 ura3Δ0 leu2Δ0 his3Δ0 lys2Δ0*	This lab
RCY4323	*MAT***a** *rtn1*ΔKAN^R *rtn2*ΔKAN^R *yop1ΔHIS5*, *ura3Δ0*, *leu2Δ0*, *his3*Δ0, *lys2Δ0*, *met15*Δ0	This lab

Table 3.2 Plasmids used in this study

Plasmid number	Construct	Source
pRC3588	pRS315 *RFP-KDEL*	This lab
pRC3589	pRS316 *RFP-KDEL*	This lab
pRC3825	pRS426 *GFP-YOP1*	This study
pRC4436	pRS426 *YOP1-GFP*	This study
pRC3822	pRS315 *RFP-RTN1*	This study

Plasmids were created using standard biological techniques and are listed in table 3.2. GFP fusions were made by linking yEGFP to the NH_2 or COOH terminus of each construct with a GGPGG linker between the GFP and the ORF. Overexpression of each construct was controlled by two means. First, by integrating the GFP-ORF fusion into a multi-copy (2μ) vector ensures many copies of each construct in cells to increase the production of the protein. Second, overexpression-constructs were placed under the control of the promotor region of *GAL1/10*, which initiates expression by the presence of galactose in the growth medium.

Purification of GFP-Yop1p tubules

1 liter culture of cells overexpressing GFP-Yop1p, as described above, were induced overnight (~16-24 hours) in galactose containing media and grown to a density of 0.5-0.8. Cells were pelleted at 3,500 rpm for 3 minutes, washed in 10 mL of SCE (1M sorbitol, 100mM citrate, 50mM EDTA) and pellleted again. Cells were then resuspended in 5mL SCE+zymolase to strip the cell walls and then gently lysed by the addition of an equal volume of 2X lysis buffer (final concentration 100mM Tris pH 8, 10mM EDTA). This suspension was then centrifuged at 300Xg for 3 minutes to pellet unbroken cells and dense material. The supernatant was then centrifuged at 20,000Xg to separate membrane and cytosolic fractions. The pellet was resuspended in 1X lysis buffer and loaded in the bottom of a stepwise sucrose flotation gradient. The flotation gradient contains 3 cushions of sucrose, 52% w/v on the bottom, 45% w/v in the center, and 10%w/v on the top. This gradient was centrifuged at 40,000 rpm for 16 hours, separating dense material (pelleted) from a heavy membrane fraction (between the 45% and 10% cushions) and a light membrane fraction (on top of the 10% cushion). GFP-Yop1p tubules are present in the heavy membrane fraction and were collected by pipette. This fraction was then loaded on the top of a linear sucrose gradient (20-60%) and centrifuged at 20,000 rpm for 1 hour, then 15 1 mL fractions were collected. GFP-Yop1p tubules were present in fraction 8 when analyzed by fluorescence microscopy. Detergent sensitivity of GFP-Yop1p tubules was done by adding an equal volume of 0.4% TritonX-100 (final concentration of 0.2%) to a small volume of resuspended tubules. Salt resistance was determined by adding an equal volume of 1M NaCl or KCl (final concentration of 500mM for each salt) to a small volume of purified tubules.

Fluorescence Microscopy

GFP fusions of *YOP1* were created using 238 amino acids of yeast enhanced green fluorescence protein (yEGFP) fused to the NH_2 terminus separated by a GGPGG linker. The promotor region of *GAL1/10* was used to induce GFP-Yop1p expression upon the addition of galactose to the growth media. RFP-KDEL expression was used to visualize ER structures. Cells were grown to mid-log phase in minimal media and pelleted, washed once in ddH_2O and resuspended in minimal media plus galactose to a density of ~0.1. Inductions were carried out for various time lengths depending on the experiment, as indicated in the results section. Images were collected using a Nikon Eclipse E600 microscope with a 100X (1.4NA) objective and 1x optivar. DIC images were collected from a single plane while fluorescence images were gathered as a series of 20-30 z steps of 0.2 μm. A CCD camera (Sensicam EM High Performance, The Cook Corporation) was used to collect images (software IP Lab version 3.6.5, Scanalytics). Blind deconvolution of each z-series was done using AutoQuant X2 program (Media Cybernetics) for 30 iterations. After deconvolution, single planes were identified that most clearly identified single tubular structures. Microscopy of purified GFP-Yop1p tubules was performed by spotting purified tubule preparations directly onto a glass slide and visualized.

Electron Microscopy

GFP-Yop1p tubules were applied to carbon coated electron microscopy grids for 5-15 seconds to allow tubules to settle on the grid then washed with buffer (100 mM Tris pH8, 50 mM NaCl). The tubules were fixed by the addition of 2% gluteraldehyde (in buffer, 100mM Tris pH 8, 50mM NaCl) for 5 minutes. Tubules were then stained by the addition of 1% uranyl acetate (in 1X lysis buffer) for 3-10 seconds. Grids were viewed on an electron microscope (Philips model 201) at 80kV.

Immunogold labeling of tubules was performed initially as described above. Prior to staining with uranyl acetate, grids were incubated for 1 hour with mouse anti-GFP monoclonal antibodies (Chemicon) in a humidification chamber, then washed 10 times with buffer (100mM Tris pH 8, 50mM NaCl). Secondary goat-anti-mouse antibody, conjuagated to 5 nm colloidal gold particles, was applied for 1 hour to the grids, then washed 15 times in buffer. Grids were then stained with uranyl acetate and viewed on the electron microscope as described above.

RESULTS

Overexpression of Yop1 p results in the formation of tubular structures.

Previous studies have established a role for Yop1p in the formation of the tubules of the peripheral ER [1-4]. Furthermore, thin section electron microscopy of cells overexpressing Yop1p show an accumulation of ER membranes [9]. These two facts suggest that the accumulated ER structures may be composed of membrane tubules. To further analyze the morphology of the ER membranes that accumulate during Yop1p overexpression, GFP-Yop1p was induced in *reg1Δ* cells by growth in galactose containing media and the morphology of the structures formed were anyalyzed by fluorescence microscopy. The overexpression of GFP-Yop1p resulted in a dramatic accumulation of tubular structures within the cell after induction (Figure 3.1). The formation of these tubular structures may indicate a direct role for Yop1p in the formation of tubular structures in vivo. Considering the fact that Yop1p is involved in forming the tubules of the peripheral ER, I examined if these tubular structures co-localize with ER membranes by fluorescence microscopy. GFP-Yop1p was induced for 24 hours and ER membranes were analyzed using RFP-KDEL expression to monitor ER structures. The results of this analysis revealed that the tubular structures

formed by overexpression of GFP-Yop1p do not co-localize with the membranes of the ER (Figure 3.1). This is an unexpected result considering Yop1p localizes to ER membranes, as well as its role in the formation of the tubules of the peripheral ER. Previous studies of a related protein, reticulon, in plant cells have suggested that the tubular structures formed by reticulon overexpression exclude ER luminal proteins due to the small diameter of the tubules [14]. Reticulon and Yop1p are thought to act in redundant roles to form the tubules of the peripheral ER [1], and purified Rtn1p forms small diameter tubules in vitro, similar to the Yop1p formed tubules [4]. Thus, the exclusion of luminal proteins from GFP-Yop1p tubular structures would account for the lack of colocalization of the tubular structures with ER membranes.

To further examine the possibility that these tubular structures are formed from ER membranes, a time-course induction of GFP-Yop1p was conducted, monitoring the formation of tubules and the structure of the ER using fluorescence microscopy. Within one hour of GFP-Yop1p induction, short tubular structures begin to appear, and these structures co-localize with ER membranes as indicated by co-localization with RFP-KDEL. Further induction results in a lengthening of these tubules, which co-localize with ER membranes for at least 16 hours. However, by 24 hours after GFP-Yop1p induction these structures no longer co-localize perfectly with ER membranes, although regions of the tubular structures formed align with regions of the peripheral ER (Figure 3.1). Taken together these results indicate that the tubular structures formed by overexpression of GFP-Yop1p are formed from ER membranes and that between 16 and 24 hours of induction these tubules obtain a small enough diameter to exclude ER luminal proteins.

Figure 3.1. Overexpression of GFP-Yop1p results in an accumulation of tubular structures. A. Fluorescence images of wild-type cells overexpressing GFP-Yop1p, 8 hours after induction. B. *reg1Δ* cells expressing RFP-KDEL to visualize the ER. Images were collected after 24 hours of induction of GFP-Yop1p. C. Timecourse induction of GFP-Yop1 in *reg1*Δ cells (RCY4274). Fluorescence images collected at 1, 8, and 16 hours after induction of GFP-Yop1p were analyzed for ER structure using expression of RFP-KDEL to visualize ER morphology. D. *reg1Δ* cells expressing vector control or GFP-Yop1p under control of the *GAL1/10* promotor grown on SD+LHKM or SGal+LHKM for 3 days.

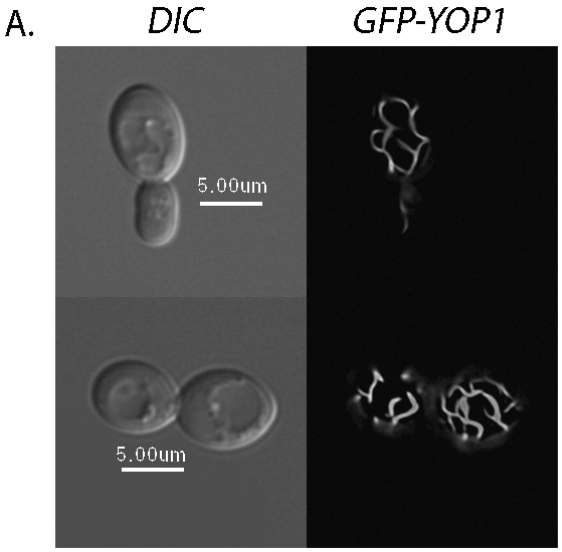
A.
DIC
GFP-YOP1
5.00um
5.00um

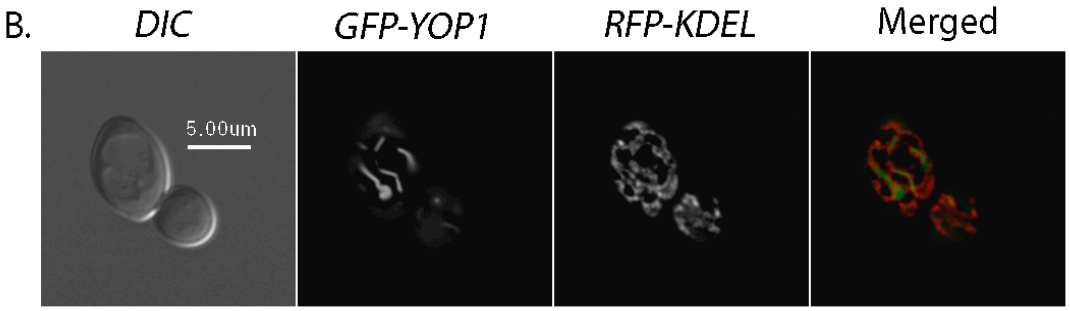
B.
DIC
GFP-YOP1
RFP-KDEL
Merged
5.00um

Figure 3.1 continued

C.

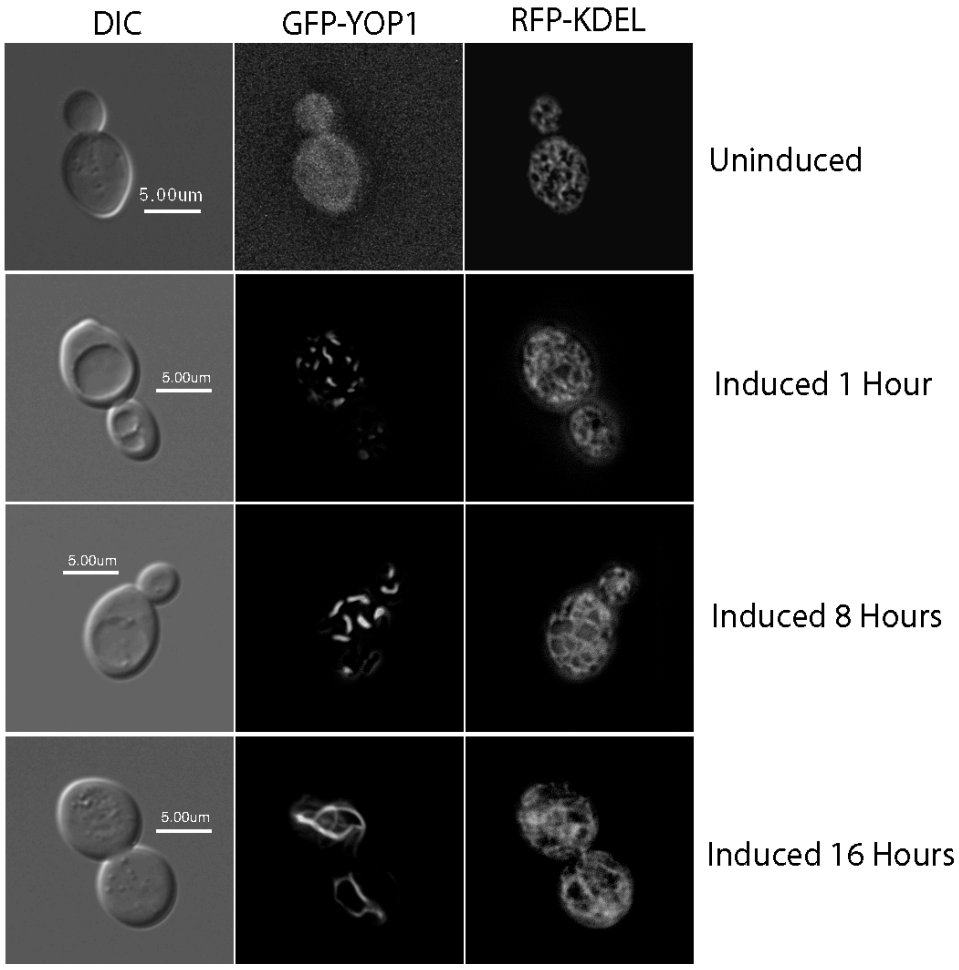

Figure 3.1 Continued

D.

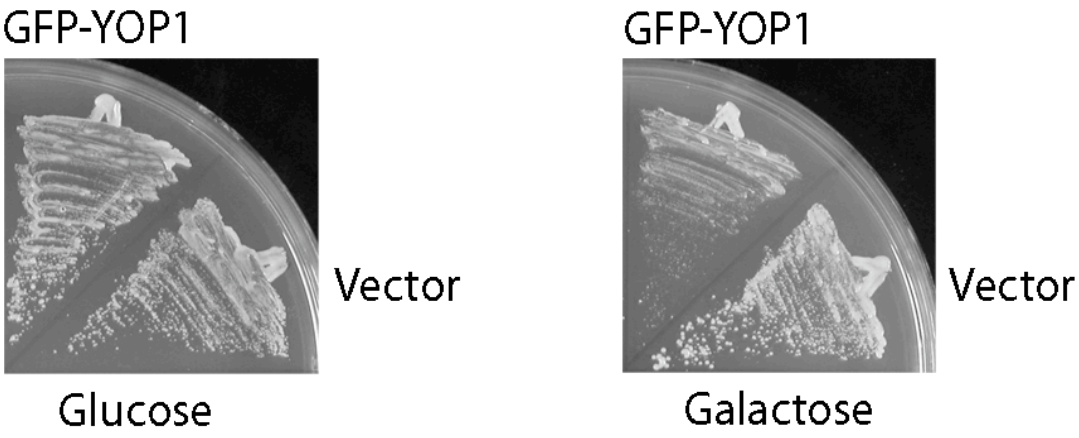

Previous studies have determined that Yop1p overexpression results in cell death after approximately 30 hours of induction [9]. In order to determine whether or not GFP-Yop1p has the same dominant negative effect on cells as genomic *YOP1*, *reg1Δ* cells (RCY4274) carrying either an empty vector or inducible GFP-Yop1p were struck on both SD and SGal plates. While the vector control cells grew normally on both the SD and the SGal plates, GFP-Yop1p induction on the SGal plate slowed cell growth (Figure 3.1). This result confirms the detrimental effect Yop1p overexpression has on cells and suggests that GFP-Yop1p overexpresssion has a similar effect.

Formation of GFP-Yop1p tubules does not require Rtn1p

Rtn1p is an ER localized membrane protein and a known binding partner of Yop1p. These proteins are thought to act in redundant roles in generating the tubules of the peripheral ER [1]. To investigate the possibility that Rtn1p is critical for the formation of the tubular structures by overexpression of GFP-Yop1p, I expressed RFP-Rtn1p and induced GFP-Yop1p expression in wild-type cells. Localization of these proteins was analyzed by fluorescence microscopy. GFP-Yop1p was localized to the tubular structures as seen before. RFP-Rtn1p localized to the ER, which also contained some punctate Rtn1p localization. The Rtn1p puncta localized mainly along the length of the GFP-Yop1p tubules perhaps indicating that some of the RFP-Rtn1p had integrated into the tubules (Figure 3.2). The tubules formed by GFP-Yop1p overexpression often align with the tubules of the peripheral ER (see Figure 3.1), thus it is possible that the RFP-Rtn1p localization could be a result of Rtn1p present on the peripheral ER binding to Yop1p in the tubular structures, and not a result of Rtn1p being integrated into the forming tubules.

I sought to determine if Rtn1p was required for the formation of the Yop1p tubular structures by overexpressing GFP-Yop1p in *rtn1Δrtn2Δ yop1Δ* cells. I found

that overexpression of GFP-Yop1p in these cells resulted in the formation of similar tubular structures (Figure 3.2), suggesting Yop1p does not require Rtn1p to form membrane tubules.

Enrichment of GFP-Yop1p formed tubular structures

I noticed an interesting property of the GFP-Yop1p tubules during fluorescence imaging, namely, that the tubular structures remained intact outside the cytosolic environment when a cell inadvertently broke open on the glass slide (Figure 3.3 A). I sought to develop an enrichment scheme to remove these tubular structures from lysed cells for analysis outside the context of the cell. Briefly, membrane fractions from cells overexpressing GFP-Yop1p were loaded on the bottom of a sucrose flotation gradient and subjected to centifugation. Membranes were separated into light and heavy fractions, with the GFP-Yop1p tubules found within the heavy fraction. This heavy membrane fraction was further subjected to centrifugation through a 20-60% linear sucrose density gradient (Figure 3.3 B). This protocol allowed for enrichment of GFP-Yop1p formed tubular structure for further analysis. Analysis of the protein composition of the GFP-Yop1p tubules was performed by SDS-PAGE and coomassie staining and revealed many protein components within the tubule-containing fraction (fraction 8, Figure 3.3 C). I determined GFP-Yop1p to be ~40 KDa by western blot (data not shown). Membrane contaminants of a similar density are also likely present within the enriched tubule fraction, thus it is possible that some of the proteins present in this fraction (besides GFP-Yop1p) are derived from these contaminating membranes.

Figure 3.2. Tubular structures formed by GFP-Yop1p are composed of ER membranes. A. *rtn1Δrtn2Δyop1Δ* cells overexpressing GFP-Yop1p for 8 hours were analyzed for ER morphology using expression of RFP-KDEL. Note that the peripheral ER is composed of tubular structures. B. *reg1Δ* cells (RCY4274) overexpressing GFP-Yop1p for 8 hours. Cells were assayed for RFP-Rtn1p localization by fluorescence microscopy. Note regions of punctate RFP-Rtn1p localization near the GFP-Yop1p tubules.

A.

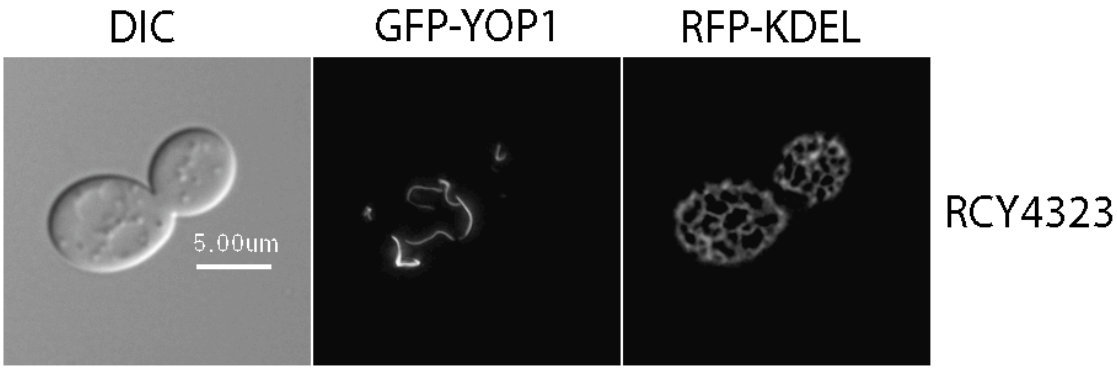
DIC
GFP-YOP1
RFP-KDEL
5.00um
RCY4323

B.

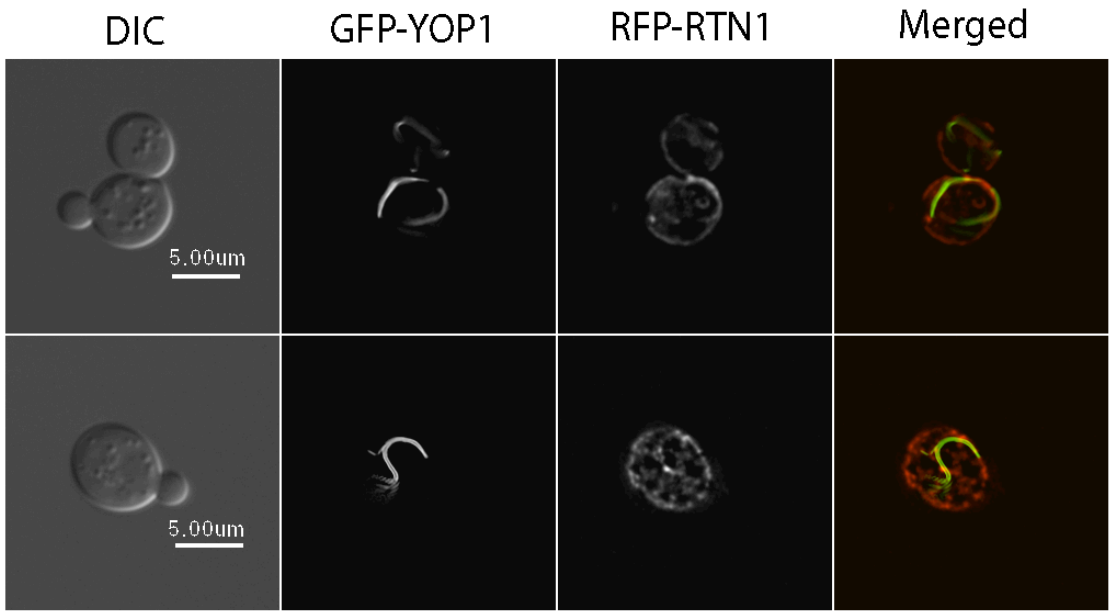
DIC
GFP-YOP1
RFP-RTN1
Merged
5.00um
5.00um

In an attempt to determine which protein bands in the coomassie stained gel may be derived from contaminating membranes of a similar density as the GFP-Yop1p tubules, wild-type cells were subjected to the same enrichment procedure (though not overexpressing GFP-Yop1p, they still expressed endogenous Yop1p). Protein profile comparison was then carried out between these cells and cells overexpressing GFP-Yop1p to identify any protein components inadvertently carried through the purification process. This analysis revealed that all protein bands present in the GFP-Yop1p lane appeared to also be present in the wild-type cell lane (Figure 3.3 D), suggesting that the major protein component of the GFP-Yop1p tubules may be GFP-Yop1p and that the other protein components present could be a result of other membranous structures carried through the purification procedure inadvertently.

Biochemical analysis of GFP-Yop1p formed tubules

The GFP-Yop1p tubules floated through up through the sucrose flotation gradient, confirming the presence of a membrane component in the tubules. It is still possible that the membranous components of the GFP-Yop1p tubules do not contribute to the stability of the tubules, but rather interactions between Yop1p proteins in the tubules are responsible for maintaining the tubule structure. To investigate this possibility tubule fractions were subjected to conditions of extremely high salt concentrations. GFP-Yop1p tubule fractions were subjected to conditions of 500 mM NaCl or KCl and analyzed for the presence of tubules by fluorescence microscopy. The addition of 500 mM NaCl or KCl did not result in the dissolution of the tubular structures (Figure 3.4 C) suggesting that they are not held together through strong protein interactions alone. Taken with the facts that Yop1p is an integral membrane protein and the GFP-Yop1p tubules floated through the membrane flotation

Figure 3.3. Enrichment of GFP-Yop1p formed tubular structures. A. Cells inadvertently broken open during slide preparation. Note the tubular structures remain in tact outside the cell wall. B. Purification scheme for GFP-Yop1p tubules. Membrane fraction of cells overexpresisng GFP-Yop1p are passed through a membrane flotation gradient followed by a linear sucrose gradient yielding in tact GFP-Yop1p tubules. C. Coomassie stained SDS-PAGE analysis of 1 mL fractions from linear sucrose gradient. GFP-Yop1p tubules are present in fraction 7. D. SDS-PAGE comparison of proteins present from wild-type cells and GFP-Yop1p overexpressing cells after enrichment procedure. E. Fluorescence images of fractions collected from the linear sucrose gradient (F1=top F12=bottom).

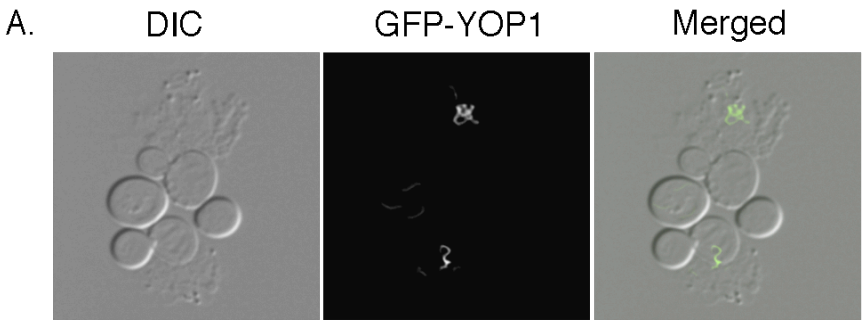
A.
DIC
GFP-YOP1
Merged

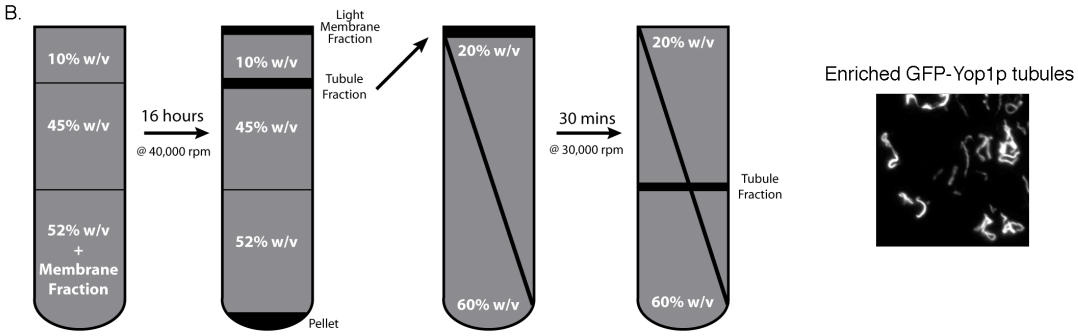
B.
10% w/v
45% w/v
52% w/v
+
Membrane
Fraction
16 hours
@ 40,000 rpm
Light
Membrane
Fraction
10% w/v
Tubule
Fraction
45% w/v
52% w/v
Pellet
20% w/v
60% w/v
30 mins
@ 30,000 rpm
20% w/v
Tubule
Fraction
60% w/v
Enriched GFP-Yop1p tubules

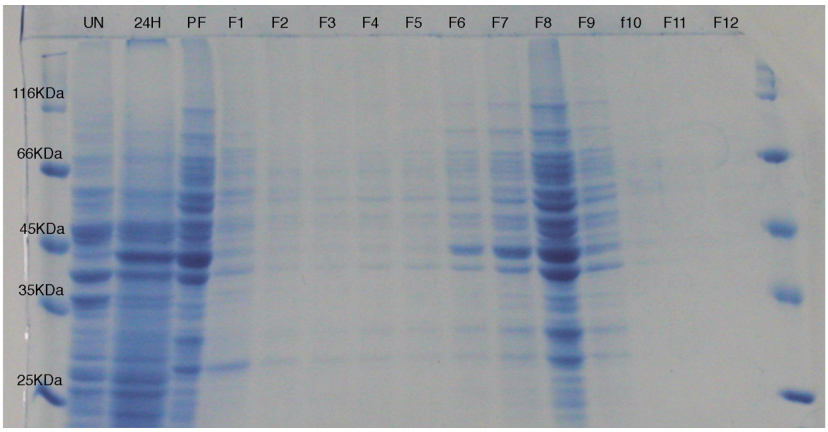
C.
UN
24H
PF
F1
F2
F3
F4
F5
F6
F7
F8
F9
f10
F11
F12
116KDa
66KDa
45KDa
35KDa
25KDa

Figure 3.3 continued

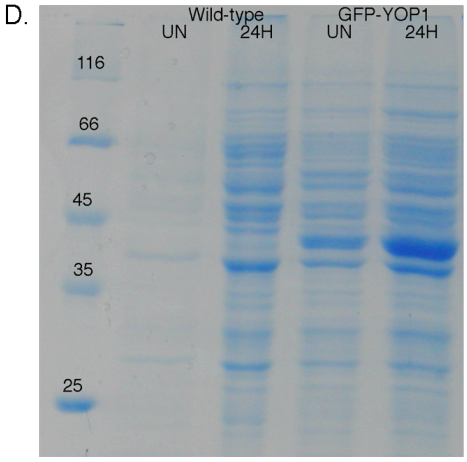

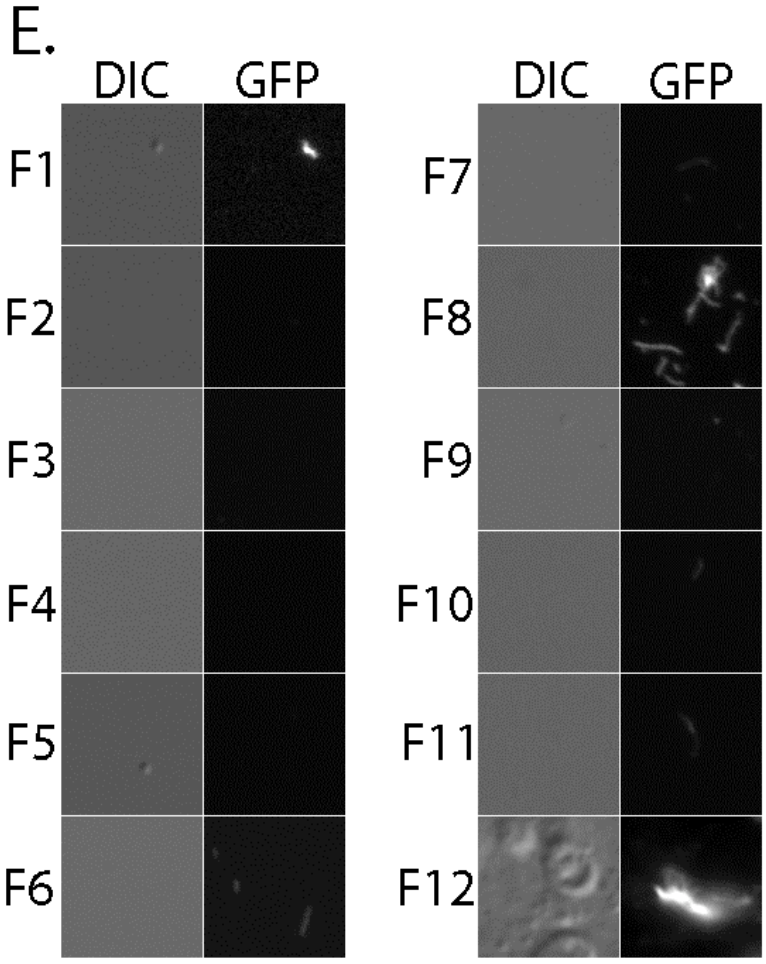

gradient, this high salt resistance suggests that the membrane component of the Yop1p tubules contributes to the stability of the tubules structure.

To further investigate the composition of these tubular structures and how their structure is formed/maintained the tubules were tested for their resistance to detergent. Membranous structures are typically sensitive to the addition of detergents through the dissolution of the membrane within the structure. GFP-Yop1p tubule fractions were subjected to the addition a solution either with or without the detergent Trition-X100 (0.2% final concentration). Fluorescence images of each sample were analyzed for the presence of tubular structures. Only in the control treated sample were tubules still present. The addition of detergent abolished the tubular structures (Figure 3.4 A), further suggesting they are composed of membrane and protein components both important to maintain the tubule structure. Additionally, fluorescence images were collected every 1 second after the addition of Trition-X100 of a single tubule. Within 15 seconds after detergent addition the GFP-Yop1p tubule had been completely solubilized (Figure 3.4 B), further confirming the membranous component of the GFP-Yop1p tubules.

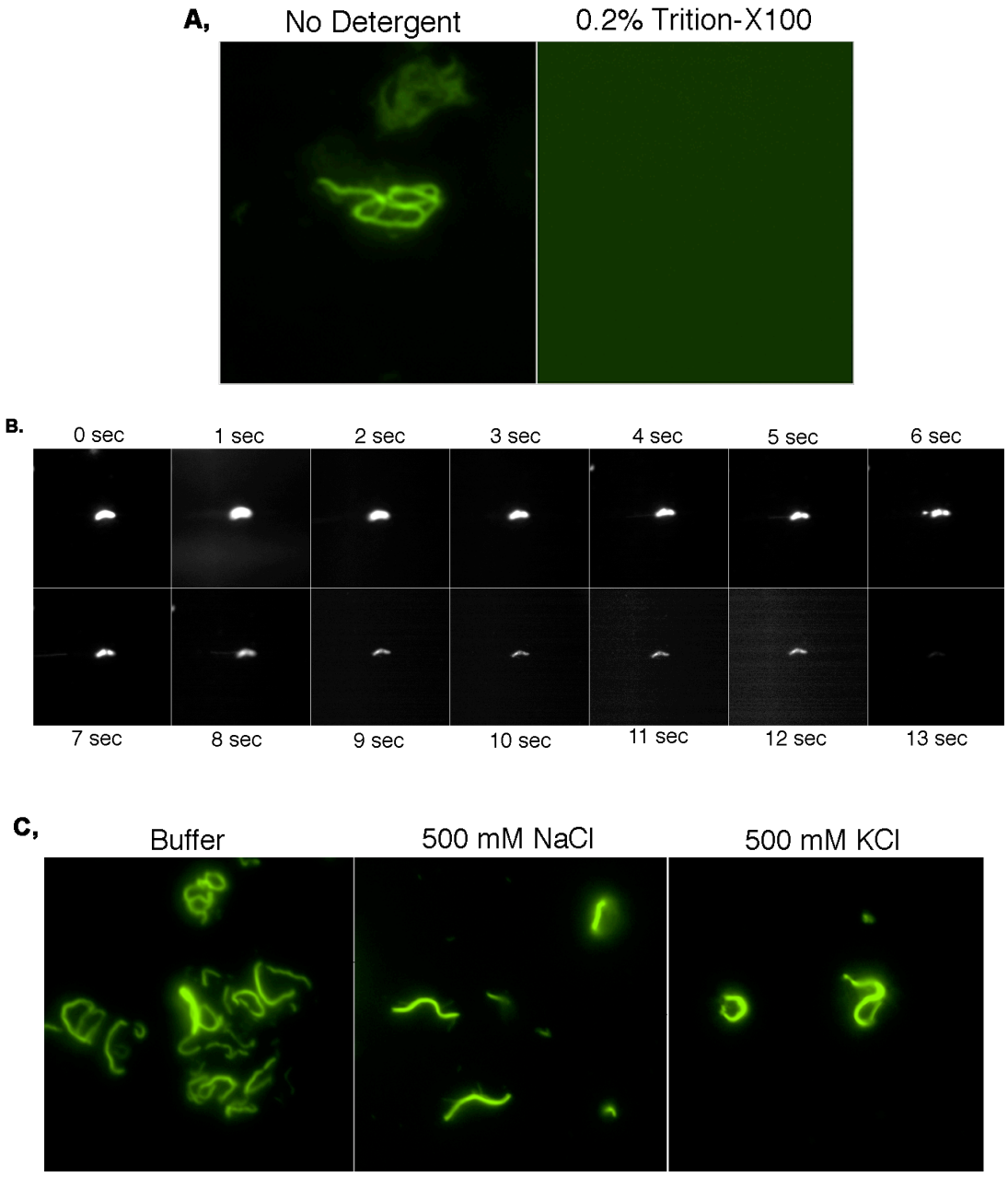

Figure 3.4. Biochemical analysis of GFP-Yop1p tubule composition. A. Enriched tubules treated with or without 0.2% Triton-X100 after purification. B. Time-course analysis of GFP-Yop1p tubules after the addition of detergent. Images captured every 1 second. C. Analysis of high salt resistance of GFP-Yop1p tubules. Purified tubules after the addition of a final concentration of 500 mM NaCl or KCl.

Morphology of GFP-Yop1p tubules

Previous studies have shown that plant reticulon overexpression results in the formation of tubular structures so small in diameter that they exclude ER luminal proteins [14]. To gain insight into the function of Yop1p in the formation of the tubules of the peripheral ER, analysis of the morphology of the GFP-Yop1p formed tubular structures was carried by negative stain electron microscopy. Enriched GFP-Yop1p tubule fractions were applied to carbon-coated grids, stained with uranyl-acetate and analyzed by electron microscopy. This analysis revealed individual tubules with a small diameter (~15 nm) often containing bulbous ends. These individual tubules were bundled together into larger, rope-like structures (Figure 3.5 A, B). Presumably, the larger, rope-like structures are the structures seen by fluorescence microscopy within cells. The morphology of the GFP-Yop1p tubules shows that Yop1p is capable of forming tubules with a very small diameter. It is unlikely that these tubules represent functional peripheral ER tubules, but are instead an artificial result of the high concentration of Yop1p due to its overexpression.

In order to eliminate the possibility that the GFP tag on Yop1p is contributing to the formation of the tubular structures, HA-tagged Yop1p was overexpressed and subjected to the tubule enrichment procedure and assayed for the presence of tubules by electron microscopy. I found that HA-Yop1p overexpression resulted in the formation of tubular structures as seen by electron microscopy (Figure 3.5 C), while wild-type cells subjected to the same treatment did not (Figure 3.5 D).

To confirm the presence of GFP-Yop1p within the tubular structures, immunogold labeling and subsequent electron microscopy was performed on enriched GFP-Yop1p tubule fractions with an anti-GFP antibody conjugated to a gold label. This analysis revealed a specific labeling of the tubular structures, while all other

membranous contaminants present remained devoid of gold labeling (Figure 3.5 E). This result confirms the presence of GFP-Yop1p within the tubular structures and further suggests that Yop1p is responsible for the formation of these structures. However, the wild-type cells do not serve as a conclusive control, thus a control where the primary antibody is omitted from the procedure, or an irrelevant primary antibody is used instead of the anti-GFP one, is needed to confirm the specific localization of Yop1p to the tubules.

Figure 3.5. Morphological analysis of purified GFP-Yop1p tubules. A-B. Negative stain electron microscopy of purified GFP-Yop1p tubules. Two examples are shown. C. Negative stain electron microscopy of HA-Yop1p formed tubules. D. Negative stain electron microscopy of similarly treated wild-type (RCY239) cells. E. Immunogold labeling of GFP-Yop1p tubules followed by negative stain electron microscopic analysis. Four examples are shown.

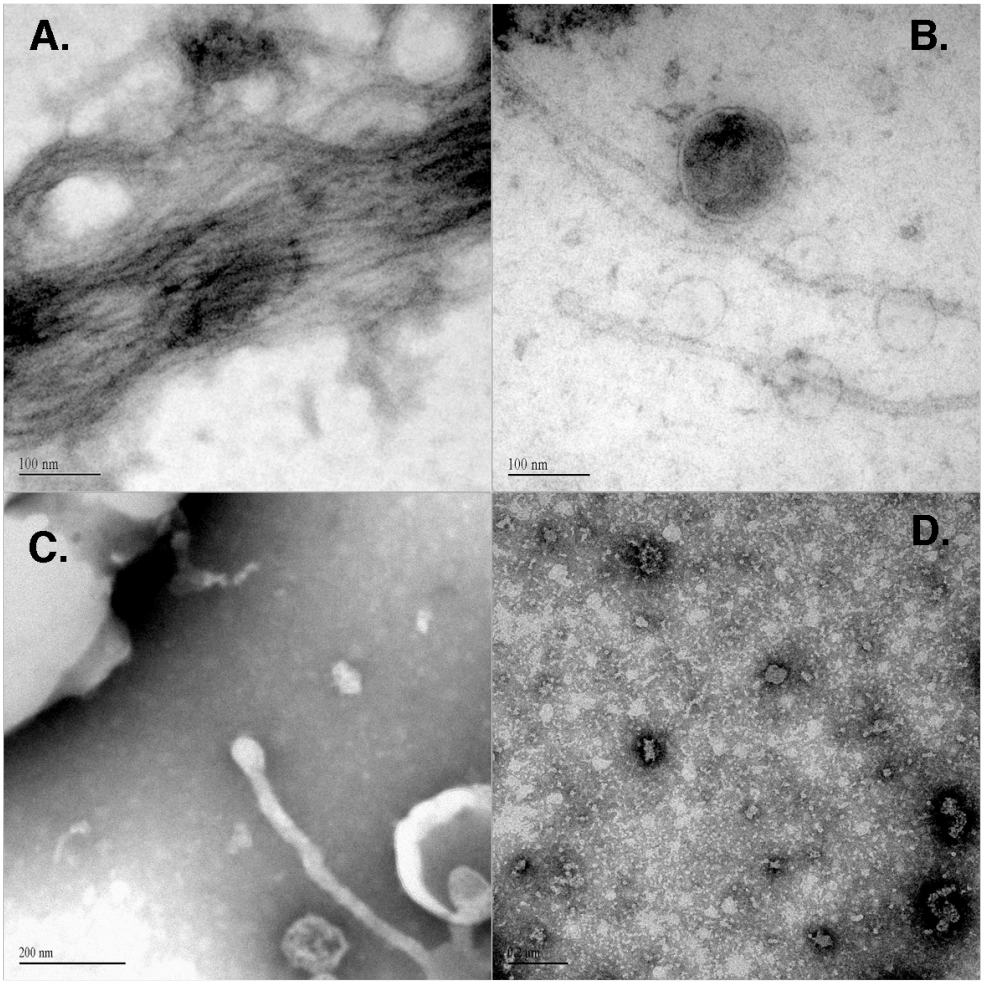
A.
100 nm
B.
100 nm
C.
200 nm
D.

Figure 3.5 Continued

E.

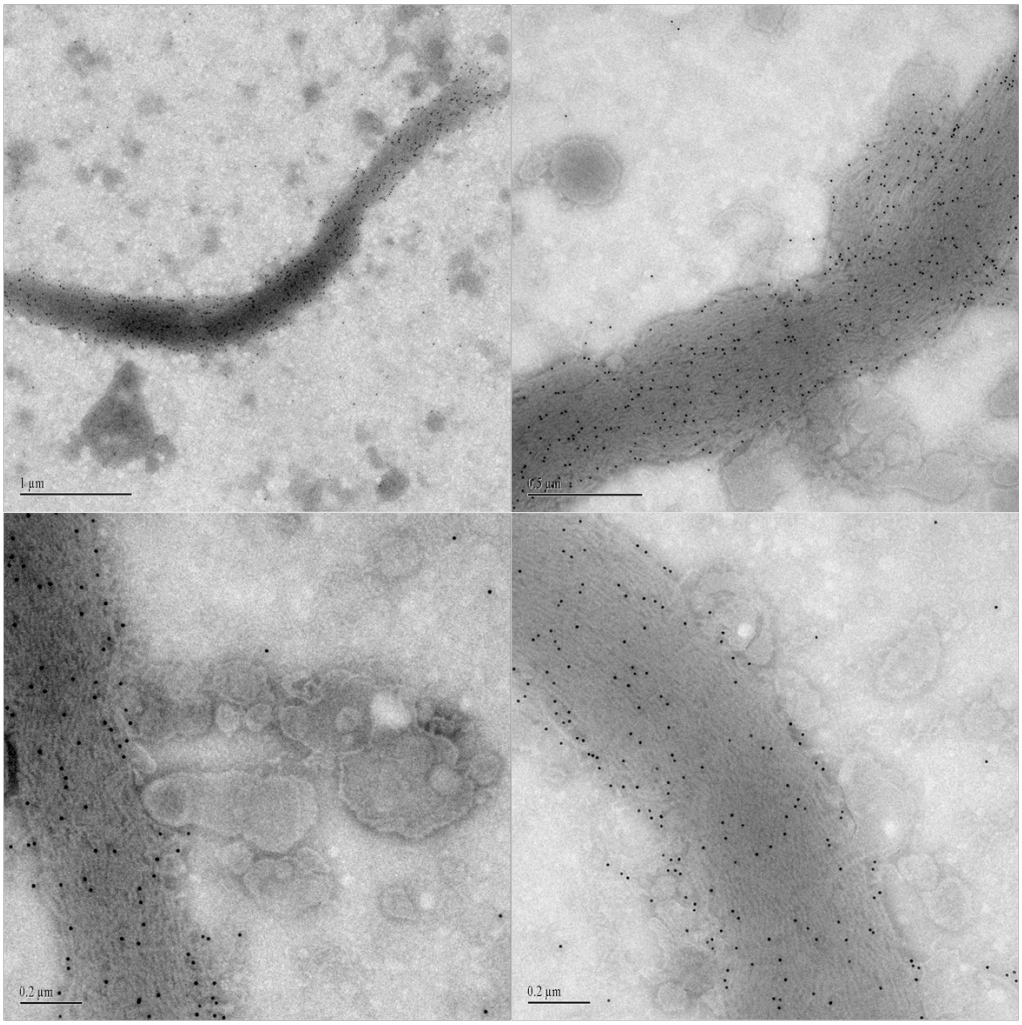

DISCUSSION

Previous studies have determined that Yop1p likely functions in generating the tubules of the peripheral ER [1-4]. A model of the molecular mechanism of Yop1p action on membranes in generating membrane curvature has been suggested based on the presence of the two long hydrophobic domains of Yop1p inserted only part of the way through the lipid bilayer [1]. This study seeks to further elucidate the mechanism of Yop1p action on membranes through analysis of the structures formed by Yop1p overexpression in vivo. Overexpression of Yop1p is known to result in an accumulation of membrane tubules though the morphology of these structures have not been studied in detail [1, 3]. I have developed a means of partially purifying these structures from cells for further morphological analysis to gain insights into how Yop1p functions in vivo.

Yop1p localizes mainly to the tubules of the peripheral ER [1]. Overexpression of Yop1p results in the formation of long, unbranched tubules within the cell [1, 3]. Interestingly, these tubular structures do not colocalize perfectly with ER membranes (Figure 3.1). Additionally, prolonged overexpression of Yop1p is dominant negative to cells, eventually resulting in a severe growth defect [9]. The stunted growth of these cells may be due to such a massive accumulation of these tubular structures that their presence interferes with other essential cellular processes. Alternatively, the formation of these tubular structures by Yop1p overexpression from ER membranes may remove so much of the ER membranes that the critical processes that occur there cannot occur.

The localization of Yop1p to ER membranes suggests that the tubular structures formed by Yop1p overexpression are likely derived from the membranes of the ER. To confirm the membranes present in the Yop1p tubules is indeed ER derived, a time-course analysis of the formation of these Yop1p tubules was performed using

RFP-KDEL expression to monitor ER membranes. Within one hour of GFP-Yop1p induction short tubular structures begin to form. These short tubules co-localize with ER membranes. As the induction of GFP-Yop1p continues the length of the tubular structures increases. Up to 16 hours after induction the tubular structures continue to co-localize with ER membranes, suggesting that the membranes contained in the tubular structures are indeed of ER origin. Sometime between 16 and 24 hours after Yop1p induction the tubular structures become distinct from the membranes of the ER, though areas of alignment can still be seen occasionally (Figure 3.1). Studies of the overexpression of a plant reticulon remodels the ER lumen as well as resulting in the formation of tubular structures that do not contain ER luminal proteins [14]. The authors of this study suggest that the tubular membranes are still continuous with the ER membrane, but the diameter of these tubules is so small as to exclude the luminal proteins. This fact, taken with our results suggest that the tubules formed by Yop1p overexpression are of ER origin and the lack of co-localization with ER membranes may be suggest that these tubular structures have a very small diameter as well.

Considering these tubules are formed from ER membranes we considered the possibility that other ER resident proteins may be necessary for the formation of the Yop1p tubules. Rtn1p is thought to act in concert with Yop1p in the formation of the peripheral ER tubules and is known to interact with Yop1p [1]. Overexpression of Yop1p was carried out in *rtn1Δrtn2Δyop1Δ* cells to investigate whether Rtn1p is necessary for the formation of the Yop1p tubules. The same long, unbranched tubular structures were seen, despite the absence of Rtn1p in these cells (Figure 3.2). These results show that Yop1p is capable of forming these structures without the help of Rtn1p. The fact that Yop1p does not require Rtn1p to form these tubular structures does not exclude the possibility that some of the Rtn1p present in ER membranes is integrated into the tubular structures through interaction with Yop1p during tubule

formation and perhaps the Rtn1p is necessary to generate the Yop1p tubules. To investigate the possibility that Rtn1p is present in these tubular structures RFP-Rtn1p was expressed during GFP-Yop1p overexpression. The localization of these proteins was monitored by fluorescence microscopy and revealed that Rtn1p is localized to ER membranes but also to puncta present along the length of the Yop1p tubules (Figure 3.2). The Rtn1p punctate localization is confined to regions where the Yop1p tubules still align with the ER tubules and is absent from the regions where the two do not align. This result suggests that Rtn1p is likely present on the ER membrane and is not incorporated into the Yop1p tubules, further suggesting that Yop1p acts alone in forming these structures.

During microscopic analysis of the Yop1p tubules I noted an interesting property of the tubular structures. Inadvertent cell lysis can occur during the preparation of slides for microscopic analysis when the coverslip is placed on the glass slide. Cells overexpressing Yop1p, when broken open by placement of the coverslip, spill their contents outside the cell wall. I noticed that the tubular structures appeared to remain intact outside the cell, suggesting they are stable enough to remain intact on their own. I sought to develop a protocol to enrich the tubular structures after cell lysis to allow a more thorough morphological analysis of these structures outside the context of the cell. Cells overexpressing Yop1p were zymolase treated to remove the cell wall, then gently lysed by the addition of high salt containing buffer. Membranes were then pelleted and loaded on the bottom of a sucrose flotation gradient and subjected to centrifugation. In this process, structures composed of membranes float up through the step-wise gradient while dense cell material is pelleted. Membranes are separated into heavy and light fractions, with the GFP-Yop1p tubules present in the heavy membrane fraction. This fraction was then further purified by means of a linear sucrose gradient. This protocol resulted in the enrichment of GFP-Yop1p tubules for

further analysis. SDS-PAGE analysis of the tubule-containing fraction indicated that many other proteins are present within the tubular structures or in the other membranous contaminants of a similar density as the tubules, but GFP-Yop1p was the major protein band in this fraction (Figure 3.3, fraction 8). To determine which proteins may have been inadvertently carried through the purification process wild-type cells were subjected to the same procedure. A comparison of the protein profiles of the wild-type cells and the cells overexpressing GFP-Yop1p revealed that all of the protein bands present in the GFP-Yop1p tubule fraction were also present in the wild-type lane, except GFP-Yop1p (~40KDa) (Figure 3.3), suggesting that GFP-Yop1p is the major component of the tubular structures and the other proteins carried through the purification are likely a result of the other membranous structures of a similar density as the GFP-Yop1p tubules. This result is in agreement with the fact that purified Yop1p is capable of forming tubular structures from lipids in vitro alone with a very small diameter [4].

To further analyze the composition of the GFP-Yop1p tubules a series of biochemical tests were performed on the partially purified tubules. Although Yop1p is an integral membrane protein, and the tubular structures floated through the membrane flotation gradient, it is possible that the tubular structures do not require a membrane component to maintain structure. To assess this possibility the enriched tubular structures were analyzed for their sensitivity to the addition of detergent. Membranous structures are broken down in the presence of detergents by solubilizing the lipids present in these structures. The addition of 0.2% Triton-X100 resulted in the complete dissolution of the GFP-Yop1p tubules (Figure 3.4), confirming that the presence of membranes within these structures contributes to their stability.

Strong protein-protein interactions are typically interfered with by the presence of high concentrations of salt. We tested the sensitivity of the GFP-Yop1p tubules to

high concentrations of salt to determine if interactions between the hydrophilic regions of Yop1p are necessary for the structuring of the tubules. The addition of extremely high concentrations of either NaCl or KCl (500 mM) was unable to disrupt the structure of the tubules (Figure 3.4), suggesting that hydrophobic interactions between Yop1p and the membrane are responsible for holding the tubules together.

The tubular structures formed in vitro by purified Yop1p have a very small diameter of ~15 nm [4]. To determine the morphology of the GFP-Yop1p tubules generated in vivo purified fractions were analyzed by negative stain electron microscopy. This analysis revealed the diameter of the tubular structures to be ~15 nm, similar to the diameter of the tubules formed by Yop1p in vitro, suggesting that the tubules could be formed solely by GFP-Yop1p. The small, individual tubules were further bundled together into larger, rope-like structures. The ends of the tubules additionally often contain rounded, bulbous ends (Figure 3.5). The bulbous ends of the tubules are likely a consequence of the energetically most stable way to terminate the tubular structures.

To confirm the presence of Yop1p within these tubules immuno-gold labeling of these structures was performed with an anti-GFP primary antibody and a secondary gold-conjugated label. The gold label was found specifically associated with the tubular structures, while contaminating membranes present on the grid lacked gold labeling (Figure 3.5). However, an additional no primary control is needed to confirm that the primary antibody is not associating with the tubular structures non-specifically. This result suggests that Yop1p is present within the tubular structures and that Yop1p is responsible for forming these structures. The fact Yop1p can form the tubular structures in the absence of Rtn1p and that these tubules have a very small diameter may suggest that Yop1p acts in concert with Rtn1p and other proteins to modulate the diameter of the tubules formed in the peripheral ER. It is also possible

that, as Hu et al [4] have suggested, that the high concentration of Yop1p due to overexpression is responsible for the small diameter of the tubules formed. Overexpression of Rtn1p or other binding partners with Yop1p may result in tubules of a larger diameter if this is the case. Further studies will determine the ability of Yop1p binding partners to modulate the diameter of the tubules formed by Yop1p by overexpressing them at the same time within cells and analyzing the morphology of the tubules formed.

REFERENCES

1. Voeltz, G.K., et al., *A class of membrane proteins shaping the tubular endoplasmic reticulum*. Cell, 2006. **124**(3): p. 573-86.
2. Shibata, Y., et al., *The reticulon and DP1/Yop1p proteins form immobile oligomers in the tubular endoplasmic reticulum*. J Biol Chem, 2008. **283**(27): p. 18892-904.
3. Prinz, W.A., et al., *Mutants affecting the structure of the cortical endoplasmic reticulum in Saccharomyces cerevisiae*. J Cell Biol, 2000. **150**(3): p. 461-74.
4. Hu, J., et al., *Membrane proteins of the endoplasmic reticulum induce high-curvature tubules*. Science, 2008. **319**(5867): p. 1247-50.
5. Dreier, L. and T.A. Rapoport, *In vitro formation of the endoplasmic reticulum occurs independently of microtubules by a controlled fusion reaction*. J Cell Biol, 2000. **148**(5): p. 883-98.
6. Shibata, Y., et al., *Mechanisms shaping the membranes of cellular organelles*. Annu Rev Cell Dev Biol, 2009. **25**: p. 329-54.
7. Shnyrova, A., V.A. Frolov, and J. Zimmerberg, *ER biogenesis: self-assembly of tubular topology by protein hairpins*. Curr Biol, 2008. **18**(11): p. R474-6.
8. Geng, J., et al., *Saccharomyces cerevisiae Rab-GDI displacement factor ortholog Yip3p forms distinct complexes with the Ypt1 Rab GTPase and the reticulon Rtn1p*. Eukaryot Cell, 2005. **4**(7): p. 1166-74.
9. Calero, M., G.R. Whittaker, and R.N. Collins, *Yop1p, the yeast homolog of the polyposis locus protein 1, interacts with Yip1p and negatively regulates cell growth*. J Biol Chem, 2001. **276**(15): p. 12100-12.

10. Chen, C.Z., et al., *Genetic analysis of yeast Yip1p function reveals a requirement for Golgi-localized rab proteins and rab-Guanine nucleotide dissociation inhibitor*. Genetics, 2004. **168**(4): p. 1827-41.
11. Calero, M. and R.N. Collins, *Saccharomyces cerevisiae Pra1p/Yip3p interacts with Yip1p and Rab proteins*. Biochem Biophys Res Commun, 2002. **290**(2): p. 676-81.
12. Hu, J., et al., *A class of dynamin-like GTPases involved in the generation of the tubular ER network*. Cell, 2009. **138**(3): p. 549-61.
13. Orso, G., et al., *Homotypic fusion of ER membranes requires the dynamin-like GTPase atlastin*. Nature, 2009. **460**(7258): p. 978-83.
14. Tolley, N., et al., *Overexpression of a plant reticulon remodels the lumen of the cortical endoplasmic reticulum but does not perturb protein transport*. Traffic, 2008. **9**(1): p. 94-102.

CHAPTER 4

ANALYSIS OF RTN1 PALMITOYLATION

ABSTRACT

Reticulon proteins are ubiquitously found in eukaryotic genomes and have recently been implicated in the formation of the highly curved tubules of the ER in both higher and lower eukaryotes. Rtn1p is thought to function in a redundant role with Yop1p in generating peripheral ER tubules in yeast through a membrane wedging mechanism. Rtn1p contains two long hydrophobic regions thought to form hairpins within the membrane, which give Rtn1p a wedge-like shape that drives membrane deformation. Palmitoylation is a post-translational modification that can alter the localization of a protein or its activity. Rtn1p is palmitoylated on four cysteine residues all located in close proximity to the putative membrane embedded regions. Here I investigate the consequences of Rtn1p palmitoylation on its ability to form the tubular peripheral ER.

INTRODUCTION

Rtn1p belongs to the eukaryotic reticulon family of integral membrane proteins, characterized by a reticulon homology domain (RHD, see Figure 1.4). This domain contains two long hydrophobic stretches (~40 amino acids) separated by a hydrophilic loop (~60 amino acids, see Figure 1.4) [Pfam PF02453][1, 2]. Yeast contain two reticulon genes, *RTN1* and *RTN2*. Rtn1p is the predominantly expressed form, but under stressed conditions the expression of Rtn2p can be induced. All reticulons studied to date localize to ER membranes [3], with the possible exception of a very small amount of mammalian RTN4 present on the plasma membrane [4]. Reticulons have been recently implicated in the formation and/or maintenance of the peripheral ER tubules in both lower and higher eukaryotes [1, 5, 6]. Previous studies have shown that reticulons form homo-oligomeric complexes [4, 7-9], which may be required for their function.

Rtn1p is also known to interact with other proteins, including Yop1p, Yip3p, Sec6p, and Sbh1p [1, 10-12]. Yop1p and Yip3p are both thought to play roles in generating or maintaining the tubules of the peripheral ER. Yip3p is a YIP-like protein (though not a YIP family member) that forms complexes with YIP family proteins [10]. Mutants of *YIP1* have been identified that contain peripheral ER sheet-like structures at the restrictive temperature [13]. It is thought that the interaction between Rab proteins and Yip1p may alter the extensive hydrophobic COOH terminal domains of Yip1p and thus affect Yip1p function in forming these tubular structures. Perhaps Yip3p provides a bridge to translate the information from the Rab-Yip1p interaction to Rtn1p and regulating its ability to form membrane tubules.

Yop1p is an integral membrane protein thought to share a redundant role with Rtn1p, through a similar mechanism of action, in the formation of the tubules of the peripheral ER. Rtn1p shares a similar domain organization with Yop1p, where two,

long hydrophobic domains are separated by a hydrophilic linker (see Figure 1.5). The NH_2 and COOH terminal ends are present on the cytoplasmic surface of the ER membrane, as well as the hydrophilic linker between the two hydrophobic domains. Each of the hydrophobic domains is inserted into the membrane, but not thought to pass all the way through. This unique topology has been proposed to give Rtn1p a wedge-like shape within the membrane. The presence of the two hydrophobic domains within the membrane are thought to drive membrane deformation through a similar mechanism of action as Yop1p (investigated in Chapters 2 and 3). Additionally, in yeast deletion of *RTN1* alone has no apparent phenotype, but *rtn1Δyop1Δ* cells (and *rtn1Δrtn2Δyop1Δ* cells) display a morphological defect of the structure of their peripheral ER, where the normal tubular structure is converted into large areas of sheet like cisternae (though some areas of tubules still exist). Expression of *RTN1* (or *YOP1*, see Figure 2.1) can rescue this morphological defect, suggesting a redundant function for Rtn1p and Yop1p in the formation of these tubular structures [1].

Post-translational lipid modifications of proteins can have a number of potential effects on the function of a protein, from localization to regulation of protein function [14-17]. For example, the acylation of Rab proteins is essential for Rab protein recruitment to membranes [18]. Additionally, protein acylation has been shown to be an important determining factor in some proteins organellular localization [19]. Palmitoylation is a reversible reaction where palmitic acid is covalently linked to cysteine residues [20]. Rtn1p has 4 cysteine residues, and the Dr. Nick Davis' lab (Wayne State University) has demonstrated that all 4 of these residues are palmitoylated. All four of these cysteines are in close proximity to the two hydrophobic domains of Rtn1p and it is possible that the palmitoylation of these residues may have alter the function of Rtn1p. Considering the proposed mechanism used by Rtn1p in generating membrane curvature through a membrane wedging

mechanism [1] the palmitoylation of these residues may have drastic effects on the shape that Rtn1p adopts within the membrane, perhaps as a potential means to regulate the action of Rtn1p on membranes. This type of reversible protein modification could act as a signal for Rtn1p to alter its action on membranes.

MATERIALS AND METHODS

Yeast strains and plasmids

All *S. cerevisiae* strains used in this study are listed in table 4.1. Manipulations of these strains were done using standard biological techniques. Cell density was determined using a Thermo Spectronic Genesys 10UV spectrophotometer (Rochester, NY) at 600nm. Endogenous level expression of each CEN construct was achieved by using the endogenous promotor region of each gene (~500 bp upstream from the start codon). Overexpression of constructs under *GAL1/10* promotor control was performed by growing cells overnight in SD media to a density of 0.4-0.8. Cells were pelleted, washed once in ddH_20, and resuspended in 1mL ddH_20. Washed cells were inoculated into minimal media containing 2% galactose to an initial density of 0.05-0.2, depending on the length of induction.

Table 4.1 *S. cerevisiae* strains used in this study

RCY Strain	Genotype	Source
RCY239	*MAT***a** *ura3-52 leu2-3,112*	This lab
RCY4274	*MAT***a/α** *reg1*ΔKAN^R/ *reg1*ΔKAN^R *ura3Δ0/ ura3Δ0*, *leu2Δ0/ leu2Δ0*, *his3*Δ0/ *his3*Δ0, *lys2Δ0/ lys2Δ0*, *met15*Δ0/*MET15*	This lab
RCY4323	*MAT***a** *rtn1*ΔKAN^R *rtn2*ΔKAN^R *yop1ΔHIS5*, *ura3Δ0*, *leu2Δ0*, *his3*Δ0, *lys2Δ0*, *met15*Δ0	This lab

Plasmids were created using standard biological techniques and are listed in table 4.2. GFP fusions were made by linking yEGFP to the NH_2 or COOH terminus of

each construct with a GGPGG linker between the GFP and the ORF. Overexpression of particular constructs was done by two means. First, by integrating the GFP-ORF fusion into a multi-copy (2μ) vector ensures many copies of each construct in cells to increase the proteins production. Second, overexpression constructs are placed under the control of the promotor region of *GAL1/10*, which responds to the presence of galactose.

Table 4.2 Plasmids used in this study

Plasmid number	Construct	Description	Source
pRC3588	pRS315 *RFP-KDEL*		This lab
pRC3589	pRS316 *RFP-KDEL*		This lab
pRC3413	pRS315 *RTN1-GFP*		This study
pRC3414	pRS315 *RTN1-PMut-GFP*	C19S, C21S, C90S, C194S	This study
pRC3437	pRS315 *RTN1-3XHA 6XHIS*		This study
pRC3438	pRS315 *RTN1-PMut-3XHA 6XHIS*	C19S, C21S, C90S, C194S	This study
pRC3501	pRS315 *GFP-RTN1*		This study
pRC3502	pRS315 *GFP-RTN1-PMut*	C19S, C21S, C90S, C194S	This study

Fluorescence Microscopy

GFP fusions of each protein were created by fusing 238 amino acids of yeast enhanced green fluorescence protein (yEGFP) to either the NH_2 or COOH terminus and separated by a unique linker sequence (GGPGG). For all peripheral ER morphology analysis experiments, expression of fusion constructs was driven by the endogenous promotor of each gene. NH_2 terminal GFP fusions contain the endogenous terminator sequences from each ORF, ~500 bp downstream from the stop codon of each gene. For COOH terminal GFP fusions, termination is controlled by 573 bp of DNA downstream of the *ADH1* ORF. All fusion constructs were created using overlap

PCR recombination with ~20 bp overlapping sequences for all PCR fragments and recombined into the specified CEN plasmid.

For the overexpression studies, the promotor region of *GAL1/10* was used to induce GFP-Rtn1p expression upon the addition of galactose to the growth media. RFP-KDEL expression was used to visualize ER structures. Cells were grown to mid-log phase in minimal media and pelleted, washed once in ddH_2O and resuspended in minimal media plus galactose to a density of ~0.1. Inductions were carried out for various time lengths depending on the experiment, as indicated in the results section. Images were collected using a Nikon Eclipse E600 microscope with a 100X (1.4NA) objective and 1x optivar. DIC images were collected from a single plane while fluorescence images were gathered as a series of 20-30 z steps of 0.2 μm. A CCD camera (Sensicam EM High Performance, The Cook Corporation) was used to collect images (software IP Lab version 3.6.5, Scanalytics). Blind deconvolution of each z-series was done using AutoQuant X2 program (Media Cybernetics) for 30 iterations. After deconvolution, single planes were identified that most clearly identified single tubular structures.

Analysis of the number of junction points

Cells expressing GFP fusions of *RTN1* or *RTN1-PMut* were expressed in wild-type, *rtn1Δ*, and *rtn1Δyop1Δ* cells and analyzed by fluorescence microscopy as described above. After deconvolution, peripheral ER structures were identified in peripheral slices of each z-series and the number of junction points between tubules was determined in each mother cell (the larger cell). The surface area in each cell was determined by measuring the diameter of the cell in two directions and averaging them to get an approximation of the diameter. Then, using πR^2 the surface area was calculated and used to correct the number of junction points for

different sized cells, yielding the number of junction points per square micrometer. Junction point quantification numbers are reported as average +/- standard deviation.

RESULTS

Overexpression of Rtn1p results in an accumulation of tubular structures in the peripheral ER

Previous studies have suggested a role for Rtn1p in the formation of the tubules of the peripheral ER, perhaps providing a redundant role to Yop1p. Rtn1p shares a similar, unique topology within the membrane as Yop1p where the presence of its two long hydrophobic hairpins are thought to be critical for the generation of peripheral ER tubules. Overexpression of GFP-Rtn1p results in an accumulation of tubular structures within the cell (Figure 4.1), similar to GFP-Yop1p overexpression (see Figure 3.1)[1].

However, the tubular structures formed by Rtn1p overexpression often contain branch points (Figure 3.1), unlike the unbranched tubules formed by Yop1p overexpression. Attempts to purify the GFP-Rtn1p tubules by a similar means used for the GFP-Yop1p tubules (see chapter 3) was unsuccessful, suggesting that Rtn1p does not form tubules that are stable enough to withstand the enrichment process (data not shown). This fact, taken with the presence of junction points in the Rtn1p formed tubular structures (Figure 4.1), may suggest that overexpressed Rtn1p is still localized to ER membranes, and that the tubules of the ER do not withstand the purification procedure. Further studies are needed to determine if Rtn1p tubules colocalize with ER membranes.

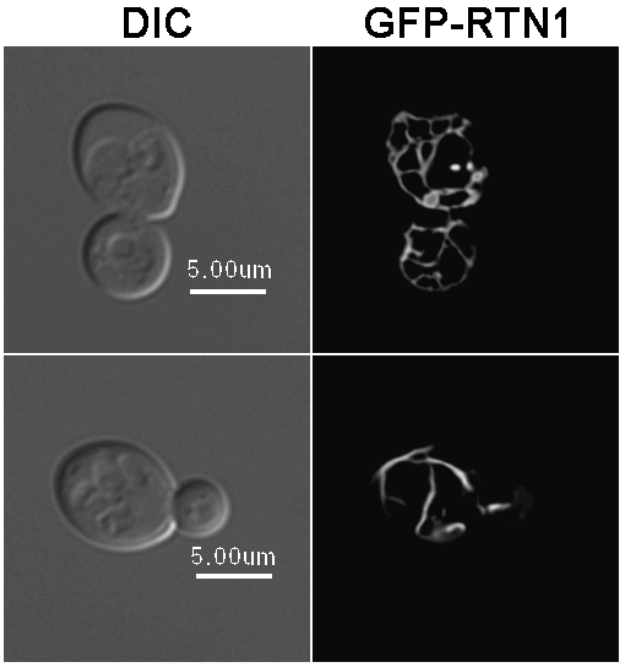

Figure 4.1 Overexpression of GFP-Rtn1p results in an accumulation of tubular structures. GFP-Rtn1p was overexpressed in RCY4274 (*reg1Δ)* cells by galactose induction for 16 hours and visualized by fluorescence microscopy. Two examples are shown highlighting that some cells have branched tubules while others do not. The cause of this discrepancy is unknown.

Expression of Rtn1p restores a tubular peripheral ER in *rtn1Δrtn2Δyop1Δ* cells

Previous studies have determined that deletion of *RTN1* or *YOP1* alone in cells has no effect on the morphology of the peripheral ER. However, *rtn1Δyop1Δ* cells (and *rtn1Δrtn2Δyop1Δ* cells) manifest abnormal peripheral ER sheet-like structures, although some areas of tubules remain. Expression of Rtn1p or GFP-Rtn1p is known to rescue this morphological defect, restoring tubular morphology typical of the peripheral ER [1]. In order to demonstrate that, in my hands, these results are reproducible, I analyzed the morphology of the peripheral ER in wild-type, *rtn1Δ*, *yop1Δ, rtn1Δyop1Δ,* and *rtn1Δrtn2Δyop1Δ* cells, using RFP-KDEL expression to visualize the structure of the ER. In wild-type, *rtn1Δ*, and *yop1Δ* cells I found the peripheral ER is composed of tubules as was previously shown (99 +/- 1%, 93.6 +/- 1.5%, 96 +/- 4% cells with normal ER, respectively) (Table 4.3, Figure 4.2). Most of the *rtn1Δyop1Δ* and *rtn1Δrtn2Δyop1Δ* cells contain large areas of membrane sheets in their peripheral ER as expected (9.3 +/- 2.6%, 5 +/- 3.6% cells with normal ER, respectively) (Table 4.3, Figure 4.2). I also found that expression of Rtn1p was sufficient to restore the sheet-like ER phenotype to a normal tubular morphology (63 +/- 7% cells with normal ER) (Table 4.3, Figure 4.2). These results confirm that Rtn1p is a player in the structuring of the tubules of the peripheral ER and demonstrates that I have the ability to use the sheet-like ER phenotype of the *rtn1Δrtn2Δyop1Δ* cells to analyze the ability of *RTN1* mutants in order to uncover the mechanism of membrane tubule formation utilized by Rtn1p.

Figure 4.2 Rtnp1 is involved in the formation of the tubules of the peripheral ER
A. RFP-KDEL expression in wild-type, *rtn1Δ, yop1Δ, rtn1Δyop1Δ, and rtn1Δrtn2Δyop1Δ* cells showing the morphology of the ER. Expression of genomic Rtn1p in *rtn1Δrtn2Δyop1Δ* cells is included in the bottom row. B. Quantification of the cells from A. with normal, tubular peripheral ER structure. Numbers are presented as average+/-standard deviation (N=300 for all cases)

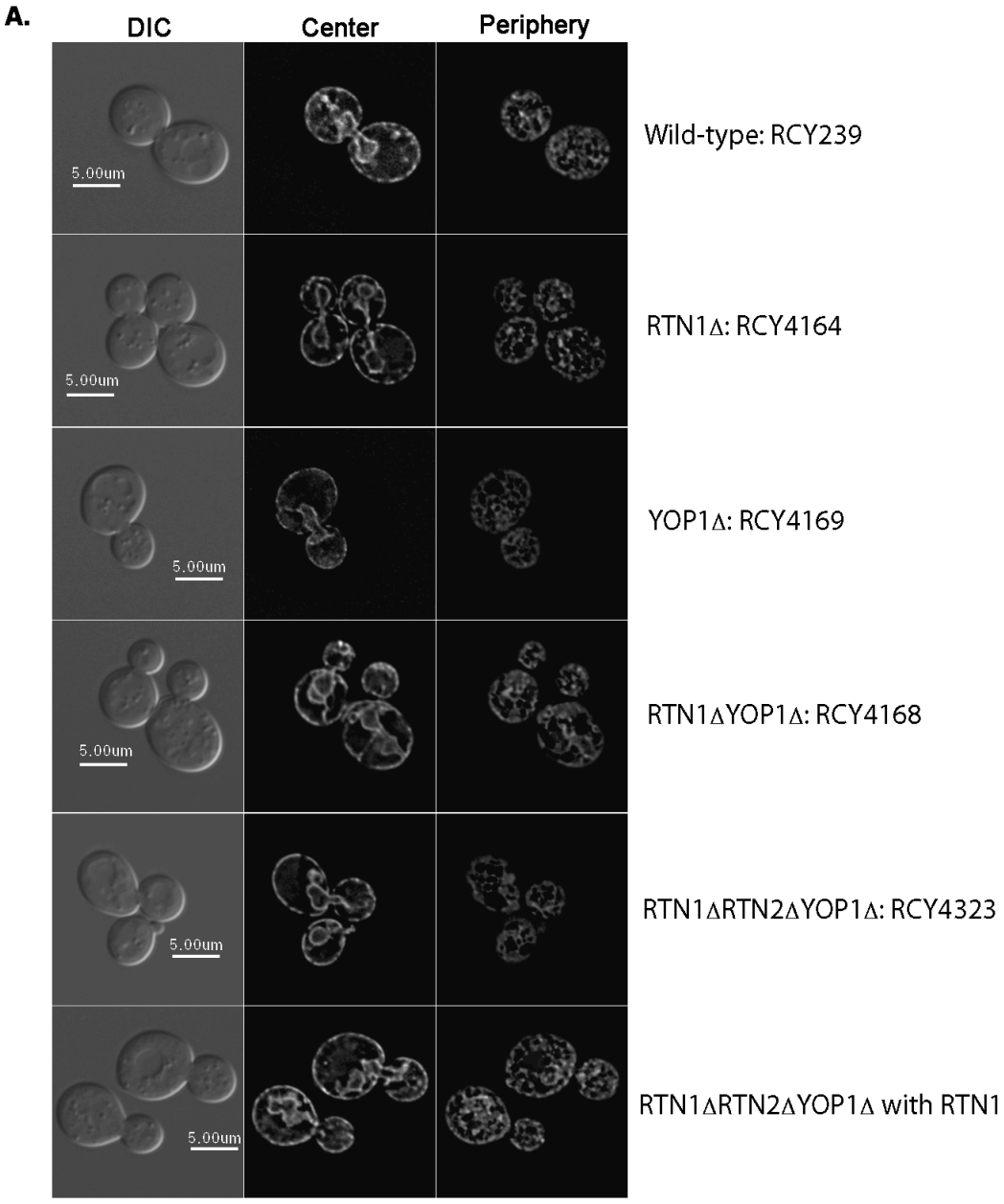
A.
DIC
Center
Periphery
5.00um
Wild-type: RCY239
RTN1Δ: RCY4164
YOP1Δ: RCY4169
RTN1ΔYOP1Δ: RCY4168
RTN1ΔRTN2ΔYOP1Δ: RCY4323
RTN1ΔRTN2ΔYOP1Δ with RTN1

Figure 4.2 Continued

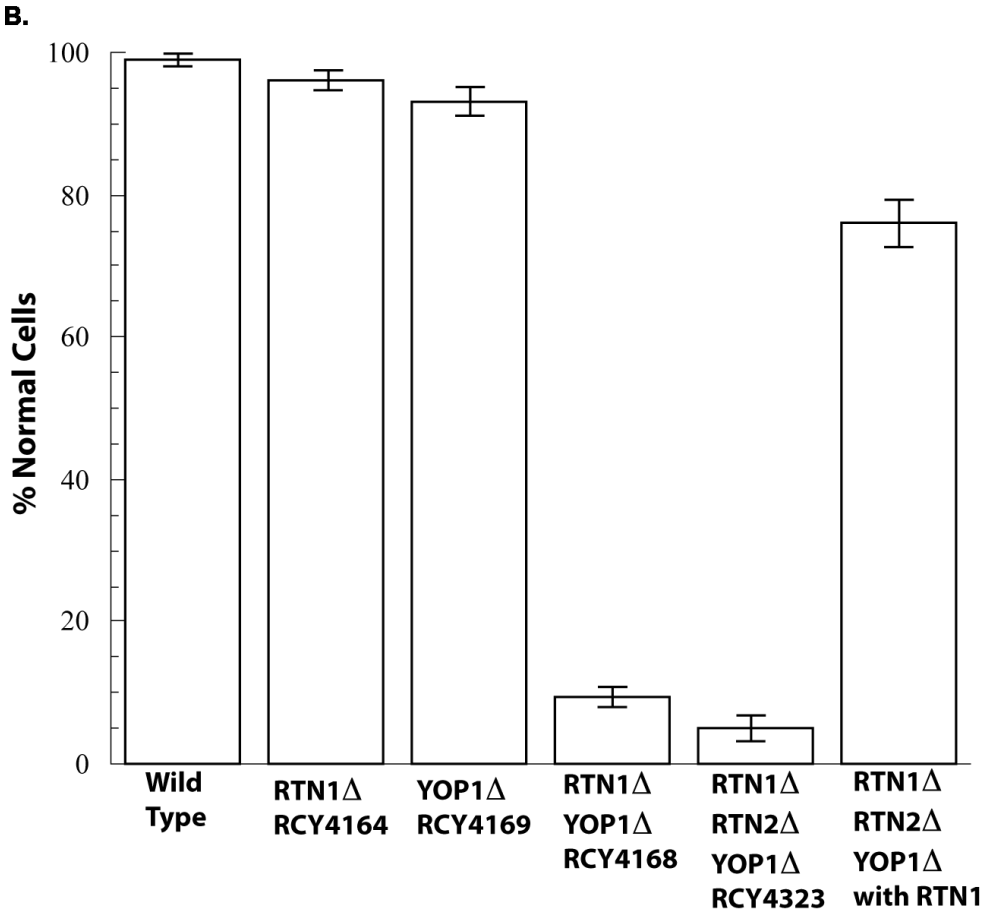

Table 4.3 Quantification of cells with a normal peripheral ER morphology, Rtn1p is involved in structuring the tubules of the peripheral ER

RCY strain	Plasmid(s)	Slide 1 100 cells counted	Slide 2 100 cells counted	Slide 3 100 cells counted	Average	St. Dev.
239	pRC3588	100	98	99	99	1
4169	pRC3588	94	92	95	93.6	1.5
4164	pRC3588	94	97	97	96	4
4168	pRC3588	3	9	16	9.3	2.6
4323	pRC3588	6	8	1	5	3.6
4323	pRC3588, pRC4560	70	56	63	63	7

GFP-Rtn1p functions in generating the tubular peripheral ER

rtn1Δrtn2Δyop1Δ cells contain large areas of membrane sheets in their peripheral ER and complementation of these cells with genomic Rtn1p restores a normal, tubular peripheral ER [1]. To determine the ability of GFP tagged Rtn1p to functionally replace *RTN1* in these cells, GFP-Rtn1p or Rtn1-GFP was expressed in *rtn1Δrtn2Δyop1Δ* cells and the morphology of the peripheral ER was analyzed by fluorescence microscopy. Expression of both NH_2 and COOH terminally tagged Rtn1p was found to restore the tubules of the peripheral ER to a similar level as genomic *RTN1* (70.3 +/-1.5%, 57.6 +/- 3.5%, 69 +/- 13.2% cells with normal ER, respectively) (Table 4.4, Figure 4.3). This analysis provides a platform to test mutants of Rtn1p for their ability to restore the tubular morphology to the peripheral ER.

Table 4.4 Quantification of cells with a normal peripheral ER morphology, GFP tagged Rtn1p is functional

RCY strain	Plasmid(s)	Slide 1 100 cells counted	Slide 2 100 cells counted	Slide 3 100 cells counted	Average	St. Dev.
4168	pRS315	10	6	11	9	2.6
4168	pRC4560	84	59	64	69	13.2
4168	pRC3501	59	69	72	70.3	1.5
4168	pRC3413	70	61	58	57.6	3.5

Figure 4.3 GFP-tagged Rtn1p is functional in restoring a tubular ER morphology in *rtn1Δrtn2Δyop1Δ* cells A. Vector control, *RTN1, GFP-RTN1* and *RTN1-GFP* was expressed in *rtn1Δrtn2Δyop1Δ* cells and peripheral ER morphology was analyzed by fluorescence microscopy. B. Quantification of the cells from A. with normal, tubular peripheral ER structure. Numbers are presented as average+/-standard deviation

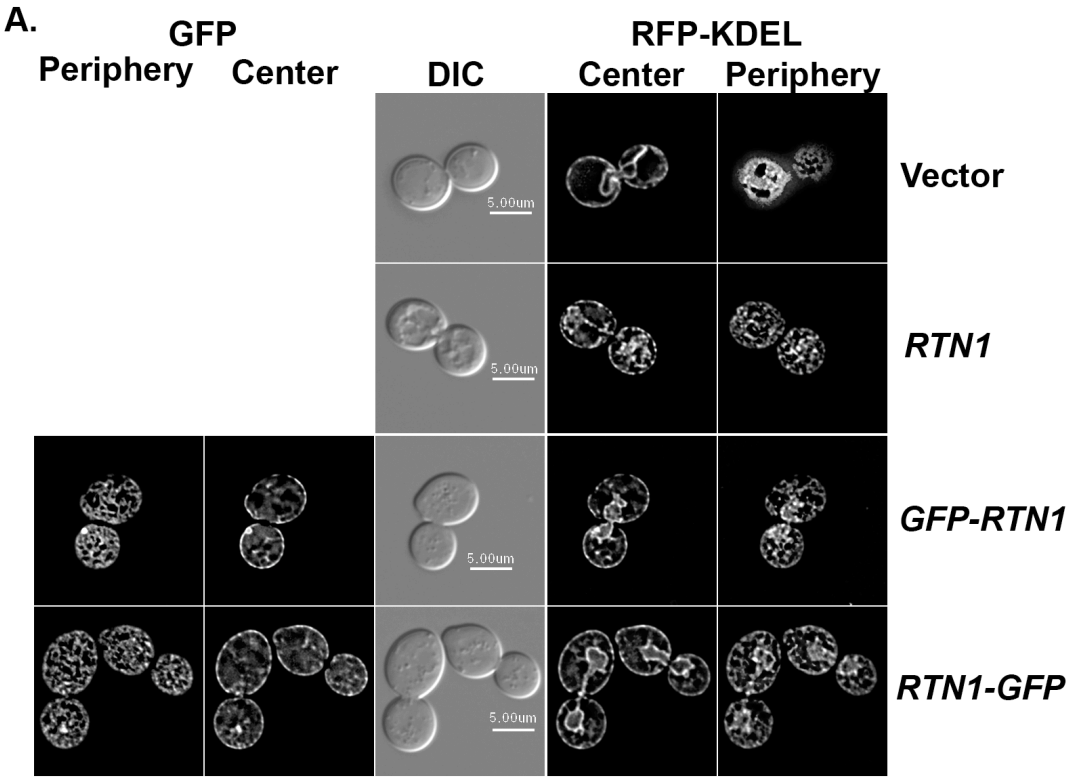
A.
GFP
Periphery
Center
DIC
RFP-KDEL
Center
Periphery
Vector
RTN1
GFP-RTN1
RTN1-GFP
5.00um

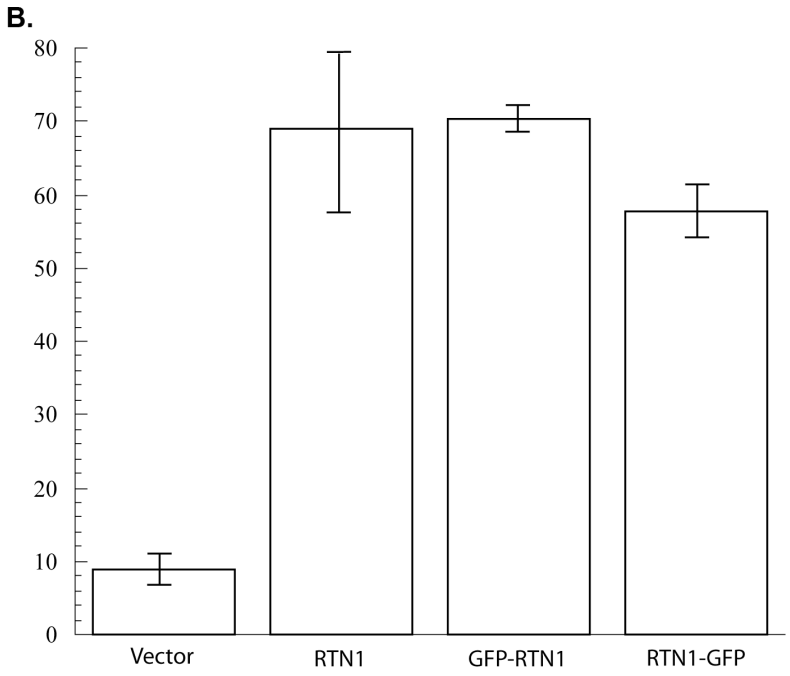
B.
80
70
60
50
40
30
20
10
0
Vector
RTN1
GFP-RTN1
RTN1-GFP

An *RTN1* mutant that cannot be palmitoylated functions in generating a tubular peripheral ER

Previous studies have shown that Rtn1p contains four cysteine residues that are post-translationally modified by the addition of a palmitoyl fatty acid. Palmitoylation of cysteines can provide a hydrophobic functional group to a protein that can be inserted into a membrane [21-24].

All 4 cysteine residues of *RTN1* are located in close proximity to the ends of the hydrophobic domains (Figure 4.4). Upon membrane insertion, these palmitoyl groups may alter the shape/topology of Rtn1p within the membrane and therefore may contribute to the ability of Rtn1p to function in membrane tubulation. A cysteine-less *RTN1* mutant was kindly provided by Dr. Nick Davis (Wayne State University) and I COOH terminally tagged it with GFP (GFP-Rtn1p-PMut). This palmitoylation mutant of GFP-Rtn1p was tested for its ability to restore a tubular peripheral ER in *rtn1Δrtn2Δyop1Δ* cells. Expression of GFP-Rtn1p-PMut in *rtn1Δrtn2Δyop1Δ* cells resulted in a normal, tubular peripheral ER (70.3 +/- 1.5% cells with normal ER) (Table 4.5, Figure 4.5), suggesting the palmitoylation of Rtn1p does not play a role in its function in generating the tubules of the peripheral ER.

Table 4.5 Quantification of cells with normal peripheral ER morphology, Rtn1p-PMut is functional

RCY strain	Plasmid(s)	Slide 1 100 cells counted	Slide 2 100 cells counted	Slide 3 100 cells counted	Average	St. Dev.
4168	pRS315	1	2	2	1.6	0.5
4168	pRC3501	84	59	64	69	13.2
4168	pRC3577	59	69	72	70.3	1.5

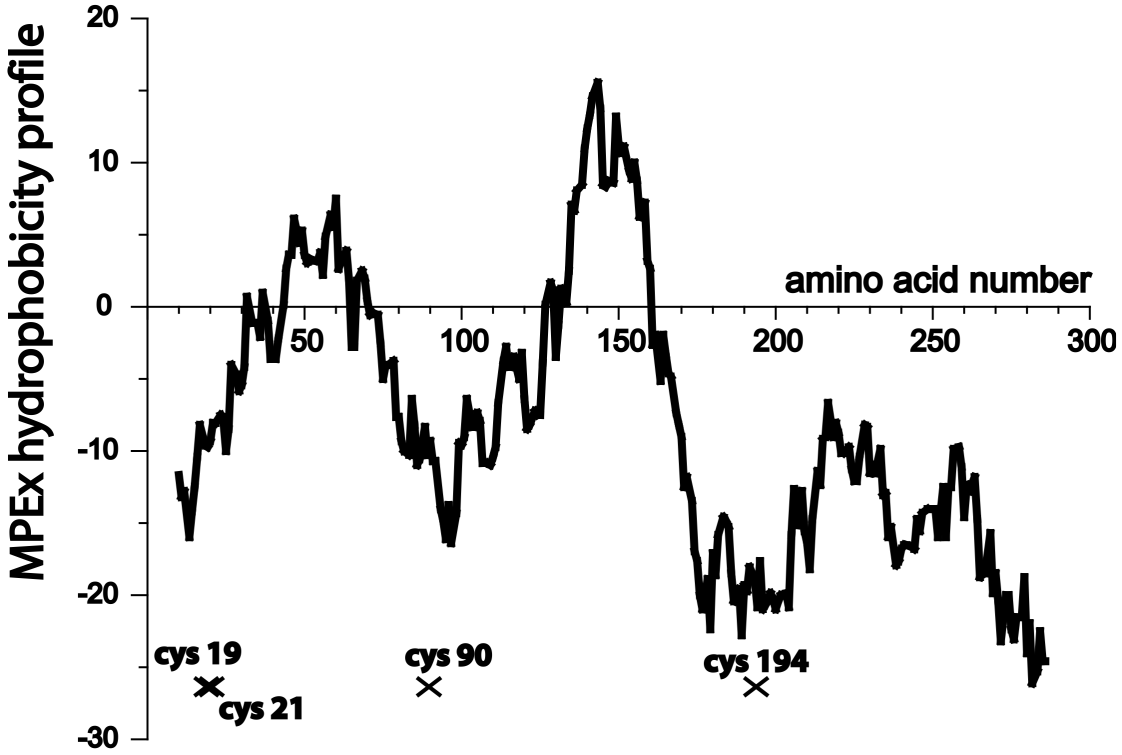

Figure 4.4 MPex hydrophobicity plot of RTN1-PMut Hydrophobicity prediction of the primary amino acid sequence of Rtn1p with the location of the four cysteine residues indicated by the black Xs.

Figure 4.5 Rtn1p-PMut is functional in restoring a normal peripheral ER morphology A. Vector control, GFP-Rtn1p and GFP-Rtn1p-Pmut were expressed in *rtn1Δrtn2Δyop1Δ* cells and peripheral ER morphology was analyzed by fluorescence microscopy. B. Quantification of the cells from A. with normal, tubular peripheral ER structure. Numbers are presented as average+/-standard deviation

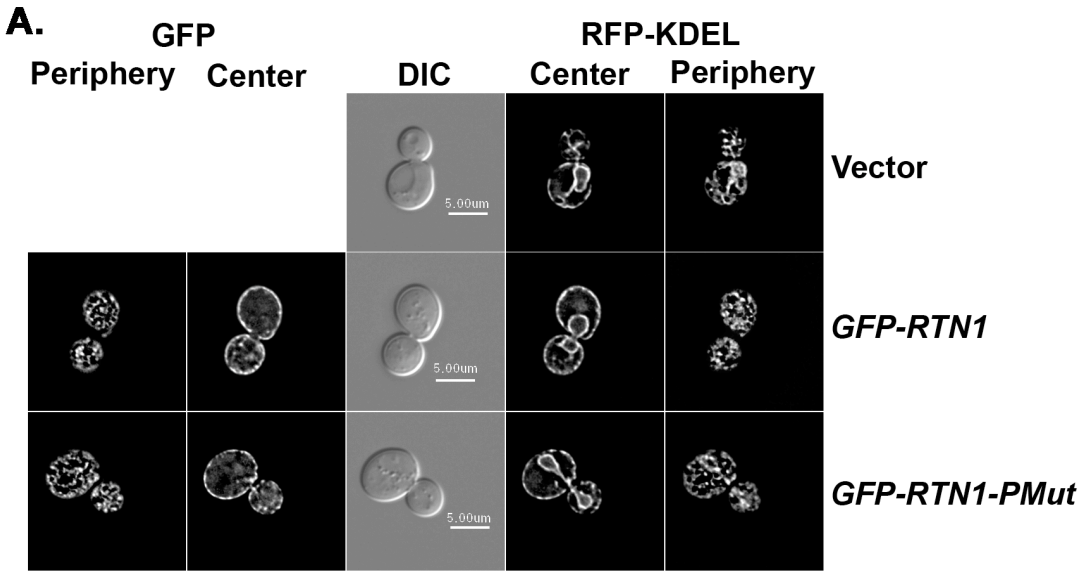
A.
GFP
Periphery
Center
DIC
RFP-KDEL
Center
Periphery
Vector
GFP-RTN1
GFP-RTN1-PMut
5.00um
5.00um
5.00um

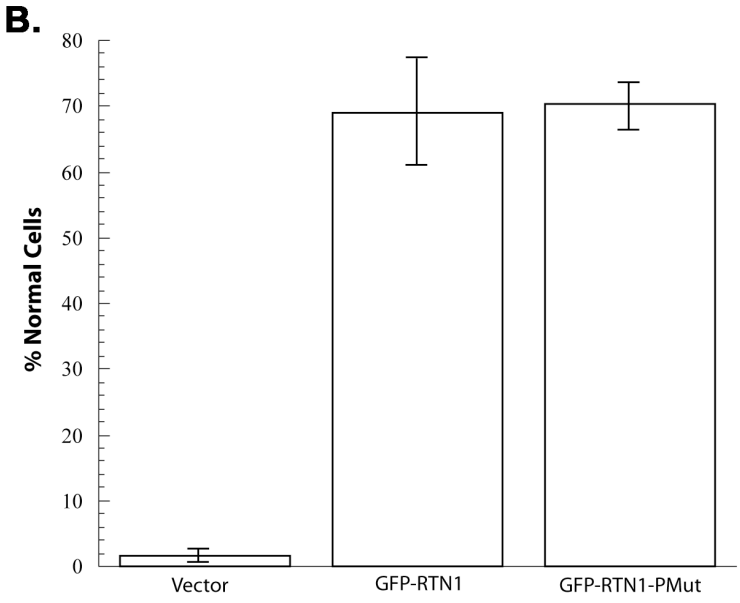
B.
% Normal Cells
80
70
60
50
40
30
20
10
0
Vector
GFP-RTN1
GFP-RTN1-PMut

Punctate localization of Rtn1p is increased in the Rtn1p-PMut

While majority of the cells expressing GFP-Rtn1p show an ER localization pattern, during this analysis I also noted that some cells show Rtn1p localization into punctate structures, though the morphologies of ER in these cells is unknown. In the palmitoylation mutant of Rtn1p it appeared the punctate localization was increased, suggesting that the palmitoylation of Rtn1p may in fact play some role in its localization. To determine if this observation was significant and to further understand how the palmitoylation of Rtn1p affects its function, the number of cells with a punctate Rtn1p localization was determined in GFP-Rtn1p and GFP-Rtn1p-PMut expressing cells. This analysis confirmed that the localization of Rtn1p to punctate structures was increased in the palmitoylation mutant of Rtn1p (61.8 +/- 4.1% cells with punctate localization) (Table 4.6, Figure 4.6) when compared to punctate localization of GFP-Rtn1p (35.4 +/- 2.3% cells with punctate localization) (Table 4.6, Figure 4.6), confirming that this modification does affect the ability of Rtn1p to localize to the tubular ER. It may be that Rtn1p has some other function in cells, distinct from its role in forming peripheral ER tubules, and the palmitoylation of Rtn1p acts to regulate its function between these two roles in cells. However, it is unclear why so many of the Rtn1p expressing cells have a punctate localization. It may be that these cells are expressing Rtn1p at a higher level that forces the formation of puncta and this effect is more severe in the palmitoylation mutant.

Table 4.6 Quantification of cells with punctate Rtn1p localization, for each slide 100 cells were counted

RCY Strain	Plasmid	Slide 1	Slide 2	Slide 3	Slide 4	Slide 5	Average	St. Dev.
239	pRC3413	35	36	34	39	33	35.4	2.3
239	pRC3414	64	60	62	56	67	61.8	4.1

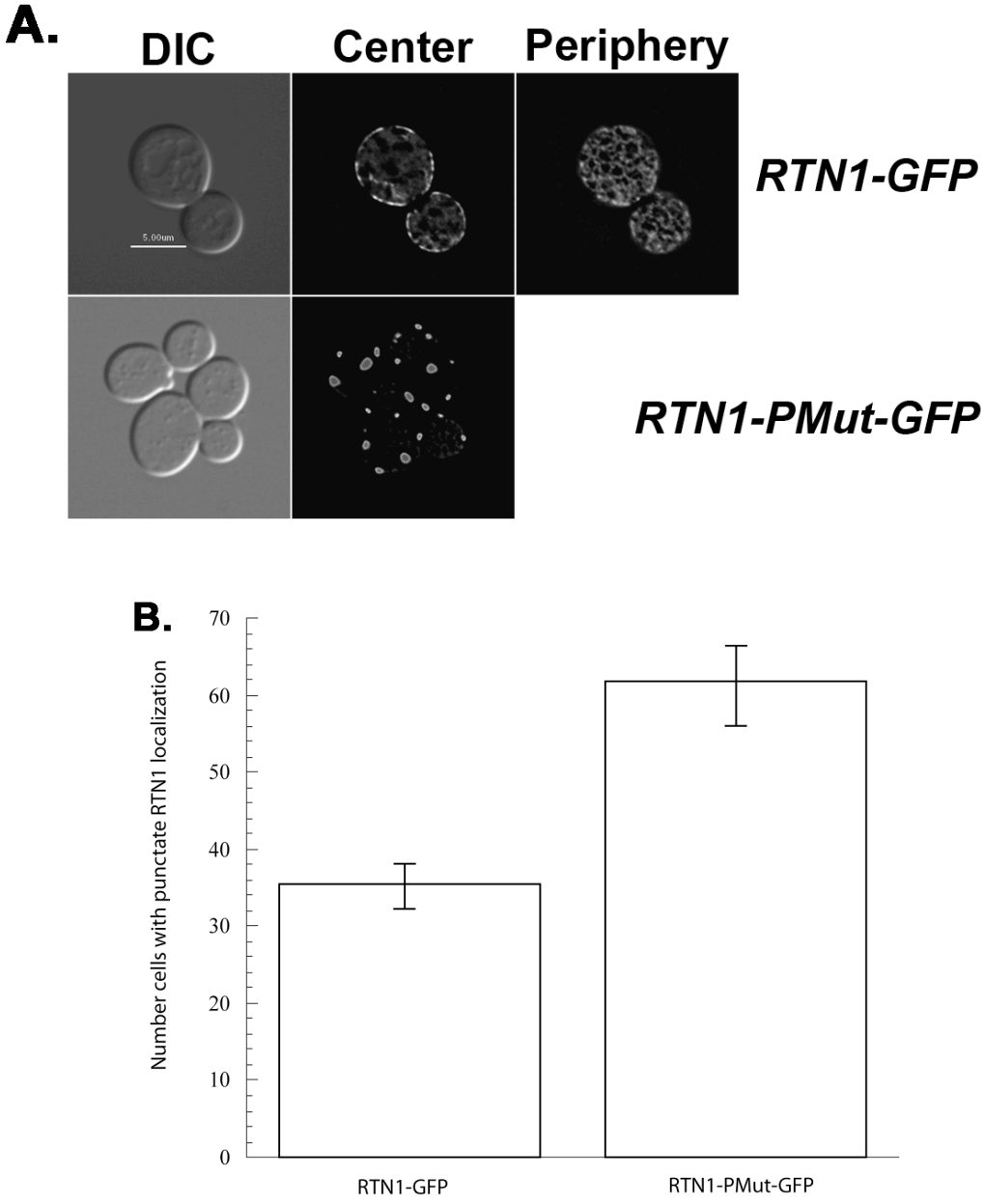

Figure 4.6 Punctate localization of Rtn1p-Pmut A. Fluorescence microscopy images of cells expressing GFP-Rtn1p or GFP-Rtn1p-PMut. B. Quantification of the number of cells displaying a punctate localization pattern of the expressed construct. Numbers are presented as average+/-standard deviation.

Formation of junction points between tubules appears unaffected by the palmitoylation of Rtn1p

The formation of tubular membrane structures requires the generation of positive membrane curvature [25]. The point that two tubules are connected in the peripheral ER, called junction points, requires localized areas of negative membrane curvature for the tubules to be joined [26]. Considering the fact that Rtn1p functions in generating the positive membrane curvature required for tubule formation [1], I reasoned that the palmitoylation of Rtn1p might act to alter its ability to generate this positive curvature. Perhaps the modification of Rtn1p specifically at the junction points allows this negative curvature to be formed by modulating the tubulating activity of Rtn1p. To assess this possibility, either GFP-Rtn1p or GFP-Rtn1p-PMut was expressed in wild-type, *rtn1Δ* cells and *rtn1Δrtn2Δyop1Δ* cells and the number of junction points per square micrometer was determined. This analysis was carried out by capturing fluorescence images of these cells then counting the number of junction points present within the mother cell. This number was then divided by the surface area of the mother cell (in square micrometers), providing the average number of junction points in a square micrometer. Surface area was determined by measuring two diameters and using πR^2. This analysis determined there was not a significant difference in the number of junction points formed by GFP-Rtn1p or GFP-Rtn1p-P-Mut expression in any of these cell types (Tables 4.7-4.12, Figure 4.7), suggesting that the palmitoylation of Rtn1p does not effect the formation of junction points in cells.

Figure 4.7 Junction point analysis GFP-Rtn1p or GFP-Rtn1p-PMut was expressed in wild-type (A. RCY239), *rtn1Δ* (B. RCY4164) or *rtn1Δyop1Δ* (C. RCY4168) cells and the number of junction points per square micrometer was determined. Numbers are presented as average +/-standard deviation.

A.

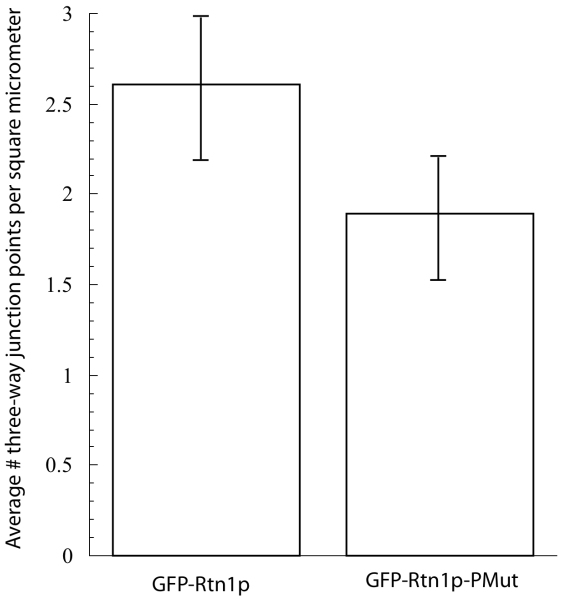
Average # three-way junction points per square micrometer
3
2.5
2
1.5
1
0.5
0
GFP-Rtn1p
GFP-Rtn1p-PMut

Figure 4.7 Continued

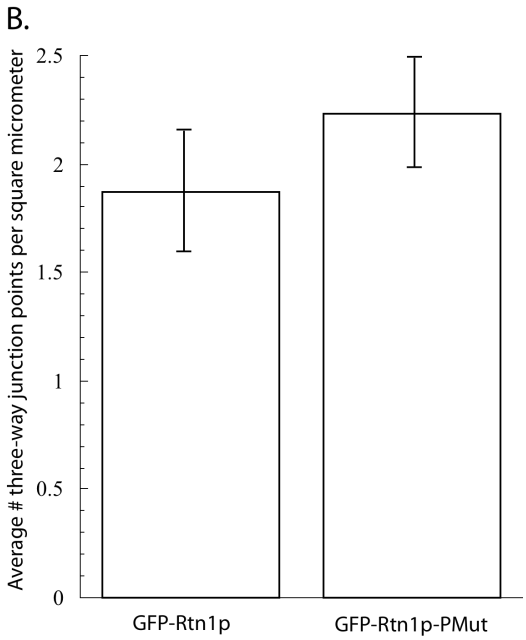

Figure 4.7 Continued

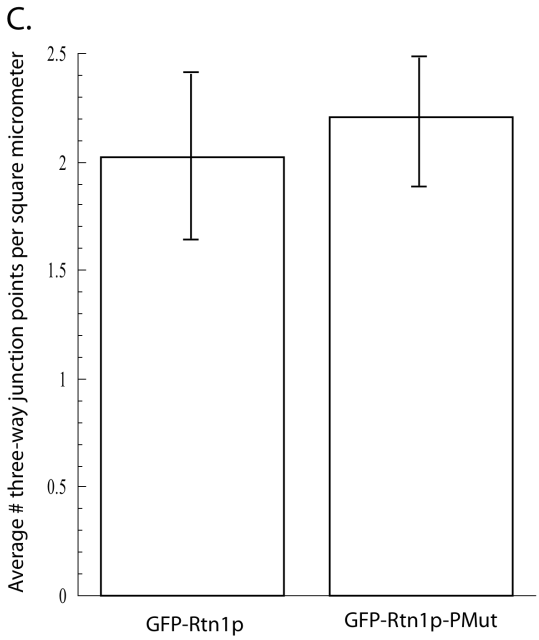

Table 4.7 Junction point analysis of wild-type cells expressing GFP-Rtn1p

Strain	Plasmid	Diameter 1 (μm)	Diameter 2 (μm)	Surface Area ($\mu m^{2)}$	# Junction Points	# Junction Points/μm^2
RCY239	pRC3501	5.8	5.5	25.0	102	4.0
RCY239	pRC3501	5.7	5.4	24.1	75	3.1
RCY239	pRC3501	5.3	5.6	23.3	58	2.4
RCY239	pRC3501	5	4.3	16.9	51	3.0
RCY239	pRC3501	5.5	5.6	24.1	72	2.9
RCY239	pRC3501	4.2	4.5	14.8	52	3.4
RCY239	pRC3501	4.6	4.3	15.5	60	3.8
RCY239	pRC3501	5.7	5.6	25.0	61	2.3
RCY239	pRC3501	5.6	5.5	24.1	64	2.4
RCY239	pRC3501	4.6	5	18.0	47	2.5
RCY239	pRC3501	5.7	6	26.8	76	2.8
RCY239	pRC3501	4.7	4.7	17.3	58	3.3
RCY239	pRC3501	5.8	6	27.3	64	2.3
RCY239	pRC3501	4.8	5.1	19.2	67	3.4
RCY239	pRC3501	5.4	5.2	22.0	55	2.4
RCY239	pRC3501	4.8	5.1	19.2	56	2.9
RCY239	pRC3501	4.8	5	18.5	50	2.6
RCY239	pRC3501	4.1	4.9	15.9	38	2.3
RCY239	pRC3501	6.4	6.1	30.6	73	2.3
RCY239	pRC3501	5.2	5.1	20.8	58	2.7
RCY239	pRC3501	5	5.2	20.4	44	2.1
RCY239	pRC3501	6.1	5.5	26.4	61	2.3
RCY239	pRC3501	4.7	5.2	19.2	48	2.4
RCY239	pRC3501	4.9	5.4	20.8	28	1.3
RCY239	pRC3501	3.9	4.4	13.5	36	2.6
RCY239	pRC3501	6.8	7	37.3	62	1.6
RCY239	pRC3501	5.8	5.3	24.1	62	2.5
RCY239	pRC3501	5.6	6	26.4	61	2.3
RCY239	pRC3501	5.9	5.3	24.6	46	1.8
RCY239	pRC3501	4.7	5	18.4	39	2.1
RCY239	pRC3501	5.3	5.9	24.3	43	1.7
RCY239	pRC3501	5.7	6	26.8	54	2.0
RCY239	pRC3501	5.2	5.2	21.2	43	2.0
RCY239	pRC3501	4.8	4.6	17.3	53	3.0
RCY239	pRC3501	4.9	5.2	20.0	49	2.4
RCY239	pRC3501	4	4.9	15.5	41	2.6
					Average	2.6
					Standard Deviation	0.6

Table 4.8 Junction point analysis of wild-type cells expressing GFP-Rtn1p-PMut

Strain	Plasmid	Diameter 1 (μm)	Diameter 2 (μm)	Surface Area ($\mu m^{2)}$	# Junction Points	# Junction Points/μm^2
RCY239	pRC3577	5.7	6	26.8	35	1.3
RCY239	pRC3577	5.1	5	20.0	54	2.6
RCY239	pRC3577	6	6	28.2	54	1.9
RCY239	pRC3577	6	6.2	29.2	40	1.3
RCY239	pRC3577	4.4	4.5	15.5	38	2.4
RCY239	pRC3577	6.4	7.2	36.3	56	1.5
RCY239	pRC3577	5.9	6.3	29.2	51	1.7
RCY239	pRC3577	5.8	5.8	26.4	48	1.8
RCY239	pRC3577	5	5	19.6	46	2.3
RCY239	pRC3577	6	6.3	29.7	50	1.6
RCY239	pRC3577	6.1	6	28.7	57	1.9
RCY239	pRC3577	5.1	5.3	21.2	47	2.2
RCY239	pRC3577	7	7.1	39.3	55	1.4
RCY239	pRC3577	5.6	5.6	24.6	48	1.9
RCY239	pRC3577	4.8	5.3	20.0	44	2.1
RCY239	pRC3577	5.2	4.9	20.0	40	1.9
RCY239	pRC3577	5.1	5.2	20.8	50	2.4
RCY239	pRC3577	5.6	6	26.4	38	1.4
RCY239	pRC3577	4.9	5.1	19.3	37	1.8
RCY239	pRC3577	4.9	4.6	17.7	35	1.9
RCY239	pRC3577	4.8	3.9	14.8	26	1.7
RCY239	pRC3577	6.6	5.8	30.1	45	1.4
RCY239	pRC3577	5	5.3	20.8	50	2.4
RCY239	pRC3577	5.5	6.2	26.7	46	1.7
RCY239	pRC3577	5.4	5.9	25.0	46	1.8
RCY239	pRC3577	4.6	5.3	19.2	36	1.8
RCY239	pRC3577	6.5	6.5	33.1	66	1.9
RCY239	pRC3577	5.1	5.7	22.9	29	1.6
RCY239	pRC3577	4.6	5	18.0	45	2.4
RCY239	pRC3577	5.6	5.9	25.9	51	1.9
RCY239	pRC3577	6	5.8	27.3	43	1.5
					Average	1.8
					Standard Deviation	0.4

Table 4.9 Junction point analysis of *rtn1Δ* cells expressing GFP-Rtn1p

Strain	Plasmid	Diameter 1 (μm)	Diameter 2 (μm)	Surface Area ($\mu m^{2)}$	# Junction Points	# Junction Points/μm^2
RCY4164	pRC3501	3.8	4	11.9	32	2.6
RCY4164	pRC3501	4.6	4.7	16.9	31	1.8
RCY4164	pRC3501	5.4	6.3	26.8	35	1.3
RCY4164	pRC3501	6.3	6.9	34.2	41	1.2
RCY4164	pRC3501	4.5	5.4	19.2	33	1.7
RCY4164	pRC3501	4.5	3.9	13.8	26	1.8
RCY4164	pRC3501	3.8	4.2	12.5	30	2.8
RCY4164	pRC3501	6.7	6.1	32.1	42	1.3
RCY4164	pRC3501	5.2	5	20.4	38	1.8
RCY4164	pRC3501	6	6.8	32.1	46	1.4
RCY4164	pRC3501	5.7	5.8	25.9	42	1.6
RCY4164	pRC3501	5.9	6	27.8	36	1.2
RCY4164	pRC3501	5	5.3	20.8	41	1.9
RCY4164	pRC3501	5	4.8	18.8	36	1.9
RCY4164	pRC3501	5.4	6.4	27.3	55	2.0
RCY4164	pRC3501	5.5	6.1	26.4	46	1.7
RCY4164	pRC3501	4.2	4.4	14.5	33	2.2
RCY4164	pRC3501	5.8	5.6	25.5	43	1.6
RCY4164	pRC3501	6.8	6.3	33.7	49	1.4
RCY4164	pRC3501	5	5.7	22.4	51	2.2
RCY4164	pRC3501	5.2	5.8	23.7	47	1.9
RCY4164	pRC3501	4.9	5	19.2	47	2.4
RCY4164	pRC3501	5.3	6.5	27.3	56	2.0
RCY4164	pRC3501	5.6	6	26.4	48	1.8
RCY4164	pRC3501	6	6.6	31.1	44	1.4
RCY4164	pRC3501	5.9	6.5	30.1	57	1.8
RCY4164	pRC3501	6	5.8	27.3	57	2.0
RCY4164	pRC3501	7	7.2	39.5	82	2.0
RCY4164	pRC3501	5.4	5	21.2	36	1.6
RCY4164	pRC3501	6	6.3	29.7	55	1.8
RCY4164	pRC3501	5.3	5.3	22.0	56	2.5
RCY4164	pRC3501	6	6.5	30.6	52	1.6
RCY4164	pRC3501	5.4	5.3	22.4	40	1.7
RCY4164	pRC3501	5.7	5	22.4	56	2.4
					Average	1.8
					Standard Deviation	0.4

Table 4.10 Junction point analysis of *rtn1Δ* cells expressing GFP-Rtn1p-PMut

Strain	Plasmid	Diameter 1 (μm)	Diameter 2 (μm)	Surface Area ($\mu m^{2)}$	# Junction Points	# Junction Points/μm^2
RCY4164	pRC3577	5.3	4.4	18.4	35	1.8
RCY4164	pRC3577	4.9	6	23.3	38	1.2
RCY4164	pRC3577	4.7	4.8	17.7	41	2.3
RCY4164	pRC3577	5	4.8	18.8	33	1.7
RCY4164	pRC3577	4	4	12.5	31	2.4
RCY4164	pRC3577	6	5.2	24.6	52	2.1
RCY4164	pRC3577	4	3.9	12.2	47	3.8
RCY4164	pRC3577	4.4	4.8	16.6	34	2.0
RCY4164	pRC3577	4.9	4.6	17.7	32	1.8
RCY4164	pRC3577	6.1	6	28.7	44	1.5
RCY4164	pRC3577	4.2	4	13.2	28	2.1
RCY4164	pRC3577	3.6	3.5	9.9	30	3.0
RCY4164	pRC3577	6	6	28.2	47	1.6
RCY4164	pRC3577	4	4	12.5	23	1.8
RCY4164	pRC3577	6.1	6.2	29.7	64	2.1
RCY4164	pRC3577	6.6	6.7	34.7	56	1.6
RCY4164	pRC3577	4.9	4.4	16.8	47	2.7
RCY4164	pRC3577	5.6	5.2	22.9	45	1.6
RCY4164	pRC3577	4.3	4.6	15.5	50	3.2
RCY4164	pRC3577	4.5	4.3	15.2	37	2.4
RCY4164	pRC3577	4.1	4	12.8	40	3.1
RCY4164	pRC3577	5.5	5.8	25.0	45	1.7
RCY4164	pRC3577	4.6	4.4	15.9	42	2.6
RCY4164	pRC3577	5	5.3	20.8	52	2.4
RCY4164	pRC3577	5.3	5.5	22.9	44	1.9
RCY4164	pRC3577	5.9	6.1	28.2	59	2.0
RCY4164	pRC3577	6	6.6	31.1	60	1.9
RCY4164	pRC3577	5.2	5.3	21.6	50	2.3
RCY4164	pRC3577	4.5	4.5	15.9	47	2.9
RCY4164	pRC3577	5.2	5.3	21.6	37	1.7
					Average	2.2
					Standard Deviation	0.5

Table 4.11 Junction point analysis of *rtn1Δyop1Δ* cells expressing GFP-Rtn1p

Strain	Plasmid	Diameter 1 (μm)	Diameter 2 (μm)	Surface Area ($\mu m^{2)}$	# Junction Points	# Junction Points/μm^2
RCY4168	pRC3501	5	5.3	20.8	43	2.0
RCY4168	pRC3501	4.2	4.9	16.2	45	2.7
RCY4168	pRC3501	3.1	3.2	7.7	22	2.8
RCY4168	pRC3501	5	4.9	19.2	43	2.2
RCY4168	pRC3501	6	6.6	31.1	66	2.1
RCY4168	pRC3501	4.4	4.2	14.5	40	2.7
RCY4168	pRC3501	7.3	8	45.9	92	2.0
RCY4168	pRC3501	5.5	5.3	22.9	59	2.5
RCY4168	pRC3501	4.7	5.5	20.4	42	2.0
RCY4168	pRC3501	5.4	5.5	23.3	40	1.7
RCY4168	pRC3501	6.1	6.1	29.2	65	2.2
RCY4168	pRC3501	6	6.1	28.7	44	1.5
RCY4168	pRC3501	5.4	5.9	25.0	42	1.6
RCY4168	pRC3501	5.2	5.5	22.4	39	1.7
RCY4168	pRC3501	4	3.8	11.9	33	2.7
RCY4168	pRC3501	5.1	5.2	20.8	32	1.5
RCY4168	pRC3501	5	4.8	18.8	40	2.1
RCY4168	pRC3501	5.1	5.2	20.8	47	2.2
RCY4168	pRC3501	5.5	5.5	23.7	42	1.7
RCY4168	pRC3501	4.5	5.8	16.9	38	2.2
RCY4168	pRC3501	5.1	4.9	19.6	45	2.2
RCY4168	pRC3501	6.5	6.6	33.6	55	1.6
RCY4168	pRC3501	6.8	7	37.3	47	1.2
RCY4168	pRC3501	6	6.4	30.1	43	1.4
RCY4168	pRC3501	5.3	5.5	22.9	37	1.6
RCY4168	pRC3501	5.3	5	20.8	29	1.3
RCY4168	pRC3501	5.5	6	25.9	45	1.7
RCY4168	pRC3501	5	5.1	20.0	38	1.8
RCY4168	pRC3501	6.1	6.2	29.7	49	1.6
RCY4168	pRC3501	5.5	5.1	22.0	53	2.4
RCY4168	pRC3501	4.6	4.8	17.3	32	1.8
RCY4168	pRC3501	4.7	4.3	15.9	35	2.2
RCY4168	pRC3501	4.5	4.3	15.2	38	2.4
					Average	2.0
					Standard Deviation	0.4

Table 4.12 Junction point analysis of *rtn1Δyop1Δ* cells expressing GFP-Rtn1p-PMut

Strain	Plasmid	Diameter 1 (μm)	Diameter 2 (μm)	Surface Area ($\mu m^{2)}$	# Junction Points	# Junction Points/μm^2
RCY4168	pRC3577	5	5.4	21.2	42	1.9
RCY4168	pRC3577	5.7	6.1	27.3	56	2.0
RCY4168	pRC3577	6.8	6.5	34.7	57	1.6
RCY4168	pRC3577	5.7	5.6	25.0	44	1.7
RCY4168	pRC3577	4.9	5.3	20.4	57	2.7
RCY4168	pRC3577	5.7	6.3	28.2	56	1.9
RCY4168	pRC3577	5	5	19.6	50	2.5
RCY4168	pRC3577	5.3	5.4	22.4	49	2.1
RCY4168	pRC3577	4.6	5	18.0	56	3.0
RCY4168	pRC3577	4.3	5	16.9	44	2.5
RCY4168	pRC3577	4.5	4.8	16.9	41	2.4
RCY4168	pRC3577	4.7	5.2	19.2	47	2.4
RCY4168	pRC3577	4.7	4.9	18.0	44	2.4
RCY4168	pRC3577	4.3	4.9	16.6	32	1.9
RCY4168	pRC3577	5.6	6.4	28.7	60	2.1
RCY4168	pRC3577	5.1	5.3	21.2	44	2.0
RCY4168	pRC3577	4.9	4.8	18.4	57	3.0
RCY4168	pRC3577	5	5	19.6	38	1.3
RCY4168	pRC3577	4.5	5.2	18.4	38	2.5
RCY4168	pRC3577	6.3	6.8	33.6	67	1.9
RCY4168	pRC3577	4.9	5.2	20.0	41	2.0
RCY4168	pRC3577	5.2	5	20.4	41	2.0
RCY4168	pRC3577	4.9	5	19.2	39	2.0
RCY4168	pRC3577	3.6	4.2	11.9	34	2.8
RCY4168	pRC3577	4.5	4.9	17.3	43	2.4
RCY4168	pRC3577	4.7	5	18.4	57	3.0
RCY4168	pRC3577	4.3	4.7	15.9	35	2.2
RCY4168	pRC3577	6	5.6	26.4	46	1.7
RCY4168	pRC3577	5.9	6.3	29.2	45	1.5
RCY4168	pRC3577	6.4	6.6	33.1	51	1.5
					Average	2.2
					Standard Deviation	0.4

DISCUSSION

Rtn1p is thought to provide a redundant function in peripheral ER tubule formation with Yop1p, considering one can functionally replace the other in this process (see figures 2.1 and 4.2) [1]. Additionally, both must be deleted in cells in order to alter the morphology of the normally tubular peripheral ER into largely, sheet-like structures [1]. I have previously shown that overexpression of Yop1p results in the formation of unbranched, long tubular structures that are stable enough to be partially purified through two sucrose gradients (see Chapter 3). Overexpression of Rtn1p results in a dramatic accumulation tubular structures within the cell, though these structures still contain junction points (Figure 4.1). I found that the Rtn1p tubules were not stable enough to withstand the enrichment procedure that yields the Yop1p tubules (data not shown, see Chapter 3), perhaps suggesting Rtn1p is more critical for the formation of the tubular structures while Yop1p is more critical for the maintenance of the tubular structure. However, a previous study provided evidence that purified Rtn1p was capable of forming tubules from pure lipids in vitro [6], thus both Rtn1p and Yop1p must share some redundancy in their function.

A model for the mechanism of Rtn1p in the formation of the tubules of the peripheral ER suggests that the insertion of the two long hydrophobic domains part-way through the membrane are responsible for its ability to generate membrane curvature [1]. The shape of Rtn1p within the membrane is thought to be responsible for its ability to function in tubule formation, though it is unclear if other factors also contribute to generating and maintaining this functional shape. It is clear that the post-translational palmitoylation of Rtn1p occurs at four cysteine residues located in close proximity to the long hydrophobic domains, though what effect this modification has on the conformation of Rtn1p, and thus its function, is unclear.

Expression of GFP-Rtn1p can restore the tubules of the peripheral ER in *rtn1Δrtn2Δyop1Δ* cells (Figure 4.3), providing a useful tool for the analysis of Rtn1p function and in determining how the palmitoylation of Rtn1p may also contribute to its function in cells. In most cells GFP-Rtn1p is localized to the peripheral ER as previously shown [1]. Interestingly, I also noted that in a subset of cells GFP-Rtn1p was localized into punctate structures. The identity of these punctate structures remains unknown, though they could be protein aggregates lacking membrane components. Alternatively a localized area with a high concentration of Rtn1p could form ER membrane aggregations resulting in the formation of karmellae. These ER membrane structures are often seen upon overexpression of ER membrane proteins [27, 28].

A mutant Rtn1p, where the four cysteine residues were all mutated to serine (C19S, C21S, C90S, C194S), was kindly provided by Dr. Nick Davis. An NH_2 terminal GFP fusion to this *RTN1* mutant (GFP-RTN1 P-Mut) was constructed and tested for its ability to restore the tubules of the peripheral ER in *rtn1Δrtn2Δyop1Δ* cells. This analysis provided insight into the contribution the palmitoylation of Rtn1p may have on its function in generating a tubular peripheral ER. I found that GFP-Rtn1p-PMut was equally as functional in restoring a normal, tubular peripheral ER as GFP-Rtn1p (Figure 4.5). This result suggests that the palmitoylation of Rtnp1 likely does not influence its ability to function in forming the tubules of the peripheral ER.

During fluorescence analysis I noticed that the number of cells with a punctate Rtn1p localization appeared to be elevated in the palmitoylation mutant when compared to GFP-Rtn1p. Upon closer analysis I confirmed that 35.4 +/- 2.3% cells expressing wild-type GFP-Rtn1p displayed a punctate localization while 61.8 +/- 4.1% cells expressing GFP-Rtn1p-PMut had this localization pattern (Figure 4.6). The increase in the unidentified puntate localization of the Rtnp1 palmitoylation mutant

may suggest that this modification plays a role in the normal localization of Rtn1p to the peripheral ER, although these structures have not been colocalized with ER labeling by RFP-KDEL. Considering the fact that Rtn1p is known to form homo-oligomeric complexes and that palmitoylation of proteins can alter their localization, it is possible that this modification may reduce Rtn1p oligomerization. Thus, in the Rtn1p-PMut, the lack of palmitoylation results in massive oligomerization of Rtn1p, resulting in aggregation seen as puncta by fluorescence microscopy. Further studies would elucidate the ability of Rtn1p-PMut to form oligomeric complexes and the influence this ability has on the formation of the puncta seen in cells.

I found that the palmitoylation of Rtn1p was not a critical modification for the generation of a tubular peripheral ER (Figure 4.5). It is possible the addition of this fatty acid to Rtn1p may be an important factor in regulating its function in generating membrane tubules, perhaps modulating the curvature generated by Rtn1p to allow the formation of junction points between tubules. The membranes at the intersection of two tubules must be bent in the negative direction, relative to the positive curvature that generates the tubules [25]. The palmitoylation of Rtn1p may decrease its ability to maintain the positive curvature of the tubule to allow fusion of two tubules. If this modification occurred specifically to the Rtn1p present at junction points it could decrease the energy required to curve the membrane in the negative direction and facilitate junction point formation.

I tested this hypothesis by analyzing the average number of junction points per square micrometer in cells. GFP-Rtn1p and GFP-Rtn1p-PMut were expressed in wild-type, *rtn1Δ* and *rtn1Δrtn2Δyop1Δ* cells and fluorescence images were captured. The number of junction points between tubules was determined within the mother cell and divided by the surface area of that cell yielding the average number of junction points per square micrometer. This analysis determined that there was not a significant

difference in the number of junction points in the Rtn1p-PMut (Figure 4.7). This result could mean that the palmitoylation of Rtn1p is not necessary for the formation of these junction points or that Rtn1p is not involved in the formation of these structures.

Palmitoylation is a modification that has been shown to alter the localization of a protein [19]. My findings suggest that the localization of Rtn1p was altered by the absence of palmitoylation (Figure 4.6), perhaps indicating that this modification functions as a localization signal to aid in the proper localization of Rtn1p to peripheral ER membranes. GFP-Rtn1p-PMut localized to punctate structures in many cells, though the exact identity of these structures is yet to be determined. In addition, in a fairly large number of GFP-Rtn1p expressing cells also displayed the punctate localization, suggesting this pattern may be exaggerated by the absence of palmitoylation. Overexpression of other ER membrane proteins is known to generate membrane aggregates called karmellae [27, 28]. It is also possible that the puncta seen in these cells are a result of aggregated Rtn1p and membranes and does not represent a true shift in localization, but is an artifact of a localized area of concentrated Rtn1p on the ER. This fact may suggest that the palmitoylation serves to stabilize Rtn1p within the membrane and prevent aggregation. Further studies aimed at identifying any membrane connections of the puncta could distinguish between a true shift in Rtn1p localization and the formation of lamellae.

REFERENCES

1. Voeltz, G.K., et al., *A class of membrane proteins shaping the tubular endoplasmic reticulum*. Cell, 2006. **124**(3): p. 573-86.
2. De Craene, J.O., et al., *Rtn1p is involved in structuring the cortical endoplasmic reticulum*. Mol Biol Cell, 2006. **17**(7): p. 3009-20.
3. Kiseleva, E., et al., *Reticulon 4a/NogoA locates to regions of high membrane curvature and may have a role in nuclear envelope growth*. J Struct Biol, 2007. **160**(2): p. 224-35.
4. Dodd, D.A., et al., *Nogo-A, -B, and -C are found on the cell surface and interact together in many different cell types*. J Biol Chem, 2005. **280**(13): p. 12494-502.
5. Shibata, Y., et al., *The reticulon and DP1/Yop1p proteins form immobile oligomers in the tubular endoplasmic reticulum*. J Biol Chem, 2008.
6. Hu, J., et al., *Membrane proteins of the endoplasmic reticulum induce high-curvature tubules*. Science, 2008. **319**(5867): p. 1247-50.
7. Hu, X., et al., *Transgenic mice overexpressing reticulon 3 develop neuritic abnormalities*. Embo J, 2007. **26**(11): p. 2755-67.
8. He, W., et al., *The membrane topology of RTN3 and its effect on binding of RTN3 to BACE1*. J Biol Chem, 2007. **282**(40): p. 29144-51.
9. Qi, B., et al., *Pro-apoptotic ASY/Nogo-B protein associates with ASYIP*. J Cell Physiol, 2003. **196**(2): p. 312-8.
10. Geng, J., et al., *Saccharomyces cerevisiae Rab-GDI displacement factor ortholog Yip3p forms distinct complexes with the Ypt1 Rab GTPase and the reticulon Rtn1p*. Eukaryot Cell, 2005. **4**(7): p. 1166-74.
11. Feng, D., et al., *The transmembrane domain is sufficient for Sbh1p function, its*

association with the Sec61 complex, and interaction with Rtn1p. J Biol Chem, 2007. **282**(42): p. 30618-28.

12. Tolley, N., et al., *Overexpression of a plant reticulon remodels the lumen of the cortical endoplasmic reticulum but does not perturb protein transport*. Traffic, 2008. **9**(1): p. 94-102.
13. Chen, C.Z., et al., *Genetic analysis of yeast Yip1p function reveals a requirement for Golgi-localized rab proteins and rab-Guanine nucleotide dissociation inhibitor*. Genetics, 2004. **168**(4): p. 1827-41.
14. Greaves, J., et al., *Regulation of SNAP-25 trafficking and function by palmitoylation*. Biochem Soc Trans, 2010. **38**(Pt 1): p. 163-6.
15. Baekkeskov, S. and J. Kanaani, *Palmitoylation cycles and regulation of protein function (Review)*. Mol Membr Biol, 2009. **26**(1): p. 42-54.
16. Uechi, Y., et al., *Rap2 function requires palmitoylation and recycling endosome localization*. Biochem Biophys Res Comm, 2009. **378**(4): p. 732-7.
17. Subramanian, K., et al., *Palmitoylation determines the function of Vac8 at the yeast vacuole*. J Cell Sci, 2006. **119**(Pt 12): p. 2477-85.
18. Pfeffer, S.R., et al., *Selective membrane recruitment of Rab GTPases*. Cold Spring Harb Symp Quant Biol, 1995. **60**: p. 221-7.
19. Uittenbogaard, A. and E.J. Smart, *Palmitoylation of caveolin-1 is required for cholesterol binding, chaperone complex formation, and rapid transport of cholesterol to caveolae*. J Biol Chem, 2000. **275**(33): p. 25595-9.
20. Smotrys, J.E. and M.E. Linder, *Palmitoylation of intracellular signaling proteins: regulation and function*. Annu Rev Biochem, 2004. **73**: p. 559-87.
21. Veit, M. and M.F. Schmidt, *Membrane targeting via protein palmitoylation*. Methods Mol Biol, 1998. **88**: p. 227-39.

22. Mundy, D.I., *Protein palmitoylation in membrane trafficking*. Biochem Soc Trans, 1995. **23**(3): p. 572-6.

23. Wedegaertner, P.B., et al., *Palmitoylation is required for signaling functions and membrane attachment of Gq alpha and Gs alpha*. J Biol Chem, 1993. **268**(33): p. 25001-8.

24. Grassie, M.A., et al., *Lack of N terminal palmitoylation of G protein alpha subunits reduces membrane association*. Biochem Soc Trans, 1993. **21**(4): p. 499S.

25. Farsad, K. and P. De Camilli, *Mechanisms of membrane deformation*. Curr Opin Cell Biol, 2003. **15**(4): p. 372-81.

26. Prinz, W.A., et al., *Mutants affecting the structure of the cortical endoplasmic reticulum in Saccharomyces cerevisiae*. J Cell Biol, 2000. **150**(3): p. 461-74.

27. Profant, D.A., et al., *The role of the 3-hydroxy 3-methylglutaryl coenzyme A reductase cytosolic domain in karmellae biogenesis*. Mol Biol Cell, 1999. **10**(10): p. 3409-23.

28. Wright, R., et al., *Increased amounts of HMG-CoA reductase induce "karmellae": a proliferation of stacked membrane pairs surrounding the yeast nucleus*. J Cell Biol, 1988. **107**(1): p. 101-14.

CHAPTER 5

CONCLUSIONS

Previous studies have identified a redundant function for Yop1p and Rtn1p in the formation of the tubular structure of the peripheral ER. Deletion of *YOP1* or *RTN1* alone has no apparent phenotype, while deletion of both together results in a morphological alteration of the tubules of the peripheral ER into large areas of sheet-like, cisternal membranes. This sheet-like ER phenotype can be restored to a normal, tubular structure by complementation with either Rtn1p or Yop1p, indicating one can functionally replace the other in this process (see Figures 2.1 and 4.2)[1]. Overexpression of either Yop1p or Rtn1p results in the accumulation of membrane tubules with a small diameter. These tubules appear to exclude ER luminal proteins due to their very small diameter, though presumably they remain continuous with the ER membrane [1-4]. These results are consistent with findings that purified Rtn1p or Yop1p have the ability to tubulate membranes in vitro. The tubules formed by purified Yop1p or Rtn1p have a small diameter of ~15 nm, small enough to exclude soluble proteins in the ER lumen. Interestingly, the tubules formed by Yop1p appear to have a very regular structure while the Rtn1p formed tubules appear to have more variation in the surface of the tubule [3]. This observation is constant with our finding that the Yop1p tubules are stable enough to withstand purification but the Rtn1p formed tubules are not able to withstand the same treatment. This difference in tubule stability between Yop1p and Rtn1p tubules may indicate a slightly different function in cells. Yop1p may mainly act to stabilize the tubules after formation in vivo, while Rtn1p may mainly initiate tubule formation, though both can accommodate the function of the other if need be. Distinguishing between the formation and the maintenance of

membrane tubules is especially difficult in this situation because of the redundancy of the function of Rtn1p and Yop1p.

Another observation made by Hu et al [3] was that purified Yop1p formed tubules contained areas where tubule junction points were present. This finding may suggest that Yop1p has the ability to form the junction points between tubules, or that junction point formation is possible without the influence of other factors. Studies have identified a small dynamin-like GTPase, Sey1p, that appears to function in regulating the formation of the three-way junction points of the peripheral ER, and the GTPase activity is required for this function [5, 6]. Sey1p is known to interact with Yop1p and it has been suggested that Sey1p may regulate the activity of Yop1p in generating the tubules of the peripheral ER, allowing junction point formation between two tubules. These authors [5] have suggested that Yop1p functions in the formation of the junction points through its interaction with Sey1p, although this role for Yop1p seems contradictory to its function in tubule formation. Sey1p is localized more heavily to the junction points, but Yop1p appears to be evenly distributed throughout the peripheral ER tubules [5]. Yop1p and Rtn1p present on the tubular structures may interact to generate the positive membrane curvature required for tubule formation [1]. When Yop1p interacts with Sey1p it may alter the function of Yop1p, through the GTPase activity of Sey1p, and function in generating the negative curvature necessary for junction point formation between two tubules [5, 6]. Perhaps the interaction between Yop1p and Sey1p abolishes the ability of Yop1p to generate positive membrane curvature, which decreases the energy required to bend the membrane in the negative direction and facilitating the formation of a junction point.

Another contradiction to the wedging mechanism used by Rtn1p/Yop1p in generating membrane curvature [1, 3] is the activity of flippases. Flippases act in many cases to rebalance the lipid distribution between the leaflets of the bilayer by

flipping lipids from one leaflet of the bilayer to the other [7-13]. A mechanism of maintaining the uneven surface area of the bilayer must exist for the wedging hypothesis to hold true. Flipases within the ER membrane must somehow sense that the high levels of curvature need to exist to allow the uneven surface areas to remain. Perhaps if the overall number of lipids remains constant between the two leaflets the flippases activity is decreased. This possibility would allow the mechanism used by Rtn1p/Yop1p to curve membranes to maintain membrane tubules by keeping the flippases from redistributing the lipids from the outer leaflet to the inner leaflet and decreasing the curvature of the peripheral ER tubules.

In recent years there has been an explosion in the field of membrane curvature generated by proteins. It would be interesting to develop a search engine aimed at locating and identifying ORFs that contain long, 30-40 amino acid, hydrophobic regions from sequenced genome databases. There are many organelles with very complex structures with no known mechanism to generate their specific morphology. The appendix of my thesis investigates an ORF from SARS-CoV contains a long hydrophobic domain which may function in generating membrane vesicles. Thus, there is evidence that viruses have hijacked the wedging mechanism of generating membrane curvature, which may suggest that the use of long hydrophobic domains to generate membrane curvature may be more widespread than we currently understand. This search engine would allow identification of other candidates for further analysis.

REFERENCES

1. Voeltz, G.K., et al., *A class of membrane proteins shaping the tubular endoplasmic reticulum*. Cell, 2006. **124**(3): p. 573-86.
2. Shibata, Y., et al., *The reticulon and DP1/Yop1p proteins form immobile oligomers in the tubular endoplasmic reticulum*. J Biol Chem, 2008. **283**(27): p. 18892-904.
3. Hu, J., et al., *Membrane proteins of the endoplasmic reticulum induce high-curvature tubules*. Science, 2008. **319**(5867): p. 1247-50.
4. Tolley, N., et al., *Overexpression of a plant reticulon remodels the lumen of the cortical endoplasmic reticulum but does not perturb protein transport*. Traffic, 2008. **9**(1): p. 94-102.
5. Hu, J., et al., *A class of dynamin-like GTPases involved in the generation of the tubular ER network*. Cell, 2009. **138**(3): p. 549-61.
6. Orso, G., et al., *Homotypic fusion of ER membranes requires the dynamin-like GTPase atlastin*. Nature, 2009. **460**(7258): p. 978-83.
7. Ezanno, P., S. Cribier, and P.F. Devaux, *Asymmetrical stress generated by the erythrocyte lipid flippase triggers multiple bud formation on the surface of spherical giant liposomes*. Eur Biophys J, 2010. **39**(8): p. 1277-80.
8. Natarajan, P., et al., *Regulation of a Golgi flippase by phosphoinositides and an ArfGEF*. Nat Cell Biol, 2009. **11**(12): p. 1421-6.
9. Sanyal, S. and A.K. Menon, *Specific transbilayer translocation of dolichol-linked oligosaccharides by an endoplasmic reticulum flippase*. Proc Natl Acad Sci U S A, 2009. **106**(3): p. 767-72.

10. Papadopulos, A., et al., *Flippase activity detected with unlabeled lipids by shape changes of giant unilamellar vesicles*. J Biol Chem, 2007. **282**(21): p. 15559-68.

11. Doerrler, W.T. and C.R. Raetz, *ATPase activity of the MsbA lipid flippase of Escherichia coli*. J Biol Chem, 2002. **277**(39): p. 36697-705.

12. Devaux, P.F., *Reconstitution of flippase activity into liposomes*. Cell Mol Biol Lett, 2002. **7**(2): p. 227-9.

13. Vishwakarma, R.A., et al., *New fluorescent probes reveal that flippase-mediated flip-flop of phosphatidylinositol across the endoplasmic reticulum membrane does not depend on the stereochemistry of the lipid*. Org Biomol Chem, 2005. **3**(7): p. 1275-83.

APPENDIX

INVESTIGATION OF SARS-CoV ORF6 REVEALS A POTENTIAL ROLE IN THE GENERATION OF DOUBLE MEMBRANE VESICLES

ABSTRACT

SARS-CoV is the causative agent of severe acute respiratory syndrome (SARS), a devastating disease that emerged in 2003. SARS-CoV has since been the subject of much research to uncover its pathogenesis. SARS-CoV is thought to form a specialized compartment within a host cell where replication of the viral genome takes place, called double membrane vesicles (DMVs) because they are composed of an inner and outer membrane barrier. Interestingly, SARS-CoV contains a group of accessory open reading frames (ORFs) with no known function. These ORFs appear to be dispensable for viral infection of tissue culture cells but it is thought that they confer some advantage to the virus during infection of a host organism. ORF6 is known to increase the replication rate of a related coronavirus and localizes to sites of viral replication within a host cell. ORF6 contains a single, long hydrophobic domain that is thought to form a hairpin within the membrane. Here I begin to investigate the possibility that this hydrophobic hairpin drives the formation of DMVs, perhaps through a membrane wedging mechanism.

INTRODUCTION

The coronaviruses represent a large family of enveloped, plus strand RNA viruses. Severe acute respiratory syndrome (SARS) is a devastating human disease that emerged in 2003 [1-4]. The SARS associated coraonavirus (SARS-CoV) was identified as the causative agent of SARS and has since been the subject of an enormous amount of research to understand the mechanism and progression of infection. Coronaviruses have the largest viral RNA genomes known and the genome of SARS-CoV is comprised of ~30 kb of RNA encoding 14 open reading frames with a similar organization pattern as other studied coronaviruses [5]. Interestingly, SARS-CoV also contains 8 accessory proteins (3a, 3b, 6, 7a, 7b, 8a, 8b, and 9b), which all appear to be non-essential during infection in tissue culture but provide some advantage to the virus during infection of a host [6]. Little is known of the function of these 8 accessory proteins. ORF3a is known to bind to spike and is postulated to provide a structural role for viral assembly [7, 8]. ORF7a localizes to ER-Golgi intermediate compartments where viral assembly is thought to occur, suggesting this protein may function in some stage of viral assembly. Additionally, ORF3a, ORF3b and ORF7a have all been shown to induce apoptosis in tissue culture, potentially as a means of lytic viral particle release [9-12].

The SARS-CoV lifecycle (Appendix Figure 1) begins with fusion of the viral envelop with a host cell plasma membrane, mediated by interactions between SARS-CoV spike protein and host ACE2 [13]. SARS-CoV (and other coronavirus) replication has been shown to occur within a series of unique vesicular structures known as double membrane vesicles (DMV), so called because the vesicles contain two lipid bilayers with replication taking place within the lumen of the inner

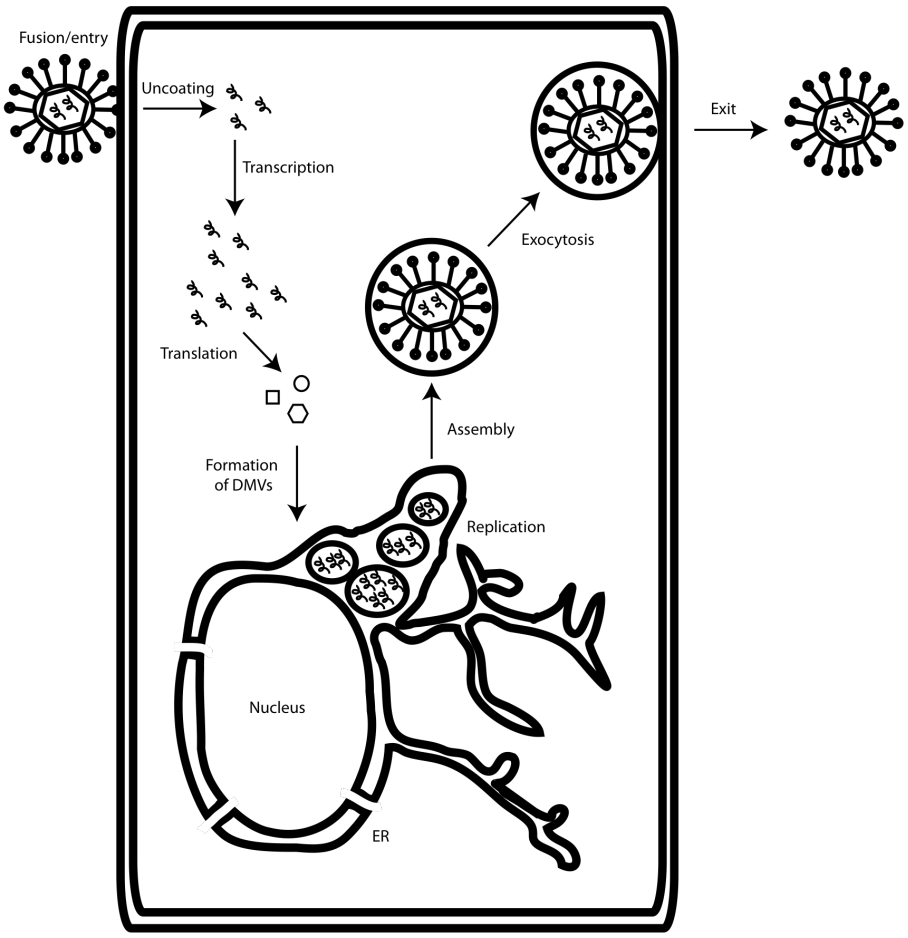

Figure 1 Simplified lifecycle of SARS CoV
Abbreviations: DMV Double Membrane Vesicles

membrane [14-16]. More recently, the morphology of these DMV structures was analyzed by electron microscopy revealing that the individual vesicles formed were also connected by a system of tubules, and that the entire tubular-vesicular structures are contained within the lumen of the ER. The unique morphology of the replication sites of SARS-CoV has led to the description of the replication sites as a reticulo-vesicular-tubular network [17]. DMV formation is thought to involve many of the host cells autophagocytic machinery [18], though the viral machinery that directs the formation of these vesicular structures has not been identified.

ORF6 expression has recently been shown to increase the replication rate and virulence of a related mouse coronavirus, murine hepatitis virus (MHV) and physically interact with nsp8, a non-structural protein that contains a RpRd domain that acts as a viral replicase [19]. These results may suggest that ORF6 functions during viral replication and acts to increase the rate of viral genome production. ORF6 may have an additional role in fighting the host cells immune response through interactions with the nuclear import adaptor molecule karyopherin alpha 2 in the cytoplasm. This interaction prevents interferon-induced nuclear import of STAT1 and decreases the host cells response to viral infection [23, 24].

In mammalian cells ORF6 localizes primarily to ER membranes as well as colocalizing with components of the SARS-CoV replication machinery and viral RNA [19-21]. ORF6 is a small integral membrane protein of 63 amino acids comprised of a hydrophilic NH_2 terminal region and a long (~43 amino acid) COOH terminal hydrophobic domain. Previous work using antibody accessibility in permeabalized and non-permeablized cells has determined that both the NH_2 and COOH termini of ORF6 are found on the cytoplasmic face of the ER membrane, suggesting the long hydrophobic domain adopts a hairpin-like conformation within the membrane [20]. Furthermore, previous work identified the hydrophobic domain of ORF6 as the

functional domain in increasing the rate of viral replication[20]. Thus, I reasoned that the presence of this hydrophobic domain within the membrane may act as a hydrophobic wedge, increasing the surface area of the outer leaflet of the membrane and driving membrane deformation, similar to the mechanism of caveolin action on membranes in generating caveolae [22].

The purpose of this study is to investigate the potential role of ORF6 in the formation of SARS-CoV replication DMV and to elucidate the mechanism of ORF6 action on membranes in remodeling the morphology of the ER into a reticulo-vesicular tubular network.

MATERIALS AND METHODS

Yeast strains and plasmids

All *S. cerevisiae* strains used in this study are listed in Appendix Table 1. Manipulations of these strains were done using standard biological techniques. Cell density was determined using a Thermo Spectronic Genesys 10UV spectrophotometer (Rochester, NY) at 600nm. Expression of ORF6 was driven by the promotor and terminator regions of *YOP1* (~500 bp upstream and downstream from the start codon, respectively). Overexpression of constructs under *GAL1/10* promotor control was performed by growing cells overnight in SD media to a density of 0.4-0.8. Cells were pelleted, washed once in ddH_20, and resuspended in 1mL ddH_20. Washed cells were inoculated into minimal media containing 2% galactose to an initial density of 0.05-0.2, depending on the length of induction.

Appendix Table 1 *S. cerevisiae* strains used in this study

RCY Strain	Genotype	Source
RCY239	*MAT***a** *ura3-52 leu2-3,112*	This lab
RCY4274	*MAT***a/α** *reg1*ΔKAN^R/ *reg1*ΔKAN^R *ura3Δ0/ ura3Δ0*, *leu2Δ0/ leu2Δ0*, *his3*Δ0/ *his3*Δ0, *lys2Δ0/ lys2Δ0*, *met15*Δ0/*MET15*	This lab

Plasmids were created using standard biological techniques and are listed in Appendix Table 2. GFP fusions were made by linking yEGFP to the NH_2 or COOH terminus of each construct with a GGPGG linker between the GFP and the ORF. Overexpression of each construct was done by two means. First, by integrating the GFP-ORF fusion into a multi-copy (2μ) vector ensures many copies of each construct in cells to increase the proteins production. Second, overexpression constructs are placed under the control of the promotor region of *GAL1/10*, which responds to the presence of galactose.

Appendix Table 2 Plasmids used in this study

Plasmid number	Construct	Description	Source
pRC3588	pRS315 *RFP-KDEL*		This lab
pRC3589	pRS316 *RFP-KDEL*		This lab
pRC4437	pRS426 ORF6-GFP		This study
pRC4438	pRS426 GFP-ORF6		This study
pRC4500	pRS315 GFP-ORF6		This study
pRC4501	pRS316 GFP-ORF66		This study
pRC4529	pRS315 H^{ORF6}-GFP	Amino acids 1-43	This study
pRC4530	pRS426 H^{ORF6}-GFP	Amino acids 1-43	This study

Fluorescence Microscopy

GFP fusions of each protein were created by fusing 238 amino acids of yeast enhanced green fluorescence protein (yEGFP) to either the NH_2 or COOH terminus and separated by a unique linker sequence (GGPGG).

For the overexpression studies, the promotor region of *GAL1/10* was used to induce ORF6 expression upon the addition of galactose to the growth media. RFP-KDEL expression was used to visualize ER structures. Cells were grown to mid-log phase in minimal media and pelleted, washed once in ddH_2O and resuspended in minimal media plus galactose to a density of ~0.1. Inductions were carried out for various time lengths depending on the experiment, as indicated in the results section. Images were collected using a Nikon Eclipse E600 microscope with a 100X (1.4NA) objective and 1x optivar. DIC images were collected from a single plane while fluorescence images were gathered as a series of 20-30 z steps of 0.2 μm. A CCD camera (Sensicam EM High Performance, The Cook Corporation) was used to collect images (software IP Lab version 3.6.5, Scanalytics). Blind deconvolution of each z-series was done using AutoQuant X2 program (Media Cybernetics) for 30 iterations. After deconvolution, single planes were identified that most clearly identified single tubular structures.

RESULTS

Localization of ORF6 in yeast

Considering the ER localization of ORF6 in mammalian cells [19-21], I sought to determine if ORF6 also localized to ER membranes in yeast and if yeast would be a useful model organism to study ORF6 function in. To accomplish this, ORF6 was tagged with GFP on its NH_2 terminus. Expression of this construct was driven by the promotor region of *YOP1* and termination by the terminator of *YOP1*. This analysis

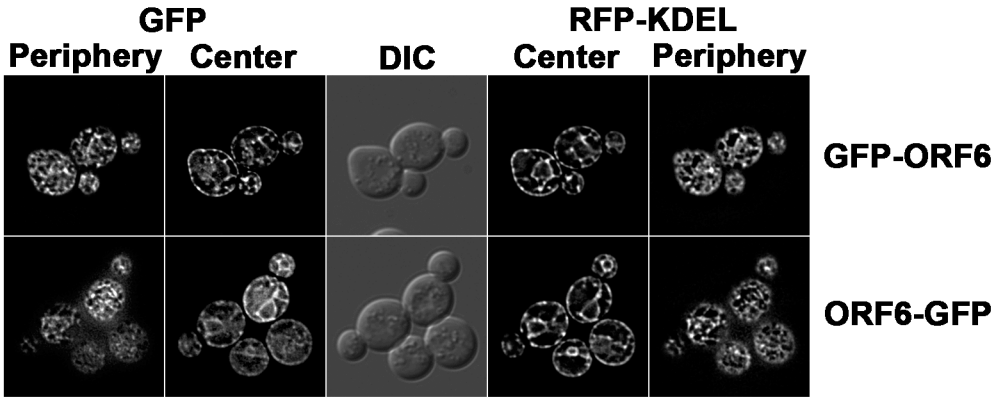

Figure 2 ORF6 localization in *S. cerevisiae* GFP-ORF6 or ORF6-GFP was expressed in wild-type (RCY239) cells and localization was analyzed by fluorescence microscopy. Co-expression of RFP-KDEL allowed visualization of ER.

revealed that GFP-ORF6 does in fact localize to what appeared to be ER membranes in yeast. Expression of the ER marker, RFP-KDEL, was co-expressed with GFP-ORF6 and confirmed that ORF6 is present on ER membranes as the two colocalized (Appendix Figure 2). This result indicates that ORF6 localizes to ER membranes through a mechanism that is conserved from yeast to mammalian cells. Furthermore, this result indicates that yeast will be a suitable organism to study the function of ORF6 in a genetically amenable cell.

Overexpression of GFP-ORF6 results in the formation of vesicular structures from ER membranes

During viral infection the concentration of viral proteins can reach very high levels, thus, I reasoned that overexpression of ORF6 in yeast might more closely mimic the levels of this protein during an actual infection. GFP-ORF6 was placed under the control of the *GAL1/10* promotor region and induced for 16 hours by the addition of 2% galactose. Examination by fluorescence microscopy revealed that ORF6 now localized to many vesicular structures spreading throughout the cytosol of the cell.

The vesicles formed resembled bunches of grapes and often appeared to surround the nuclear membrane of the cell (Appendix Figure 3). The grape-like bunches of vesicles appeared distinct in morphology from the ER membranes ORF6 localized to when lower protein levels were present so I performed a time-lapse experiment of the induction of GFP-ORF6 to determine the membrane source of the ORF6 formed vesicles. Cells were induced for GFP-ORF6 expression and protein localization was determined by fluorescence microscopy at 1 hour, 2 hours, 3.5 hours, 7 hours, 16 hours and 24 hours after induction. At early time points after induction, GFP-ORF6 localized to what appeared to be ER membranes with visible vesicular

Figure 3. Overexpression of ORF6 A. Wild-type cells overexpressing GFP-ORF6 by galactose induction after 24 hours. Fluorescence images of three planes taken through the indicated level of the cell are shown. B. A time-course induction of GFP-ORF6 by galactose induction. Fluorescence images were collected at 1 hour, 2 hours, 3.5 hours, 7 hours, 16 hours and 24 hours after induction. The images represent a cross sectional view through the center of the cell. C. Fluorescence images of wild-type cells overexpressing GFP-ORF6 for 16 hours. RFP-KDEL expression was used to monitor the morphology of the ER. D. Wild-type (RCY239) and *reg1Δ* (RCY4274) carrying either vector control or inducible GFP-ORF6 were struck onto minimal media plates containing either glucose (SD) or galactose (SGal) and grown at 30°C for three days and analyzed for growth.

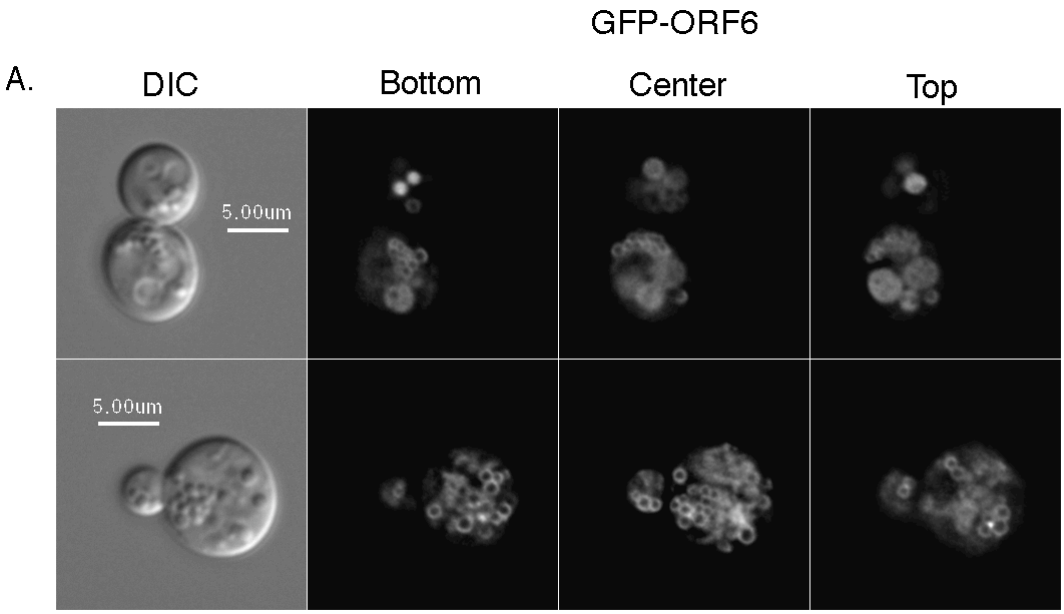
GFP-ORF6
A.
DIC
Bottom
Center
Top
5.00um
5.00um

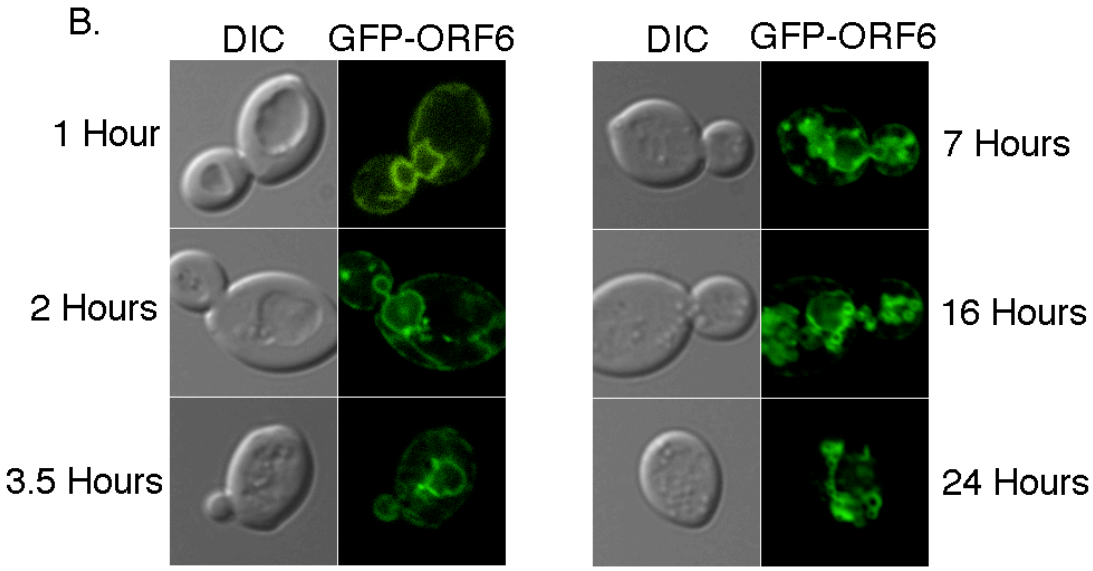
B.
DIC
GFP-ORF6
DIC
GFP-ORF6
1 Hour
2 Hours
3.5 Hours
7 Hours
16 Hours
24 Hours

Figure 3 Continued

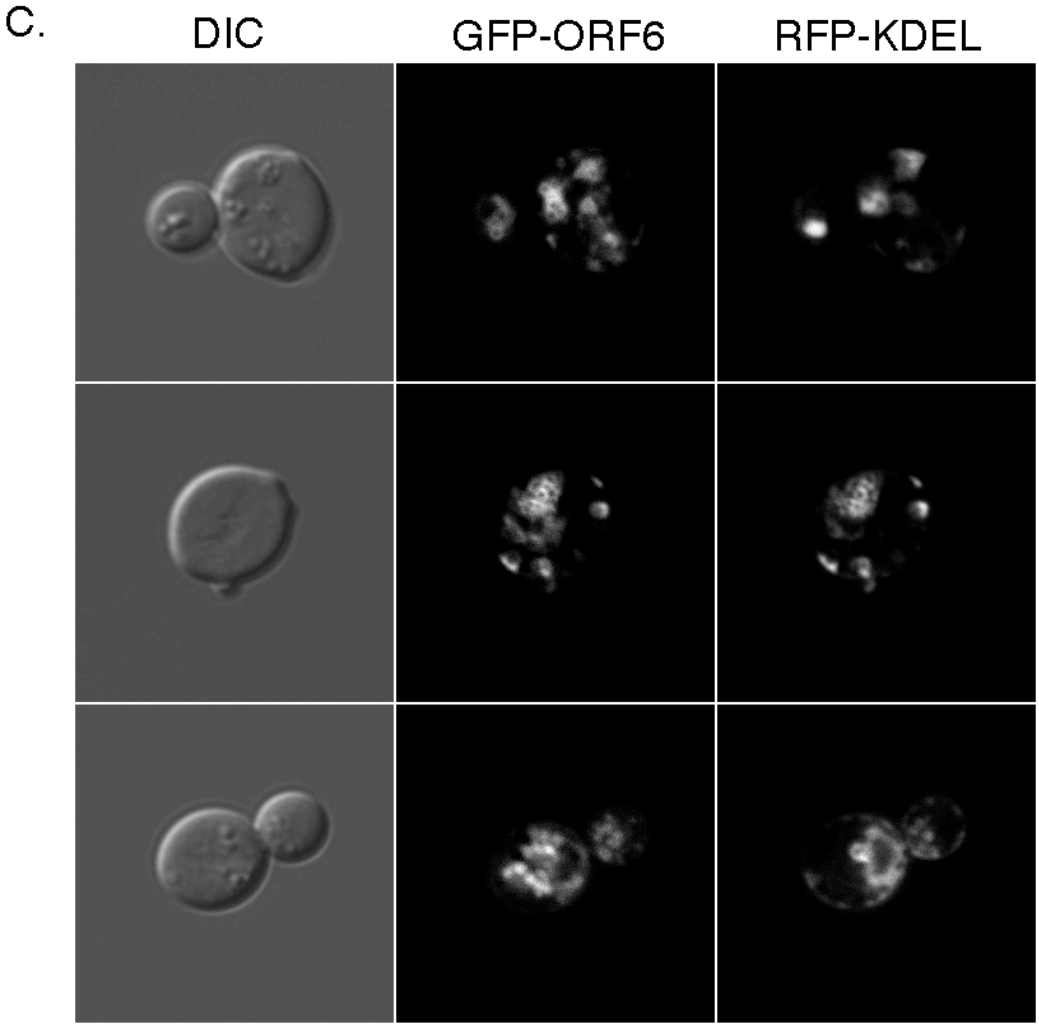

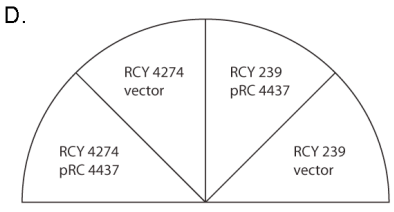

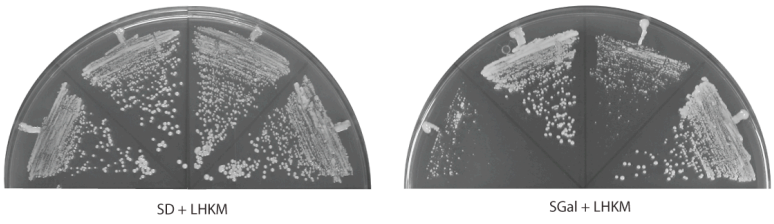

structures near the nuclear envelope by 7 hours. By 24 hours after induction, GFP-ORF6 localized completely to the vesicular structures and the ER localization was no longer discernable (Appendix Figure 3).

Since the vesicular structures form from ER membranes but the ER morphology is no longer discernable by 24 hours after induction, I sought to understand if the ER membranes were converted into the vesicular structures by ORF6 overexpression or if the ORF6 vesicles become distinct from the ER by 24 hours post-induction. If the vesicles are distinct from the ER, then I would expect the ER morphology to remain intact after the induction of ORF6. I used the expression of RFP-KDEL to monitor the morphology of the ER after the induction of GFP-ORF6 by fluorescence microscopy. After 24 hours GFP-ORF6 induction, RFP-KDEL localized solely to the ORF6 vesicles, and the typical ER morphology was no longer apparent. Interestingly, upon closer examination I noticed that the RFP-KDEL seemed to specifically localize around the vesicles, and was not present within the lumen of the vesicles (Appendix Figure 3). This localization, taken with the fact that the vesicles are formed from ER membranes, suggests that the vesicles may form within the ER lumen or that they form by budding into the ER lumen. Coronaviruses replicate within a unique membrane vesicle within the cell during infection known as a double membrane vesicle (DMV) ([14-16]. The DMV is thought to derive its membranes from the ER, and also form within the ER lumen [17]. It is thought that these vesicular structures are formed mainly by viral proteins, but also using host factors as well [18]. These results suggest that ORF6 may in part drive the formation of the DMV during infection, either directly or by recruiting host factors to bud membrane vesicles into the ER lumen.

ORF6 overexpression results in a slow growth phenotype

I noticed that cells overexpressing GFP-ORF6 appeared to grow somewhat more slowly than wild-type cells did, based on a decreased cell density after overnight growth (empirical observation). To confirm this observation vector control cells and cells containing the inducible GFP-ORF6 were struck onto minimal media plates containing either glucose or galactose as a carbon source. As expected, both cell lines grew normally on the glucose plate, and the GFP-ORF6 overexpressing cells showed decreased growth on the galactose plate when compared to the vector control cells (Appendix Figure 3). This result confirms that overexpression of GFP-ORF6 results in a slower division time. When this result is considered with the fact that overexpression of GFP-ORF6 appears to convert most of the ER membranes into the vesicular structures (Appendix Figure 3), it seems likely that the decreased cell growth may be due to the disruption of the morphology of the ER. Further studies aimed at analyzing the function of the ER, perhaps an ER to Golgi trafficking defect, would more definitively determine the reason for the decreased viability.

Localization of the hydrophobic domain of ORF6

Inspection of the predicted hydrophobic character of ORF6 primary amino acid sequence shows that ORF6 contains a long hydrophobic domain, ~43 amino acids long. Previous studies have determined that both the NH_2 and COOH termini are located on the cytoplasmic face of the ER membrane in mammalian cells, suggesting the hydrophobic domain of ORF6 may adopt a hairpin structure within the ER membrane [20]. There are other examples of long hydrophobic domains with the capacity to act as “wedges” within the membrane resulting in membrane bending. In order to determine if the hydrophobic domain of ORF6 is responsible for the action of ORF6 on the membrane, I created a GFP-tagged ORF6 truncation, containing only the

Figure 4 Localization of GFP-H^{ORF6} A. Fluorescence images of wild-type cells expressing GFP-H^{ORF6} to assess its localization. RFP-KDEL expression allowed visualization of ER structures. B. MPeX plot of hydrophobicity of the amino acid sequence of ORF6. Black bar indicates the highly hydrophobic region. C. Primary amino acid sequence of ORF6. Black bar indicates the highly hydrophobic region.

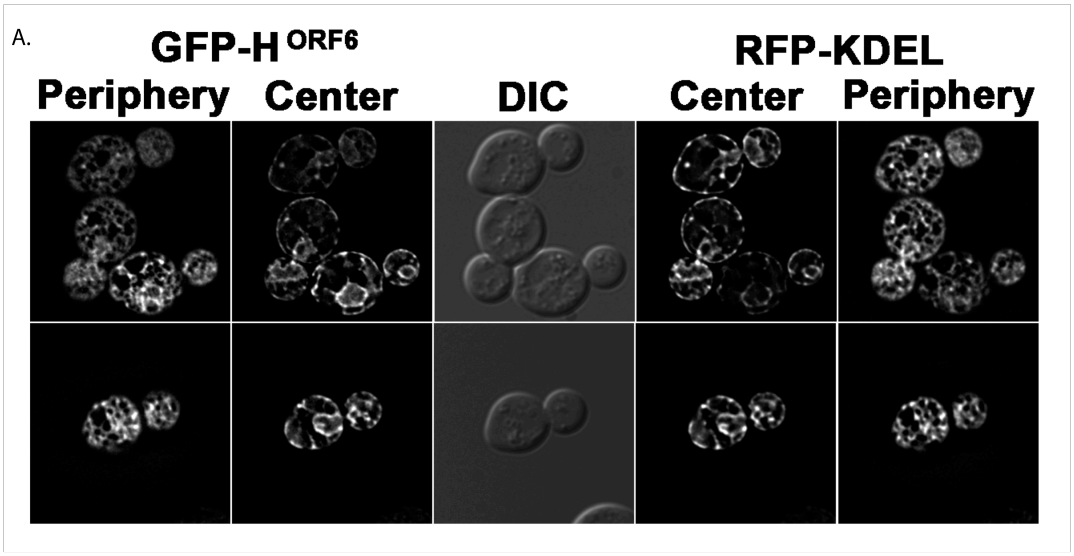
A.
GFP-H ORF6
Periphery
Center
DIC
RFP-KDEL
Center
Periphery

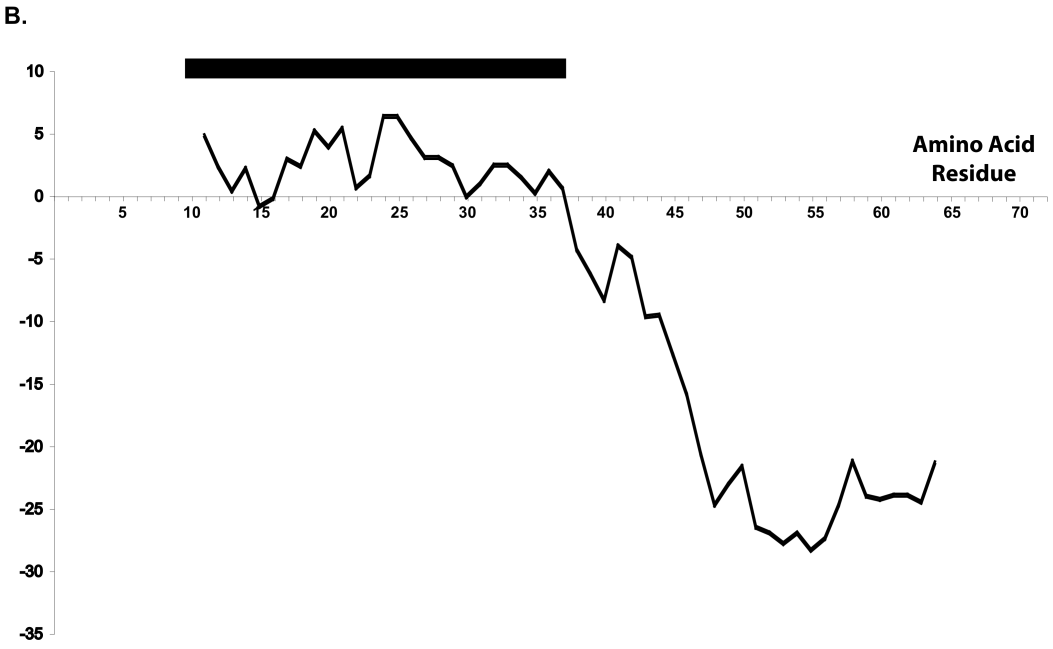
B.
10
5
0
-5
-10
-15
-20
-25
-30
-35
5
10
15
20
25
30
35
40
45
50
55
60
65
70
Amino Acid Residue


C.
MFHLVDFQVT IAEILIIIMR TFRIAIWNLD VIISSIVRQL FKPLTKKNYS ELDDEEPMEL DYPYPYDVPD YA
10
20
30
40
50
60
70

43 amino acid hydrophobic domain of ORF6 fused to GFP (separated by a GGPGG linker sequence). I expressed this construct in cells at low levels using the promotor region of *YOP1*. The GFP-H^{ORF6} localized to the ER membrane, similar to the full-length protein (Appendix Figure 4). The fact that GFP-H^{ORF6} localizes to the ER, similar to the full-length protein, allowed me to further assess whether the hydrophobic domain is responsible for the formation of the vesicular structures upon ORF6 overexpression.

Overexpression of GFP-H^{ORF6}

To further investigate my model that ORF6 acts on membranes through a hydrophobic wedging mechanism to drive the formation of the vesicle structures I placed the GFP-H^{ORF6} construct under the control of the *GAL1/10* promotor region. GFP-H^{ORF6} localization was monitored by fluorescence microscopy at 1 hour, 4 hours, 8 hours, 16 hours, and 24 hours after induction. Similar to the full length GFP-ORF6 construct, GFP-H^{ORF6} initially localized to the ER membranes (Appendix Figure 5). By 4 hours after induction the appearance of vesicular structures was seen close to the nuclear envelope. The vesicular structures formed by GFP-H^{ORF6} at 4 hours post-induction were formed more quickly than full-length ORF6 vesicles (see Figure 3) and may suggest the hydrophobic domain alone can act more quickly to form the vesicular structures. Consistent with this observation, the morphology of the ER is indiscernible in cells overexpressing GFP-H^{ORF6} by 8 hours after induction (Appendix Figure 5) while the full length ORF6 did not have this effect on cells until between 16 and 24 hours after induction (see Figure 3). Perhaps the NH_2 and COOH terminal hydrophilic domains of ORF6 serve some regulatory function, slowing the formation of the vesicular structures during infection until the virus has progressed through its lifecycle far enough to begin replication, and hence have a need for the DMV.

Figure 5 Overexpression of GFP-H^{ORF6} A. Fluorescence images of *reg1Δ* (RCY4274) overexpressing GFP-H^{ORF6} taken 16 hours after induction with galactose. Images represent a cross-sectional view through the center of the cell. B. A time-course induction of GPF-H^{ORF6} with fluorescence images collected at 1 hour, 4 hours, 6 hours, 8 hours, 16 hours and 24 hours after induction. Images represent a cross-sectional view through the center of the cell.

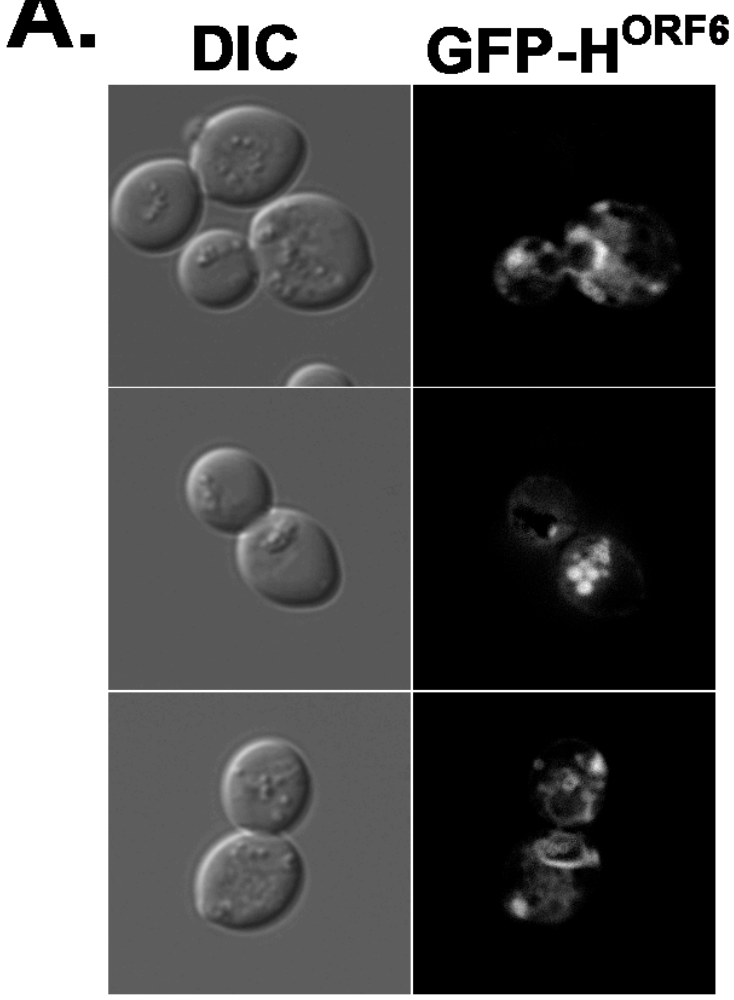
A.
DIC
GFP-H^ORF6

Figure 5 Continued

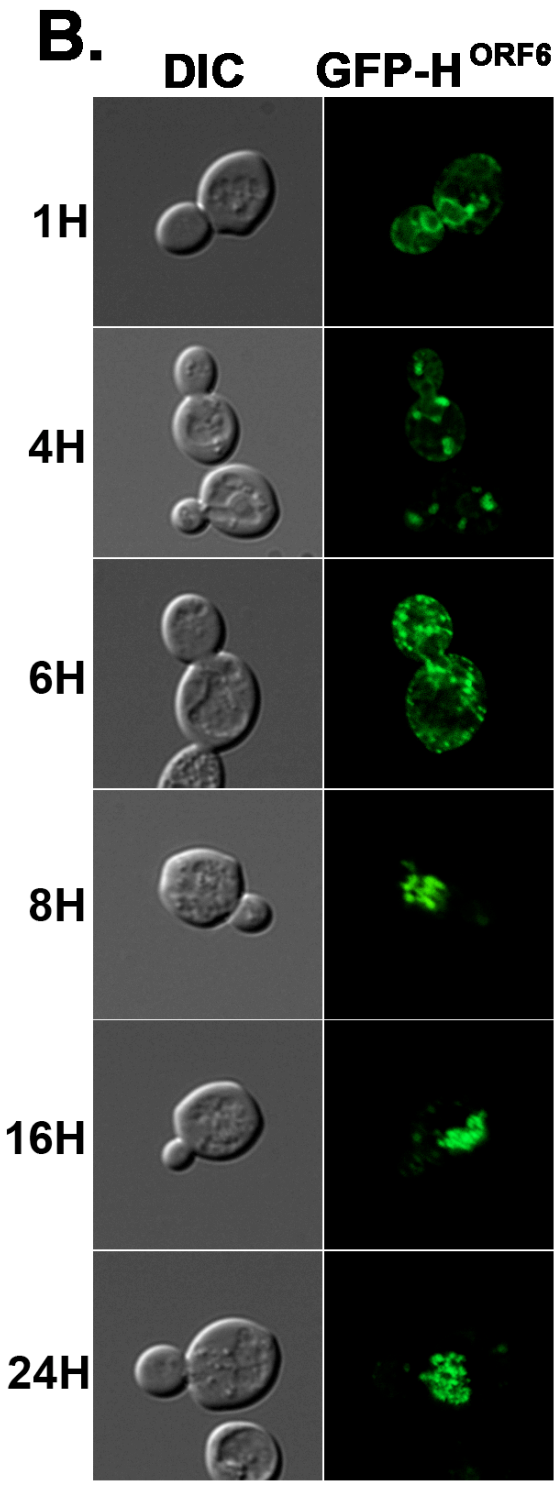

DISCUSSION

To accomplish my investigation of the function of ORF6 in cells I utilized budding yeast as a model organism for the ease of genetic manipulation and live cell imaging. In mammalian cells ORF6 is expressed during infection of a host cell and localizes to ER membranes and sites of viral replication [19-21]. GFP-tagged ORF6, expressed at levels similar to a yeast endogenous protein (*YOP1* promotor control), was found to localize to ER membranes (Figure 2), suggesting a conservation of the mechanism of ORF6 localization to these membranes. The conservation of the localization of ORF6 from yeast to mammalian cells may further suggest that the function of ORF6 may be conserved as well and indicate that yeast may be a suitable cell to study in more detail the function of ORF6 during SARS-CoV infection.

During a viral infection, host cell machinery is hijacked by viral factors for the purpose of making more viral particles, and as such, viral protein levels can reach relatively high levels when compared to host proteins. The ER localization of ORF6 was determined using a yeast endogenous promotor region (promotor region of *YOP1*) (Figure 2), thus presumably the protein levels of ORF6 in these cells was similar to the levels of Yop1p. I increased the expression of ORF6, reasoning that higher levels would more closely mimic the levels of ORF6 in an infected host cell, by placing the GFP-ORF6 construct under the control of the promotor region of the galactose inducible *GAL1/10* within a mult-copy vector (pRS425).

Overexpression of GFP-ORF6 was found to result in the formation of many vesicular structures within the cell with membranes derived from the ER membranes (Figure 3). High levels of ORF6 appeared to convert the typical cisternal and tubular morphology into the vesicular structures resembling bunches of grapes. Interestingly, the vesicular structures formed by GFP-ORF6 overexpression appeared to colocalize with the ER lumenal marker, RFP-KDEL, however the RFP signal was restricted to

outside the lumen of the vesicle (Figure 3). This localization pattern suggests that the vesicular structures are formed inside the lumen of the ER, either by formation de novo or by membrane budding into the ER luminal space. After prolonged overexpression (24 hours) the vesicular structures formed fill most of the cytoplasmic space of the cell and a complete conversion of normal ER morphology into the vesicular structures (Figure 3). Considering the vital functions the ER provides to the cell it is not surprising that the extended overexpression of ORF6 results in cell death, though further studies are needed to identify the functional defects imparted on the ER by high levels of ORF6.

Previous work has identified the long hydrophobic domain of ORF6 to function to similar levels as the full-length protein in increasing the replication rate and virulence during infection [20]. I have ascertained that the hydrophobic domain of ORF6 is sufficient to localize this protein to the correct compartment of the cell for proper function (the ER) and upon overexpression the hydrophobic domain alone is capable of forming the vesicular structures seen by overexpression of full length ORF6 (Figures 4 and 5). These results confirm that the hydrophobic domain of ORF6 is the functional unit of the protein and suggests that this domain may directly deform membranes through a hydrophobic wedging mechanism. Although these results suggest ORF6 acts directly on membranes, it is likely that this protein does not act alone in this process. Interactions between the hydrophobic domain of ORF6 and other viral proteins and/or host proteins may also contribute to the formation of the DMV replication site for SARS-CoV.

The formation of the DMV structures by SARS-CoV during infection requires some of the host cells autophagocytic machinery, for example microtubule associated light chain 3 (LC3), Apg12, and Apg5, and these proteins colocalize with DMV [18]. However, successful infection occurs even in the absence of ORF6 [19-21]. Thus it

seems likely that ORF6 functions in a redundant role with some as yet unidentified protein (host or viral) and/or interacts with the host autophagocitic machinery. Perhaps interactions between the hydrophobic domain of ORF6 and other proteins accelerates the formation of the vesicular structures as well as the viral replication rate, but removing ORF6 does not abolish the ability of the virus to form replication sites.

REFERENCES

1. Kuiken, T., et al., *Newly discovered coronavirus as the primary cause of severe acute respiratory syndrome.* Lancet, 2003. **362**(9380): p. 263-70.
2. Rota, P.A., et al., *Characterization of a novel coronavirus associated with severe acute respiratory syndrome.* Science, 2003. **300**(5624): p. 1394-9.
3. Ksiazek, T.G., et al., *A novel coronavirus associated with severe acute respiratory syndrome.* N Engl J Med, 2003. **348**(20): p. 1953-66.
4. Peiris, J.S., et al., *Coronavirus as a possible cause of severe acute respiratory syndrome.* Lancet, 2003. **361**(9366): p. 1319-25.
5. Thiel, V., et al., *Mechanisms and enzymes involved in SARS coronavirus genome expression.* J Gen Virol, 2003. **84**(Pt 9): p. 2305-15.
6. Yount, B., et al., *Severe acute respiratory syndrome coronavirus group-specific open reading frames encode nonessential functions for replication in cell cultures and mice.* J Virol, 2005. **79**(23): p. 14909-22.
7. Zeng, R., et al., *Characterization of the 3a protein of SARS-associated coronavirus in infected vero E6 cells and SARS patients.* J Mol Biol, 2004. **341**(1): p. 271-9.
8. Tan, Y.J., et al., *A novel severe acute respiratory syndrome coronavirus protein, U274, is transported to the cell surface and undergoes endocytosis.* J Virol, 2004. **78**(13): p. 6723-34.
9. Khan, S., et al., *Over-expression of severe acute respiratory syndrome coronavirus 3b protein induces both apoptosis and necrosis in Vero E6 cells.* Virus Res, 2006. **122**(1-2): p. 20-7.

10. Tan, Y.J., et al., *Overexpression of 7a, a protein specifically encoded by the severe acute respiratory syndrome coronavirus, induces apoptosis via a caspase-dependent pathway.* J Virol, 2004. **78**(24): p. 14043-7.
11. Yuan, X., et al., *G1 phase cell cycle arrest induced by SARS-CoV 3a protein via the cyclin D3/pRb pathway.* Am J Respir Cell Mol Biol, 2007. **37**(1): p. 9-19.
12. Yuan, X., et al., *G0/G1 arrest and apoptosis induced by SARS-CoV 3b protein in transfected cells.* Virol J, 2005. **2**: p. 66.
13. Li, W., et al., *Angiotensin-converting enzyme 2 is a functional receptor for the SARS coronavirus.* Nature, 2003. **426**: p. 450-4.
14. Pedersen, K.W., et al., *Open reading frame 1a-encoded subunits of the arterivirus replicase induce endoplasmic reticulum-derived double-membrane vesicles which carry the viral replication complex.* J Virol, 1999. **73**(3): p. 2016-26.
15. Gosert, R., et al., *RNA replication of mouse hepatitis virus takes place at double-membrane vesicles.* J Virol, 2002. **76**(8): p. 3697-708.
16. Goldsmith, C.S., et al., *Ultrastructural characterization of SARS coronavirus.* Emerg Infect Dis, 2004. **10**(2): p. 320-6.
17. Knoops, K., et al., *SARS-coronavirus replication is supported by a reticulovesicular network of modified endoplasmic reticulum.* PLoS Biol, 2008. **6**(9): p. e226.
18. Prentice, E., et al., *Coronavirus replication complex formation utilizes components of cellular autophagy.* J Biol Chem, 2004. **279**(11): p. 10136-41.
19. Kumar, P., et al., *The nonstructural protein 8 (nsp8) of the SARS coronavirus interacts with its ORF6 accessory protein.* Virology, 2007. **366**(2): p. 293-303.

20. Netland, J., et al., *Enhancement of murine coronavirus replication by severe acute respiratory syndrome coronavirus protein 6 requires the N-terminal hydrophobic region but not C-terminal sorting motifs.* J Virol, 2007. **81**(20): p. 11520-5.

21. Frieman, M., et al., *Severe acute respiratory syndrome coronavirus ORF6 antagonizes STAT1 function by sequestering nuclear import factors on the rough endoplasmic reticulum/Golgi membrane.* J Virol, 2007. **81**(18): p. 9812-24.

22. Rothberg, K.G., et al., *Caveolin, a protein component of caveolae membrane coats.* Cell, 1992. **68**(4): p. 673-82.

23. Frieman, M., et al., *Severe acute respiratory syndrome coronavirus ORF6 antagonizes STAT1 function by sequestering nuclear import factors on the rough endoplasmic reticulum/Golgi membrane.* J. Virol., 2007. **81:** 9812–9824.

24. Kopecky-Bromberg, S. A., et al. *Severe acute respiratory syndrome coronavirus open reading frame (ORF) 3b, ORF 6, and nucleocapsid proteins function as interferon antagonists*. J. Virol., 2007. **81:**548–557.